Design of vaccine nanotechnology-based delivery systems: The effect of CpGODN TLR9 agonist-protein antigen conjugates anchored to liposomes

Despo Chatzikleanthous

Under the supervision of

Prof. Yvonne Perrie and Dr. Roberto Adamo

A thesis presented in fulfilment of the requirements for the degree of Doctor of Philosophy

Strathclyde Institute of Pharmacy and Biomedical Sciences,
University of Strathclyde
Glasgow G4 0RE

December 2019

DECLARATION OF AUTHENTICITY

This thesis is the result of the author's original research. It has been composed by the author and has not been previously submitted for examination which has led to the award of a degree. The copyright of this thesis belongs to the author under the terms of the United Kingdom Copyright Acts as qualified by University of Strathclyde Regulation 3.50. Due acknowledgement must always be made of the use of any material contained in, or derived from, this thesis.

ACKNOWLEDGEMENTS

The research project was funded by the European Commission Project Leveraging Pharmaceutical Sciences and Structural Biology Training to Develop 21st Century Vaccines (H2020-MSCA-ITN-2015 grant agreement 675370). Despo Chatzikleanthous is a PhD candidate at the University of Strathclyde (Glasgow, UK) participated in the project at GSK (Siena, Italy). This project was cosponsored between the University of Strathclyde and GSK.

Supervision: Yvonne Perrie (University of Strathclyde), Roberto Adamo (GSK)

Experiments were conducted within GSK and University of Strathclyde facilities. All experiments were conducted by Despo Chatzikleanthous, apart from NF-κB luciferase reporter assay (Ida Paciello, GSK), Opsonophagocytosis killing assay (Giada Buffi, GSK) and Cryo-TEM (Mairi Clarke, Scottish Centre for Macromolecular Imaging, University of Glasgow).

Signe Tandrup Schmidt (University of Strathclyde) was involved on the design and performance of biodistribution studies.

Table of Contents

List of figures

List of tables

List of abbreviations

APCs	Antigen presenting cells
BSA	Bovine serum albumin
CDC	Centers for disease control and prevention
CFS	Colony forming unit
CpGODN	CpG oligonucleotides
CTL	Cytotoxic T lymphocyte
CSF	Cerebrospinal fluid
Cryo-TEM	Cryo transmission electron microscopy
DCs	Dendritic cells
DDA	Didodecyldimethylammonium bromide
DLS	Dynamic light scattering
DMPG	1, 2-dimyristoyl-sn-glycero-3-phospho-(1'-rac-glycerol) (sodium salt)
DOTAP	1, 2-dioleoyl-3-trimethylammonium-propane (chloride salt)
DOTIM	1-[2-(oleoyloxy) ethyl]-2-oleyl-3-(2-hydroxyethyl) imidazolinium chloride
DOTMA	1,2-di-O-octadecenyl-3-trimethylammonium propane (chloride salt)
DSPC	1, 2-distearoyl-sn-glycero-3-phosphocholine
DSPE	1,2-distearoyl-sn-glycero-3-phosphoethanolamine
EOD	Early-onset disease
FRR	Flow rate ratio
FCS	Fetal calf serum
GBS	Group B Streptococcus
HPLC	High-performance liquid chromatography
HSPC	L-α-phosphatidylcholine, hydrogenated (Soy)
IAP	Intrapartum antibiotic prophylaxis

IFN	Interferon
IL	Interleukin
IVS	Inactivated injectable polio vaccine
LOD	Late-onset disease
LUV	Large unilamellar vehicles
MenB	Meningococcal serogroup B
MHC	Major histocompatibility complex
OPKA	Opsonophagocytosis killing assay
OVA	Oral polio vaccine
OVA protein	Ovalbumin
Pam_2Cys	S-[2,3-bis(palmitoyloxy)propyl]cysteine
Pam_3Cys	N-α-Palmitoyl-S-[2,3-bis(palmitoyloxy)-(2RS)-propyl]-L-cysteine
PAMP	Pathogen-associated molecular pattern
PBS	Phosphate-buffered-saline
PDI	Polydispersity index
PEG	Polyethylene glycol
Poly I:C	Polyinosinic: polycytidylic acid
PRRs	Pattern recognition receptors
RPMI	Roswell Park Memorial Institute
SUV	Small unilamellar vehicles
TDB	Trehalose 6, 6’-dibehenate
TFR	Total flow rate
Th	T helper
TLC	Thin layer chromatography
TLR	Toll like receptor
TNF-α	Tumour necrosis factor alpha
RT	Room temperature
WBC	White blood cells
WHO	World health organization

Abstract

The efficiency of CpG oligonucleotides as Toll like receptor (TLR) 9 agonist has been well established along the last few years. Although CpGODN has shown promising results as vaccine adjuvant in preclinical and clinical studies, its *in vivo* stability and potential systemic toxicity have generated concern for the use of CpGODN. In an effort to increase stability, localise action and reduce dosage, different strategies have been approached, such as conjugation of CpGODN with immunogenic agents or encapsulation/adsorption of CpGODN into/onto liposomes resulting in enhanced immunopotency compared to coadministration of free CpGODN and antigen. Despite the advances in the field, the effect of conjugation of TLR9 to antigen in combination with liposomes on the immunogenicity of protein-based vaccines has not been explored yet.

In this present study, thiol-maleimide chemistry was utilised for the covalent ligation between protein antigen and CpGODN TLR9 agonist, which did not alter protein's ability to be recognised by specific antibodies or activation of receptor by TLR9 agonist. Thanks to its negative charge, protein conjugate was electrostatically bound to cationic liposomes composed of 1, 2-distearoyl-sn-glycero-3-phosphocholine (DSPC), cholesterol and dimethyldioctadecylammonium bromide (DDA). The designed system GBS67-CpGODN+L shared similar vesicle characteristics (size and charge) compared to free liposomes but exhibited different structure and morphology. Following immunisation through the intramuscular (i.m.) route, cationic liposomes-protein conjugate complex (GBS67-CpGODN+L) formed a vaccine depot at the injection site, which translated into notable increase of functional immune responses compared to the simple coadministration of GBS67, CpGODN and liposomes (GBS67+CpGODN+L). This effect seems due to increased total IgG level and specifically of IgG2a subtype, although no specific Th1/Th2-driven response was found.

This work demonstrates that the conjugation of TLR9 agonist to GBS67 in conjunction with adsorption on cationic liposomes, can promote codelivery leading to the induction of a multifaceted immune response at low antigen and CpGODN doses. The findings of this study highlight the potential for harnessing the immunostimulatory properties of different adjuvants to develop more effective nanostructure-based vaccine platforms achieving therapeutic effect at lower doses.

Chapter 1 Introduction

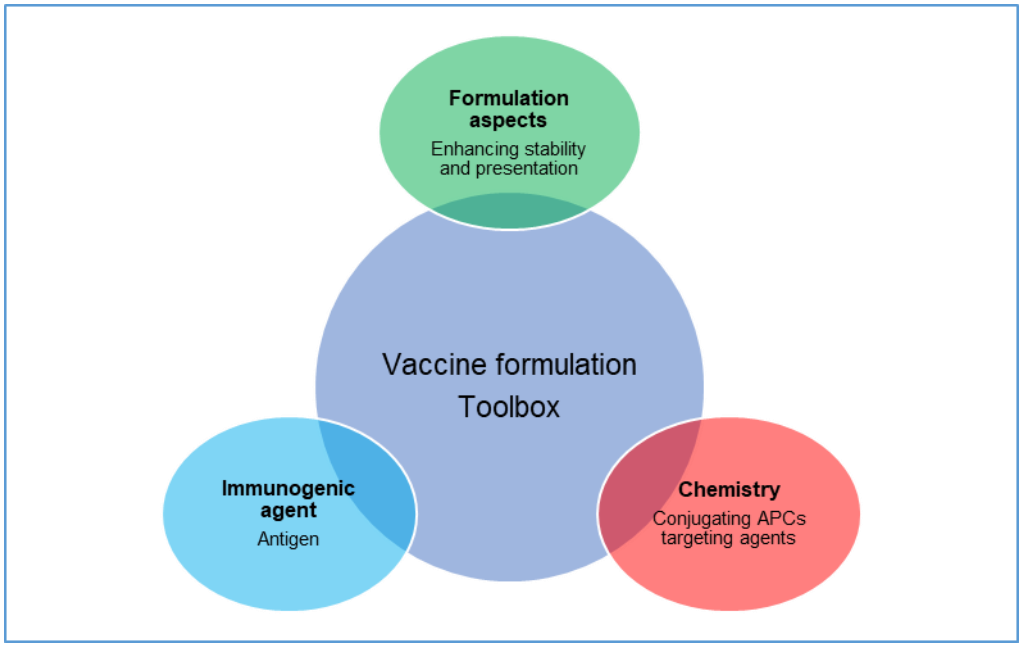

1.1 Vaccination

Despite advancements in the prevention, early detection and treatment of many diseases the overall mortality rate due to infectious diseases remains high at 15-20%, demonstrating the need for more effective prevention cures and therapies (World Health Organization). Existing treatments for many diseases suffer from several limitations. First, there is a portion of patients who do not respond to conventional therapies, fully or partially. Examples include the decreased meningococcal susceptibility to penicillin which has been reported in several areas in the world (Nudelman and Tunkel, 2009). Moreover, many of the treatments are empirical and based on antibiotics and antimicrobial agents. However, there are concerns about the use of antibiotics, as they are associated with high levels of toxicity which combined with the fact that drugs are not side-specific, cause side effects resulting in damage of the healthy cells of the organism. Thus, combining this and the disease prevention ability of vaccines, much research is focused on the development of vaccines.

Traditional live-attenuated vaccines (e.g. polio, tetanus and poliomyelitis) have been effective for the elimination and control of many diseases. However, concerns about their safety have restricted their development and protein and peptide-based vaccines have arisen as a safer alternative. Example is the switch from live oral polio vaccine (OVA) to inactivated injectable polio vaccine (IVS) in the UK, due to side effects connected with OVA as is Vaccine Associated Paralytic Poliomyelitis (VAPP) and Circulating Vaccine Derived Poliovirus (cVDPV). Since 2004, people in the UK have been vaccinated using IVS (World Health Organization). In contrast, although subunit vaccines are safer than conventional vaccines, they are less immunogenic. In the development of vaccines, a second consideration is the composition of the today's societ which is quite different from the one which most of the vaccines were developed. Today, most of the developed countries have a lower proportion of children and higher proportion of adults and elderly. Thus, adults and elderly are very important target groups for the development of new vaccines. However, the development of vaccines for these groups can be challenging as they are more susceptible to infections. The adaptive immunity, responsible for the defence of the organism against the pathogens, is decreased by age. More specifically, the production of naïve lymphocytes and the antigen-recognition repertoire diversity are decreased. So, there is a need for the design of more advanced vaccine formulations with broader coverage and augmented immune responses. Novel approaches and

alternative strategies are required for the development of upgraded vaccine formulations that are able to address the needs of the today's society. One new strategy is the development of a novel therapeutic modality, which can be applied separately or coupled with current treatments for the treatment of a disease. One of these novel approaches is nanotechnology-based vaccination.

1.2 Nanotechnology-based therapy

Over the past few years, nanotechnology has been used in medicine for human vaccine delivery, particularly to enhance the immunogenicity of subunit vaccines. Despite the advantages of increased safety and ability to carry large quantities of antigens due to their recombinant form, subunits vaccines are still less efficient than traditional vaccines. Subunit vaccines use a portion of the pathogen (antigens) which in many cases itself is very weakly immunogenic. Thus, there is a need for the development of delivery systems and adjuvants which can boost their immunogenicity. Nanotechnology platforms have been incorporated into vaccine development as delivery system and/or adjuvants (Peek *et al.*, 2008). Nanocarrier-based delivery systems are continuously improved aiming the maximal humoral and cellular immune responses and the minimal undesirable side effects.

Efficient and specific delivery of antigens and controlled release of the antigen to antigen presenting cells (APCs) are necessary preconditions and the ultimate goal for effective vaccination. Numerous nanocarriers have been designed and investigated for their ability to deliver therapeutic or immunogenic agents to cells in order to overcome problems associated with them (e.g. dendrimers, liposomes, polymers). The large size of therapeutic and immunogenic molecules and their hydrophilic nature due to the negatively charged phosphate groups are obstacles to the cellular uptake (Al-Dosari and Gao, 2009; Kim *et al.*, 2014; Zhang *et al.*, 2019). The entrance of charged molecules into the cells is not feasible because they lack the ability to cross the lipophilic and negatively charged membrane due to the charge repulsion. In addition, therapeutic and immunogenic moieties are susceptible to nucleases which are contained in the extracellular environment secreted by the surrounding bacteria (Blokesch and Schoolnik, 2008). Therefore, the use of carriers becomes imperative in circumventing degradation and thus stabilising the therapeutic and immunogenic molecules by nucleases (Patil *et al.*, 2005). Nanoscience focuses on the development of carriers which can selectively transfer the drug or antigens to target cells by minimising its degradation and preventing side effects (Gullotti and

Yeo, 2009; Fernando *et al.*, 2018). It has been proven that the morphological features of carriers such as size, shape and surface charge can strongly influence the vaccine adjuvanticity properties, which in turn affects the quality and magnitude of immune responses (Oyewumi *et al.*, 2010; Watson *et al.*, 2012; Kumar *et al.*, 2015; Comberlato *et al.*, 2019). Hence, the manufacture of particulate vaccine carriers is a key consideration.

An ideal vector should have a particle size in the range 10-1000 nm and resistance to degradation by the immune system (Zhao *et al.*, 2014) Several studies have demonstrated that nanoparticles exhibit some advantages over microparticles such as enhanced uptake into lymphatics and greater uptake into APCs (Courant *et al.*, 2017). In addition, carriers should be biocompatible and easily functionalised (Holland *et al.*, 2019). Essential characteristics for a vector are also the low levels of toxicity and the extended circulating half-life (Peer *et al.*, 2007). The long circulation time is strongly related with the nanoparticle size. The reduction of particle size increases the circulation time of particles (Gullotti and Yeo, 2009). Nanoparticles, such as liposomes (Perrie *et al.*, 2016), polymeric nanoparticles, virus-like nanoparticles, silk nanoparticles (Seib, 2017), proteosomes and emulsions have been extensively studied as delivery systems and/or adjuvants over the past three decades (Mohan *et al.*, 2013). The work within this thesis focuses on the use of liposomes as adjuvant and nanocarriers.

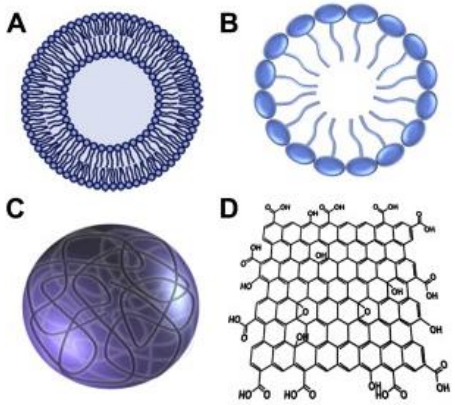

Figure 1.1 *Structures of nanocarriers for vaccine antigen delivery. (A) Liposomes (B) Emulsions (C) Polymeric nanoparticles (D) Graphene oxide nanosheets (Kim et al., 2014).*

1.3 Liposomes

Liposomes were discovered by Alec D. Bangham in the 1960s at the Babraham Institute, University of Cambridge and consist of biocompatible and biodegradable

phospholipid bilayers (Bangham and Horne, 1964). The liposomal size depends on the number of bilayers. Liposomes are usually divided, according to their morphology, into two major types, unilamellar and multilamellar vesicles. Unilamellar liposomes are formed when a single bilayer of phospholipids surrounds the aqueous core. Small Unilamellar Vehicles (SUV) with size less than 100 nm and the Large Unilamellar Vehicles (LUV) with size up to a few microns are some of the most extensively used (Marasini *et al.*, 2017). Liposomes have the ability to load and codeliver hydrophilic and hydrophobic molecules as antigens and immunopotentiators. An immunogenic agent may be either encapsulated in the core of the liposome or adsorbed on the surface for presentation to APCs (Peek *et al.*, 2008).

In addition, the physicochemical properties of liposomes including their size, surface charge and lipid composition are versatile. They can be easily surface modified by adding a ligand, antigen or another type of lipid. Moreover, they can incorporate almost any drug independent of its solubility in water (Solaro *et al.*, 2010). All the above characteristics make liposomes useful for delivery purposes. Surface-modified liposomes have been designed and studied for targeting immune cells, codelivering immunostimulatory agents, and enhancing both humoral and cell-mediated immune responses simultaneously aiming the augmentation of vaccine efficiency (Ludewig *et al.*, 2000; Henriksen-Lacey *et al.*, 2010a; Maji *et al.*, 2016; Nisini *et al.*, 2018; Wilkinson *et al.*, 2018).

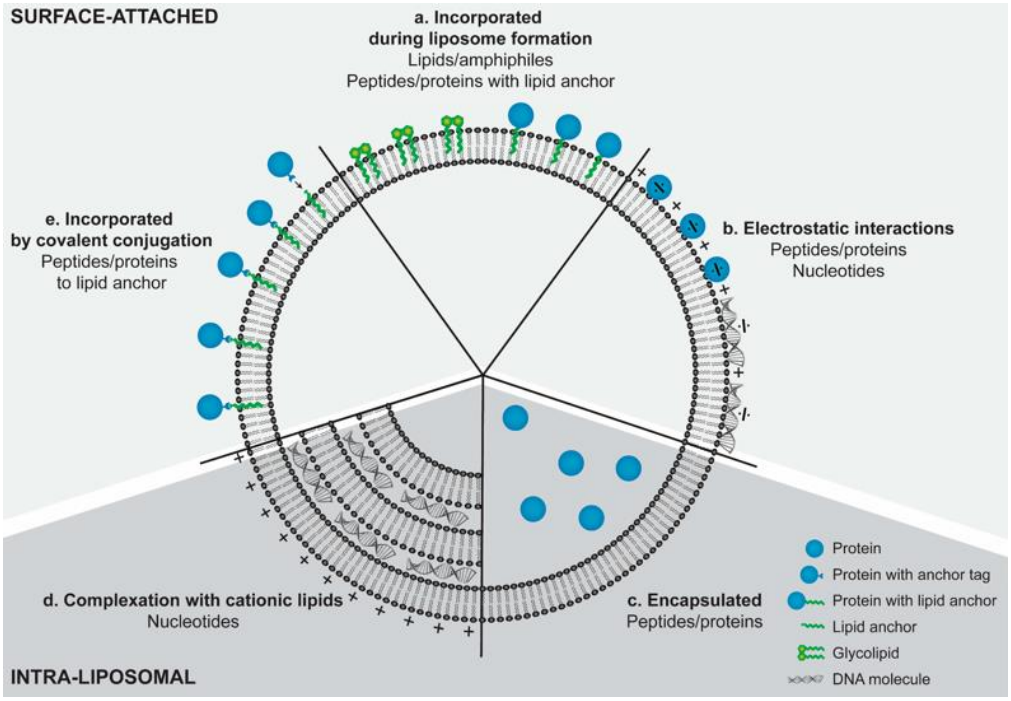

Figure 1.2 *Strategies used for incorporation of immunogenic agents and other adjuvants into liposomes depending on the type and purpose of the molecules in question. (a) Hydrophobic molecules and lipids can be incorporated into the lipid bilayer by addition to the dissolved lipids prior liposomes manufacturing. (b) Peptides/proteins and nucleotides can be electrostatically adsorbed to oppositely-charged lipids on the surface of liposomes. (c) Peptides and proteins can be encapsulated into the aqueous interior of the liposomes. (d) Nucleotides can be complexed with cationic lipids being embedded between multiple lipid bilayers. (e) Post-liposome manufacture attachment of peptides and proteins can be achieved by covalent conjugation to functionalised lipid anchors (Tandrup Schmidt et al., 2016).*

Gregoriadis and Allison were the first to report the use of liposomes as immunological adjuvants in 1974. They found that negatively charged liposomes containing dicetyl phosphate could promote robust immune responses against diphtheria toxoid (Perrie *et al.*, 2016). Since then, numerous studies have shown the benefits of the use of liposomes for therapeutic purposes and liposomal vaccines have been investigated in human trials against malaria, HIV, hepatitis A, influenza and prostate cancer (Bulbake *et al.*, 2017).

In 1998, Guan *et al*. investigated the effects of physical association of an antigen widely expressed in most human carcinomas MUC1 peptide BP25 with liposomes, on immune responses. Lipid conjugated and non-conjugated MUC1 peptides were incorporated in liposomes with a composition of 3:1:0.25 molar ratio (1,2-distearoyl-sn-glycero-3-phosphocholine (DSPC) / cholesterol / 1, 2-dimyristoyl-sn-glycero-3-phospho-(1'-rac-glycerol) (DMPG)) containing Monophosphoryl lipid A (1% w/w of the total lipids). C57BL/6 mice vaccinated subcutaneously with peptide alone, peptide mixed with peptide-free liposomes, and peptide associated with liposomes in

entrapped or surface-exposed forms. Their studies showed that liposome-associated (encapsulated or surface-exposed) with MUC1 peptide produced stronger antigen-specific T cell responses (6-10-fold higher) than the formulations with the lipopeptide alone or peptide mixed with peptide-free liposomes (Guan *et al.*, 1998).

Cationic liposomes are highly effective as carriers of immunogenic agents (antigens) and other adjuvants. Due to their cationic charge, they have the capability to electrostatically bind and codeliver negatively charged molecules as antigens and adjuvants enhancing antigen delivery, uptake and presentation to APCs. They are known for the formation of a depot effect leading to the attraction of APCs at the site of injection (Schwendener, 2014; Perrie *et al.*, 2016). Even though there is a plethora of lipid combinations/liposome constructs that can be considered, they usually composed by neutral phospholipids such as DSPC, L-α-phosphatidylcholine (HSPC) and 1,2-dioleoyl-sn-glycero-3-phosphocholine (DOPC) which is the principle lipid giving the structure of lipid bilayer to liposomes particles, cholesterol which enhances stability of the lipid bilayer and a cationic lipid such as dimethyldioctadecylammonium (DDA) and 1,2-dioleoyl-3-trimethylammonium-propane (DOTAP) which gives the cationic charge. One of the most known cationic lipid formulation is CAF01 which is composed by the DDA cationic lipid and trehalose 6,6-dibehenate (TDB) immunopotentiator. The cationic lipid DDA has been shown to greatly enhance the protective immunity of the associated antigen and generate high levels of both humoral and cell-mediated responses (Kaur *et al.*, 2012; Kaur *et al.*, 2014).

Lay *et al*. demonstrated that the combination of lipoplexes and Fluzone[1], an influenza vaccine, elicited enhanced antibody responses and cell immunity in mice. They injected intramuscularly combined formulation of the JVRS-100 adjuvant which consists of 1-[2-(oleoyloxy)ethyl]-2-oleyl-3-(2-hydroxyethyl)imidazolinium chloride (DOTIM)/cholesterol cationic liposome–DNA complexes with a split trivalent influenza vaccine (Fluzone-Sanofi Pasteur). They observed that mice vaccinated with JVRS-100–Fluzone had higher grade protection, as measured by attenuation of weight loss and increased survival, compared to vaccination with Fluzone alone. More specifically, they demonstrated that mice received vaccination with adjuvanted JVRS-100 Fluzone formulation showed a 10-fold higher level of total Fluzone-specific IgG compared to animals immunised with Fluzone alone. Regarding the T-cell specific

[1] Fluzone is a registered trademark of Sanofi Pasteur Inc.

immune responses, JVRS-100–Fluzone vaccination resulted in an approximately 10-fold increase in antigen-specific splenocyte response when compared with Fluzone alone as measured by IFNγ production. To further evaluate the impact of JVRS-100 adjuvant on the efficiency of Fluzone vaccine, mice vaccinated with JVRS-100–Fluzone and Fluzone alone were tested against drifted influenza strains. Mice vaccinated with JVRS-100–Fluzone and challenged with 2× LD50 of PR/8/34 (H1N1) or HKx31 (H3N2) had 10–15% weight loss and 100% survival. In contrast, mice treated with unadjuvanted Fluzone had more than 30% weight loss and 0% survival. Mice vaccinated with JVRS-100–Fluzone and challenged with 2× LD50 of B/Lee/40 showed a similar weight loss profile compared to unadjuvanted Fluzone until day 6, after which the infection was lethal for the control and unadjuvanted groups. In contrast, the JVRS-100–adjuvanted group recovered with 80% survival. Their observations indicated that JVRS-100 adjuvant increases immunogenicity and may induce cross-protection to influenza strains (Lay *et al.*, 2009).

Henrisken-Lacey *et al.* reported that liposomes have the ability to promote a depot effect of antigens. In particular, they used radioisotopes H^3 and I^{125} to determine the *in vivo* fate of DDA and DDA: TDB liposomes and Ag85B-ESAT-6 their associated antigen. Mice vaccinated intramuscularly with I^{125}-antigen with or without the coadministration of cationic liposomes H^3-DDA or H^3 DDA: TDB. Their studies demonstrated that Ag85B-ESAT-6 antigen was cleared rapidly from the site of injection when administrated alone with only 5.7% of antigen dose found at the injection site after one day post injection. In contrast, the coadministration of cationic liposomes with the antigen promoted the slower release of it with approximately 76% of the antigen remaining at the site of injection one day after vaccination. However, no significant differences were found when the two different liposomal formulations were used. The same conclusions were reached when subcutaneous administration was used. Moreover, during their *in vivo* studies they proved that when Ag85B-ESAT-6 antigen was administrated with either DDA or DDA: TDB liposomes, the antigen specific immune responses were enhanced. IFNγ, IgG1 and IgG2c were obtained using DDA or DDA: TDB liposomes were found to be around 2-fold higher than that observed when Ag85B-ESAT-6 antigen was administrated alone. Their results support that the inclusion of cationic liposomes into Ag85B-ESAT-6 antigen based vaccines significantly enhanced the immunogenicity of antigen-based vaccine (Henriksen-Lacey *et al.*, 2010a).

Another group of researchers (Thoryk *et al.*, 2016) during their studies proved that the use of lipid nanoparticles can enhance the immune responses to subunit vaccine antigens in mice. They performed immunogenicity studies using HBsAg and Ovalbumin (OVA) as model antigens and they observed that the coadministration of lipid nanoparticles with antigens at the same injection site and the same time can boost the antigen specific B-cell and T-cell immune responses. Notably, the immune responses achieved with lipid nanoparticles were higher than those elicited by aluminium-based adjuvant (MAA).They found that the B-cell specific IgG titres obtained with lipid nanoparticles were 4-fold higher than those obtained when HBsAg antigen was coadministrated with MAA adjuvant. The coadministration of HBsAg antigen with lipid nanoparticles resulted in high levels of antigen specific CD4+ and CD8+ T-cell responses which were 3-5-fold higher than that those induced when HBsAg was coadministrated with MAA adjuvant. Similar results obtained with OVA (Thoryk *et al.*, 2016).

Furthermore, the ability of liposomes to promote antigen presentation and immunogenicity of HIV DNA vaccines was investigated by many researchers. Qiao *et al*. designed a DNA adjuvant (man-ZCL) consisting of zwitterionic lipid mannosylated distearoyl phosphoethanolamine-polycarboxybetaine (DSPE-PCB) (mannose-DSPE-PCB), cationic lipid DOTAP and cholesterol for HIV vaccination. HIV DNA plasmid Env was chosen as a model antigen for the investigation of the cytotoxicity and transfection efficiency levels of the adjuvant/DNA system. Their *in vivo* and *in vitro* studies demonstrated that man-ZCL lipoplexes had lower toxicity profile compared to CpG/DNA and Lipofectamine2000/DNA and had the ability to enhance the anti-HIV immune response. In addition, their studies indicated that man-ZCL could assist to activate T cells through a non-inflammasome pathway suggesting that the man-ZCL could be potentially applied as a safe and efficient DNA adjuvant for HIV vaccines (Qiao *et al.*, 2016).

At least 8 liposome-based adjuvant systems have been approved or are in clinical trials for human use (Table 1.1). Since 1997, Inflexal[2] and Epaxal[3] are marketed vaccines against influenza and hepatitis A respectively. Both of them are composed of “virosomes”, which are consisted of unilamellar phospholipid membrane vesicle incorporating virus membranes. Furthermore, Stimuvax and RTS, S/AS01 are

[2] Inflexal is a registered trademark of Crucell.
[3] Epaxal is a registered trademark of Crucell.

liposomal vaccines for therapy of non-small cell lung cancer and prevention of malaria and are both in clinical trials phase III. They are comprised of more conventional lipids like cholesterol, phosphatidylglycerol and Monophosphoryl Lipid A (Watson *et al.*, 2012; Li *et al.*, 2019).

Table 1.1 *Selected liposome and lipid-based vaccines approved for human use or in clinical trials (Watson et al., 2012).*

Name	Company	Disease	Description	Status
Inflexal	Crucell	Influenza	Virosomes-reconstituted influenza viral membranes (phospholipids, hemagglutinin, and neuraminidase) supplemented with PC	Marketed
Epaxal	Crucell	Hepatitis A	Formalin-inactivated Hepatitis A virus adsorbed to virosomes	Marketed
Stimuvax	Merck KGaA, Oncothyreon	Non-small cell lung cancer	BLP25 (palmitoylated MUC1), MPL, DPPC, DMPG, Chol	Phase 3
RTS,S/AS01	GlaxoSmithKline	Malaria	Recombinant fusion of P. falciparum circumsporozoite protein and Hepatitis B surface antigen, PC, Chol, MPL, QS21	Phase 3
Vaxisome	NasVax	Influenza	Inactivated influenza vaccine, CCS, Chol	Phase 2
JVRS-100	Juvaris BioTherapeutics	Influenza	Inactivated influenza vaccine, DOTIM, Chol, non-coding plasmid DNA	Phase 2
Vaxfectin	Vical	Influenza	Plasmid DNA-encoded influenza proteins, GAP-DMORIE, DPyPE	Phase 1
CAF01	Statens Serum Institut	Tuberculosis	Subunit protein antigen Ag85B-ESAT, DDA, TDB	Phase 1

1.4 Immune potentiators

Despite the evolvement of the research, one of the main problems with the use of protein-based vaccines is the low immunogenicity levels. Enhancement of vaccines immune responses is ultimate goal of vaccine research. It has been reported by many researches that surface engineering improves vaccines formulations in several different ways. Overcoming immune senescence, vaccine and antigen dose sparing as B-cell and T-cell immune responses broadening are some of the potential benefits of the use of adjuvants.

Studies have established that the efficiency of the nanoparticle-based system is increased when the nanoparticle is conjugated with a specific ligand, which can bind specific receptors on the cell surface. Proteins (mainly antibodies and their fragments), nucleic acids (aptamers), or other receptor ligands such as peptides, vitamins, and sugars can be potential cell activators (Peer *et al.*, 2007). This strategy has arisen as one approach to overcome the deficiency in specificity and maximise the immunogenicity. Therefore, the use of appropriate ligands that can be preferentially recognised from the cells as receptors can have positive effect on them (Ghosh and Heston, 2004).

Toll-like receptors agonists (TLR) are some of the most used immune potentiators for vaccines. TLR receptors are type I single-pass transmembrane proteins found on the surface of cells. These proteins are able to recognise classes of pathogens including Gram-positive and Gram-negative bacteria, fungi, DNA or RNA viruses. Stimulation of these receptors by specific ligands leads to the activation of the innate immune cells, such as dendritic cells (DC) resulting on the robustness of immune response. To date, 14 TLRs have been identified. The Toll gene was first discovered in 1985 by Christiane Nüsslein-Volhard in Drosophila melanogaster (Lemaitre *et al.*, 1996; Thakur *et al.*, 2017).

Through a variety of signalling pathways, engagement of TLRs result in quantitative and qualitative changes in immunological functions, including antigen presentation (Cluff *et al.*, 2005). Myeloid differentiation primary-response protein 88(MyD88)-dependent (production of inflammatory cytokines) and -independent pathways (induction of interferon beta (IFN-β)) are two distinct pathways of TLR signalling. All TLRs except TLR3 use the MyD88-dependent pathway (Figure 1.3).

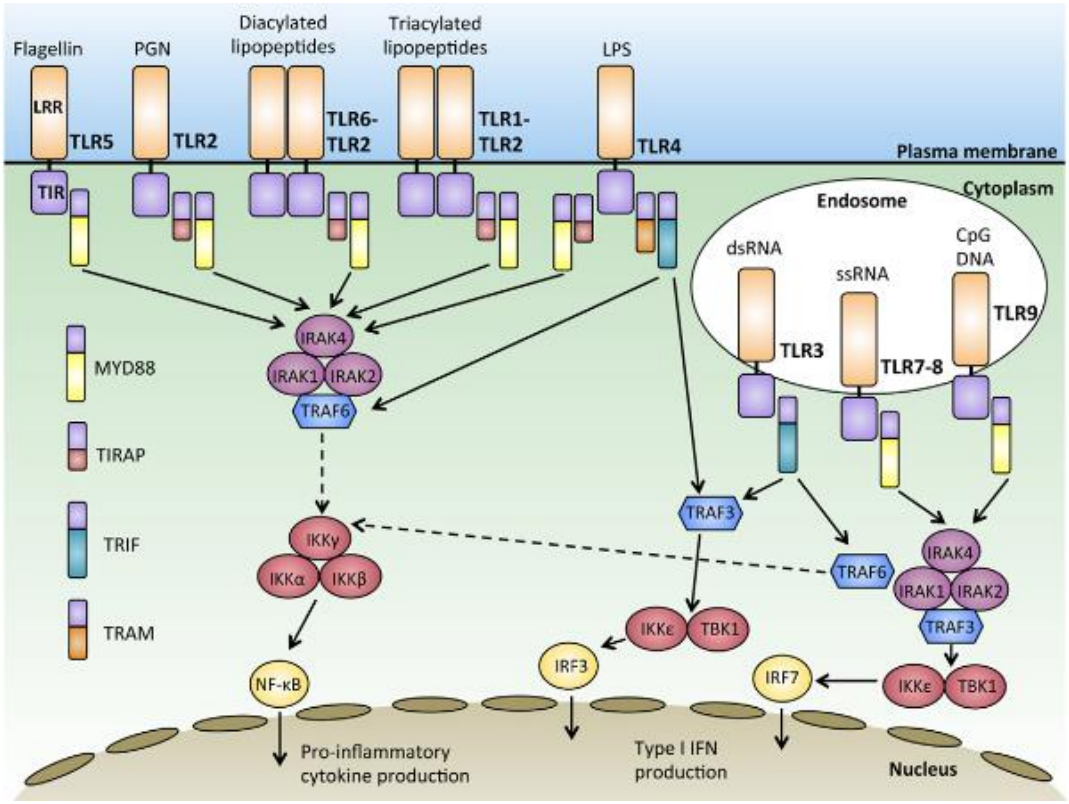

Figure 1.3 *Signal transduction downstream of MYD88-dependent and independent pathways. Activation of Toll-like receptors (TLRs) through binding of their ligand leads to receptor dimerisation and the recruitment of adaptor proteins such as MYD88, TIRAP, TRIF, and TRAM. Most of the TLRs form homodimers upon activation while TLR2 can also form heterodimers with either TLR6 or TLR1 to recognise diacylated and triacylated lipopeptides, respectively. Downstream signals are propagated through the activation of IRAKs-TRAF6 and the IKK complex, culminating in the activation of transcription factors such as nuclear factor-κB (NF-κB) and interferon-regulatory factors (IRFs), which regulate the production of pro-inflammatory cytokines and type 1 interferon (IFNs) (Wang et al., 2014).*

Several studies have explored the use of various molecules as ligands. Donadei *et al.* investigated the adjuvant effect of TLR7 agonist in a meningococcal serogroup C glycoconjugate vaccine. They conjugated Meningococcus serogroup C antigens with CRM_{197} protein, which was in turn conjugated with TLR7 agonist.Their *in vitro* studies showed that MenC-CRM_{197}-TLR7 vaccine could activate TLR7 in a greater extent compared to the MenC-CRM197 ligand alone. TLR7 agonist augmented the IgG2a subclass inducing a Th1 shift (Donadei *et al.*, 2016). Smith *et al*. designed novel oxoadenine TLR7/8 agonists and they evaluated their ability to enhance immunity using CRM197 as a model antigen. Their studies indicated that antigen-specific antibody production was 800-fold higher compared to that obtained from pigs vaccinated with the non-adjuvanted vaccine. Furthermore, they proved that antigen-specific antibody production was increased in a dose dependent manner. Vaccination of pigs with the highest dose of adjuvant-antigen formulation resulted in a 13-fold

increase of antigen-specific CD3+/CD8+ T cells compared to pigs vaccinated unadjuvanted antigen (Smith *et al.*, 2016).

Fallon *et al*. tested the impact on the immune response of a RSV fusion protein vaccine when conjugated to a TLR4 agonists. Specifically, they conjugated RSV protein with glucopyranosyl lipid A (GLA), a TLR4 agonist. One group of patients received vaccination containing adjuvanted antigen and another group was vaccinated with unadjuvanted vaccines. The addition of adjuvant into the vaccine increased both humoral and cellular immune responses compared to the group vaccinated with the non-adjuvanted vaccine. Antibody titres from patients who were vaccinated with GLA-RSV formulation were 3-fold higher in comparison with titres obtained with RSV vaccine alone (Falloon *et al.*, 2017).

Another class of TLRs is also TLR2 agonists which are very promising adjuvants for human use. This class includes bacterial and synthetic lipopeptides such as Lipoteichoic acid, MALP-2 and MALP-404 and S[2,3 bis (palmitoyloxy)propyl]cysteine (Pam_2Cys),N-α-Palmitoyl-S-[2,3-bis(palmitoyloxy)-(2RS)-propyl]-L-cysteine (Pam_3Cys) which can be conjugated or mixed with antigens providing adjuvant activity. Adjuvant activity partially involves signaling through TLR2, leading to antibody-mediated and cellular immunity. Several studies have evaluated the adjuvant activity of TLR2 on vaccines. For example, Zeng *et al.* tested the effect of lipidation of proteins on their immunogenicity. Specifically, they investigated the impact of attachment of the TLR2 Pam_3Cys to the intact hen egg white lysozyme (HEL) protein. They synthesised three different water soluble lipid moieties, $Pam_2CysSer_2Lys_8Cys$ (Lipid 1), $(Pam_2Cys)_2LysSerLysSerLys_8Cys$ (Lipid 2), $Pam_2CysSer_2PEG_{11}Cys$ (Lipid 3) and they covalently attached them with the HEL protein producing the following lipidated protein molecules: HEL-S-$(Lipid\ 1)_1$, HEL-S-$(Lipid\ 1)_2$, HEL-S-$(Lipid\ 2)_1$, HEL-S-S-$(Lipid\ 1)_1$ and HEL-S-$(Lipid\ 3)_1$. They performed *in vivo* studies on C57BL/6 mice using lipidated and non-lipidated form of HEL protein non-adjuvanted or adjuvanted with Freund's complete adjuvant (CFA) or alum and they proved that all the lipidated proteins were able to induce significantly higher anti-HEL antibody titres compared to that produced using non-lipidated proteins, with no significant differences observed between the different lipidated protein forms. Anti-HEL antibody titres obtained using lipidated HEL protein were approximately 2-fold higher than that observed using HEL in CFA and HEL alone.(Zeng *et al.*, 2011).

The same conclusions were reached by Moyle *et al*. who developed a nanoparticulate lipoprotein vaccine development platform, which enables the site-specific conjugation of TLR2 to antigens. More specifically, they conjugated three different synthetic TLR2 agonists, lipid core peptides, Pam_2Cys and Pam_3Cys to Group A Streptococcus recombinant antigens and they studied their capacity to elicit high titre antigen-specific IgG antibodies against each antigen in the polytope sequence, in order to select the optimal TLR2 agonist. Their results demonstrated that Pam_2Cys or Pam_3Cys adjuvants induced the highest antigen-specific antibody titres. Mice received vaccination with Pam_2Cys or Pam_3Cys showed 16-fold higher average J14-specific antibody levels and 2-fold higher M protein N terminal antigen-specific antibody titres, compared with the ones vaccinated with alum formulated polytope and LCP, before the final boost at day 35. In order to determine the level of antibody titres against each of the seven individual M protein N-terminal antigens in the polytope sequence, they performed ELISA using synthetic peptides corresponding to each antigen. They observed that all adjuvants produced antibodies able to target all antigens with Pam_2Cys or Pam_3Cys showing the higher average antibody titres compared to the alum and LCP groups, with no significant differences observed between these groups (Moyle *et al.*, 2013; Moyle *et al.*, 2014).

Sekiya *et al.* investigated the effect of pegylation of TLR2 Pam_2Cys on the size, activity and efficacy of formed antigen-lipopeptide complexes using OVA as model antigen. In particular, they used PEG_5, PEG_{11} and PEG_{22} to produce Pam_2Cys-PEG_5, Pam_2Cys-PEG_{11} and Pam_2Cys-PEG_{22} respectively mixing it with OVA. During their studies, they observed that inclusion of PEG into formulations increased the solubility of formulations and resulted in decreased sizes in a PEG-length-dependent manner. Their *in vivo* studies using Pam_2Cys-PEG_{11} and Pam_2Cys mixed with different doses of OVA showed that PEGylated lipopeptide induced significantly higher antibody titres at low antigen doses compared to those achieved with non-PEGylated lipopeptide suggesting that pegylation improves the ability of vaccine delivery vehicles to allow dose-sparing for antibody titres. Furthermore, they indicated that Pam_2Cys-PEG_{11} induced 3-fold higher cell-mediated CD8+ immune responses compared to Pam_2Cys when they mixed with an equal amount of OVA. Vaccination of mice with OVA formulated with Pam_2Cys resulted in increased CD8+ T cells production compared to mice vaccinated with OVA alone (2-3-fold higher). To investigate the antigen drainage to lymph nodes mediated by Pam_2Cys and Pam_2Cys-PEG_{11}, they vaccinated C57BL/6 mice with Alexa Fluor 680-labelled OVA (OVA-AF680) formulated with one

or other lipopeptide and they measured the presence of it in the lymph nodes after 6, 12 and 34 hours. They found that mice vaccinated with OVA-AF680+Pam_2Cys-PEG_{11} displayed significantly higher presence of DCs, fact that correlated with higher numbers of CD8+ T cells and higher levels of MHC Class II. These results indicated that when Pam_2Cys-PEG_{11} was used, the antigen was transported faster to the lymph nodes (Sekiya *et al.*, 2017).

CpG oligonucleotides (or CpGODN) is one of the very promising classes of TLR9 and their ability to enhance immune responses has been well documented. CpGODN are short single-stranded synthetic DNA molecules that contain a cytosine triphosphate deoxynucleotide ("C") followed by a guanine triphosphate deoxynucleotide ("G"). The "p" refers to the phosphodiester link between consecutive nucleotides, although some ODN have a modified phosphorothioate (PS) backbone instead. When these CpG motifs are unmethylated, they act as immunostimulants (Tam, 2006). They are capable of recognising highly conserved molecular structures associated with microorganisms as danger signals indicating infection and trigger vigorous immune responses. Responsiveness to CpG motifs is mediated through TLR9, a receptor localised to and signalling from the endosomal compartment of APCs, such as dendritic cells (DCs) and macrophages.

Synthetic CpGODN oligonucleotides can be divided into 4 classes based on their CpG motifs sequence, sugar, base and backbone modifications as well as secondary and tertiary structures which affect their immune modulatory properties. A-class CpGODN are characterised by a phosphodiester central CpG-containing palindromic motif and a phosphorothioate -modified 3’ poly-G string. This class is well known for the activation and proliferation of T cells and induction of high levels of IFNα and IFNγ. The main characteristic of B-class CpGODN is the full phosphorothioate backbone with one or more CpG dinucleotides. B-class CpGODN are strong stimulators of B cells with moderate effect on IFN. A combination of A-and B-class is the C-class CpGODN which combine the features of both classes inducing strong B and T cell responses. The A and C-class are expressed in different endolysosomal compartments than B-class. IRF-7 mediated signalling pathway is triggered by A and C-class CpGODN leading to strong IFN responses, in opposition to B class, which stimulate NF-κB mediated signalling pathway resulting in B cell responses (Honda *et al.*, 2005). Finally, P-class CpGODN, similarly to C-class stimulate B and T cell activation the IFN-α response being as strong as in A-class CpGODN.

TLR9 binding of CpG-containing DNA results in the induction of rapid innate immune responses to prevent or limit early infection, subsequent highly specific adaptive responses to facilitate pathogen clearance and finally, memory responses for long-lived protection. Supported by the induction of immunostimulatory T helper Th1-biasing cytokines and chemokines including interleukin (IL)-12, tumour necrosis factor alpha (TNF-α) and IFN α/β and γ, CpGs directly (i.e., APCs) or indirectly (i.e., natural killer (NK) cells and T lymphocytes) activate a variety of immune cells, ultimately resulting in enhanced immune function (Vollmer and Krieg, 2009).

De Titta *et al*. investigated the effect of CpGODN-polymeric nanoparticles conjugation on the cellular immunity. Ultra-small polymeric nanoparticles (25 nm) yielding from emulsion polymerisation of propylene sulphide with Pluronic F127 as an emulsifier, were conjugated to CpGODN class B and C via disulphide bond (van der Vlies *et al.*, 2010). *In vitro* test of the designed systems proved that NP-CpG induced enhanced maturation and up-regulation of costimulatory molecules (CD80 and CD86) on the surface of DCs compared to free CpG-B. The response to NP-CpG-B induced significantly higher levels of IL-12p70 secretion by DCs than did free CpG-B, whereas no significant differences observed between NP-CpG-C and free CpG-C. Intradermal coadministration of NP-CpG-B or NP-CpG-C with NP-OVA in mice showed that NP-CpG-B increased levels of CD4+ and CD8+ T cells responses compared with free CpG-B, when NP-CpG-C was not able to induce T cell responses *in vivo* at the adjuvant dose used. In addition, the total amount of IFNγ was enhanced 6.5-fold in mice vaccinated with NP-CpG-B compared with about a two-fold increase in mice vaccinated with free CpG-B. Challenge of vaccinated mice with E.G7-OVA tumour cells revealed that a delayed tumour onset and longer tumour-free survival were observed in mice vaccinated with NP-CpG-B conjugate compared with free CpG-B. Further studies of the same group demonstrated that both NP-CpG-B and NP-CpG-C were capable to induce 2-fold higher cytotoxicity in memory CD8+ T cells than CpG free forms. In order to determine whether NP-coupled CpG was more effective at recalling memory than free CpG, they challenged mice with B16-F10-OVA tumours 4–6 months after vaccination with free CpG-B and NP-OVA and 5 days after memory cells were recalled with various formulations. Their studies demonstrated that NP-CpG-B was the only adjuvant formulation capable of killing B16-F10-OVA tumours and prolonging survival (de Titta *et al.*, 2013).

CpGODN has been used also in conjunction with other molecules, peptides or sugars, which act as immunostimulators and immunomodulators in order to modulate immunity. Combinations of immunopotentiators are required to trigger multiple activation pathways and to elicit robust and multifunctional antitumour immune responses. Silva *et al*. investigated the efficiency of combinations of TLR agonists with ISCOMATRIX adjuvant, which composed of purified fractions of Quillaia saponaria extract (ISCOPREP saponin), cholesterol, and phospholipid, in mouse models of melanoma and pancreatic cancer. It has previously reported that the efficacy of the ISCOMATRIX-OVA vaccine as a single adjuvanted vaccine is limited in the therapeutic cancer setting of established tumours. To this end, CpGODN TLR9 and poly(I:C) TLR3 have been combined with ISCOMATRIX. Their *in vivo* studies demonstrated that mice vaccinated with ISCOMATRIX-OVA and combination of CpG, poly(I:C) showed significant tumour regression and longer survival time. On the contrary, ISOMATRIX-OVA in combination with CpG or poly(I:C) did not induce any protection to therapeutic cancer models, despite the enhancement of T cell responses obtained compared to ISOMATRIX-OVA alone (Silva *et al.*, 2015). Similar conclusions were reached by Zhao *et al*. who investigated the ability of the TLR 7/8 agonist 3M-052 and TLR9 agonist CpGODN to synergistically combine and enhance immunity. Results showed that mice vaccinated with the combination of TLR agonist completely rejected their 200 mm^3 tumours. Furthermore, double adjuvanted system led to approximately 90% reduction of tumour infiltrating mMDSK cells, which are considering an important marker of immune suppression as they suppress the activity of NK, and CTL cells. As a result, the number of NK and CTL cells increased 5-fold, fact that was consistent also with the elevated IFNγ responses obtained from restimulated splenocytes (8-fold) after treatment with CpGODN/3M-052. Finally, when large tumours were studied, therapy with combination of CpGODN/3M-052 resulted in 80-90% cure rates. In contrast, mice vaccinated with each agonist alone barely shown any tumour growth progression (Zhao *et al.*, 2014).

Kovacs-Nolan *et al*. evaluated the immunostimulatory properties of TLR9 agonist CpGODN 1826 combined with indolicidin and polyphosphazene in mice. Indolicidin is a bovine host defence peptide known for inducing expression of IL-8 in human bronchial epithelial cells. Polyphosphazene is a water-soluble polymer with high adjuvant activity, able to induce long-lasting immune responses. Their studies revealed that when CpGODN 1826 was combined with indolicidin, an enhanced, more balanced and robust immune response was obtained. Further studies with

combination of CpGODN, indolicidin and polyphosphazene demonstrated that no-significant differences were observed between the total anti-OVA igG titres in CpG/ indolicidin, CpG/polyphosphazene and CpG/indolicidin/polyphosphazene groups. Although similar trend was observed on IgG1 titres, significantly higher IgG2a antibody levels were obtained with the triple adjuvant combination. Analysis of cell-mediated responses by measurement of IFNγ, showed that 5-fold increased IFNγ secreting cells in mice vaccinated with CpG/indolicidin/polyphosphazene compared to mice vaccinated with combinations of two of the adjuvants or non-adjuvanted group (Kovacs-Nolan *et al.*, 2009).

The majority of the vaccine studies performed up to today, have used B-class CpGODN including CpG 1018, 1826, 2007 (Scheiermann and Klinman, 2014; Shi *et al.*, 2019). B-class CpGODN has been incorporated in Heplisav B[4], a prophylactic vaccine approved by the FDA in 2017. This vaccine combines the Hepatitis B surface antigen (HBsAg) with the CpG adjuvant 1018 resulting in high antigen specific antibody responses even 2 weeks after the priming dose demonstrating superiority over Engerix B[5], a currently licensed HBV vaccine adjuvanted with aluminium hydroxide (Sablan *et al.*, 2012; Janssen *et al.*, 2013; Shi *et al.*, 2019).

1.5 The role of chemical conjugation of CpGODN TLR9 agonist on protein antigens

It is proven by multiple studies that conjugation of CpG motifs with protein antigens creates a more potent immunogen compares to physical mixture of antigen with the same amount of CpG motifs corresponds to the conjugation (Datta *et al.*, 2004). As a result, this protein-CpG conjugates achieve therapeutic effect at lower doses, which is always a goal in vaccine development.

Colocalisation, antigen uptake and presentation and thus elevated immune response levels are some of the benefits of protein conjugates (Tighe *et al.*, 2000; Heit *et al.*, 2005; Kramer *et al.*, 2017). Protein-CpG conjugates can be efficiently internalised by the same DCs through endocytosis. Protein-CpG mixtures have the limitation of inconsistent colocalisation as a portion of the CpG is taken up by cells that do not come in contact with antigen, and a portion of the antigen is taken up by cells that do not come in contact with CpG.

[4] Heplisav B is a registered trademark of Dynavax Technologies Corporation.
[5] Engerix-B is a registered trademark of the GSK group of companies.

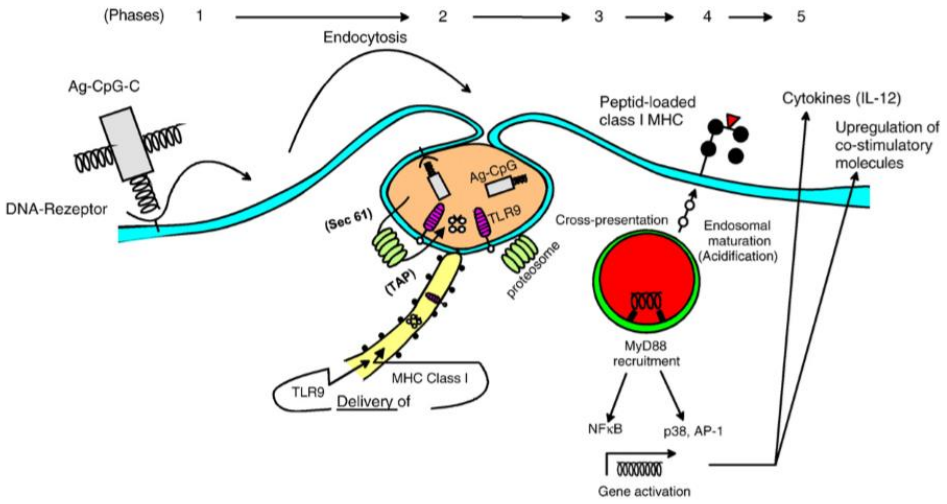

Figure 1.4 *Endosome targeting by CpGODN-antigen complexes. TLR9 signalling drives the maturation of cross-presenting DCs into professional APCs with competence for crosspriming. Phase1: CpGODNs conjugated to proteinaceous antigen (Ag) bind to a cell surface bound DNA receptor thus causing efficient endosomal translocation (via phagocytosis) of both CpGODNs (to drive TLR9 activation) as well as exogeneous Ag for TAP/proteasomal processing (Phase 2). The mechanisms controlling cross-presentation appear to operate within or in the vicinity of endosomal compartments, and are enhanced by TLR activation. Sec 61 represents a pore forming protein, TAP stands for "transporter associated with Ag processing". Phase 3: Ag becomes processed; CD8 epitopes are loaded on MHC class 1 and loaded MHC class 1 molecules (red triangles) translocate to the membrane. Upon maturation (red colour, acidification) of the endosome the CpGODN liberated from Ag activates TLR9 which causes MyD88 recruitment and thus (phase 4) activation of DC via the TLR9 signal pathway. As a consequence (phase 5) DCs mature into professional APCs by upregulation costimulatory molecules and cytokine production (Wagner, 2009).*

A plethora of studies have demonstrated the effect of protein conjugates on immunity as well as their superiority over physical mixture including asthma, infectious diseases and cancer applications. Shirota *et al*. showed that conjugating CpGODN directly to antigen can boost immunity up to 100-fold over that induced by simply mixing CpGODN with immunogen, proposing an approach for control of bronchial asthma. In particular, they designed a covalently linked CpG-antigen conjugate and examined the efficacy on airway eosinophilia. Their experiments revealed that the conjugate not only induce higher immune responses that unconjugated form but was also able to inhibit the airway hyperresponsiveness and Th2 cytokine levels. Improvement of airway eosinophilia and airway hyperresponsiveness was accompanied by a reduction in the responsiveness of Ag-specific Th2 cells in the regional lymph nodes (Shirota *et al.*, 2000). The same group in further studies, demonstrated that the increased activation of Th1 cells by CpG-antigen conjugates resulted in the enhanced antigen uptake and the coincorporation of both antigen and CpG by the same DCs (Shirota *et al.*, 2001). Similar conclusions were reached by Tighe *et al*. who evaluated the efficiency of ISS-ODN-Amb1 allergen conjugate *in vivo*. Their experiments

demonstrated that chemical conjugation of an ISS-ODN to allergen Amb a 1 enhances its immunogenicity and reduces its allergenicity. Physical mixture of Amb a1 with ISS-ODN also induced a Th1 response in mice but weaker than that induced with the corresponding conjugate. In particular, vaccination of mice with a mixture of Amb a1 and ISS-ODN induced a lower IgG2a titre and 10-fold less IFNγ than mice immunised with the conjugate. Further *in vivo* studies on rabbits and monkeys confirmed all the above (Tighe *et al.*, 2000).

Kramer *et al.* compared the *in vitro* immunostimulatory activity of CpG conjugated via either its 5′ or 3′ end to the model antigen OVA. Their results suggest that the APCs were activated to the same extent with class B CpG conjugated to OVA via either the 5′ or 3′ end or unconjugated class B CpG in the mixture with OVA. However, *in vitro* T-cell assays demonstrated that both the 5′ and 3′ CpG−OVA conjugates induced the same percentage of proliferation of CD8+ and CD4+ T-cells, which was significantly higher than the proliferation induced by the mixture of CpG and OVA and the untreated control. Further studies on the production of the proinflammatory cytokine IFNγ revealed that both the 5′ and 3′ CpG−OVA conjugates induced statistically the same level of IFNγ production in CD8+ and CD4+ T-cells, which was significantly higher than the amount of IFNγ produced in response to the mixture of CpG and OVA (Kramer *et al.*, 2017).

Maurer *et al.* explored the immunobiology of CpG-DNA conjugated soluble antigen and CpG-DNA mixed with OVA, *in vitro* and *in vivo.* Their studies demonstrated that CpGDNA-OVA conjugates were able to trigger *in vivo* peptide-specific CTL responses at 10-fold lower antigen doses compared to a mixture of CpG-DNA with OVA. In addition, they found that CpGODN covalently linked to antigen resulted in enhancement of antigen uptake yielding in efficient antigen cross-presentation by DCs and their activation into professional DCs by triggering up-regulation of the costimulatory molecules CD40 and CD86 (Maurer *et al.*, 2002). Similar conclusions were reached by Heit *et al.* who proved that CpG-OVA conjugate can be translocated to the endosome of DCs 10 to 50-fold more efficient compared to OVA alone. Upon receptor-mediated endocytosis the CpG-OVA complex becomes translocated to LAMP-1-positive endosomal-lysosomal compartments which express TLR9 and competence for cross-presentation. In contrary, cellular uptake of OVA-FITC was poor and only minute amounts of OVA-FITC were found in vesicular structures some of which colocalised with LAMP-1-positive compartments. Furthermore, they

analysed the ability of CpG-OVA complex to drive MHC class I-restricted CD8+ T cell responses and compared it with the ability of LM-OVA live vaccine. They demonstrated that single subcutaneous challenge of C57BL/6 mice with CpG-OVA complex triggered primary as well as secondary clonal expansion and contraction of SIINFEKL-specific CD8+ T cells similar in kinetic and magnitude as that observed with live vaccine LM-OVA. In contrast, a single challenge with CpG-DNA admixed to OVA failed to trigger significant clonal expansion of CD8+ T cells (Heit *et al.*, 2005).

1.6 The beneficial use of liposomes in combination with CpGODN TLR9 agonist

The efficiency of CpG oligonucleotides as TLR9 agonist has been well established along the last few years. It is proven that CpG is a potential immunotherapy for malignant, infectious and autoimmune diseases. Although CpGODN has shown promising results in preclinical studies, clinical use of CpGODN still encounters several obstacles including poor *in vivo* stability mainly due to their digestion by endonucleases, acute adverse side effects, unfavourable pharmacokinetic and biodistribution profiles and poor cellular uptake characteristics (Tam, 2006).

In an effort to overcome the aforementioned issue related to *in vivo* delivery of free CpGODN, optimised lipid based nanoparticulate carriers were developed and used in combination with CpGODN (Wilson *et al.*, 2009). Various types of liposomal CpGODN have been developed for different purposes like immunostimulation and vaccine adjuvants. Several studies have demonstrated that encapsulation or coadministration of CpG motifs into/with liposomes enhanced dramatically the immunopotency compared to free CpGODN (Kuramoto *et al.*, 2008; Erikci *et al.*, 2011; Bayyurt *et al.*, 2017; Nikoofal-Sahlabadi *et al.*, 2018).

Nikoofal-Sahlabadi *et al.* evaluated the therapeutic anti-tumour effects of cationic liposomes (DOPE: DOTAP: Cholesterol 40:40:20) containing phosphodiester CpGODN formulations in mice bearing C26 colon carcinoma or B16F0 melanoma. Their studies demonstrated that mice vaccinated with liposomes encapsulating CpGODN showed improvement in mice survival (32 days) and tumour growth delay (43%) which was comparable with the amount of these parameters in the chemotherapeutic drug Doxil used as positive control (38% and 94% for median survival time and tumour growth delay, respectively). In contrary, groups of mice vaccinated with empty liposomes or liposomes encapsulated with non-CpG had

shown minimal to zero effect on survival time and a tumour growth delay improvement of 15%, highlighting the importance of liposomes-CpG combination (Nikoofal-Sahlabadi *et al.*, 2018). Their results are in agreement with Bayyurt *et al*. who coencapsulated CpGODN TLR9 and poly(I:C) TLR3 into PC: Cholesterol neutral liposomes and they tested their efficiency on cancer models *in vivo*. They demonstrated that their liposomes-CpG formulations were able to provide long lasting antigen specific humoral and cellular immunity capable of preventing E.G7 tumour development. Specifically, a 5-fold tumour size reduction was observed in mice vaccinated with liposomes encapsulating CpG, poly(I:C) and OVA 14 days after inoculation (Bayyurt *et al.*, 2017).

Erikçi *et al*. demonstrated that encapsulation of CpG motifs into liposomes have a significant impact on the elicited immune responses. Two types of CpG motifs, A and B-class (D and K-type, respectively), were encapsulated within five different kinds of liposomes possessing different surface charge, lamellarity and size. The efficiency of the designed formulations was evaluated *in vitro* and *in vivo*. Their studies proved that when the TLR9s CpG was used in combination with liposomes, the IFNγ and IL-6 production was augmented significantly compared to the free CpGs and liposomes form. In addition, coencapsulation of the model antigen OVA with B-class CpGODN adjuvant in anionic liposomes induced 150-fold higher antigen specific antibody titres over free antigen-CpG mixture, after primary vaccination. After a boost immunisation, a 22-fold increase on the IgG titres was noted when anionic liposomes formulations was used compared to simple mixture of CpG and OVA. Similar conclusions were reached when they analysed the IFNγ levels production after stimulation of splenocytes with OVA, indicating that incorporation of anionic liposomes induced strong humoral and cell mediated anti-OVA specific immune compared to OVA+CpG physical mixture (Erikci *et al.*, 2011).

Kuramoto *et al.* tested the antitumour activity of lipoplex formulations composed by the chemically modified phosphorothioate (PS)-CpG DNA or natural phosphodiester (PO)-CpG DNA with DOTMA/cholesterol cationic liposomes (PS-CpG DNA-lipoplex and PO-CpG DNA-lipoplex prepared in 5% dextrose solution) in a peritoneal dissemination mice model. PS-CpG DNA-lipoplex inhibited the proliferation of tumour cells more effectively compared to PO-CpG DNA-lipoplex after intraperitoneal administration in a CpG DNA dose-dependent manner. However, both formulations were more effective than 5% dextrose, naked PS-CpG DNA, and naked PO-CpG

DNA. It has been observed also that TNF-α production from PS-CpG DNA-lipoplex-treated cells was significantly higher than that from PO-CpG DNA-lipoplex. In contrast, no TNF-α production was observed after treatment with a CpG-free formulation indicating the impact of TLR9 CpG on the response. Finally, Kuramoto *et al.* underlined the contribution of cationic liposome formulations showing that naked PS-CpG DNA or PO-CpG DNA failed to inhibit the proliferation of tumour cells in the mouse peritoneal dissemination model as naked formulations were not able to be distributed to the lymph organs (Kuramoto *et al.*, 2008).

1.7 Model diseases

1.7.1 Diphtheria toxin

Diphtheria is caused by infection with the Gram-positive bacillus *Corynebacterium diphtheriae,* which carries a lysogenic bacteriophage containing the gene coding for diphtheria toxin (Kabanova and Rappuoli, 2011). Yersin and Roux were the first to show that an extracellular toxin, diphtheria toxin secreted by *Corynebacterium diphtheriae* is responsible for toxicity. The formaldehyde-treated detoxified form of diphtheria toxin, diphtheria toxoid, has been successfully used for mass vaccination making diphtheria toxin a rare disease nowadays (Malito *et al.*, 2012).

A major contribution to the understanding of the mode of action of DT was the discovery of mutated forms in the early 1970s. These proteins were called cross-reacting material (CRM), since they were immunologically related to diphtheria toxin. CRM197 is the most popular mutant obtained. It is an enzymatically inactive and nontoxic form of diphtheria toxin, that contains a single amino acid substitution from Glycine to Glutamate in position 52 (Giannini *et al.*, 1984; Malito *et al.*, 2012). Subsequently, CRM197 was found to be an ideal carrier for conjugate vaccines against encapsulated bacteria. Today CRM197 is the carrier for licensed conjugate vaccines against *Haemophilus influenzae*, pneumococcus, and meningococcus, and is used to vaccinate most children globally (Kabanova and Rappuoli, 2011).

1.7.2 Meningitis serogroup B

Meningitis is characterised by an acute inflammation of the protective membranes covering the brain and spinal cord, collectively known as meninges (Saez-Llorens and McCracken, 2003). The inflammation is characterised by an abnormal number of white blood cells (WBCs) in the cerebrospinal fluid (CSF) and is typically caused by infection with viruses, bacteria, or other microorganisms. The types of bacteria vary

according to the infected age group. Neisseria meningitidis, a Gram-negative diplococcus pathogen, is the most common cause of meningitis in children and young adults, and is associated with an overall mortality rate of 3–13% (Schuchat *et al.*, 1997).

Virulent strains of *Neisseria meningitidis* have a polysaccharide capsule, which is the major virulence factor for this bacterium. Thirteen serogroups have been identified based on the biochemical composition of their polysaccharide capsule. Among them, six (A, B, C, W-135, X, and Y) are responsible for the majority of the cases of meningococcal disease occurred worldwide. Meningococci of serogroups B, C and Y are the most common causes of the disease in the USA (Nudelman and Tunkel, 2009). Before of the introduction of meningococcal vaccination it was estimated that, serogroup C caused 35%, serogroup B caused 32% and serogroup Y caused 26% of the cases occurred (Rosenstein *et al.*, 1999). In total, meningococcal disease in the USAaffects around 3,000 people each year, with the highest incidence in children younger than 2 years. In case of UK, serogroup B infection has been the most common cause of bacterial meningitis. It is estimated that about 3,200 people get bacterial meningitis and associated septicaemia each year in UK (Meningitis Research Foundation, 2017). Sub-Saharan Africa has one of the world's greatest disease burdens caused by the meningeal pathogens. During the past 10 years, *Neisseria meningitidis* was responsible for recurrent epidemics of meningitis that accounted for approximately 700,000 cases with serogroups A and X being the most common in this region (Centers of Disease control and Prevention, 2009). In recent years, considerable progress has been made in understanding the pathogenetic and pathophysiological mechanisms of meningococcal disease (Tunkel and Scheld, 1993; van de Beek *et al.*, 2012).

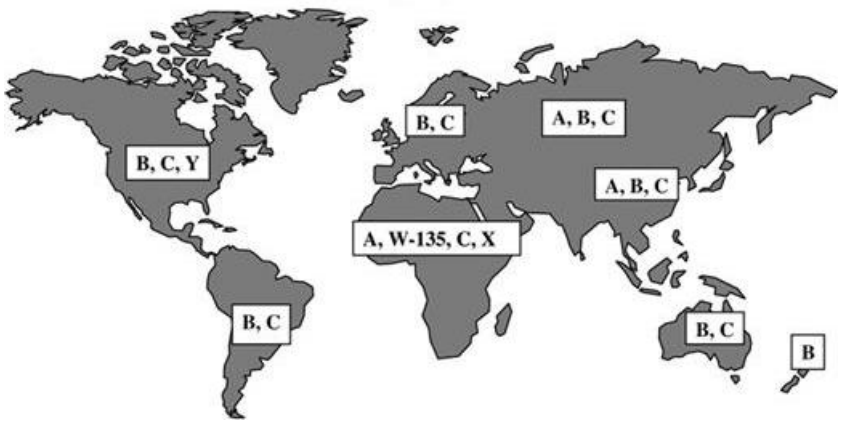

Figure 1.5 *Global meningococcal serogroup distribution (Stephens et al., 2007).*

Bacterial meningitis ensues when bacteria overcome the defence mechanisms of host. More specifically, bacterial meningitis occurs when bacteria sequentially colonise host mucosal epithelium, invade and survive in the intravascular space, cross the blood–brain barrier, and survive in the CSF(Quagliarello and Scheld, 1992). The expression of the subcapsular surface components such as the pneumococcal cell walls and lipopolysaccharide of bacteria, important bacterial virulence factors of meningitis, helps bacteria overcome host defences and allow the pathogen to enter the central nervous system leading to influx of leukocytes. Studies showed that bacterial meningitis is characterised by pleocytosis of theCFS, consisting predominantly of polymorphonuclear leukocytes (Zwijnenburg *et al.*, 2006).

Research supports that Gram-negative bacteria induce inflammation through the local central nervous system releasing inflammatory mediators such as IL-1, IL-6, TNFand prostaglandins (Nudelman and Tunkel, 2009). Inflammatory mediators increase leukocyte influx, blood-brain barrier permeability and brain oedema, which may correlate with morbidity and mortality in patients with bacterial meningitis. Experiments demonstrated that inoculation of IL-1 and TNF-α within CSFof rats induced meningeal inflammation and blood-brain barrier injury. In addition, inoculation of a combination of the cytokines into CSFresulted in a synergistic inflammatory response manifested by a more rapid and significantly increased influx of white blood cells into the CSF(Ramilo *et al.*, 1990; Quagliarello *et al.*, 1991; Hoffman and Weber, 2009).

The increase of the CSFvolume and the increase in the water content of the brain, which occurs due to cerebral oedema, are directly related to an increase of intracranial pressure. Intracranial pressure often increases in patients with bacterial

meningitis. Moreover, cerebral oedema leads to alterations in cerebral blood flow, which are intimately related to the loss of cerebrovascular autoregulation, such that cerebral blood flow fluctuates directly with the mean arterial blood pressure (Pfister *et al.*, 1990; Tureen *et al.*, 1990; Quagliarello and Scheld, 1992). Decrease on the arterial blood pressure can cause parallel decreases in cerebral blood flow and reduce oxygen delivery to the brain leading to death due to hyperperfusion or hypoperfusion of the brain.

1.7.2.1 Treatments for Meningitis

The type of meningitis treatments hinges on several factors including the stage of disease, the age and the overall health of the patient. If the disease is detected at an early stage, before sepsis is identified, empirical antibiotic therapy usually consists since effective antibiotics immediately stop the proliferation of *Neisseria meningitidis*. In contrast, targeted antibiotic therapy is used when the patient is diagnosed with purulent meningitis. The antibiotic therapy can include benzylpenicillin, ampicillin, cefotaxime, vancomycin and third-generation cephalosporin, which are effective antibiotics, and the selection of them based on the specific isolated pathogen. The administration should be intramuscular in children and intramuscular or intravenous in adults. The duration of the therapy is usually 7-10 days.

Adjunctive dexamethasone therapy recommended to patients with acute bacterial meningitis. This therapy applied in combination with the antimicrobial therapy. Corticosteroids are administrated before or with the first dose of the antibiotics. Although the small reduction of morbidity and mortality in high-income countries due to adjunctive dexamethasone therapy, there is no clear evidence of the benefit of the use of it in patients with meningococcal disease in low-income countries (Tunkel *et al.*, 2004). In addition, several studies indicated that experts have concerns about the use of adjunctive dexamethasone with antibiotics as dexamethasone can significantly reduce the antibiotic penetration into CSFand delay CSFsterilisation (Ricard *et al.*, 2007).

The epidemiology of bacterial meningitis has significantly changed the last decades due to vaccination. The overall mortality of meningococcal disease prior to passive immunity or antibiotic treatment was 70-85% (Flexner, 1913). Fortunately, the introduction of effective conjugate vaccines against the common meningococcal pathogens led to the reduction of the case fatality rate in many countries. Conjugate

vaccines are composed of carrier proteins that are covalently linked to a polysaccharide component of the pathogen. They are safe and their use is recommended also for young children. They facilitate a T-cell-dependent antigen response leading to immunological memory (Nudelman and Tunkel, 2009).

Vaccines against some of the main serogroups have been licensed. There are currently three vaccines available in the USA and other countries to prevent meningococcal disease, all quadrivalent in nature, targeting serogroups A, C, W-135, and Y: two conjugate vaccines (MCV-4), Menactra[6] and Menveo[7], and one polysaccharide vaccine (MPSV-4), Menomune[8].

Sanofi Pasteur licensed the first meningococcal conjugate vaccine (MCV-4), Menactra, in the USA in 2005; Novartis (currently GlaxoSmithKline) licensed Menveo in 2010. The FDA has approved both MCV-4 vaccines for people 2 to 55 years old. Menactra received FDA approval for use in children as young as 9 months in April 2011 while Menveo received FDA approval for use in children as young as 2 months in August 2013. The CDC has not made recommendations for or against its use in children less than 2 years. These vaccines have been very effective for the control of meningococcal serogroup C as it has been nearly eliminated in high-income countries. Example is the significant decrease of the rate of serogroup C disease in UK after the introduction of the vaccine to all children and young adults in 2000. Meningococcal polysaccharide vaccine (MPSV-4), Menomune, produced by Sanofi Pasteur and has been available since the 1970s. It may be used if MCV-4 is not available, and is the only meningococcal vaccine licensed for people older than 55. It is recommended for people who have not received MenACWY previously and require one single dose as travellers.

Two other vaccines, Mencevax[9] and Nimenrix[10] were licensed by GlaxoSmithKline. Mencevax is a single-dose meningococcal ACWY unconjugated polysaccharide vaccine used to control outbreaks of meningococcal infection and for travellers in countries where the disease is endemic or highly epidemic. Mencevax is indicated for use across all age groups from 2 years of age, and is currently registered and approved in 78 countries across Africa, Asia, Australia, Europe, Latin America, Middle

[6] Menactra is a registered trademark of Sanofi Pasteur Inc.
[7] Menveo is a registered trademark of GSK group of companies.
[8] Menomune is a registered trademark of Sanofi Pasteur Inc.
[9] Mencevax is a trademark of Pfizer Inc.
[10] Nimenrix is a trademark of Pfizer Inc.

East and New Zealand. Nimenrix is a single-dose quadrivalent conjugate vaccine against serogroups A, C, W-135, and Y. It is indicated for all age groups above one year of age and it is currently available in 63 countries across the European Economic Area.

The greatest challenge in vaccine development was the design of vaccine for Meningococcal serogroup B (MenB). It is known that MenB polysialic acid and polysialic acid found on neural cell adhesion molecules are structurally identical. Thus, it has been proposed that infection with MenB or vaccination with polysialic acid may be associated with subsequent autoimmune. As a result, new strategies were evaluated for the design of an effective vaccine for MenB. In 2000, Rino Rappuoli introduced the use of reverse vaccinology against serogroup B meningococcus. The method based on the scanned sequence of MenB genome for the identification of potential antigens. Six hundred antigens were identified which then were tested *in vitro* and *in vivo* for their ability to induce immune response. They discovered that a number of surface-exposed proteins in combination with the outer membrane proteins adjuvants, were able to induce high levels of immune response. These novel proteins provided an optimal basis for the development of a novel and effective vaccine against MenB (Rappuoli, 2000).

Since then, new vaccines have been developed based on protein antigens, with the capacity to protect against MenB. 4CMenB (Bexsero[11]; GlaxoSmithKline, UK) has been approved for use in more 37 countries including Europe, Australia, Canada, Chile, Colombia, and Uruguay and is recently approved in the USA (Nolan *et al.*, 2015). 4CMenB vaccine contains four major antigenic components: Neisseria adhesin A (NadA), Neisseria heparin-binding antigen (NHBA) fused with GNA1030 and factor H-binding protein (fHbp) fused with GNA2091 and New Zealand NZ98/254 strain outer membrane vesicles (NZ OMV) with PorA 1.4 (Medini *et al.*, 2015).

[11] Bexsero is a trademark of the GSK group of companies.

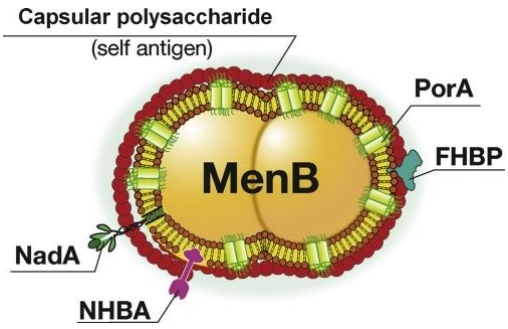

Figure 1.6 *Composition of Bexsero vaccine (Rappuoli et al., 2011).*

Several studies have contributed to the elucidation of the functional role of each of the vaccine components. NadA is a surface exposed trimeric protein which belongs to the class of trimeric autotransporter adhesins. It is present in approximately 50% of pathogenic meningococcal isolates and is associated mostly with strains that belong to three of the four hypervirulent serogroup B lineages (Malito *et al.*, 2014). There are two genetically distinct groups of NadA. Group I includes NadA 1, NadA 2 and NadA 3 variants, which are the most common. NadA 4, NadA 5 and NadA 6 constitute group II and are rarer. NadA 3 is the variant included in Bexsero vaccine. It is proven that NadA expressed on the surface of *Escherichia coli* promotes adhesion to and invasion of Chang epithelial cells (Capecchi *et al.*, 2005; Bambini *et al.*, 2014). NadA presents a tripartite structural organisation with an N-terminal globular domain ('head' domain), an intermediate α-helix region with high propensity to form coiled-coil structures (coiled-coil 'stalk') and a conserved C-terminal membrane anchor domain (Comanducci *et al.*, 2002). Epitope mapping studies showed that the head of NadA3 contains immunogenic regions responsible for the generation of a protective bactericidal response (Malito *et al.*, 2014). Up to today, NadA is the most well characterised and known antigen between the ones included in Bexsero and for this reason has been selected as model antigen for this study.

Neisseria heparin-binding antigen (NHBA), also known as GNA2132 is a surface-exposed lipoprotein, which is present in all the meningococcal strains. NHBA binds heparin and heparin sulphate structures through a conserved Arg-rich region that is the target of human lactoferrin and meningococcal NaIP proteases (Esposito *et al.*, 2011; Vacca *et al.*, 2016). NHBA is able to induce antigen-specific bactericidal antibodies in animals and humans.

Factor H-binding protein (fHbp) is a surface-exposed lipoprotein that binds human complement factor H, which is key regulator of the alternative complement pathway

that helps the organism evade host innate immunity (Mascioni *et al.*, 2009; Malito *et al.*, 2013; McNeil *et al.*, 2013). fHbp is present in the vast majority of circulating meningococcal strains and is classified in three main variant groups (1, 2 and 3) or two subfamilies (A and B) with poor cross protection. Clinical trials have shown 4CMenB to induce bactericidal antibody responses against meningococcal antigens in a high proportion of infants, adolescents, and adults, with an acceptable tolerability profile (Masignani *et al.*, 2003; Fletcher *et al.*, 2004).

Another vaccine, rLP2086 (Trumenba[12]; Pfizer Inc, US), has been licensed recently with promising results. Bivalent rLP2086 vaccine contains two variants of the meningococcal surface protein factor H-binding protein (fHbp): Variant A05 (or 3.45) from fHbp subfamily A and variant B01 (or 1.55) from subfamily B (Taha *et al.*, 2017). The efficacy of rLP2086 has been broadly reviewed and recognised in many countries around the world. Previous clinical studies demonstrated the safety, tolerability, and immunogenicity of bivalent rLP2086 in children, adolescents and young adults (Richmond *et al.*, 2012; Marshall *et al.*, 2013).

1.7.3 *Streptococcus agalactiae* or Group B Streptococcus (GBS)

Group B Streptococcus (GBS) or *Streptococcus agalactiae* are Gram-positive, β-hemolytic, chain-forming cocci that are normal residents of the vaginal flora in 25% of healthy women (Rajagopal, 2009) . GBS can convert from the asymptomatic mucosal carriage state to a bacterial pathogen causing infections in pregnant women and newborns. The main transmission of GBS is the maternal colonisation leading to serious neonatal infections like meningitis, sepsis and pneumonia. By 1970s, GBS emerged as leading cause of neonatal mortality and morbidity in USA (Dermer *et al.*, 2004). By the 1980s, it was estimated that neonatal infections caused by GBS had an incidence of 0.5–2 per 1000 live births, a mortality rate of 20–25% and permanent neurologic sequelae in the majority of survivors (Schuchat, 1999; Nuccitelli *et al.*, 2015).

[12] Trumenba is a registered trademark of Pfizer Inc.

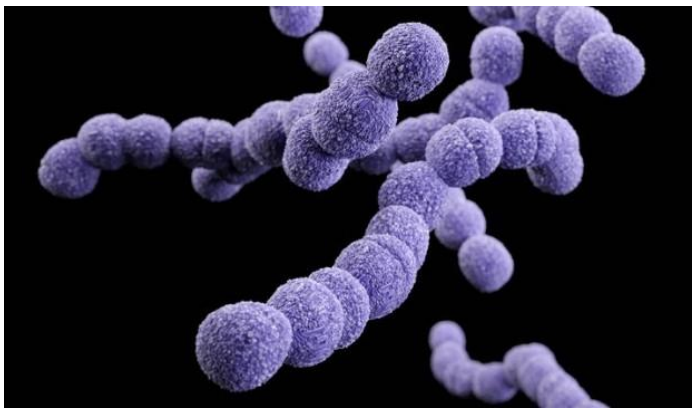

Figure 1.7 *GBS bacteria morphology (Center for disease control).*

GBS disease in neonates is classified into two categories: the early-onset disease (EOD) and the late-onset disease (LOD). EOD refers to the disease develops within the first week after birth and can spread during birth through neonatal aspiration of contaminated amniotic or vaginal fluids. EOD manifests as respiratory failure and pneumonia that rapidly progresses into bacteremia and septic shock syndrome. LOD develop between the 7th day of birth and 2 or 3 months of age. Although the route of LOD is not fully understood, it is suggested that result primarily from transmission after birth, either from the mother (contaminated breast milk) or other sources (nosocomial transmission) (Zimmermann *et al.*, 2017). LOD present often with meningitis. Globally, over the same 20-year period, the incidence of GBS LOD has remained relatively steady with 0.3–0.4 cases per 1000 live births and GBS remains the most important cause for neonatal meningitis in children aged less than 5 years.

GBS has also emerged as an important cause of invasive infections in non-pregnant adults, particularly among the elderly (>65 years). Susceptibility to GBS is increased in the elderly and immunocompromised individuals with underlying conditions such as diabetes, cancer, and HIV. Clinical manifestations of adult GBS infection are varied and include skin, soft tissue and urinary tract infections, bacteremia, pneumonia, arthritis and endocarditis. The case fatality rate for GBS infection in elderly adults is estimated at 15% in the USA and is significantly higher than in neonates.

Capsular polysaccharide is one of the main virulence factors of GBS and has been extensively studied for many years. Variation in polysaccharide composition corresponds to strain classification and serotypes. At present, as many as 10 serotypes (Ia, Ib, and II–IX) are recognised. In the 1970s, serotype III GBS (GBSIII) was the dominant cause of neonatal disease, but over time GBSIa, GBSII, and GBSV

have increased in prominence as well. The distribution and predominance of certain serotypes is susceptible to variations and can change over time. Serotypes Ia, Ib, II, III, and V are prevalent colonisers in the USA and Europe (Johri *et al.*, 2006; Ippolito *et al.*, 2010; Lamagni *et al.*, 2013; Melin and Efstratiou, 2013; Fabbrini *et al.*, 2016). Serotypes VI and VIII are the most prevalent among pregnant women in Japan (Lachenauer *et al.*, 1999; Matsubara *et al.*, 2002) while serotypes IV and V predominate in the United Arab Emirates and Egypt, respectively (Shabayek and Spellerberg, 2018; Raabe and Shane, 2019). The most recently characterised novel GBS serotype IX was reported from Denmark (Slotved *et al.*, 2007; Schrag and Verani, 2013).

1.7.3.1 Treatments for GBS

The treatment provided relies on the stage of the disease and most importantly to the age of the patient. EOD may be prevented by intrapartum antibiotic prophylaxis (IAP). IAP refers to the antibiotics administration given intravenously to the mother during labour. Peripartum antibiotic prophylaxis has markedly decreased the incidence and case fatality rate of EOD from 1.8 cases/1000 live births in the early 1990s to 0.26 cases/1000 live births in 2010 as it was demonstrated from clinical trials in USA (Landwehr-Kenzel and Henneke, 2014). Despite the success of intrapartum antibiotic prophylaxis in prevention of mother–infant transmission of GBS, rates of GBS-related stillbirths, prematurity and LOD have not decreased. No prevention strategy is currently totally effective in the eradication of EOD and, most important, IAP has had no impact on LOD where the burden is still substantial.

In 2010, American College of Obstetricians and Gynecologists (ACOG), CDC and the American Academy of Pediatrics (AAP) issued updated guidelines recommending a universal culture-based screening for pregnant women at 35–37 weeks of pregnancy in order to limit IAP to a certain risk group. The screening-based approach is recommended in the US, Japan and a number of European countries (Belgium, France, Germany, Italy, Poland, Spain and Switzerland). At the moment there is no routine GBS screening in UK. Based on the NHS guidelines, as 3 to up in 10 women carry GBS, routine screening mean that a high number of pregnant women would be given high dose of antibiotics that may not need. The antibiotic administration during pregnancy also is associated with safety concerns as the exposure of babies to antibiotics in their early lives may have other effects.

In addition, the recent emergence of antibiotic-resistant GBS strains, particularly those resistant to penicillin, imposes a significant threat to the successful treatment of infections. Also, GBS resistance to clindamycin and erythromycin has already affected IAP options for penicillin allergic women. It is reported that of clinical GBS isolates, 20% are resistant to clindamycin and 30–40% to erythromycin (Castor *et al.*, 2008). The evolution of clinically meaningful resistance among GBS to the beta lactams would jeopardise IAP effectiveness and also affect treatment of invasive infections. Taking into consideration all the above limitations of current guidelines, the need for the development of alternate prevention and therapeutic measures is reinforced (Rajagopal, 2009).

The ability of GBS to cause neonatal invasive infections is dependent on the maternal antibody titre. Early work done by Rebecca Lancefield in the 1930s (Lancefield, 1938) reported protection against GBS infection in mice by CPS-specific antiserum in rabbits. Baker and Kasper (1976) demonstrated an inverse association between the levels of maternal serotype-specific capsular antibodies and the increased susceptibility to invasive GBS disease in newborns. This association was confirmed in later investigations (Lin *et al.*, 2001; Lin *et al.*, 2004; Baker *et al.*, 2014). Vaccination seems, therefore, to be an effective strategy to protect neonates against GBS infection.

Many candidate vaccines have been tested in clinical trials or are still under pre-clinical trials. A monovalent conjugate vaccine has been evaluated in clinical trials I and II demonstrating immunogenicity and safety in a satisfactory level. However, this monovalent vaccine is not capable enough to provide protection against multiple GBS serogroups as it was proven later. Thus, multivalent vaccines have been arisen as an alternative able to offer broader vaccine coverage. An example is the pentavalent vaccine based on serotypes Ia, Ib, II, III, V which is currently under pre-clinical trials (Kobayashi *et al.*, 2016).

At present there is no licensed vaccine to prevent GBS. Current strategies have focused on the development of effective vaccines for prevention of GBS infection. A trivalent (serotypes Ia, Ib and III) GBS conjugated to CRM197 vaccine developed by Novartis (currently GlaxoSmithKline), has been evaluated in phases I and II clinical trials in pregnant South African women in order to stimulate production of functionally active antibodies that can cross the placenta and provide protection (Chen *et al.*, 2013). The results demonstrated that the investigational GBS vaccine used showed

an acceptable tolerability profile and was immunogenic with antibody transfer rates to infants in line with those reported for other vaccines targeting polysaccharides (Madhi *et al.*, 2016). A phase III clinical trial is currently under consideration (Madhi *et al.*, 2013). In 2017, Pfizer started to evaluate a pentavalent GBS PCV targeting Ia, Ib, II, III, and V in a phase I trial on healthy volunteer. Despite the promising result from the clinical trial, recent change of serotype distribution worldwide requires the replacement of old serotypes, or the addition of new serotypes in the GBS PCV (Lin *et al.*, 2018).

Pilus proteins have been identified through reverse vaccinology as promising vaccine candidates as they play a key role in the adhesion and attachment of Gram-negative and Gram-positive pathogens to host cells (Margarit *et al.*, 2009). Three pilus variants (PI-1, PI-2a and PI-2b) are present in the human GBS pathogen. GBS67 is one of the model antigens used in this study. GBS67 is an ancillary highly conserved three-domain protein of pilus 2a, which contributes to bacterial adherence to respiratory and intestinal epithelial cells, and to biofilm formation (Rosini *et al.*, 2006; Nobbs *et al.*, 2008; Sharma *et al.*, 2013; Nilo *et al.*, 2015).

1.8 Aim and objectives of the project

The aim of this thesis was to develop a novel nanotechnology-based vaccine delivery system for enhanced immune responses. Building on the previous work in this field, the use of liposomes in combination with a TLR agonist, was investigated for the development of a new effective adjuvanted vaccine system using different proteins as model antigens (CRM197- a non-toxic mutant of diphtheria toxin, NadA-Meningococcal serogroup B protein antigen, GBS67- Group B Streptococcus pilus protein). This novel system combines the use of delivery systems and immunopotentiators, two different approaches which have been investigated by many groups for generating next generation adjuvants. Delivery systems help to improve the uptake and presentation of antigens, and immunopotentiators help to activate the innate immune system, with the combination of both approaches providing the best opportunity to produce highly potent vaccines. In addition, significant improvement of immune responses is associated with the use of antigen-adjuvant conjugates making conjugates technology platform extremely promising for the development of next generation vaccines. Our working hypothesis is that conjugation of TLR agonist to a protein could favour presentation to the TLR and liposome could in turn further enhance the multivalent antigen-TLR agonist presentation resulting in enhanced immunogenicity. To achieve this aim, the objectives of the work were the following:

1. The development of antigenic protein-TLR agonist conjugates
2. The manufacturing of DSCP:Cholesterol:DDA cationic liposomal formulations
3. The surface association of protein conjugate on liposomes
4. To evaluate the immunological efficiency of the designed system *in vivo*
5. To investigate the pharmacokinetics properties of the designed system

Chapter 2 Conjugation of TLR2 agonist Pam_3Cys on model protein

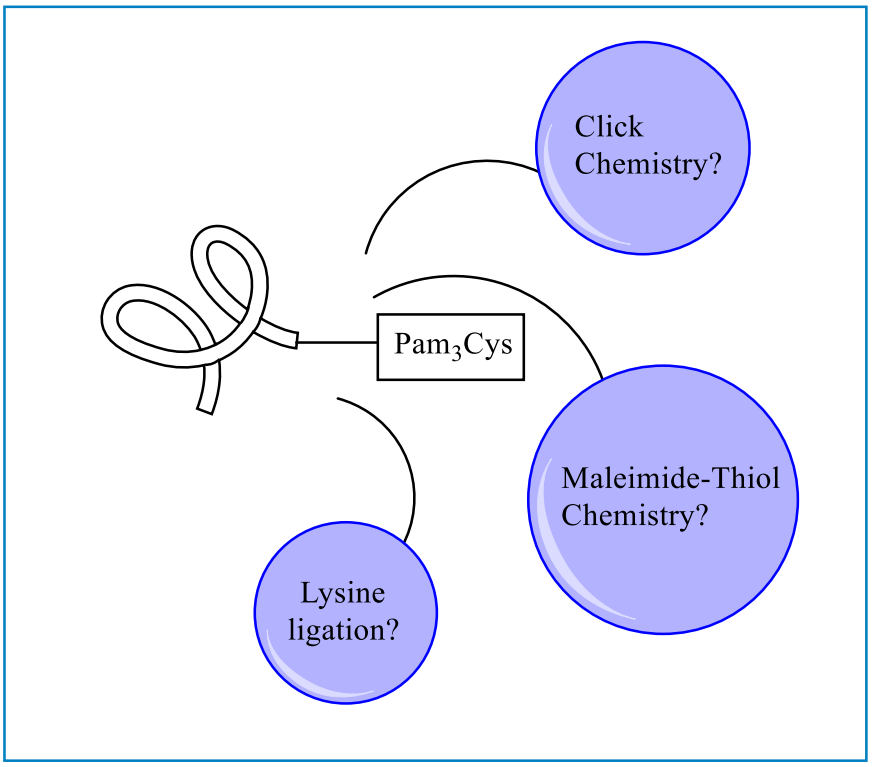

2.1 Introduction

TLR2 ligands can elicit antigen-specific cellular and antibody-mediated immune responses. Clinical trials have demonstrated that these molecules promote rapid activation of innate immunity through induction of inflammatory cytokines and upregulation of costimulatory molecules, effect that subsequently leads to effective immunity. Thus, TLR2 ligands represent a very promising class of adjuvants for human use.

The selection of TLR2-targeting adjuvants for subunit vaccines has focused on bacterial lipopeptides and their synthetic analogues Pam_2Cys and Pam_3Cys. These lipid moieties have been studied extensively coadministrated or conjugated to antigens and other adjuvants demonstrating substantial potential as vaccine adjuvants (Zaman and Toth, 2013). Despite their adjuvant activity, these molecules are very hydrophobic due to their lipid nature, thus their use is more challenging.

2.2 Aim and objectives

The aim of the work described in this chapter was the conjugation of a model carrier protein (CRM197- a non-toxic mutant of diphtheria toxin) with the TLR2 agonist Pam_3Cys in order to design a novel non-viral vaccine delivery system with upgraded therapeutic efficacy. The research herein suggests the use of lipopeptide Pam_3Cys in vaccine protein-based delivery systems as immunostimulant. This TLR agonist selected for this work was based on previous investigations, which proved the efficiency of it to augment immune responses (Moyle *et al.*, 2013; Moyle *et al.*, 2014). To achieve this aim, the objectives were:

1. The synthesis of protein conjugated to Pam_3Cys TLR2 agonist
2. The confirmation of the designed system
3. The characterisation of the protein conjugate

2.3 Materials

Table 2.1 lists the materials used within this work.

Table 2.1 *List of materials.*

Material	**Supplier**
CRM197	GSK, Siena, Italy
EDC ($C_8H_{17}N_3 \cdot HCl$)	Sigma Aldrich, UK
endo-BCN-PEG8-NHS ester ($C_{34}H_{54}N_2O_{14}$)	Broadpharm, USA
EMCS ($C_{14}H_{16}N_2O_6$)	Sigma Aldrich, Italy
N_3-PEG10-NH_2 ($C_{22}H_{46}N_4O_{10}$)	Broadpharm, USA
Pam_3Cys ($C_{54}H_{103}NO_7S$)	Sigma Aldrich, Italy
p-nitrophenol ($O_2NC_6H_4OH$)	Sigma Aldrich, Italy
SH-PEG7-NH_2 linker	Sigma Aldrich, Italy
SBAP ($C_9H_{11}N_2O_5Br$)	Sigma Aldrich, Italy
Sinapinic acid	Sigma Aldrich, Italy
TCEP 0.0005 M solution	Sigma Aldrich, Italy

2.4 Methods

2.4.1 Conjugation of Pam_3Cys on protein using PEG as crosslinker

The synthesis of the Pam_3Cys-protein system was done based on a similar way to previously reported (Zeng *et al.*, 2002; Moyle *et al.*, 2013; Moyle *et al.*, 2014). The synthesis is composed of 3 reaction-steps. The reactions scheme is shown in Figure 2.1.

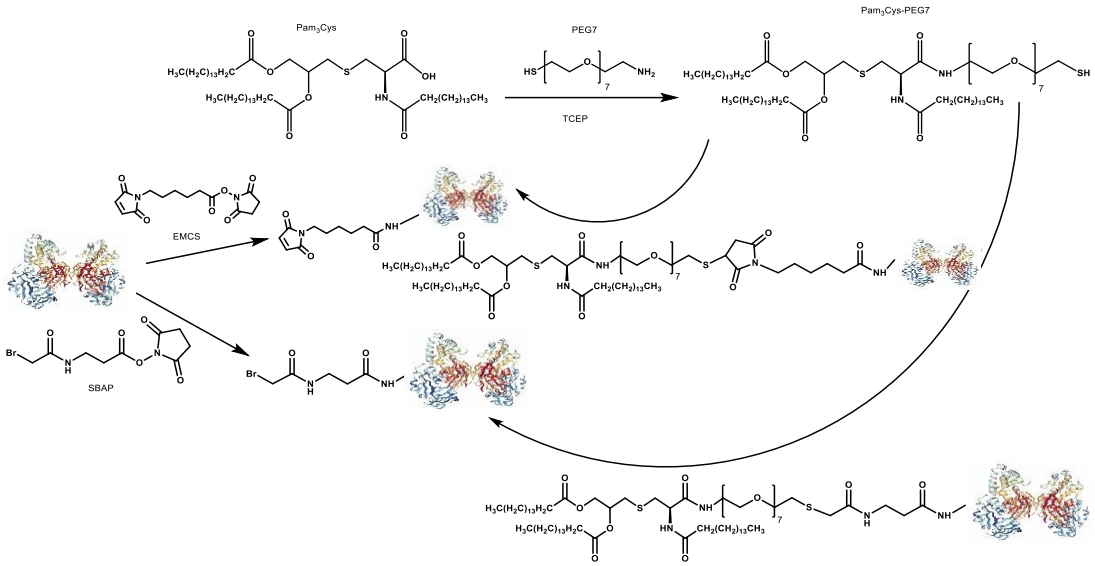

Figure 2.1 *Reaction scheme for conjugation of Pam₃Cys on protein. Pam₃Cys was modified with SH-PEG7-NH₂ for the introduction of sulphide group. Model protein was modified with EMCS and SBAP linkers for the introduction of a maleimide moiety and bromoacetyl group, respectively. Sulfhydryl group in the Pam₃Cys-PEG7 reacts with maleimide and bromoacetyl group in slightly acidic environment (pH range 6.5-7.5) and basic environment (pH>7.5), respectively forming a stable thioether linkage.*

2.4.1.1 Modification of Pam_3Cys with PEG7 linker

For the synthesis of Pam_3Cys-protein construct, the modification of the Pam_3Cys was necessary, so as to be able to further conjugate this with the model protein. For the purpose of this conjugation, a SH-PEG7-NH_2 linker was added on Pam_3Cys for the introduction of sulphide group for subsequent coupling to the protein. In particular, the primary amine group on SH-PEG7-NH_2 will be conjugated with the activated with p-nitrophenol carboxyl group on Pam_3Cys. The reactions scheme is presented in Figure 2.2.

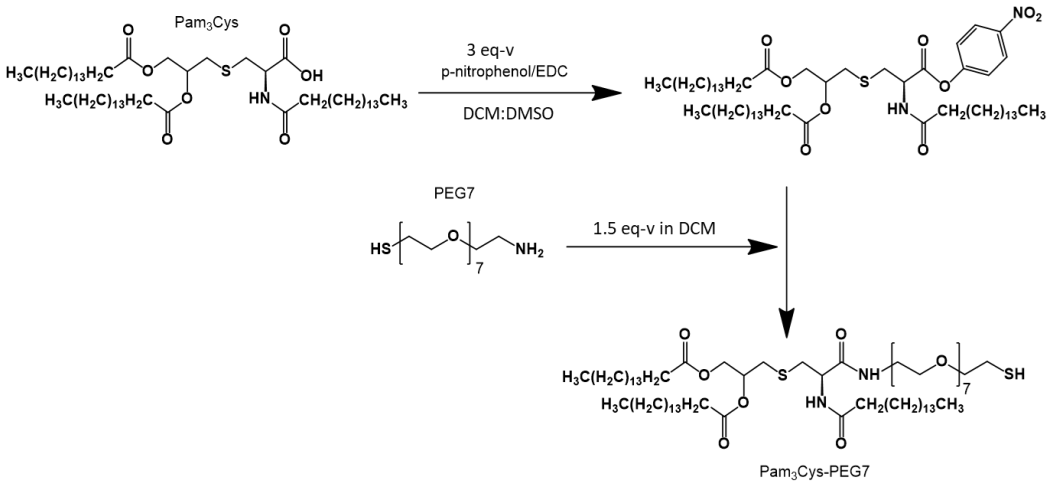

Figure 2.2 *Reaction scheme for modification of Pam₃Cys with PEG7.*

An amount of 10 mg (11.1 µmol) of Pam_3Cys (MW 910.46) were mixed with 3 eq-v (6.38 mg, 33.3 µmol) EDC (MW 191.70) and 3 eq-v (4.63 mg, 33.3 µmol) molar excess p-nitrophenol (MW 139.11) in 1 mL of DCM. The reaction was incubated for 30 minutes under continuous mixing at room temperature (RT). The activation of carboxyl group on Pam_3Cys was assessed by Thin Layer Chromatography (TLC).

An amount of 1.5 eq-v (7 mg, 16.5 µmol) molar excess of NH_2-PEG7-SH (MW 422) was dissolved in 0.2 mL of DCM. The PEG7 solution was added to the Pam_3Cys-p-nitrophenol reaction mixture under an inert nitrogen atmosphere for preventing the reaction of components with air. A quantity of 5 µL of triethylamine was also added to the reaction mixture. Reaction was stirred for 24 hours at RT. The reaction mixture was purified by gel filtration for removing of excess reactants. Success of the reaction was assessed by ^{1}HNMR spectroscopy. Finally, ESI-MS was performed in order to determine the exact molecular weight of the product.

2.4.1.2 Modification of protein with EMCS and SBAP linker

This is the second step of the two step reaction scheme for the synthesis of Pam_3Cys-protein system and refers to the modification of model protein (CRM197) with EMCS and SBAP linkers. The modification was done based on a similar way to that stated before (Donadei *et al.*, 2016). EMCS and SBAP linkers are amine-to-sulfhydryl crosslinkers that contains NHS-ester and maleimide and NHS ester and bromoacetyl reactive groups, respectively. The success of the modification of proteins with EMCS and SBAP was assessed by MALDI-TOF.

An amount of 1.52 mg of EMCS and SBAP linkers were dissolved in 50 μL of DMSO, and 17.2 μL of prepared mixtures (10 eq-v molar excess, 1.71 μmol) were added to a solution of 10 mg (0.17 μmol) CRM197 protein in 100 mM NaPi, pH 7.2, respectively. Reactions were running for 3 hours on a plate shaker at RT. After 3 hours, reaction mixtures were purified using 30 kDa Viva spin filter units 0.5 mL (5 cycles) dialysing against 10 mM NaPi, 1 mM EDTA pH 7.2. The protein content was quantified by colorimetric assay (MicroBCA assay). The linker/protein molar ratio was determined by MALDI-TOF mass spectrometry analysis run in an UltraFlex III MALDI-TOF/TOF instrument (Bruker Daltonics) in linear mode and with positive ion detection. The samples for analysis were prepared by mixing 2.5 μL of product and 2.5 μL of sinapinic acid matrix. A quantity of 2.5 μL of each mixture was deposited on a samples plate, dried at RT for 10 min, and subjected to the spectrometer.

2.4.1.3 Ellman's assay

To ensure the presence of free thiol groups on Pam_3Cys-PEG7 linker, Ellman's assay was performed prior to the conjugation with the protein. The principle of this method is based on the reaction of the thiol with DTNB to give the mixed disulphide and 2-nitro-5-thiobenzoic acid (TNB). Under conditions of oxidative stress, free sulfhydryls decrease and disulphides increase. The intensity of the coloured reaction product is a direct function of thiol group amount that can be estimated by comparing its absorbance value at 412 nm to a standard curve composed of known concentrations of a sulfhydryl-containing compound such as cysteine (Thermo Scientific).

2.4.1.4 Pam_3Cys – protein conjugation

The next and final step for the synthesis of these protein adjuvanted conjugate was the conjugation of modified protein. The maleimide moiety in the EMCS reacts with the modified sulfhydryl group in the Pam_3Cys-PEG7 in slightly acidic environment (pH range 6.5-7.5). In contrast, the bromoacetyl group on SBAP linker reacts with sulfhydryl groups at basic environment (pH>7.5). In both cases, the result is the formation of a stable thioether linkage that is not reversible. Various molar ratios (5 eq-v, 10 eq-v and 20 eq-v molar excess regarding the thiol groups quantified by Ellman's assay) were investigated to achieve optimal reaction conditions between the protein and Pam_3Cys-PEG7. The reaction scheme for the Pam_3Cys-protein conjugation is presented in Figure 2.3.

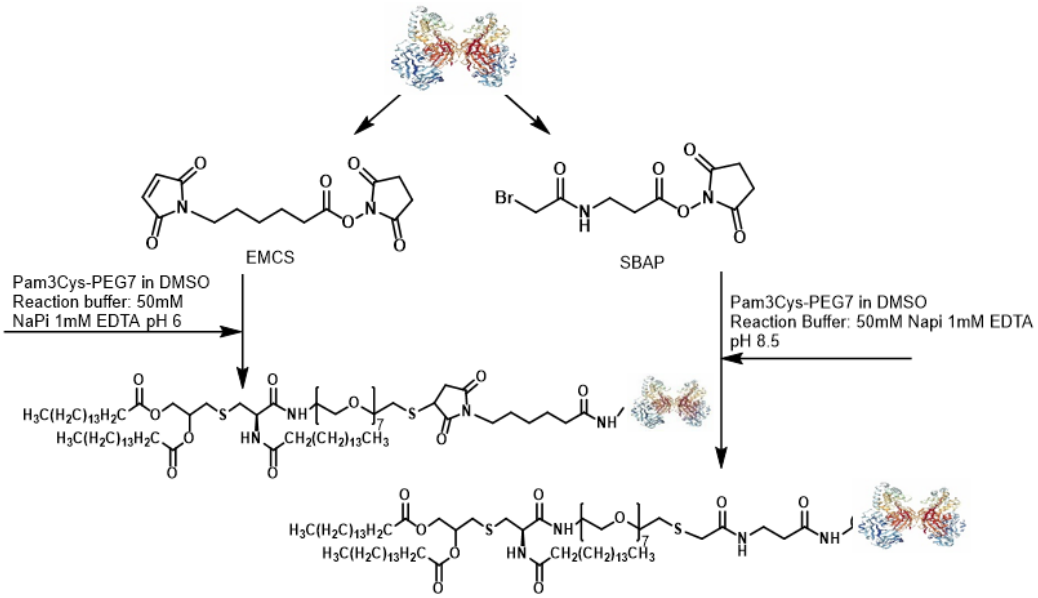

Figure 2.3 *Reaction scheme for modification of protein with EMCS and SBAP linkers.*

Amounts of 5 eq-v (0.024 μmol), 10 eq-v (0.046 μmol) and 20 eq-v (0.097 μmol) molar excess of Pam_3Cys-PEG7 (MW 1278) dissolved in DMSO (32 μg, 63 μg, 130 μg respectively), were added to 300 μg of CRM197-EMCS (MW 60719, $4.94x10^{-3}$ μmol) in 100 mM NaPi, 1 mM EDTA pH 6 and CRM197-SBAP (MW 61754, $4.86x10^{-3}$ μmol) in 100 mM, 1 mM EDTA pH 8.5 protein solutions, respectively. The reactions were incubated overnight at RT under continuous mixing and was monitored by SDS-PAGE.

2.4.2 Click chemistry

The click chemistry for the synthesis of the Pam_3Cys-protein system was carried out based on a similar way to that stated before (Kolb *et al.*, 2001). The process is an alkyne-azide [2+3] Huisgen cycloaddition and composed by 3 reaction-steps. First step is the modification of Pam_3Cys with N_3-PEG10-NH_2 linker in order to introduce the azide group (-N_3) on Pam_3Cys. Second step is the modification of protein with endo-BCN-PEG8-NHS linker for the insertion of endo-BCN (cyclooctyne) group on model protein. Third and last step is the addition of protein-PEG8-endoBCN to the Pam_3Cys-PEG10-N_3, which they “click” when they meet in solution. The reactions scheme is shown in Figure 2.4.

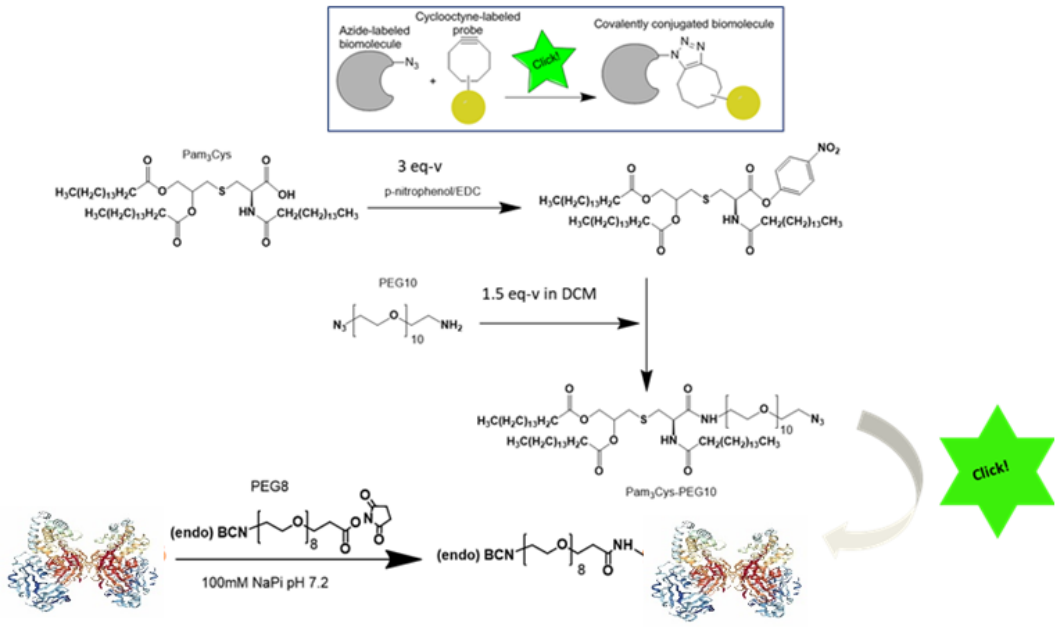

Figure 2.4 *Click chemistry reaction scheme for conjugation of Pam_3Cys with protein.*

2.4.2.1 Modification of Pam_3Cys with PEG10 linker

An amount of 10 mg (11.1 µmol) of Pam_3Cys (MW 910.46) were reacted with 3 eq-v (6.38 mg, 33.3 µmol) EDC (MW191.70) and 3 eq-v (4.63 mg, 33.3 µmol) molar excess p-nitrophenol (MW 139.11) in DCM. The reaction was incubated for 30 minutes at RT under continuous mixing and was followed by TLC. An amount of 1.5 eq-v (8.69 mg, 16.5 µmol) molar excess of N_3-PEG10-NH_2 (MW 526.62) was dissolved in 0.2 mL of DCM solvent. The PEG10 solution was added to the Pam_3Cys-p-nitrophenol reaction mixture under an inert nitrogen atmosphere for preventing the reaction of components with air. The reaction was stirred for 24 hours at RT and purified manually by gel filtration for excess removal of p-nitrophenol and PEG10. Reaction was followed by TLC.

2.4.2.2 Modification of model protein with PEG8 linker

An amount of 0.61 mg (5 eq-v molar excess, 0.85 µmol) of endo-BCN-PEG8-NHS linker (MW 714.8) (dissolved in 100 mM NaPi pH 7.2) was mixed with 10 mg (0.17 µmol) CRM197 protein in 100 mM NaPi, pH 7.2. Reaction was incubated for 3 hours on a plate shaker. After 3 hours, reaction mixture was purified using a G25 Sephadex column. The linker/protein molar ratio was determined by MALDI-TOF mass

spectrometry analysis using sinapinic acid matrix and the protein content was determined by colorimetric assay (MicroBCA assay).

2.4.2.3 "Click" between modified Pam_3Cys and protein

Amounts of 0.03 (0.0171 μmol), 0.07 (0.0513 μmol), 0.24 mg (0.171 μmol) (10 eq-v, 30 eq-v and 100 eq-v molar excess) of Pam_3Cys-NH_2-PEG10-N_3 (MW 1084.16) dissolved in DMSO were added to 100 μg of CRM197- endo-BCN-PEG8-NHS (MW 59,016, $1.71x10^{-3}$ μmol) in a DMSO: Buffer ratio 1:9, respectively. TWEEN20 in 0.01% was added also to one reaction with 100 eq-v of Pam_3Cys. The reactions were incubated overnight at RT, under continuous mixing and SDS-PAGE and MALDI-TOF analysis were performed to assess the success of the conjugations.

2.4.3 Direct conjugation of Pam_3Cys TLR2 agonist on model protein

Direct conjugation of Pam_3Cys on CRM197 protein was the last method tested. This method is composed by two reaction-steps. First step is the activation of carboxyl group on Pam_3Cys using p-nitrophenol and EDC. Then, the modified Pam_3Cys reacts directly with the free amine groups on CRM197 protein. The reaction scheme is presented in Figure 2.5.

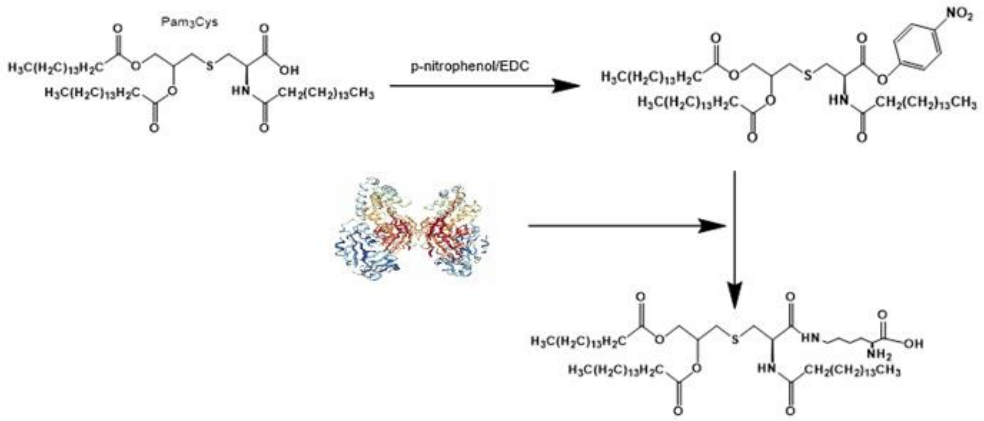

Figure 2.5 *Reaction scheme for direct conjugation of Pam_3Cys on protein.*

An amount of 10 mg (11.1 μmol) of Pam_3Cys (MW 910.46) were mixed with 3 eq-v (6.38 mg, 33.3 μmol) EDC (MW 191.70) and 3 eq-v (4.63 mg, 33.3 μmol) molar excess p-nitrophenol (MW 139.11) in 1 mL of DCM. The reaction was incubated for 30 minutes at RT, under continuous mixing and was followed by TLC. Reaction mixture was purified by gel filtration for excess removal of p-nitrophenol and EDC and

isolation of the final product. Success of the reaction was assessed by ^{1}HNMR spectroscopy. An amount of 30 eq-v (19.45 mg, 333 μmol) molar excess of CRM197 in 100Mm NaPi, pH 7.2, was added to the Pam_3Cys-p-nitrophenol reaction mixture. The reaction was incubated for 24 hours at RT, under continuous mixing and SDS-PAGE and MALDI-TOF mass spectrometry analysis were performed to assess the success of the conjugation.

2.5 Results

2.5.1 Conjugation of Pam_3Cys on protein using PEG7 linker

The synthesis and characterisation of the Pam_3Cys-protein was done as described in the Methods part of this chapter (Section 2.4). EMCS, SBAP and NH_2-PEG7-SH act as heterobifunctional cross-linkers allowing the protein conjugation on Pam_3Cys TLR2 agonist with a controlled, two-step reaction. The proposed chemical reaction and the structure of the final product is shown in Figure 2.3.

2.5.1.1 Modification of Pam_3Cys with PEG7 linker

Based on the ^{1}HNMR performed on the final purified product, the desired product was obtained. The chemical structures of reactants and product as also the^{1}HNMR spectrums are presented in Figure 2.6-Figure 2.9. ^{1}HNMR for Pam_3Cys (400 MHz, $CDCl_3$): δ 6.58 (d, 1H, NH), 5.20-5.09 (m, 1H, S-glyceryl-*CH*), 4.75-4.64 (m, 1H, Cys-*CH*), 4.37-4.28 (m, 1H, S-glyceryl-OCH_{2a}), 4.10 (dd, 2H, S-glyceryl-OCH_{2b}), 3.18-2.97 (m, 2H, Cys-CH_2), 2.72 (d, 2H, S-glyceryl-OCH_2), 2.35-2.23 (m, 6H, 3xPal-C(O)CH_2), 1.68-1.52 (m, 6H, 3xPal-CH_2), 1.35-1.17 (m, 72H, 36xPal-CH_2), 0.90-0.82 (m, 9H, 3xPal-CH_3). ^{1}HNMR for PEG7 (400MHz, $CDCl_3$): δ 3.67 (m, 36H, O-CH_2-CH_2), 2.73 (m, 2H, CH_2-NH_2), 1.91 (m, 2H, NH_2), 1.40 (m, 1H, SH). ^{1}HNMR for Pam_3Cys-PEG7 (400 MHz, $CDCl_3$): δ 7.7 (s, 1H, CH-NH), 7 (m, 1H, NH), 5.53 (m, 1H, S-glyceryl-*CH*), 4.81 (m, 1H, Cys-*CH*), 4.37-4.28 (m, 2H, S-glyceryl-OCH_{2a}), 4.10 (dd, 2H, S-glyceryl-OCH_{2b}), 3.67 (m, 36H, 7xpolyethylene glycol), 3.18-2.97 (m, 2H, Cys-CH_2), 3.07 (s, 2H, NH_2-CH_2), 2.73 (m, 1H, CH_2-SH), 2.72 (d, 2H, S-glyceryl-OCH_2), 2.35-2.23 (m,

6H, 3xPal-C(O)CH_2), 1.68-1.52 (m, 6H, 3xPal-CH_2), 1.35-1.17 (m, 72H, 36xPal-CH_2), 0.90-0.82 (m, 9H, 3xPal-CH_3).

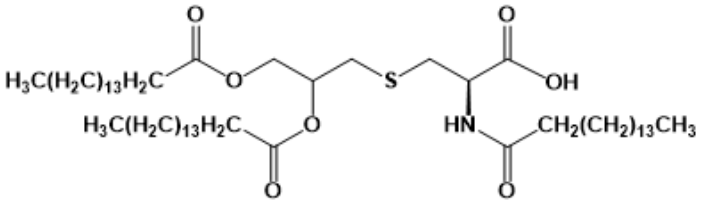

Figure 2.6 *Chemical structure of Pam_3Cys.*

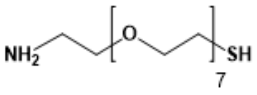

Figure 2.7 *Chemical structure of PEG7 linker.*

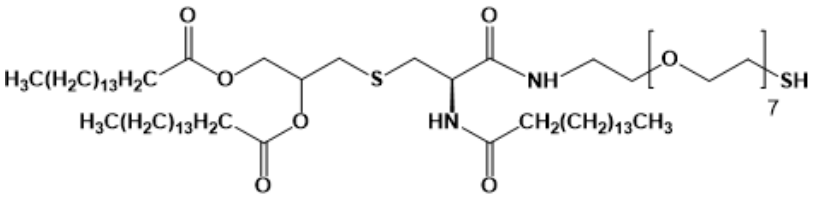

Figure 2.8 *Chemical structure of Pam_3Cys-PEG7.*

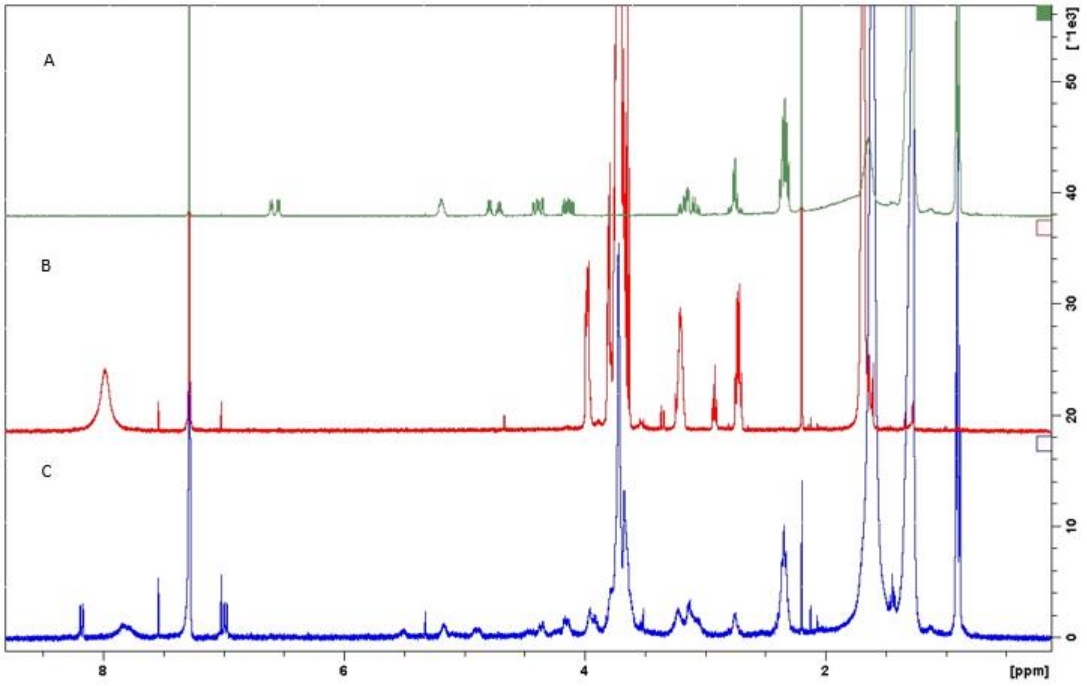

Figure 2.9 *^{1}HNMR spectrums for the modification of Pam_3Cys with PEG7 A) Pam_3Cys B) PEG7 C) Pam_3Cys-PEG7. Spectrums obtained in $CDCl_3$ for all the samples.*

ESI-Mass Spectrometry was followed for the determination of the exact molecular weight of the obtained product. As illustrated in Figure 2.10, the determined molecular weight (1277.94) is in agreement with the expected molecular weight of Pam_3Cys-PEG7 (1277.96).

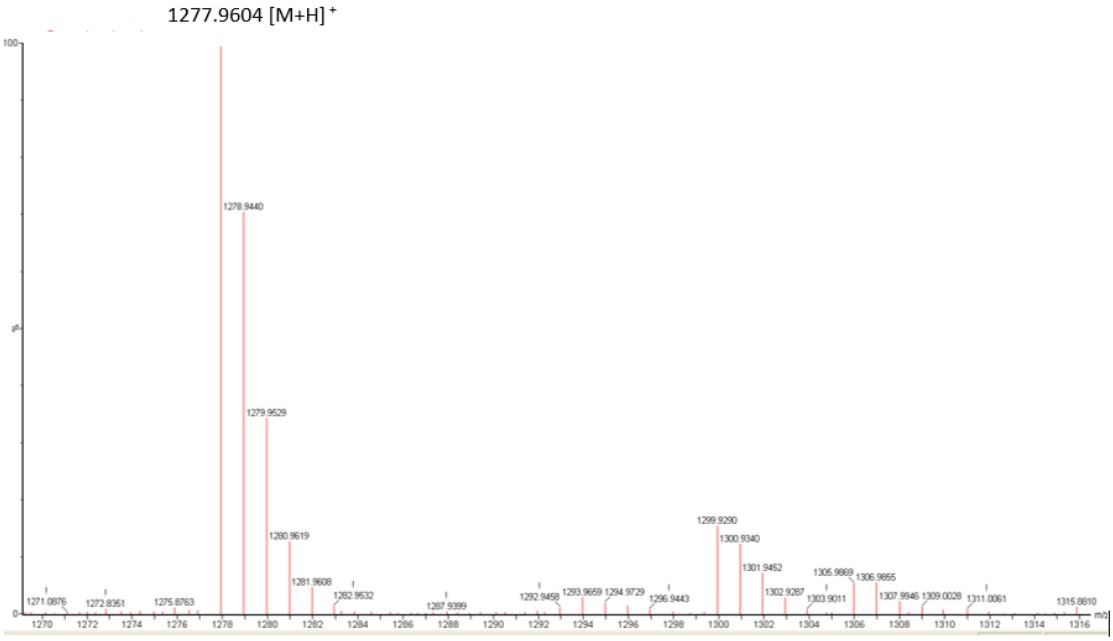

Figure 2.10 *ESI-MS on Pam$_3$Cys-PEG7.*

Table 2.2 *ESI-MS analysis result.*

Calculated MW	MW by ESI-MS
1277.96	$[M+H]^+$ 1277.94

2.5.1.2 Modification of protein with EMCS and SBAP linker

The concentration of protein solutions before and after the reactions was determined by BCA assay to ensure that protein solutions are enough concentrated for the next step of the experiments. Table 2.3 summarises all the above.

Table 2.3 *Concentrations of protein constructs.*

Sample	Final Concentration (mg/mL)
CRM197-EMCS	28.6
CRM197-SBAP	24

The success of the protein modification was demonstrated by MALDI-TOF mass spectrometry analysis using sinapinic acid matrix. As indicated from the analysis results (Figure 2.11-Figure 2.12), the modification of CRM197 protein using EMCS

and SBAP was successful. The molecular weight of protein is increased as was expected due to the introduction of 6 linkers for EMCS (EMCS/protein molar ratio=7) and 10 linkers for SBAP (SBAP/protein molar ratio=10).

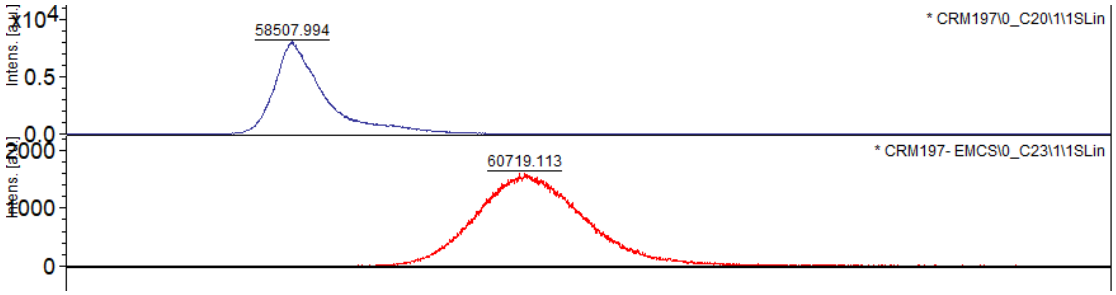

Figure 2.11 *MALDI-TOF analysis for CRM197-EMCS. by MALDI-TOF mass spectrometry analysis run in an UltraFlex III MALDI-TOF/TOF instrument (Bruker Daltonics) in linear mode and with positive ion detection.*

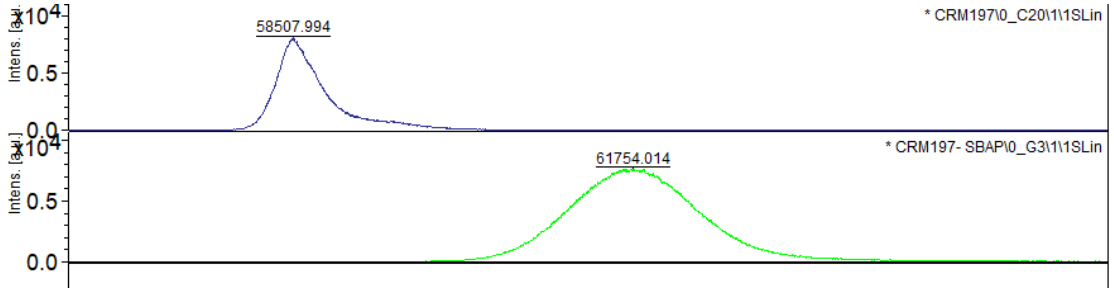

Figure 2.12 *MALDI-TOF analysis for CRM197-SBAP. by MALDI-TOF mass spectrometry analysis run in an UltraFlex III MALDI-TOF/TOF instrument (Bruker Daltonics) in linear mode and with positive ion detection.*

Table 2.4 *MALDI-TOF analysis results.*

Structure	MW Protein (Da)	MW Protein-EMCS (Da)	MW Protein-SBAP (Da)	Number of EMCS introduced on protein	Number of SBAP introduced on protein
CRM197	58,508	60,719	61,754	7	10

2.5.1.3 Ellman's assay

The Ellman's assay was performed for an estimation of the free thiol groups, which are available on Pam_3Cys-PEG7. The Table 2.5 presents the results. This assay indicated that thiol groups are available on the linker for conjugation with the protein.

Table 2.5 *Ellman's assay results.*

Compound	-SH concentration (μmol/mL)
Pam$_3$Cys-PEG7	0.7

2.5.1.4 Conjugation on proteins

The success of the conjugations was evaluated by the performance of SDS-PAGE (Figure 2.13). Aggregation and cross-linking of the protein was observed for all the molar excess of Pam$_3$Cys-PEG7 tested. It is of note that visual changes were observed in the protein-linker solutions after a certain point of time. Protein solutions were getting cloudy and formation of micelles was noticed.

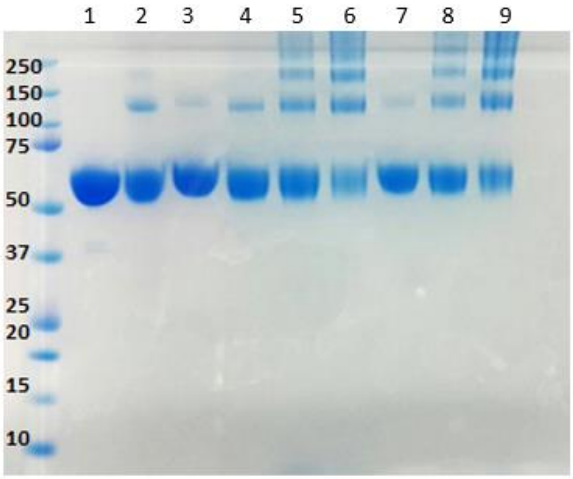

Figure 2.13 *SDS-PAGE for confirmation of CRM197-Pam$_3$Cys conjugation (Bands: 1.CRM197 2.CRM197-EMCS 3.CRM197-SBAP 4.CRM197-EMCS-Pam$_3$Cys-PEG7 5 eq-v 5.CRM197-EMCS-Pam$_3$Cys-PEG7 10 eq-v 6.CRM197-EMCS-Pam$_3$Cys-PEG7 20 eq-v 7.CRM197-SBAP-Pam$_3$Cys-PEG7 5 eq-v 8.CRM197-SBAP-Pam$_3$Cys-PEG7 10 eq-v 9. CRM197-SBAP-Pam$_3$Cys-PEG7 20 eq-v.*

2.5.2 Click chemistry

SDS-PAGE was performed in first place to assess the success of the click chemistry for the conjugation of Pam$_3$Cys on CRM197 protein. As presented by Figure 2.14, aggregation and crosslinking of the protein obtained after the introduction of PEG8 and Pam$_3$Cys linkers on it. Although there is a slight increase in the molecular weight for bands 2 and 3, the band referring to the free protein indicating high amount of unconjugated protein in the sample. MALDI-TOF analysis was followed for the determination of exact molecular weight of final product and the evaluation of the insertion of Pam$_3$Cys on protein. As illustrated in Figure 2.15, PEG8 linkers have been

successfully inserted on CRM197 as indicated from the increase in the molecular weight (yellow line). However, no Pam_3Cys-PEG10 tail was added on CRM1987-PEG8 as the CRM197-Pam_3Cys had shown the same molecular weight as CRM197-PEG8.

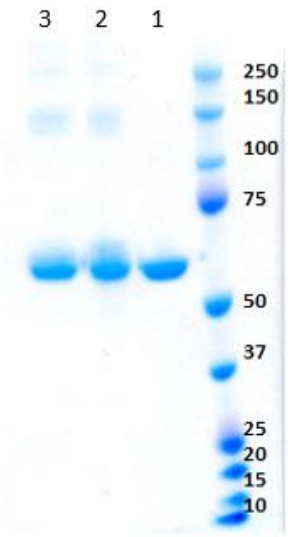

Figure 2.14 *SDS-PAGE for confirmation of CRM197-Pam_3Cys sythesis by click chemistry (Bands: 1. CRM197 2.CRM197-NHS-PEG8-endo(BCN) 3.CRM197- NHS-PEG8-endo(BCN)-N_3-PEG10-NH_2-Pam_3Cys (30 eq-v).*

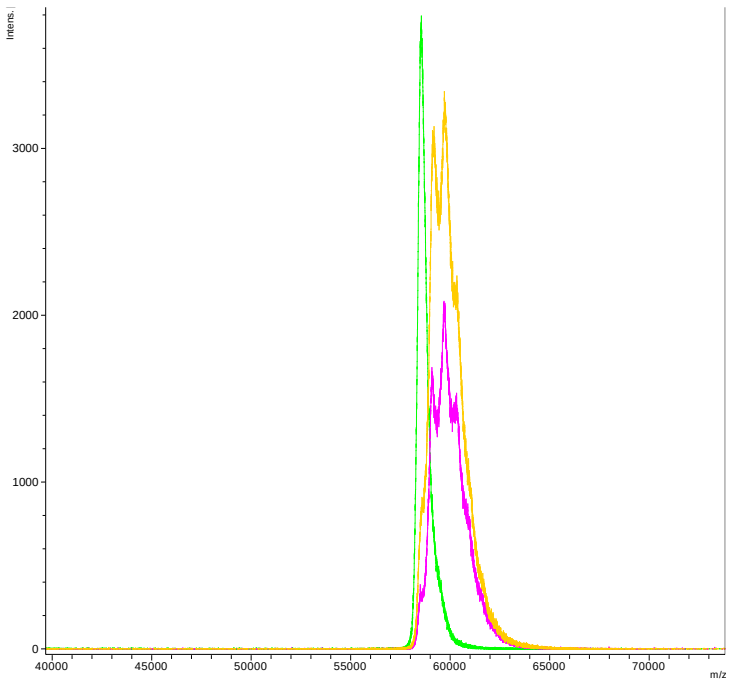

Figure 2.15 *MALDI-TOF analysis for CRM197 (green line), CRM197-NHS-PEG8-endo(BCN) (pink line) and CRM197- NHS-PEG8-endo(BCN)-N_3-PEG10-NH_2-Pam_3Cys (yellow line). by MALDI-TOF mass spectrometry analysis run in an UltraFlex III MALDI-TOF/TOF instrument (Bruker Daltonics) in linear mode and with positive ion detection.*

As the addition of 30 eq-v molar excess of Pam_3Cys on protein led to aggregation, different molar excess were tested to evaluate if either or not the reason behind the aggregation is the amount of linker added. Two molar ratios were tested, 10 eq-v and 100 eq-v molar excess and the results presented in the Figure 2.16. The SDS-PAGE revealed that protein was aggregating and crosslinking regardless the molar excess of linker used for the reaction. It was also observed that, no conjugation was obtained as almost all the free protein was in the reaction mixture.

In order to test the hypothesis for the formation of micelles in protein solution after the addition of Pam_3Cys liker, reaction was repeated with TWEEN20 solubilising agent, added in reaction mixture in 0.01%. Furthermore, a reaction between CRM197-PEG8 and PEG10 was carried out to assess how the protein will react in the absence of Pam_3Cys. As indicated from Figure 2.16, the inclusion of TWEEN20 did not make any difference and protein macroscopic aggregates were obtained which were also visible by eye. Interestingly, the reaction between protein and PEG10 without Pam_3Cys had

shown slight increase in the molecular weight indicating that PEG10 reacted with protein and no precipitation and aggregation were observed in solution.

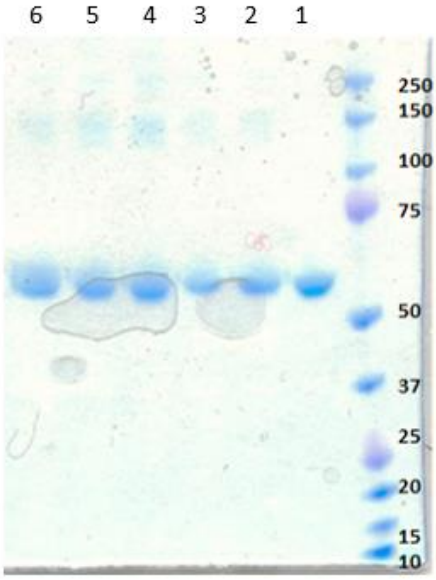

Figure 2.16 *SDS-PAGE for confirmation of CRM197-Pam$_3$Cys sythesis by click chemistry (Bands: 1. CRM197 2.CRM197-NHS-PEG8-endo(BCN) 3.CRM197- NHS-PEG8-endo(BCN)-N$_3$-PEG10-NH$_2$-Pam$_3$Cys (10 eq-v) + TWEEN20 0.01% 4. CRM197- NHS-PEG8-endo(BCN)-N$_3$-PEG10-NH$_2$-Pam$_3$Cys (100 eq-v) + TWEEN20 0.01% 5. CRM197- NHS-PEG8-endo(BCN)-N$_3$-PEG10-NH$_2$-Pam$_3$Cys (100 eq-v) 6. CRM197- NHS-PEG8-endo(BCN)-N$_3$-PEG10-NH$_2$.*

2.5.3 Direct conjugation of Pam$_3$Cys on protein

Another method considered was the direct addition of Pam$_3$Cys TLR2 on CRM197 protein without the use of any PEG crosslinker to assess the protein reaction. The performance of SDS-PAGE (Figure 2.17) had shown no indication of aggregation and crosslinking of the protein, fact that was quite interesting. As the molecular weight of Pam$_3$Cys (MW 910.46 g/mol) is relatively small compared to the molecular weight of CRM197 protein (MW 58400 Da), was difficult to identify any difference in the molecular weight between the bands. Thus, MALDI-TOF was ultilised for the determination of the exact molecular weight of the reaction product. MALDI-TOF analysis revealed that the molecular weight of reaction product is the exact molecular weight of free CRM197 protein, so no Pam$_3$Cys tail was attached to it (Figure 2.18).

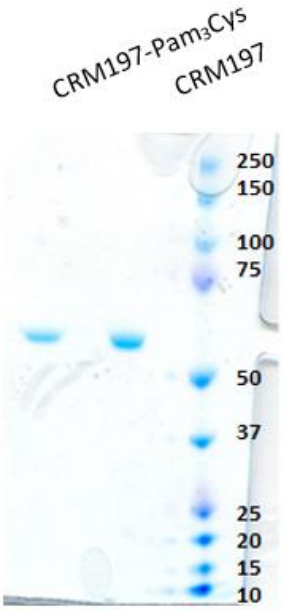

Figure 2.17 *SDS-PAGE for confirmation of CRM197-Pam$_3$Cys sythesis by direct conjugation.*

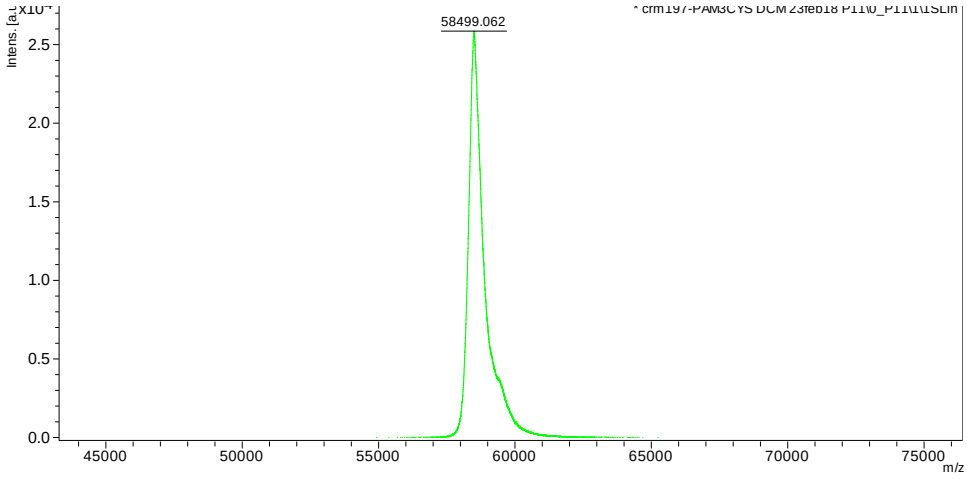

Figure 2.18 *MALDI-TOF analysis for CRM197-Pam$_3$Cys. by MALDI-TOF mass spectrometry analysis run in an UltraFlex III MALDI-TOF/TOF instrument (Bruker Daltonics) in linear mode and with positive ion detection.*

2.6 Discussion

Lipoproteins are a very promising class of vaccine candidates and are recognised as one category of self-adjuvanting vaccines (Kovacs-Simon *et al.*, 2011). Examples are the two lipidated fHbp variants included in Trumenba vaccine, a licensed vaccine for the prevention of MenB. Studies proved that lipidated forms of fHbps were more immunogenic compared to the non-lipidated forms. This immune-enhancing effect is a result of the presence of the N-terminal lipids on fHbp proteins serving as an adjuvant via the recognition by TLR2 (Luo *et al.*, 2016). Nevertheless, bacterial lipoproteins are challenging to express. Fletcher *et al.* reported that the lipidated form of the fHbp protein is expressed at approximately 5 to 8% of total cellular protein (Fletcher *et al.*, 2004). Thus, the existence of a synthetic version of lipoprotein, would help increase their production. A potential strategy for the development of lipoproteins is the chemical ligation of a lipid tail such as Pam_3Cys on antigenic proteins. Three different methods for conjugation of the Pam_3Cys lipid tail on protein, were attempted in this part of the study, including conjugation of Pam_3Cys using PEG7 crosslinker, the click chemistry and the direct conjugation of Pam_3Cys on protein avoiding the use of any crosslinker.

Pam_3Cys is lipid moiety comprised of three palmitic acid groups that are bound in an ester and amide linkage to a cysteine residue. It is the synthetic analog of Braun's lipoprotein from *Escherichia coli* which was identified in the cell-wall of Gram-negative bacteria. It was first engineered to enhance the immunogenicity of epitopes derived from influenza virus and enhance virus-specific CTLs when mice were injected with a MHC class I epitope conjugated to Pam_3Cys (Khan *et al.*, 2009). Since then, Pam_3Cys has been extensively tested for the development of peptide vaccines demonstrating high efficiency. While highly immunogenic and effective at adjuvanting peptide and protein epitopes (Chua *et al.*, 2008; Moyle, 2017), lipopeptides that contain Pam_3Cys have poor solubility characteristics, making dosing, and formulation difficult. This is predominantly due to the hydrophobic moiety that results from the lipid chains (Zaman and Toth, 2013).

The lipophilic nature of Pam_3Cys made its conjugation with antigens challenging. Many methods have been contacted aiming to solve this issue. It is referred in the literature that, small peptides and PEGs have been attached on Pam_3Cys in order to enhance solubility under aqueous conditions (Moyle *et al.*, 2013). Zeng *et al*.

observed that the conjugation site between Pam_3Cys and immunogen plays an essential role in the solubility of Pam_3Cys-immunogen complexes. They reported that when lipopeptide was attached to the N-terminal of the immunogen, opalescent solution were obtained even at very low concentrations. In contrast, when Pam_3Cys was added between a B and T cell epitope at the approximate centre of the molecule, solubility was improved dramatically (Zeng *et al.*, 2002).
In addition, investigations have focused on the structurally similar derivative, Pam_2Cys which is a synthetic analogue of MALP-2 (macrophage activating lipopeptide-2) derived from the cytoplasmic membrane of *Mycoplasma fermentans*. Pam_2Cys contains one less palmitic acid group compared to Pam_3Cys and a free amino group with improved solubility characteristics (Zeng *et al.*, 2002; Chua *et al.*, 2008; Zaman and Toth, 2013).

Taking into consideration the hydrophobic properties of Pam_3Cys, a modification of Pam_3Cys with a PEG-SH chain was explored in order to increase its solubility and introduction of thiol group for conjugating with the maleimide or bromide group on modified protein. PEG7 linker was added on Pam_3Cys with success as was demonstrated from NMR and ESI-MS but no difference in hydrophobicity of Pam_3Cys was observed. At the same time, CRM197 was modified with EMCS or SBAP linker and 7 or 10 linkers respectively were introduced on protein as was confirmed by MALDI-TOF. These results were in agreement with work reported previously for the modification of other proteins (Donadei *et al.*, 2016). Pam_3Cys-PEG7 was added on protein in different molar ratios (1:5, 1:10, 1:20) in order to optimise the reactions conditions and to avoid saturation of protein surface (Martinez-Jothar *et al.*, 2018). The reaction resulted in the formation of aggregates regardless of the molar ratio.

The pH is another factor to consider in maleimide thiol or bromoacetyl reactions. The pH of the reactions was checked in order to ensure that for maleimide-thiol reaction the pH is slightly acidic (pH range 6.5-7.5) and bromoacetyl-sulfhydryl is in basic environment (pH>7.5). When the maleimide-thiol reaction occurs in more basic conditions (pH >8.5), the reaction favours primary amines and also increases the rate of hydrolysis of the maleimide group to a non-reactive maleamic acid (Hermanson, 2013). For this purpose, the pH was checked prior, during and after the process to ensure optimal reaction conditions.

It can be concluded that the stoichiometry of reaction is not the reason behind the aggregation as protein aggregates were observed even at lower excess molar ratio

of Pam_3Cys added on protein. In addition, the failure of the reactions cannot be based on non-optimum pH reaction conditions as pH was monitored. A possible reason behind the reactions outcome could be the hydrophobicity of Pam_3Cys- PEG7 moiety. The incorporation of a PEG linker into Pam_3Cys did not favour the water solubility of lipopeptide as expected. Potential reason behind this could be the length of PEG used. Conjugation of a longer hydrophilic PEG chain on Pam_3Cys could affect its lipophilic nature and increase its water solubility. In addition, utilisation of a longer PEG could increase further the distance between protein and Pam_3Cys, thus potentially preventing protein aggregation.

Chemical conjugation of Pam_3Cys to model protein through random conjugation process has been challenging. Random conjugation targeting lysine residues on immunogen is characterised by heterogeneity and complexity, which can affect the solubility, stability and pharmacokinetics of the mixtures (Boylan *et al.*, 2013; Perez *et al.*, 2014). Conversely, site specific conjugation approaches are preferable as the site of conjugation can be selected and resulting in more homogenous products (Badescu *et al.*, 2014). Click chemistry or linkage chemistry is one of these approaches, which attracted interest the latest years. It has the benefit of simplicity as consists from few simple reaction steps and the starting materials are commercially available.

Click chemistry universe is comprised by many reactions with the Huisgen 1,3-dipolar cycloaddition being the premier example of a click reaction (Kolb *et al.*, 2001). This cycloaddition refers to the copper-catalysed reaction of alkynes and azides resulting to the formation of 1,4-disubsituted-1,2,3-triazoles which cannot be cleaved hydrolytically or otherwise, and unlike benzenoids and related aromatic heterocycles, they are almost impossible to oxidise or reduce (Tornøe *et al.*, 2002; Kolb and Sharpless, 2003; Presolski *et al.*, 2011). Strain-Promoted Alkyne-Azide Cycloadditions (SPAAC) are a modified version of these reactions, which are preferable as they don't require a toxic metal as catalyst and proceed efficiently at RT (Mbua *et al.*, 2011). A SPAAC catalyst-free cycloaddition was approached herein for the selective incorporation of Pam_3Cys lipid tail on CRM197 model protein. Protein has been modified with a cyclooctyne linker (NHS-PEG8-endo(BCN)), where 3 alkyne sides were introduced on protein based on the MALDI analysis performed. The same time, Pam_3Cys was modified successfully with an azide linker (N_3-PEG10-NH_2), as indicated from the TLC was performed. However, precipitation and protein

aggregates were obtained during the reactions, irrespective of the molar ratios (10 eq-v, 30 eq-v, 100 eq-v).

Identifying the molar ratio at which molecule surface saturation occurs is important in order to avoid the use of high molar excess, which may result in aggregation, and precipitation of reaction mixture. The potential reason for protein aggregation in this case could be the overload of protein with lipopeptide leading to formation of micelles and precipitation of protein. As referred in the literature, high yields of alkynes-azides cycloaddition can be achieved even at 1:1 molar ratio (Manetsch *et al.*, 2004; Zhang *et al.*, 2005). However, these reactions have been using catalyst and heat. On the other hand, when cycloaddition takes place in the absence of catalyst and heat, 10-250 eq-v molar excess of azide compared to alkyne was used. The reaction is very slow and runs for 24 hours in ambient conditions (Mbua *et al.*, 2011). Therefore, excess of Pam_3Cys-azide was needed for ensuring the coupling with protein-alkyne. However, excess of hydrophobic Pam_3Cys in solution did not favour the reaction as caused the lipid moieties surrounded the protein surface causing precipitation and aggregation. Reaction outcome was not preventable even in the presence of TWEEN 20 surfactant, which is widely used in the pharmaceutical industry for protein stabilisation, inhibition of protein aggregation and maintenance of solution viscosity and density.

Finally, direct conjugation of Pam_3Cys on CRM197 protein was attempted. As previous attempts with excess of Pam_3Cys caused formation of aggregates, the use of CRM197 protein in excess was decided for this last trial. Although, no aggregates, precipitation or change in appearance was observed after eye inspection, conjugation still did not work as was demonstrated by MALDI-TOF. Results come in agreement with what was observed before by Moyle *et al*. who tried to incorporate the Pam_3Cys lipid adjuvant at the C-terminus of the recombinant protein. They referred that where a PEG linker was not included, no reactivity was observed (Moyle *et al.*, 2014).

2.7 Conclusion

Overall, it has been demonstrated that incorporation of Pam_3Cys into protein is not straight forward. The solubility issues due to the lipid nature of Pam_3Cys made its addition on protein and peptide antigens is challenging. As a result, pharmaceutical development moved towards the synthesis and use of Pam_3Cys variances and alternatives with the focus on more simplified TLR2 ligands. Simple lipid moieties

have the benefit of shorter hydrophobic tail with potentially more favoured water solubility properties. It is established that the lipid moiety on lipopeptides is responsible for the self adjuvanting activity of lipopeptides. Thus, many groups have used simpler acyl moieties for lipopeptide vaccine development with palmitic acid and the lipoamino acids being two of the most studied examples (Bueno *et al.*, 2004; Moyle *et al.*, 2006). Acyl moieties are more easily synthesised and incorporated into antigens than either Pam_2/Pam_3Cys. Development of these types of molecules can be the basis for the development of lipopeptide-based vaccines targeting many diseases.

Due to the challenges described in this chapter, the replacement of a Pam_3Cys TLR2 agonist with TLR9 agonist CpGODN was decided. CpGODN was used for all the work described in the next chapters.

Chapter 3 Conjugation of TLR9 agonist CpGODN on model proteins

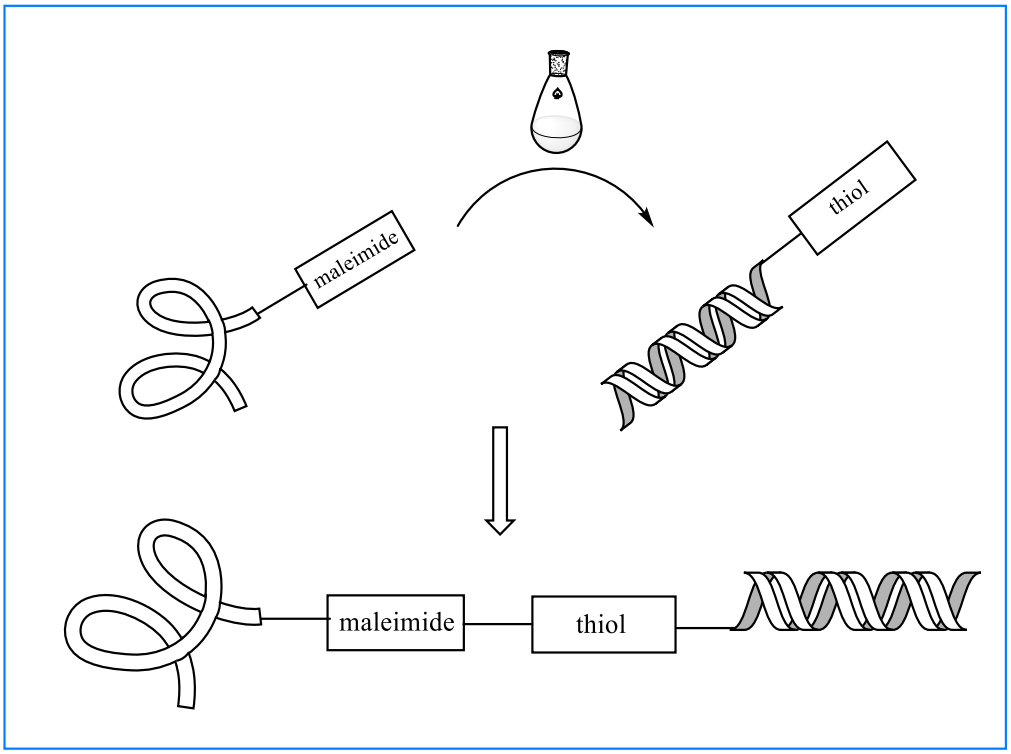

3.1 Introduction

Agonists of Toll like receptor 9 (TLR9) can activate innate immunity and initiate a cascade of immune responses that can impact the magnitude and the persistence of the immune response. Numerous studies have demonstrated that these molecules lead to activation of the cells initiating pro-inflammatory reactions that result in the production of cytokines such as type-I IFN, IL-6, TNF and IL-12 (Vollmer and Krieg, 2009). These features render TLR9 a very promising class for the development of vaccine adjuvants. Synthetic oligodeoxynucleotides (ODN) that contain unmethylated CpGODN dinucleotide repeats are widely used as TLR9 agonists coadministrated with antigens and other adjuvants. TLR9 agonists have demonstrated substantial potential as vaccine adjuvants, and as mono- or combination therapies for the treatment of cancer and infectious and allergic diseases (Scheiermann and Klinman, 2014). Although the immunological potency of CpGODN has been extensively studied, no work has investigated the effect of chemical linkage of CpGODN with immunological agents attaching on liposomes and its *in vivo* efficiency.

3.2 Aim and objectives

The aim of the work described in this chapter was the conjugation of different model proteins (CRM197- a non-toxic mutant of diphtheria toxin, NadA-Meningococcal serogroup B protein antigen, GBS67- Group B Streptococcus protein) with the TLR9 agonist CpGODN in order to design a novel non-viral vaccine delivery system with upgraded therapeutic efficacy. Building on the previous work in this field, this research suggests the use of CpGODN1826 in vaccine protein-based delivery systems as immunostimulant. This TLR agonist selected for this experimental test based on previous investigations, which proved the efficiency of it to augment immune responses. To achieve this aim, the objectives of this work weres:

1. The preparation of proteins conjugated to CpGODN TLR9 agonist
2. The confirmation of the designed systems by SDS-PAGE and SEC-HPLC
3. The characterisation of the protein conjugates by NF-κB luciferase reporter assay and dot blot

3.3 Materials

Table 3.1 outlines the materials used within this chapter.

Table 3.1 *List of materials.*

Material	Supplier
CpGODN 1826 (5'-[AmC6]TCCATGACGTTCCTGACGTT)	Sigma Aldrich, Italy
CRM197 as model protein	GSK, Siena, Italy
EMCS ($C_{14}H_{16}N_2O_6$)	Sigma Aldrich, Italy
GBS67	GSK, Siena, Italy
NadA	GSK, Siena, Italy
SPDP ($C_{12}H_{12}N_2O_4S_2$)	Sigma Aldrich, Italy
TCEP 0.0005 M solution	Sigma Aldrich, Italy

3.4 Methods

3.4.1 Conjugation of CpGODN on proteins

The synthesis of the CpGODN-protein system was done based on a similar manner to that reported before for the synthesis of CpG-protein or other conjugate of TLR7 agonist and glucan adjuvant (Maurer *et al.*, 2001; Heit *et al.*, 2005; Donadei *et al.*, 2016; Clauson *et al.*, 2019). The synthesis consists of 3 reaction-steps, as described in Figure 3.1. The same protocol was used for conjugation of all three proteins CRM197, NadA, GBS67.

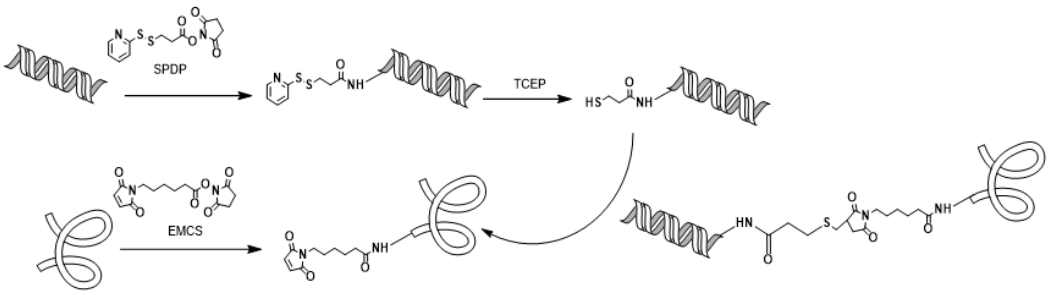

Figure 3.1 *Reaction scheme for conjugation of CpGODN on proteins.*

3.4.1.1 Modification of CpGODN with SPDP linker

For the synthesis of CpGODN-protein system, the modification of the CpGODN was necessary, so as to be able to further conjugate this with model proteins. For the purpose of this conjugation, an SPDP linker was added on CpGODN for the introduction of disulphide group. SPDP is a short-chain crosslinker for amine-to-sulfhydryl conjugation via NHS-ester and pyridyldithiol reactive groups that form cleavable (reducible) disulphide bonds with cysteine sulfhydryls. The CpGODN-SPDP was then pre-treated with TCEP reducing agent in order to break the disulphide bonds on SPDP linker so the thiol groups will be free to further conjugate with the protein.

An amount of 20 mg (3.21 μmol) of CpGODN 1826 (5'-[AmC6] TCCATGACGTTCCTGACGTT, MW 6238) were mixed with 10 eq-v molar excess (10 mg, 32.1 μmol) of SPDP linker (MW 312.37) in 100 mM NaPi pH 7.2: DMSO 9:1 (100 μL:900 μL) solution. The reaction was incubated for 3 hours at RT under continuous mixing and was purified by size exclusion chromatography (G25 column, V=105 mL) using H_2O as eluent buffer. ^{1}HNMR was performed in order to assess the success of the reaction.

A quantity of 6.35 mg (0.98 μmol in H_2O) of CpGODN-SPDP (MW 6460) were pre-treated with 3 eq-v molar excess (5.6 μL) of 0.0005 M TCEP solution for 3 hours at RT under the dark. The reaction mixture was purified by size exclusion chromatography using G25 column (V=105 mL) in H_2O. The amount of CpGODN-SPDP recovered was quantified by measuring UV absorption at 260 nm. Sample was dried and stored in 4 °C until using it.

3.4.1.2 Modification of proteins with EMCS linker

This is the second step of the two step reaction scheme for the synthesis of CpGODN-protein system and refers to the modification of model proteins (NadA, CRM197, and GBS67) with EMCS. EMCS is an amine-to-sulfhydryl crosslinker that contains NHS-ester and maleimide reactive groups. Proteins were modified using EMCS in different molar excess, in order to optimise the reaction conditions. The success of the modification of proteins with EMCS was assessed by MALDI-TOF. Sinapinic acid was used as matrix for the analyses.

An amount of 10 mg (211 μL, 0.17 μmol) of CRM197 stock solution (47.4 mg/mL in 100 mM NaPi pH 7.2) were mixed with 6 eq-v (1 μmol) and 10 eq-v (1.71 μmol) molar

excess (11 µL and 17 µL respectively, from a stock solution of 1.52 mg EMCS/50 µL DMSO) of EMCS linker in appropriate quantity of 100 mM NaPi 1 mM EDTA pH 8.1 buffer solution, so that the final concentration of protein solutions being 20 mg/mL. Reactions were incubated for 3 hours at RT. After 3 hours, reaction mixtures were purified using 30 kDa Viva spin filter units 0.5 mL (5 cycles) dialysing against 50 mM NaPi, 1 mM EDTA pH 7.5. Protein content was determined by colorimetric assay. The linker/protein molar ratio was determined by MALDI-TOF mass spectrometry analysis run in an UltraFlex III MALDI-TOF/TOF instrument (Bruker Daltonics) in linear mode and with positive ion detection.

3.4.1.3 CpGODN – protein conjugation

For conjugation of adjuvant to the modified protein, Micheal addition of the sulfhydryl group in CpGODN-SPDP with the maleimide moiety in the EMCS activated protein was used. The reaction which is illustrated in Figure 3.2, occurs in a pH range 6.5-7.5 to form a stable thioether linkage. The first bioconjugation reaction was carried out was with CRM197. In order to optimise the reaction conditions different pH as also different CpGODN-SPDP: protein-EMCS ratios were tested (Table 3.2).

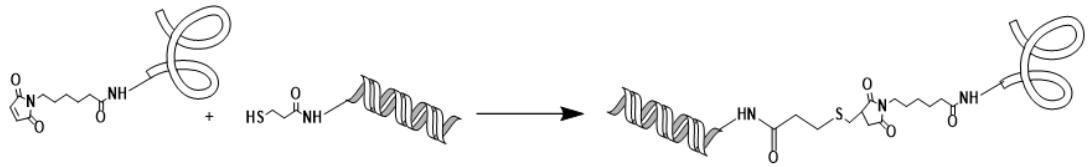

Figure 3.2 *Conjugation of CpGODN on proteins.*

Table 3.2 *Reaction conditions tested for bioconjugation.*

Reaction condition	Conditions tested
Reaction pH	6.5 and 7.5
CpG-SPDP: protein-EMCS molar ratio	10:1 and 20:1

To this end, 5.23 mg (0.81 µmol) CpGODN-SPDP (MW 6460) was pre-treated with TCEP, purified by G25 column, and the recovered material was quantified by UV. An amount of 4.85 mg (0.081 µmol) of CRM197-EMCS (MW 59,783) were mixed with 10 eq-v (5.23 mg, 0.81 µmol) or 20 eq-v (10.46 mg, 1.62 µmol) molar excess of CpGODN-SPDP. CpGODN-SDPD crude was dissolved in 400 µL of 50 mM NaPi 1 mM EDTA pH 6.5 or 50 mM NaPi 1 mM EDTA pH 7.5 so that the final concentration

of protein in solution being 10 mg/mL. The reactions were incubated overnight at RT under continuous mixing and SDS-PAGE 4-12% Bis-Tris gel using MOPS was performed to assess the success of the conjugation.

Protein conjugate was purified using 30 kDa Viva spin filter units 0.5 mL (40 cycles), and recovered in PBS (1x) buffer. The protein content was quantified using BCA colorimetric assay and CpGODN content was quantified by UV measuring absorbance at 260 nm. Finally, the conjugation of protein to CpGODN was evaluated by SDS-PAGE and SEC-HPLC.

3.4.2 NF-κB luciferase reporter assay

TLR-specific activation assay was performed using human embryonic kidney 293 (HEK293) cells expressing luciferase under control of the NF-kB promoter and stably transfected with mice TLR9. HEK293-transfected cells were maintained in DMEM complemented with 4.5 g/L glucose and HEPES (Invitrogen), 10% fetal bovine serum (FBS), 1% penicillin/streptomycin solution (Invitrogen), puromycin (5 µg/mL), and blasticidin (5 µg/mL). For the NF-κB luciferase assay, 25,000 cells/well were seeded in 90 µL of complete DMEM without antibiotics in 96-well µClear luciferase plates (PBI International) and incubated for 24 hours at 37 °C. Successively, cells were stimulated with 10 µL of serial 2-fold dilutions of CRM197-CpGODN or CpGODN alone in PBS (Starting concentration 12.5 µg/mL). All compound concentrations were tested in triplicate. After incubation for 6 hours at 37 °C, supernatants were discarded from each well, and cells were lysed for 20 minutes at RT using 20 µL/well of 1:5 diluted 'passive lysis buffer' (Promega). Luciferase assay reagent (100 µL/well) (Promega) was added, and emitted light was immediately quantified using a Tecan microplate reader. NF-κB activation of stimulated cells was expressed as fold-increase in emitted light over the average result of PBS stimulated control cells (Donadei *et al.*, 2016).

3.4.3 Dot Blot

Test samples and controls (2 mg/mL) spotted on nitrocellulose membranes and the membranes were let drying for 20 minutes. Non-specific sites were blocked by soaking the membranes in PBS-5% w/v BSA-0.05% v/v TWEEN20 in a 10 cm Petri dishes for 1 hour at RT. After 3 washes with PBS 0.05% v/v TWEEN20, membranes were incubated with antiserum versus protein diluted in 1:1000 with PBS-5% w/v BSA-0.05% v/v TWEEN20 (positive serum) or serum from non-immunised mice (1:1000 in PBS-5% w/v BSA-0.05% v/v TWEEN20) (negative serum) for 1 hour at

RT. Membranes were washed three times with PBS 0.05% v/v TWEEN20 (3 x 5 minutes). Finally, membranes were incubated with fluorescent anti-mice IgG secondary antibody (1:10000 in PBS-5% w/v BSA-0.05% v/v TWEEN20) for 45 minutes at RT. Membranes were washed with PBS 0.05% v/v TWEEN20 (3 x 5 minutes) and were scanned using Odyssey fluorescent imaging system (LI-COR).

3.5 Results

3.5.1 Conjugation of CpGODN on proteins

The synthesis and characterisation of the CpGODN-protein was done in a similar way as described in the Methods part of this chapter (Section 3.4). The proposed chemical reactions and the structure of the final product are shown in Figure 3.2.

3.5.1.1 Modification of CpGODN with SPDP linker

The chemical structures of reactants and product as also the ^{1}HNMR spectrums are presented in Figure 3.3-Figure 3.5. ^{1}HNMR for SPDP (400MHz, DMSO): δ 7.2-8.5 (pyridine), 3.3 (m, 2H, S-CH_2-*CH_2*), 3.1 (m, 2H, S-S-*CH_2*), 2.5 (succinimide). ^{1}HNMR for CpGODN-SPDP (400MHz, D_2O): δ 7.6-7.8 (m, pyridine), 7.5 (s, 1H, *CH*-NH), 2.8–3.0 (m, cysteine). The peak analysis confirmed the successful preparation of modified CpG-SPDP.

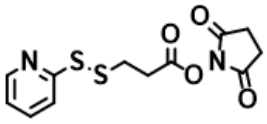

Figure 3.3 *Chemical structure of SPDP.*

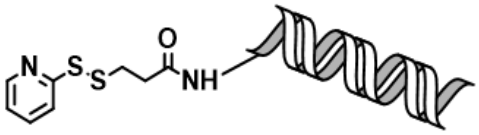

Figure 3.4 *Chemical structure of CpGODN-SPDP.*

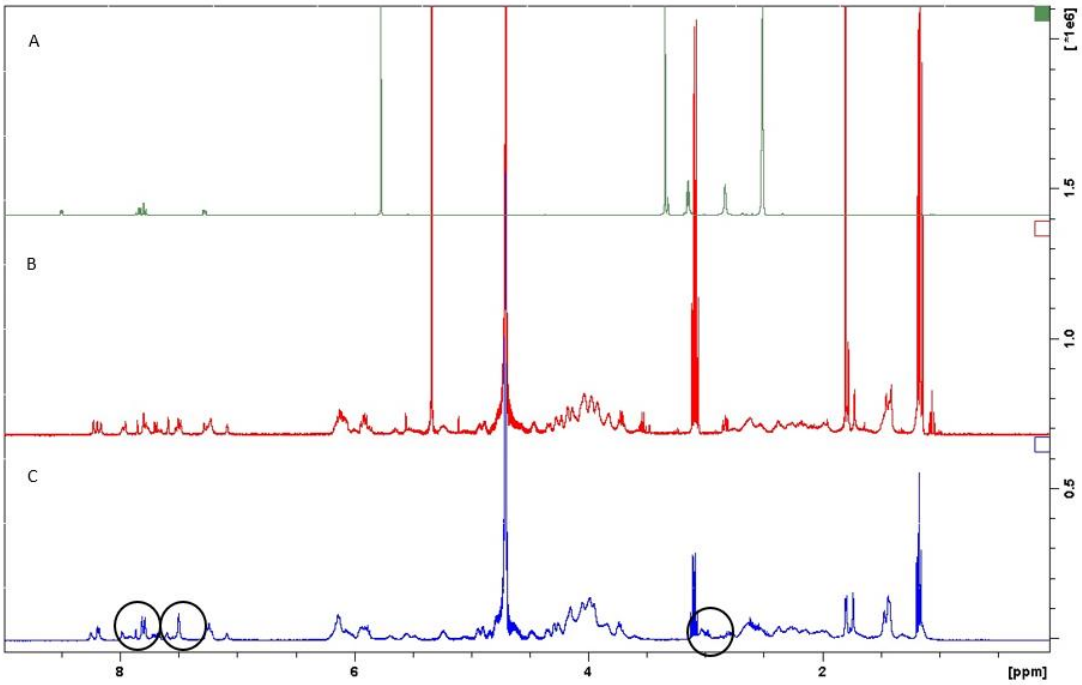

Figure 3.5 *^{1}HNMR spectrums for the modification of CpGODN with SPDP (A) SPDP (B) CpGODN (C) CpGODN-SPDP. CpGODN and CpGODN-SPDP spectrums obtained in D_2O. SPDP spectrum obtained in DMSO.*

3.5.1.2 Modification of proteins with EMCS linker

The exact molecular weight of proteins and proteins modified with EMCS linker were determined by MALDI-TOF. The obtained molecular weight of proteins were in agreement with the calculated molecular weight. The molecular weight of modified

proteins increased compared to the one obtained for unmodified proteins indicating the addition of EMCS linkers (Figure 3.6-Figure 3.8). The increase in the molecular weight is analogous to the number of EMCS linker introduced on proteins. CRM197 protein was the first protein modified for this reason, different molar excess ratios of EMCS (6 and 10 eq-v molar excess) were tested in order to determine the ideal reaction conditions for the introduction of a sufficient number of linkers (Figure 3.6). It was observed that, the use of 6 eq-v molar excess of EMCS on protein was enough to introduce an average number of 4 EMCS linkers on protein. Thus, NadA and GBS67 proteins were modified accordingly. The Figure 3.7shows the MALDI-TOF analysis for NadA protein. The molecular weight of the monomeric structure of the protein is determined at first place (25,581 Da) which was as expected around 25 kDa for the full-length monomer of NadA. Then, the modified NadA was analysed and the number of introduced linkers was determined by the increase in the molecular mass of the proteins and the number of peaks obtained as demonstrated in Figure 3.7. Finally, the modification of GBS67 protein was assessed where the shift in the molecular weight of protein indicates successful modification of protein with EMCS linker (Figure 3.8). Table 3.3 summarises the information collected from the analysis.

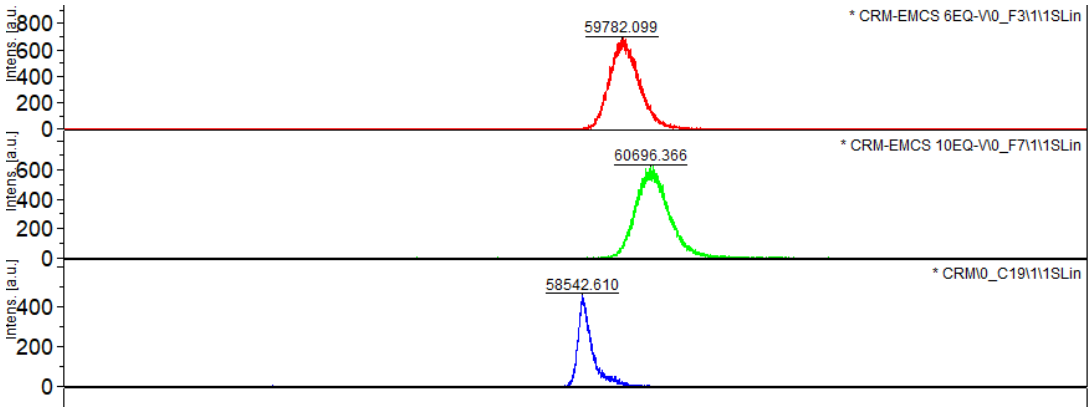

Figure 3.6 *MALDI-TOF analysis for CRM197 and CRM197-EMCS. by MALDI-TOF mass spectrometry analysis run in an UltraFlex III MALDI-TOF/TOF instrument (Bruker Daltonics) in linear mode and with positive ion detection.*

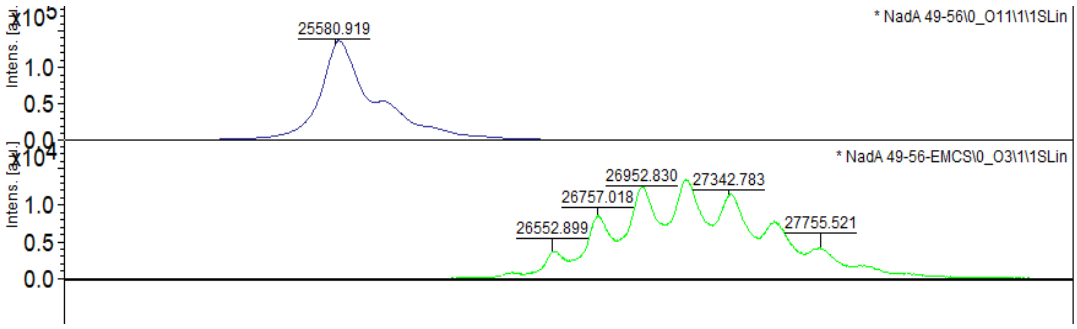

Figure 3.7 *MALDI-TOF analysis for NadA and NadA-EMCS. by MALDI-TOF mass spectrometry analysis run in an UltraFlex III MALDI-TOF/TOF instrument (Bruker Daltonics) in linear mode and with positive ion detection.*

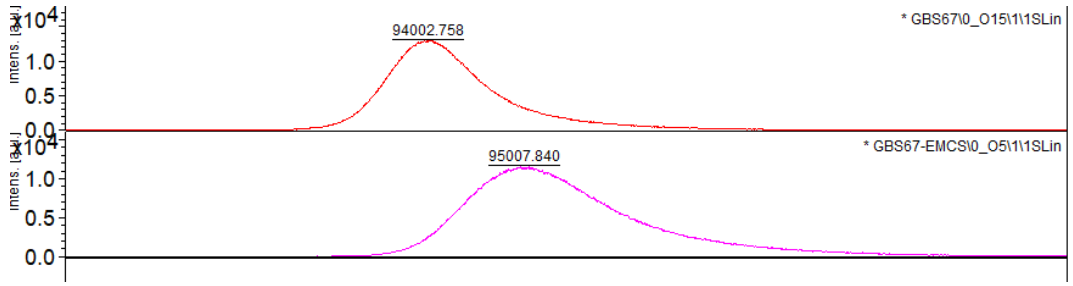

Figure 3.8 *MALDI-TOF analysis for GBS67 and GBS67-EMCS. by MALDI-TOF mass spectrometry analysis run in an UltraFlex III MALDI-TOF/TOF instrument (Bruker Daltonics) in linear mode and with positive ion detection.*

Table 3.3 *Information summarised from MALDI-TOF analysis.*

Structure	MW Protein	MW Protein-EMCS	Number of EMCS introduced on protein
CRM197	58,543	59,782 (6eq-v)	4
		60,696 (10 eq-v)	7
NadA	25,581	27,756 (6 eq-v)	7
GBS67	94,003	95,998 (6eq-v)	4

3.5.1.3 Conjugation on proteins

The impact of pH and CpGODN-SPDP: protein-EMCS molar ratio used for the reactions were evaluated in order to achieve optimum reaction conditions. First, conjugation of CRM197-EMCS with CpGODN-SPDP was carried out using a slightly acidic pH (pH 6.5) or a slightly basic-neutral pH (pH 7.5) in 20:1 CpGODN-SPDP: CRM197-EMCS excess. As it is demonstrated by the SDS-PAGE presented in Figure 3.9A, conjugation occurred in both conditions, proving that both of pH are suitable for the reactions. In order to test a different molar ratio between modified CRM197 protein

and CpG, pH 7.5 was chosen for further experiments. Chemical ligation between CpGODN-SPDP and CRM197-EMCS using 10:1 molar ratio resulted in protein-CpGODN coupling demonstrating that conjugation occurred even in presence of lower CpGODN excess (Figure 3.9B). All further experiments adopted the following reaction conditions: pH 7.5 and CpGODN: protein 10:1 ratio.

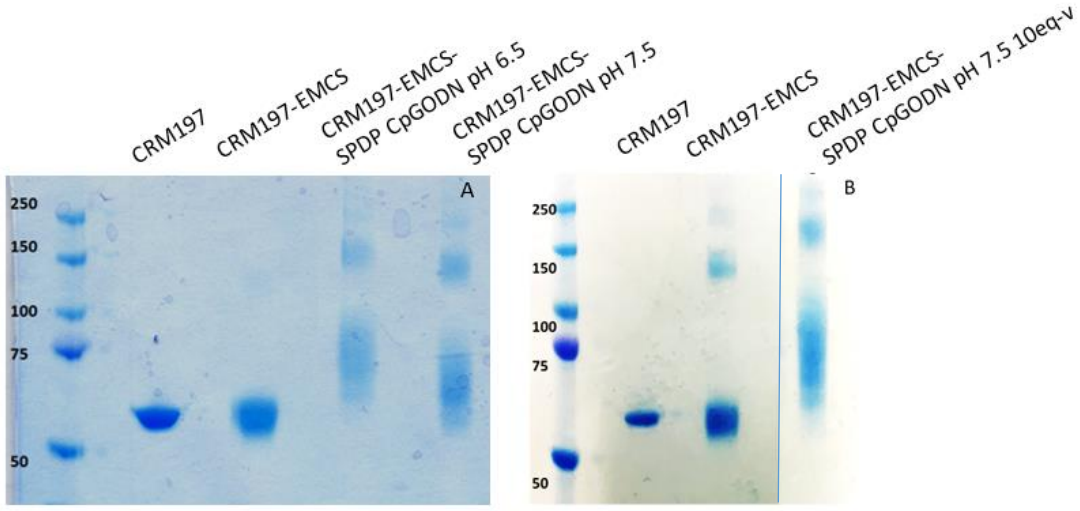

Figure 3.9 *SDS-PAGE for reaction conditions optimisation for CRM197-CpGODN conjugation (A) pH (B) CpGODN:protein molar ratio. (For the panel B, gel image was cropped to remove lanes that were not required).*

The success of the conjugations was tested by SDS-PAGE and SEC-HPLC. SDS-PAGE electrophoresis and HPLC demonstrated that CpGODN was conjugated to the modified proteins evidenced by bands of higher molecular weight compared to unmodified protein. (Figure 3.10-Figure 3.14). Then, MALDI-TOF analysis was followed in order to determine the exact molecular weight of conjugates but unfortunately did not work, regardless of the different matrixes were tested. Thus, the conjugations were confirmed with the performance of SEC-HPLC with the protein conjugates eluting faster from the SEC-HPLC column as was expected due to their higher molecular weight compared to protein-EMCS and protein alone.

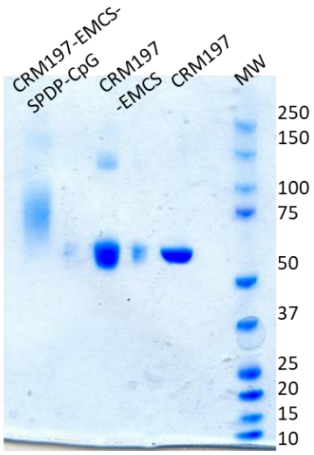

Figure 3.10 *SDS-PAGE for confirmation of CRM197-CpGODN conjugation (Bands 1: CRM197 protein, 2: CRM197 modified with EMCS 3: CRM197-CpGODN conjugate).*

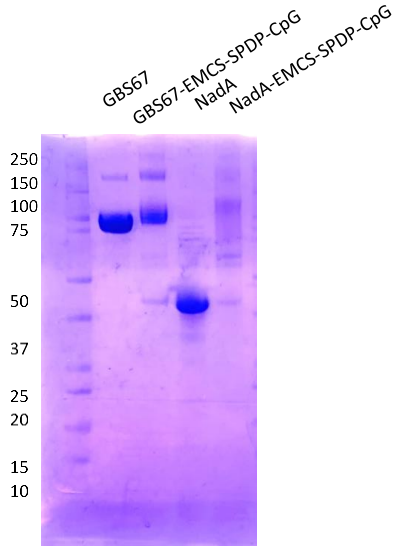

Figure 3.11 *SDS-PAGE for confirmation of NadA-CpGODN and GBS67-CpGODN conjugations (Bands 1: NadA protein, 2: NadA modified with EMCS, 3: NadA-CpGODN conjugate, 4: GBS67 protein, 5: GBS67 modified with EMCS, 6: GBS67-CpGODN conjugate).*

Based on the molecular weight differences obtained from MALDI and SDS-PAGE between protein-EMCS and protein-CpGODN conjugates structures, the numberof CpGODN chains attached on proteins was estimated. Based on results obtained, the average number of CpGODN chains introduced on all the proteins was 3-4. The Table 3.4 summarises all the above.

Table 3.5 summarises the protein and CpGODN content for all three conjugates have been synthesised.

Table 3.4 *Introduction of CpGODN chains on proteins.*

Structure	CpGODN: protein stoichiometry (mol/mol)	MW protein-CpGODN conjugate	CpGODN: protein in conjugate (mol/mol)	[a] Conjugation efficiency (%)
CRM197	10:1	100,000	6:1	60%
NadA	10:1	100,000	4:1	40%
GBS67	10:1	120,000	4:1	40%

[a] Amount of conjugated CpGODN vs amount of CpGODN used for conjugation.

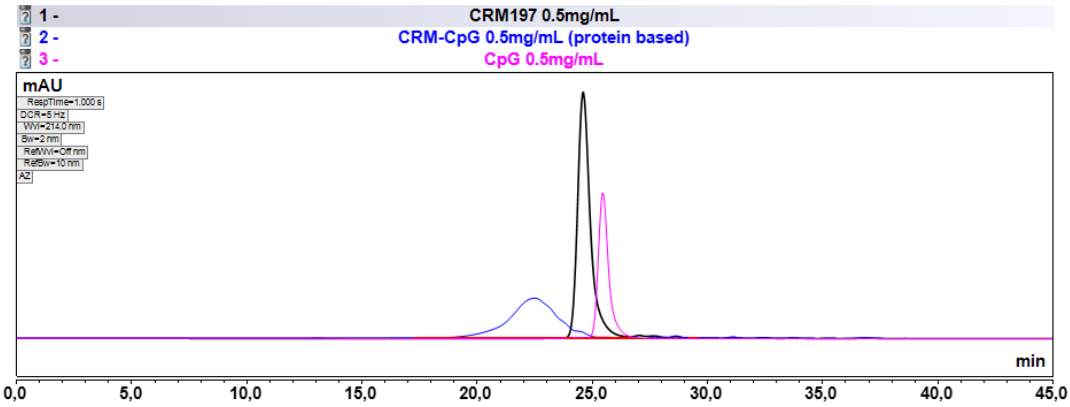

Figure 3.12 *SEC-HPLC for CRM197, CRM197-EMCS, CRM197-CpG. Experiments performed using a Phenomenex SEC-4000 column and 100 mM NaPi, 100 mM Na_2SO_4, ACN 5%, pH 7.1 as running buffer. All samples were injected in a protein concentration of 0.5 mg/mL for CRM197 and CRM197-CpG and 0.5 mg/mL for free CpG. Injection volume: 50 µL.*

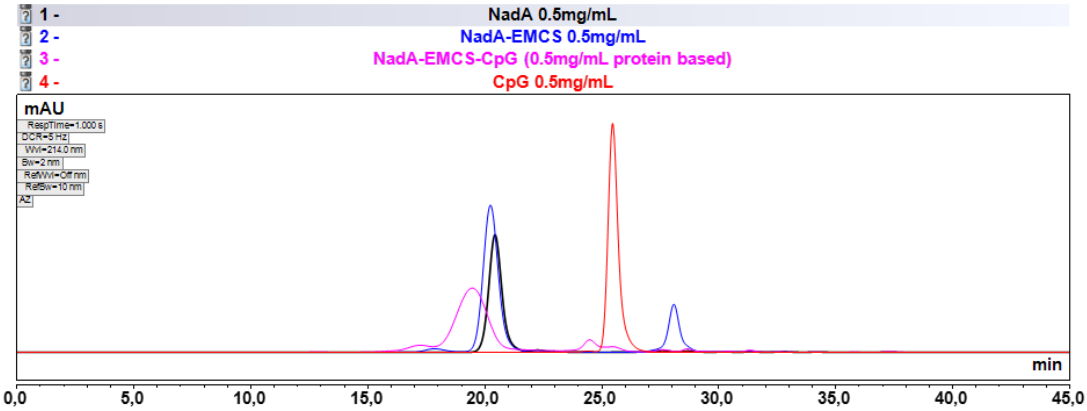

Figure 3.13 *SEC-HPLC for NadA, NadA-EMCS, NadA-CpG. Experiments performed using a Phenomenex SEC-4000 column and 100 mM NaPi, 100 mM Na_2SO_4, ACN 5%, pH 7.1 as running buffer. All samples were injected in a protein concentration of 0.5 mg/mL for NadA, NadA-EMCS and NadA-EMCS-CpG and 0.5 mg/mL for free CpG. Injection volume: 50 µL.*

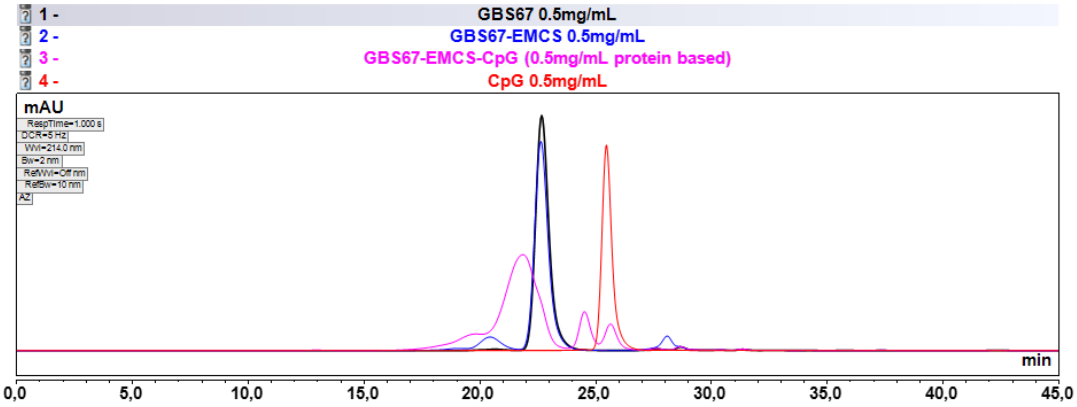

Figure 3.14 *SEC-HPLC for GBS67, GBS67-EMCS, GBS67-CpG. Experiments performed using a Phenomenex SEC-4000 column and 100 mM NaPi, 100 mM Na_2SO_4, ACN 5%, pH 7.1 as running buffer. All samples were injected in a protein concentration of 0.5 mg/mL for GBS67 and GBS67-EMCS and GBS67-EMCS-CpG and 0.5 mg/mL for free CpG. Injection volume: 50 µL.*

Table 3.5 *Summarised information for all the conjugates obtained.*

Conjugate	NadA-CpGODN	CRM197-CpGODN	GBS67-CpGODN
Protein concentration (mg/mL)	6.65	5.36	6
CpGODN concentration (mg/mL)	0.65	1.05	0.9

3.5.2 *In vitro* testing

The capacity of the adjuvanted CRM197 protein to engage TLR9 was evaluated *in vitro*, using human embryonic kidney 293 (HEK293) cells expressing luciferase under control of the NF-κB promoter and stably transfected with a murine TLR9 agonist (Figure 3.15). In this assay, NF-κB activation is measured by monitoring the levels of luciferase expression following stimulation of cells with serial dilutions of TLR9 agonists. The CpGODN1826 used for the conjugations (custom synthesis by Sigma-Aldrich in order to contain a primary amine at the 5') as also the commercially available CpGODN, were chosen as positive controls. As illustrated by the Figure 3.15, TLR9 attached to the protein improved the receptor activation compared to the unconjugated form. NF-kB fold induction starts at 3.13 µg/mL for both of the positive controls used. In contrast, CRM197-CpGODN conjugate is able to induction receptor activation starting from much lower concentration (0.39 µg/mL).

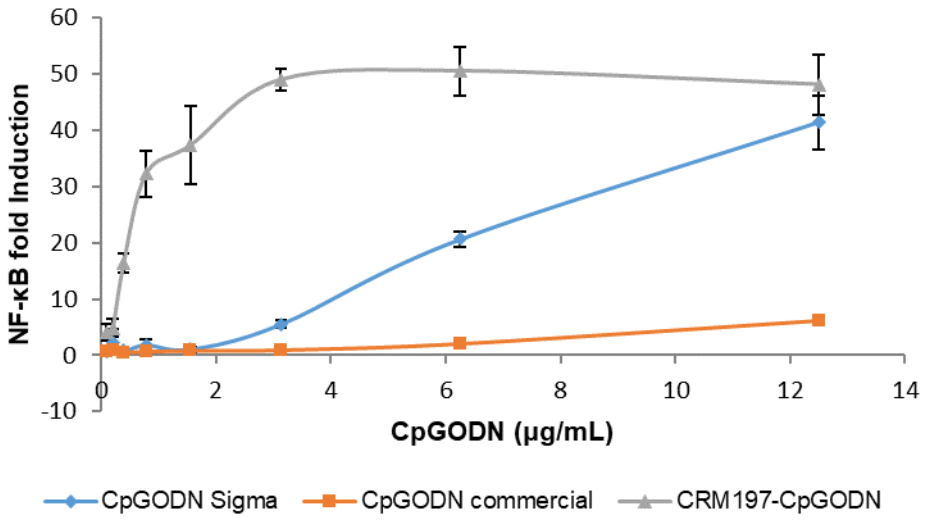

Figure 3.15 *NF-kB luciferase reporter assay for CRM197-CpGODN conjugate. Activation of TLR9 reporter cell line by CRM197-CpGODN conjugate. 25,000 TLR9-HEK293 cells/well were stimulated with 0.1–12.5 µg/mL (2-fold steps) of TLR9 agonists. Commercial CpGODN as CpGODN used for conjugation (custom synthesis by Sigma) were used as a positive controls. After 6 hours, luciferase expression was measured and expressed as fold-induction compared to cells incubated with PBS and plotted as mean ± SD of triplicates.*

3.5.3 Dot blot

The capacity of the conjugate to be recognised by primary antibodies (antiserum versus protein) was tested using dot blot technique. In this technique, protein detection occurred when test sample is capable to be bind by the serum antibodies. Figure 3.16 demonstrates that CRM197-CpGODN, NadA-CpGODN and GBS67-CpGODN conjugates are recognised by serum antibodies indicating that the incorporation of CpGODN chains on the protein was not impacting on protein epitopes binding to the primary antibodies. . OVA was used as control for the experiment as unrelated protein proving that the recognition is protein specific.

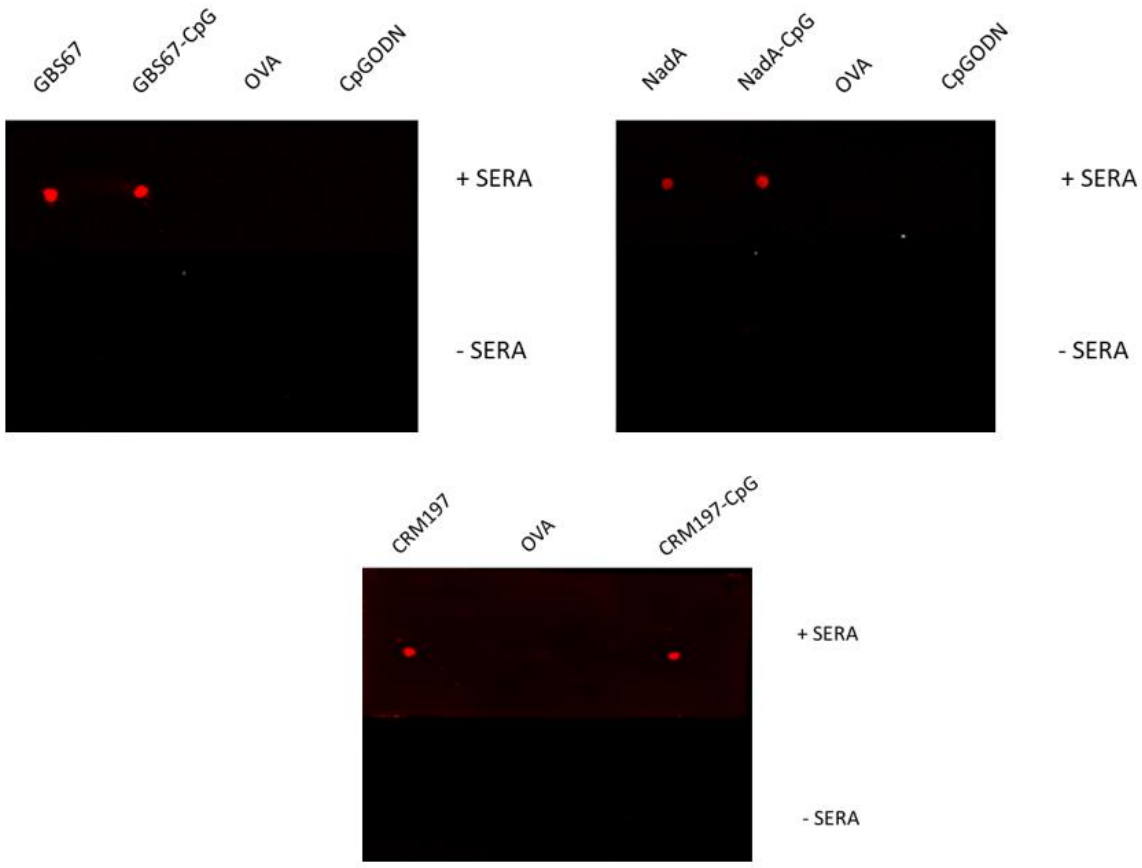

Figure 3.16 *Dot blot for CRM197-CpG, NadA-CpGODN and GBS67-CpGODN conjugates. Free CpGODN and OVA protein were used as negative controls.*

3.6 Discussion

The chemical ligation of CpGODN 1826 into three different model proteins (CRM197, NadA, GBS67 was performed in this part of the work described in this chapter. Thiol-maleimide bioconjugation chemistry was used for the CpGODN introduction on proteins. The modification of CpGODN with SPDP linker and protein with EMCS were performed using 6 eq-v molar excess of linker on CpGODN/protein in order to achieve controlled functionalisation of linker and thus more homogenous and defined products. Previous studies demonstrated that in a range of 5-15 eq-v molar excess of linker, the linker content in the resulting product is increased linearly. A test on CRM197 protein with 10 eq-v EMCS resulted in the introduction of 7 EMCS linkers. High molar excess of linker could potential led to highly heterogeneous mixtures containing different protein conjugates species and also overload of modified molecule (Slutter *et al.*, 2010; Clauson *et al.*, 2019). Using 6 eq-v excess, EMCS linker was inserted onto the protein in a level of 4-7 mol/mol of protein, as was estimated

by MALDI analysis. This result agrees with what has been reported before for the modification of different protein with maleimide linker (Donadei *et al.*, 2016; Jones *et al.*, 2016).

As previously described elsewhere, a molar ratio of 5:1 of CpGODN: protein is capable for the addition of 2-3 CpGODN/protein molecule (Maurer *et al.*, 2002; Heit *et al.*, 2003; Heit *et al.*, 2005). In this study, 10:1 CpG: protein ratio was used in order to ensure the presence of CpGODN in excess favouring the coupling with protein. Bioconjugation between modified protein and CpGODN resulted in protein conjugates containing 4 CpGODN chains for GBS67-CpGODN and NadA-CpGODN and 6 CpGODN chains for CRM197-CpGODN conjugate. These results come in agreement with what has been previously published for the preparation of CpGODN conjugates using other proteins (Maurer *et al.*, 2002; Heit *et al.*, 2003; Heit *et al.*, 2005). Although, the conjugation reaction efficiency is relatively low due to the high excess of CpGODN used, this finding was in agreement with previous investigations on CpGODN conjugates.

Coupling of the TLR9 CpGODN on protein could favour the uptake and thus create a positive effect on the elicited immune response, given that the complexity of the construct does not affect the activity of individual components. As was demonstrated by NF-κB assay, protein conjugate showed significant increase in the TLR9 activation compared to CpGODN unconjugated form indicating that the presence of protein was not preventing its binding to TLR9. The multivalent presentation of the TLR9 ligand attached to protein significantly improved the receptor activation compared to unconjugated form. This effect may add further *in vivo* benefits due to the localisation and the increase in the avidity interactions with specific receptors on APCs. However, further experiments are needed in order to evaluate this hypothesis. The presence of TLR9 CpGODN on protein did not impair its ability to be recognised by primary antibodies coming from anti-protein serum, as was demonstrated by dot blot fact that indicates that conjugation did not affect the protein epitopes.

3.7 Conclusion

In conclusion, three different protein conjugates have been synthesised in this part of the work. All three proteins have been successfully conjugated with CpGODN TLR9 agonist and well characterised.The immunological evaluation of the antigenic protein conjugate GBS67-CpGODN will be evaluated in a following stage of this work.

Chapter 4 Preparation of cationic liposomal formulations

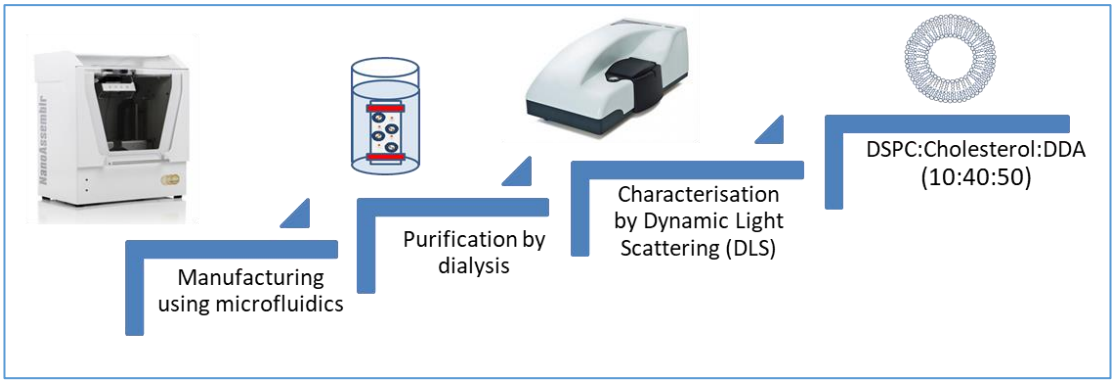

4.1 Introduction

Liposomes as carrier systems offer advantages in terms of the development of vaccine formulations. Key advantages liposome-based vaccine delivery systems offer include their ability to protect incorporated antigen and their versatility in design such that they can be formulated to manipulate biodistribution promote cell uptake and induce cell activation (Perrie *et al.*, 2016; Marasini *et al.*, 2017). Liposome composition and preparation that can be chosen to achieve such desired features include selection of lipid, charge, size, size distribution, entrapment and location of antigens or adjuvants. Depending on the chemical properties, water-soluble antigens (proteins, peptides, nucleic acids, carbohydrates, haptens) are entrapped within the aqueous inner space of liposomes, whereas lipophilic compounds (lipopeptides, antigens, adjuvants, linker molecules) are intercalated into the lipid bilayer and antigens or adjuvants can be attached to the liposome surface either by adsorption or chemical linking (Tandrup Schmidt *et al.*, 2016). Coformulations containing different types of antigens or adjuvants can be combined with the parameters mentioned to tailor liposomal vaccines for individual applications (Watson *et al.*, 2012; Schwendener, 2014).

4.2 Aim and objectives

The aim of the work described in this chapter was to design and formulate cationic liposomes able to adsorb immunogenic agents. The primary aim was the optimisation of liposomes manufacturing conditions for the production of well-defined, stable cationic liposome formulations. Building on the previous work in this field (Kuramoto *et al.*, 2008; Erikci *et al.*, 2011; Bayyurt *et al.*, 2017; Nikoofal-Sahlabadi *et al.*, 2018), in this study cationic liposomes were investigated as carrier and/or adjuvants for protein-conjugated to CpGODN.The cationic liposomes selected were based on DDA as this has previously been shown to offer strong immunogenic properties (Davidsen *et al.*, 2005; Henriksen-Lacey *et al.*, 2011a; van Dissel *et al.*, 2014). To further develop these formulations and investigate their potential to delivery protein-CpGODN conjugates, the objectives of this chapter were:

1. To optimise the manufacturing conditions for the preparation of cationic liposomes formulations using microfluidics
2. To evaluate the impact of purification methods on the formulations characteristics

3. To test the stability of cationic liposomes
4. To associate liposomes with immunogenic agents and CpGODN by adsorption

4.3 Materials

Table 4.1 lists the materials used for within the work reported in this chapter.

Table 4.1 *List of materials.*

Material	Supplier
Cholesterol	Sigma Aldrich, UK
CRM197	GSK, Siena, Italy
1,1′-Dioctadecyl-3,3,3′,3′-tetramethylindocarbocyanine perchlorate (DiI)	Sigma Aldrich, UK
DSPC	Avanti lipids, USA
DDA	Avanti lipids, USA
GBS67	GSK, Siena, Italy
OVA	Sigma Aldrich, UK

4.4 Methods

4.4.1 Preparation of liposomes

The preparation of DSPC: Cholesterol: DDA cationic liposomes was achieved via microfluidics processes based on previously developed methods (e.g. (Kastner *et al.*, 2014; Joshi *et al.*, 2016; Guimarães Sá Correia *et al.*, 2017; Khadke *et al.*, 2019; Roces *et al.*, 2019; Wongpinyochit *et al.*, 2019). For this, a microfluidic micro-mixer, known as a Nanoassemblr[13] (Benchtop, Precision NanoSystems Inc., Vancouver, Canada) was used for the manufacturing of liposomes. The Nanoassemblr uses mixing cartridges, which have two stream inlets that merge into a micro-channel that has a staggered herringbone design. A nanoprecipitation reaction occurs and results in the formation of nanoparticles (Figure 4.1).

[13] Nanoassemblr is a trademark of Precision Nanosystems Inc.

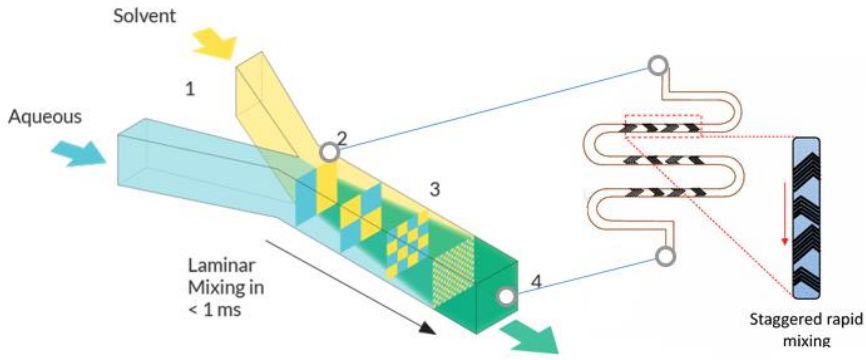

Figure 4.1 *Rapid, controlled and homogenous mixing of an aqueous phase and a miscible solvent containing dissolved nanoparticle precursors produces homogeneous nanoparticles (Precision nanosystems; (Gdowski et al., 2018).*

Here, lipids were dissolved in ethanol in different molar ratios (µM) as indicated in Table 4.2. The ethanol-lipid solution was injected into the first inlet and an aqueous buffer (TRIS 10 mM, pH 7.4) into the second inlet of the microfluidic mixer using disposable syringes. During initial studies, different Flow Rate Ratios (FRR) of the solvent and aqueous phases were tested (1:1 and 3:1) keeping constant the Total Flow Rate (TFR) at 12 mL/min. Aqueous dispersions of liposome formulations, were collected from the outlet stream and initially two different purifications methods were tested for the removal of any residual solvent.

4.4.2 Purification of liposomes

To purify the liposomes via dialysis, liposome solution was placed into a semi-permeable membrane dialysis tube (14,000 MWCO) and the dialysis tubing sealed and placed into a beaker containing 1:200 v/v of liposomes: TRIS 10 mM, pH 7.4 and dialysis was run for 2 hours under continuous stirring. TFF was the second method tested for the purification of liposomes. A KrosFlo[14] Research 2i Tangential flow filtration system (Spectrum labs, California, USA) was used with a MicroKros[15] 500 kDa hollow fibre cassette made from modified polyethersulfone (mPES) at a feed rate of 27 mL/ min.

4.4.3 Sterilisation of liposomes

Finally, 0.22 µm syringe filters (Millex-GP Syringe Filter Unit 0.22 µm Polyethersulfone PES 33 mm Millipore) were tested for the sterilisation of the

[14] KrosFlo is a registered trademark of Repligen Corporation.
[15] MicroKros is a registered trademark of Repligen Corporation.

liposome formulations. The suitability of filtration sterilisation on these formulations was assessed by the determination of liposome recovery and physicochemical attributes after sterilisation.

Table 4.2 *Lipid composition of DSPC:Cholesterol:DDA liposomes.*

Lipid (molar ratio)/ Formulation	F1	F2	F3	F4	F5
DSPC	66	63	60	50	10
Cholesterol	34	32	30	30	40
DDA	0	5	10	20	50

4.4.4 Quantification of liposome recovery

A fluorescence technique is used to study the lipid recovery after purification and sterilisation of liposome formulations using the DiI lipophilic fluorescent molecule. A DiI stock solution 1 mg/mL was prepared in ethanol and lipid stocks were loaded with 0.2 mol% of tracer dye, DiI before microfluidic production of the liposomes. The lipid recovery after purification and sterilisation was determined from a calibration standard curve as a direct function of the measured absorbance (Appendix, Figure A.1). A POLARstar Omega plate reader spectrophotometer was used for the measurement of the fluorescence using an excitation wavelength of 482 nm and emission wavelength of 520 nm.

4.4.5 Adsorption of protein on liposomes

In order to evaluate the impact of the protein:liposome mixing ratio on the final liposome-protein characteristics, various amount of protein were loaded onto DSPC:Cholesterol:DDA cationic liposomes in a similar manner to that of Hamborg *et al*. (Hamborg *et al.*, 2013). Briefly, amount of 1, 5, 10, and 20 µg of protein was mixed with 50 µg of liposomes in a final volume of 200 µL (Protein: liposomes 1:20, 1:10, 1:5, 1:2.5 w/w, respectively). Samples were left to equilibrate for 30 minutes in RT and then they characterised in terms of size, PDI and zeta potential.

After optimisation of protein: liposome ratio, this ratio was used in the next series of studies to consider adsorption of CpGODN and/or proteins and protein conjugates. To achieve this protein/protein conjugate (250 µg) were mixed with 5 mg of liposomes in a final volume of 1 mL (protein: liposomes 1:20 w/w). The amount of CpGODN

equal to that conjugated on protein was also added to one of the formulations (Protein: CpGODN 1:0.15 w/w). Dialysis using Biotech CE tubing (300 kDa MWCO) was carried out overnight at 4°C with two buffer changes, for removal of unbound protein. BCA assay and UV was used for quantification of protein (280 nm) and CpGODN (260 nm) quantification respectively. The amount of protein adsorbed on liposomes surface was calculated by subtracting the amount of protein remaining in solution from the amount of protein initially added to the liposome dispersion. GBS67, CRM197 and OVA were the proteins selected for this part of the study.

4.4.6 Characterisation of liposomes by DLS

The size distribution (mean diameter and polydispersity index (PDI)), and the zeta potential of the liposomes were performed by dynamic light scattering using photon correlation spectroscopy on a Zetasizer Nano-ZS (Malvern Instruments Ltd., UK). Measurements were made at 25 °C with liposomes being diluted in 1/10 using their aqueous phase (1/300 v/v TRIS:H_2O 10 mM pH 7.4). Sizes quoted are the z-average mean (dz) for the liposomal hydrodynamic diameter (nm).

4.4.7 Liposome morphology

Geometry of liposomes was observed by cryo-TEM as described previously (Sangra *et al.*, 2017; Forbes *et al.*, 2019; Lou *et al.*, 2019) with minor modifications. For TEM observations, a Jeol Jem F-200 microscope (Jeol, Tokyo, Japan) operating at 200,000 V was used. Samples were prepared by placing 5 µL of liposomes onto a 400-mesh lacey carbon-coated grid, blotting from both sides for approximately 2 s and then plunging into nitrogen cooled ethane (100% ethane). Samples were then observed in a cryo-holder in electron microscope Jem F-200 microscope (Jeol, Tokyo, Japan) at liquid nitrogen temperature and 200,000 V.

4.4.8 Stability test

Liposome formulations were stored in 4 °C and their physical appearance and their characteristics (particle size, size distribution, zeta potential) were evaluated for 1 week to confirm the short-term shelf-life of these systems.

4.4.9 Statistical analysis

Statistical significance was determined by ANOVA followed by Tukey's (HSD) test. Significance was acknowledged for p values less than 0.05 (marked with *). All calculations were made in Minitab 18.

4.5 Results

4.5.1 The impact of cationic content and purification method on the liposomes characteristics

Liposomes consisting of DSPC, Cholesterol and DDA were formulated using the microfluidics method in a final concentration 0.5 mg/mL. Manufacturing parameters as FRR and TFR were constant for this part of the study (3:1, 12 mL/min). As shown in Figure 4.2-Figure 4.5, increasing the cationic lipid concentration did not significantly impact the particle size (average size 80-90 nm; Figure 4.2) post dialysis purification but did increase the zeta potential as expected (Figure 4.5). On the other hand, TFF purification had a major impact on vesicle size of the cationic formulations as it is shown in Figure 4.2; liposomes composed of DSPC: Cholesterol remained at the same size pre and post-TFF purification (70 - 80 nm; Figure 4.2) but as the cationic lipid content increased the difference in particle size pre and post TFF increased up to a 6 fold increase when the liposomes contained a 50% cationic lipid content (Figure 4.2). This increase in size is accompanied by an increase in the polydispersity index (PDI) (Figure 4.3). The change in the particle size in terms of particle size distribution is also confirmed in Figure 4.4; Figure 4.4A shows a similar size distribution profile for all the liposomes after dialysis whilst after TFF a shift to a more heterogeneous population of particles is measured (Figure 4.4B).

The change in size and PDI of the liposomes was also accompanied by a reduction in liposome recovery (Table 4.3). Whilst good (65-100 %) recovery of liposomes was noted when dialysis was employed as a purification method, purification of the liposomes via TFF reduced notably with the addition of cationic lipid with high (~100%) recovery of neutral (DSPC:Cholesterol) liposomes, reducing to almost total liposome loss when the liposomes contained 20% cationic lipid (Table 4.3).

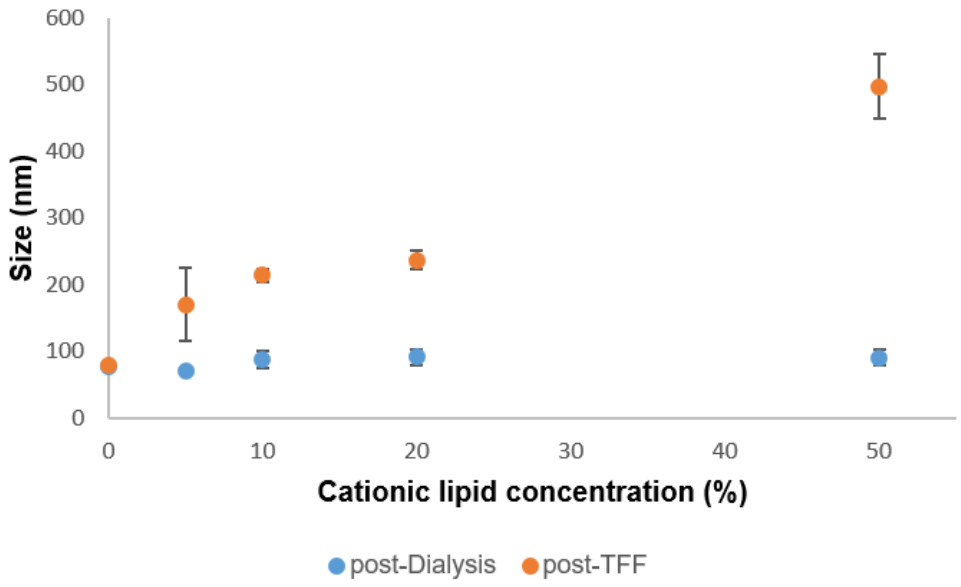

Figure 4.2 *The effect of cationic lipid concentration and purification method on the liposomes size produced by microfluidics. DSPC:Cholesterol:DDA liposome formulations with increasing molar percentages of DDA were manufactured using microfluidics at a 3:1 FRR, 12 mL/min TFR and purified using dialysis or TFF with a final lipid concentration 0.5 mg/mL. Purified liposomes were characterised in terms of sizeA and PDI by DLS. Results represent mean ± SD, n = 3 independent batches.*

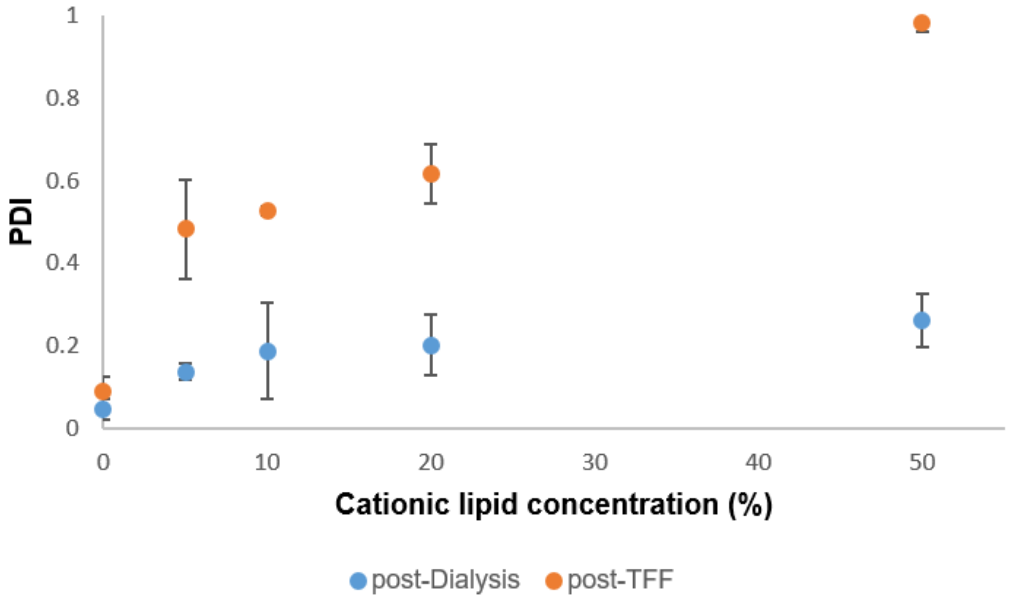

Figure 4.3 *The effect of cationic lipid concentration and purification method on PDI of liposomes produced by microfluidics. DSPC:Cholesterol:DDA liposome formulations with increasing molar percentages of DDA were manufactured using microfluidics at a 3:1 FRR, 12 mL/min TFR and purified using dialysis or TFF with a final lipid concentration 0.5 mg/mL. Purified liposomes were characterised in terms of size and PDI by DLS. Results represent mean ± SD, n = 3 independent batches.*

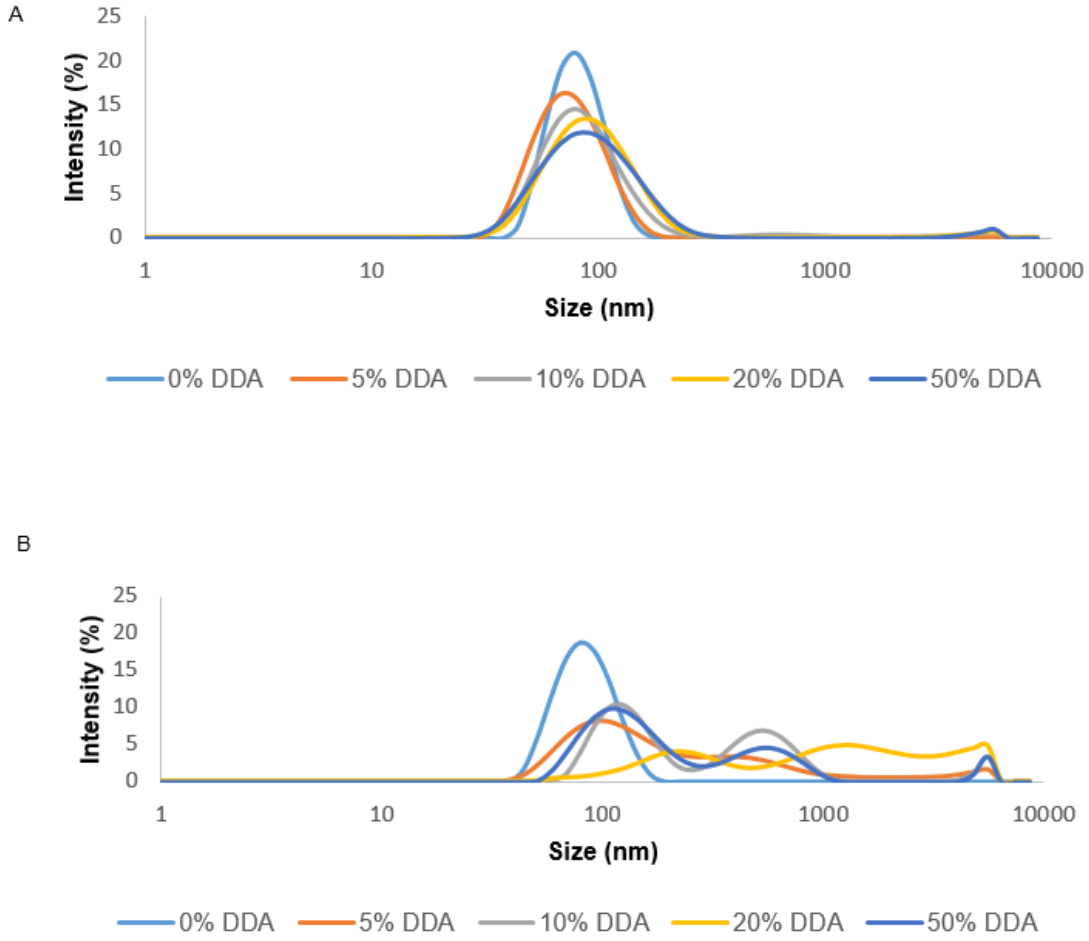

Figure 4.4 *The effect of cationic lipid concentration and purification method on size distribution of liposomes produced by microfluidics. DSPC:Cholesterol:DDA liposome formulations with increasing molar percentages of DDA were manufactured using microfluidics at a 3:1 FRR, 12 mL/min TFR and purified using (A) dialysis or (B) TFF with a final lipid concentration 0.5 mg/mL. Size distribution plots were obtained by DLS. Results represent mean ± SD, n = 3 independent batches.*

.

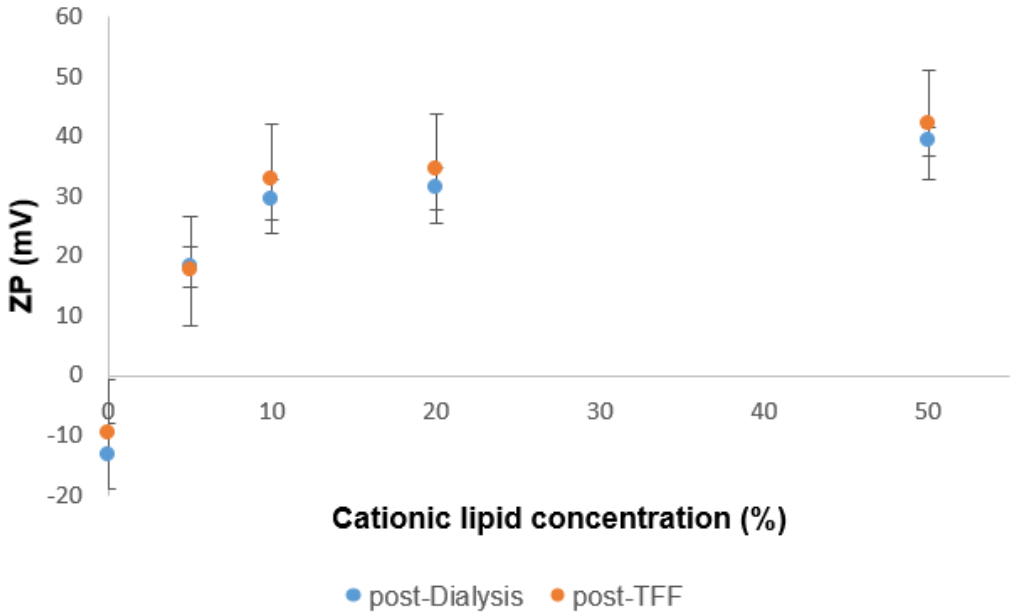

Figure 4.5 *The effect of cationic lipid concentration and purification method on zeta potential of liposomes produced by microfluidics. DSPC:Cholesterol:DDA liposome formulations with increasing molar percentages of DDA were manufactured using microfluidics at a 3:1 FRR, 12 mL/min TFR and purified using dialysis or TFF with a final lipid concentration 0.5 mg/mL. Purified liposomes were characterised in terms of zeta potential by DLS. Results represent mean ± SD, n = 3 independent batches.*

Table 4.3 *Lipid recovery in liposomes produced by microfluidics. DSPC:Cholesterol:DDA liposome formulations with increasing molar percentages of DDA were manufactured using microfluidics at a 3:1 FRR, 12 mL/min TFR and purified using dialysis or TFF with a final lipid concentration 0.5 mg/mL. Lipid recovery was calculated by fluorescense. Results represent mean ± SD, n = 3 independent batches.*

	Recovery (%)	
Cationic lipid concentration (%)	**Dialysis**	**TFF**
0	75 ± 4	106 ±11
5	64 ± 2	70 ± 3
10	66 ± 9	18 ± 31
20	101 ± 16	32 ± 56
50	72 ± 9	5 ± 9

4.5.2 The impact of sterilisation on liposomes characteristics

Given the potential interactions of the cationic liposomes with filter membranes, the impact of filter sterilisation was also tested. Liposomes consisting of DSPC, Cholesterol and DDA were formulated using the microfluidics method in a final concentration 0.5 mg/mL. TFR and FRR were constant for this part of the study (12 mL/min, 3:1). Samples were purified by dialysis or TFF and subject to sterile filtration.

As it is illustrated in Figure 4.6-Figure 4.13, sterile-filtration of liposomes can impact on the liposome physicochemical attributes and liposomes recovery. Figure 4.6-Figure 4.9 show the size and PDI of the various liposome formulations after purification and sterile filtration. In general, the liposomes attributes increase after sterilisation in terms of size and PDI irrespective if they were first purified by dialysis or TFF. This change in particle size attributes is also shown in the particle size distribution plots (Figure 4.10-Figure 4.11). The zeta potential was also notably changed after sterile filtration (Figure 4.12-Figure 4.13) with the zeta potential of the cationic liposomes being near neutral for all the cationic liposomes irrespective of their initial purification process. Whilst purification of liposomes by dialysis did not impact on liposome recovery, subsequent filter sterilisation resulted in notable losses in liposome concentration (Table 4.4) with recovery dropping to 3% even when low levels of cationic lipid is incorporated within the formulation. The combination of TFF and filter sterilisation also resulted in very low liposome recovery with a cumulative effect of losses during TFF and sterilisation (Table 4.4). These results confirmed that cationic liposomes should be purified by dialysis and could not be filter sterilised and as such for *in vivo* studies, aseptic methods were followed as much as possible.

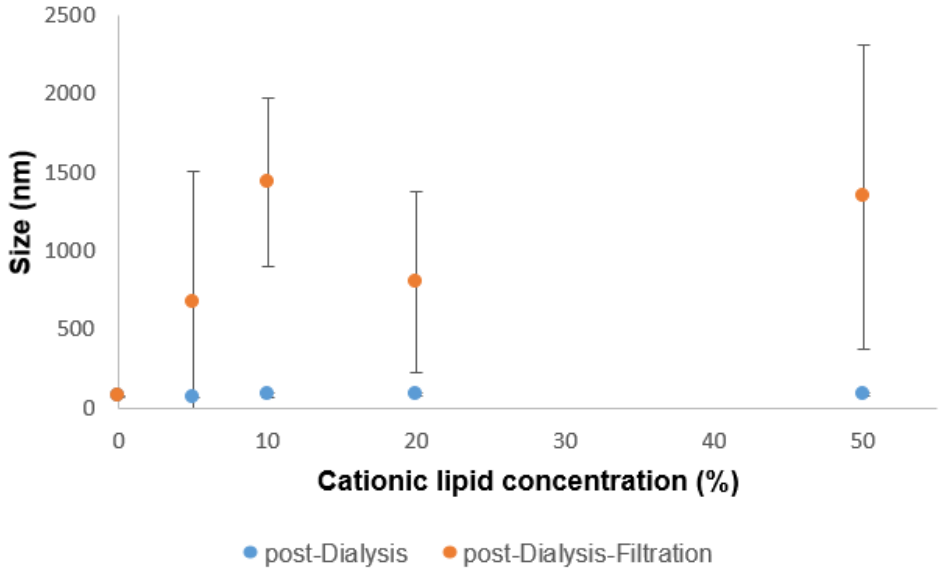

Figure 4.6 *The effect of filtration on size of liposomes purified by dialysis. DSPC:Cholesterol:DDA liposome formulations with increasing molar percentages of DDA were manufactured using microfluidics at a 3:1 FRR, 12 mL/min TFR, purified by dialysis and sterilised by filtration with a final lipid concentration 0.5 mg/mL. Sterilised liposomes were characterised in terms of size and PDI by DLS. Results represent mean ± SD, n = 3 independent batches.*

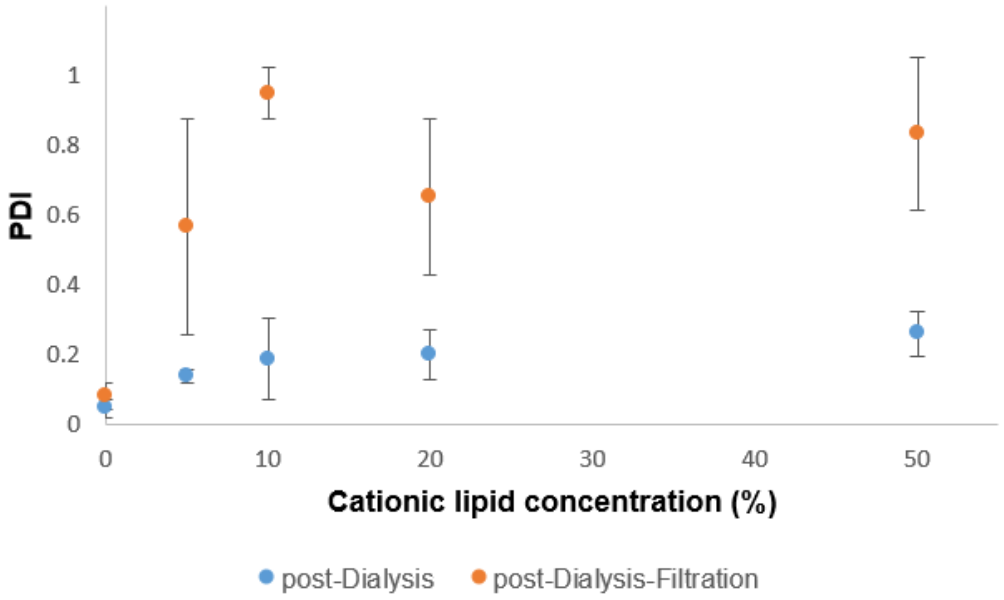

Figure 4.7 *The effect of filtration on PDI of liposomes purified by dialysis. DSPC:Cholesterol:DDA liposome formulations with increasing molar percentages of DDA were manufactured using microfluidics at a 3:1 FRR, 12 mL/min TFR, purified by dialysis and sterilised by filtration with a final lipid concentration 0.5 mg/mL. Sterilised liposomes were characterised in terms of size and PDI by DLS. Results represent mean ± SD, n = 3 independent batches.*

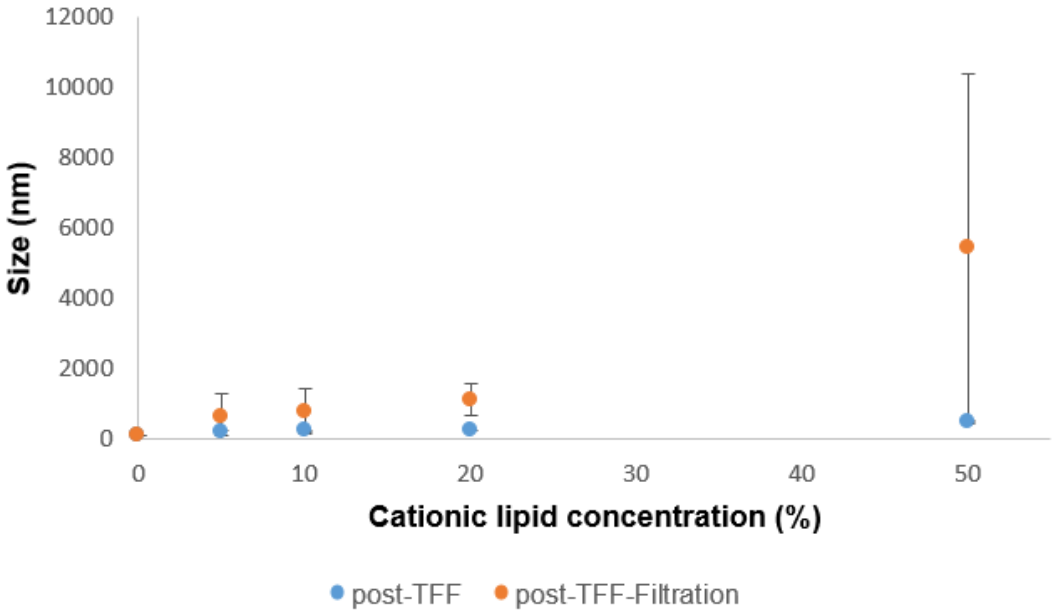

Figure 4.8 *The effect of filtration on size of liposomes purified by TFF. DSPC:Cholesterol:DDA liposome formulations with increasing molar percentages of DDA were manufactured using microfluidics at a 3:1 FRR, 12 mL/min TFR, purified by TFF and sterilised by filtration with a final lipid concentration 0.5 mg/mL. Sterilised liposomes were characterised in terms of size and PDI by DLS. Results represent mean ± SD, n = 3 independent batches.*

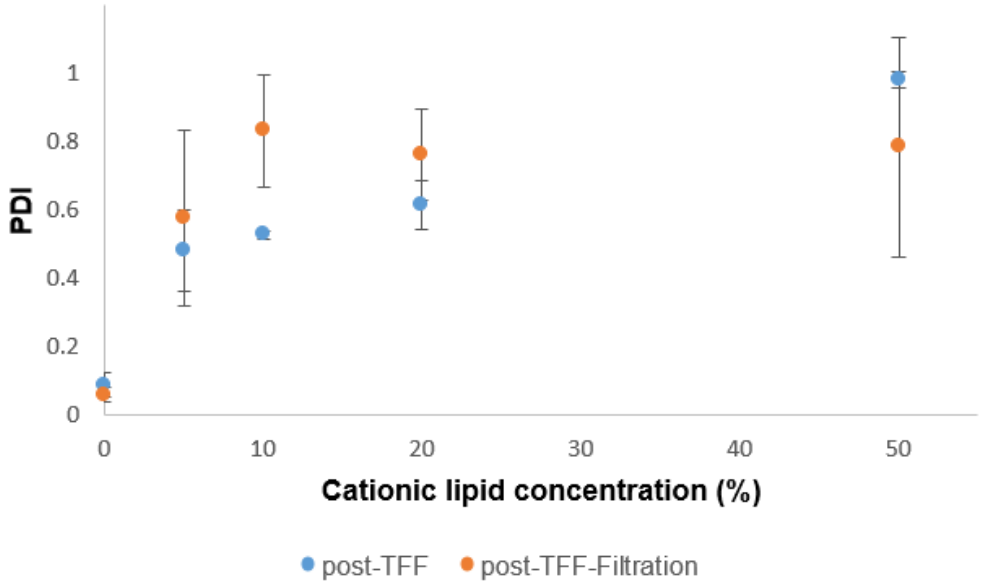

Figure 4.9 *The effect of filtration on PDI of liposomes purified by TFF. DSPC:Cholesterol:DDA liposome formulations with increasing molar percentages of DDA were manufactured using microfluidics at a 3:1 FRR, 12 mL/min TFR, purified by dialysis and sterilised by filtration with a final lipid concentration 0.5 mg/mL. Sterilised liposomes were characterised in terms of size and PDI by DLS. Results represent mean ± SD, n = 3 independent batches.*

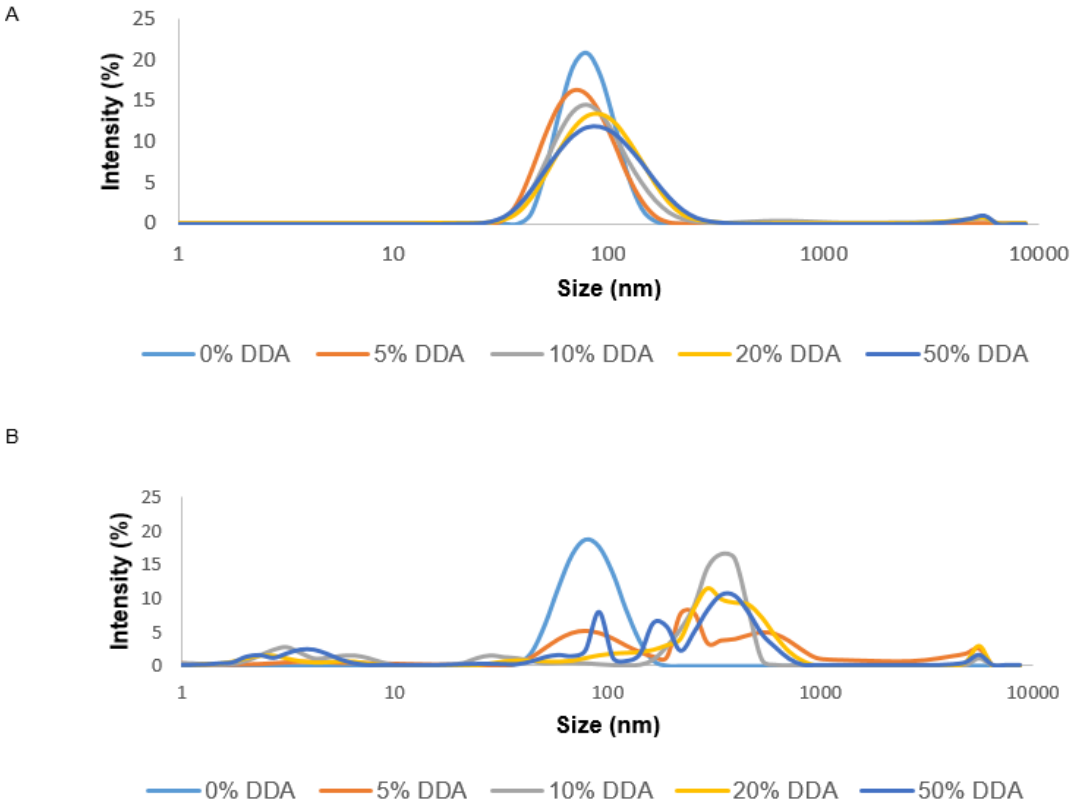

Figure 4.10 *The effect of filtration on size distribution of liposomes purified by dialysis. DSPC:Cholesterol:DDA liposome formulations with increasing molar percentages of DDA were manufactured using microfluidics at a 3:1 FRR, 12 mL/min TFR, purified by dialysis and sterilised by filtration with a final lipid concentration 0.5 mg/mL. Size distribution plots for (A) post-Dialysis (B) post-Dialysis-Filtration liposomes were obtained by DLS. Results represent mean ± SD, n = 3 independent batches.*

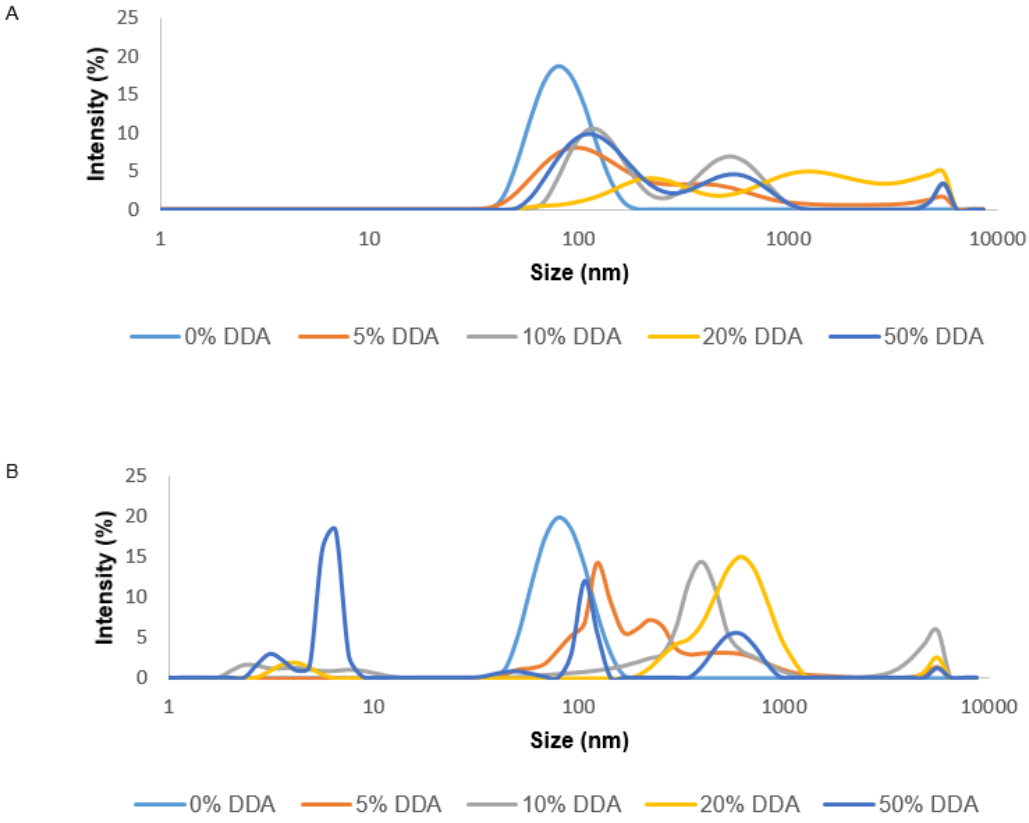

Figure 4.11 *The effect of filtration on size distribution of liposomes purified by TFF. DSPC:Cholesterol:DDA liposome formulations with increasing molar percentages of DDA were manufactured using microfluidics at a 3:1 FRR, 12 mL/min TFR, purified by TFF and sterilised by filtration with a final lipid concentration 0.5 mg/mL. Size distribution plots for (A) post-TFF (B) post-TFF-Filtration liposomes were obtained by DLS. Results represent mean ± SD, n = 3 independent batches.*

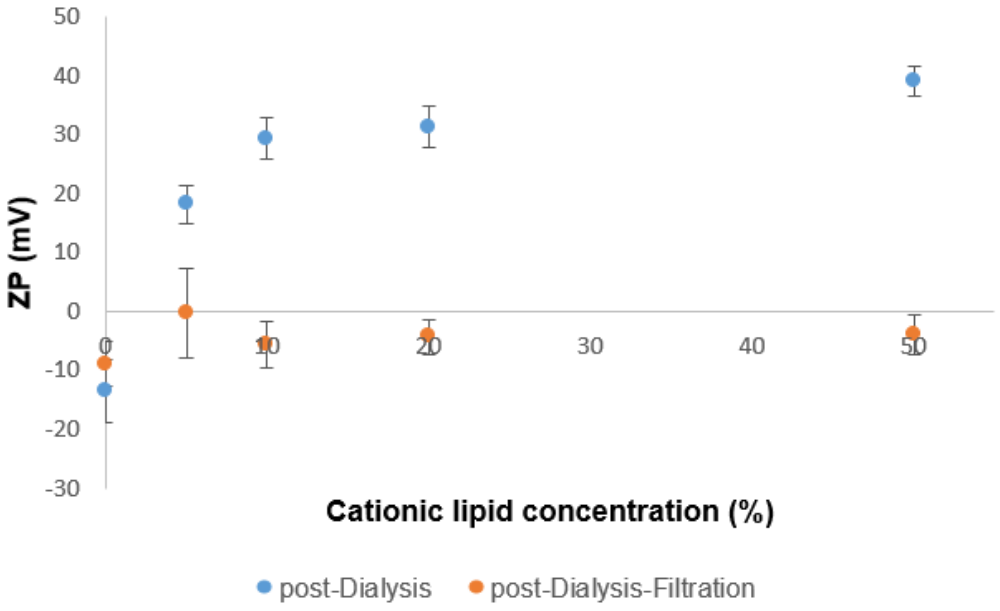

Figure 4.12 *The effect of filtration on zeta potential of liposomes purified by dialysis. DSPC:Cholesterol:DDA liposome formulations with increasing molar percentages of DDA were manufactured using microfluidics at a 3:1 FRR, 12 mL/min TFR, purified by dialysis and sterilised by filtration with a final lipid concentration 0.5 mg/mL. Sterilised liposomes were characterised in terms of zeta potential by DLS. Results represent mean ± SD, n = 3 independent batches.*

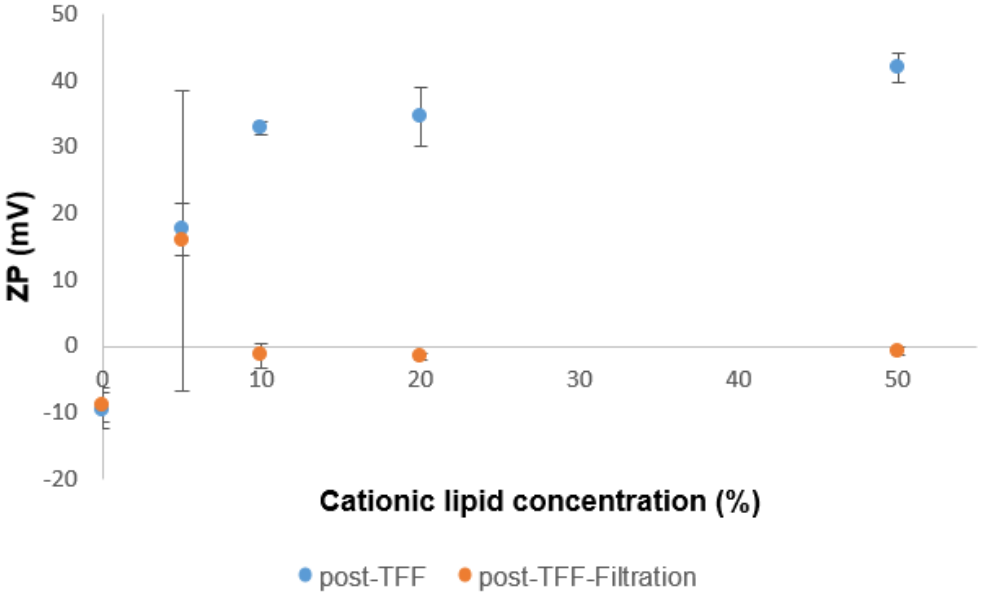

Figure 4.13 *The effect of filtration on zeta potential of liposomes purified by TFF. DSPC:Cholesterol:DDA liposome formulations with increasing molar percentages of DDA were manufactured using microfluidics at a 3:1 FRR, 12 mL/min TFR, purified by TFF and sterilised by filtration with a final lipid concentration 0.5 mg/mL. Sterilised liposomes were characterised in terms of zeta potential by DLS. Results represent mean ± SD, n = 3 independent batches.*

Table 4.4 *Impact of sterilisation on liposome recovery. DSPC:Cholesterol:DDA liposome formulations with increasing molar percentages of DDA were manufactured using microfluidics at a 3:1 FRR, 12 mL/min TFR and purified using dialysis or TFF with a final lipid concentration 0.5 mg/mL. Lipid recovery was calculated by fluorescense. Results represent mean ± SD, n = 3 independent batches.*

	Recovery (%)	
Cationic lipid concentration (%)	**Dialysis/Filtration**	**TFF/Filtration**
0	63 ±15	80 ±18
5	3 ± 22	0 ±13
10	0 ± 2	0 ±10
20	0 ± 4	0 ±12
50	0 ± 7	0 ±83

4.5.3 The impact of manufacturing conditions on the liposomes characteristics

Given the method of purification and removal of solvent had been identified, the next step was to consider the impact of the manufacturing conditions used within microfluidics. To achieve this, liposomes consisting of DSPC, Cholesterol and DDA were formulated using the microfluidics method by varying the FRR between 3:1 and 1:1, in a final concentration of 10 mg/mL. TFR was constant for this part of the study (12 mL/min) and samples were purified by dialysis.

As it is shown in Figure 4.14, when a flow rate ratio of 3:1 was used compared to 1:1, a significant ($p<0.05$) reduction of liposome size with the vesicle size changing from 164 nm to 131 nm for 3:1 and 1:1, respectively. However, increasing the FRR also resulted in a significant increase ($p<0.05$) in PDI values with a FRR 1:1 giving the lowest value (0.07) compared to FRR 3:1 (0.3) indicating that 1:1 gives larger particles but a more homogeneous size distribution compared to particles prepared at a FRR of 3:1. This is also confirmed by the size distribution plots (Figure 4.15). In both cases, liposomes were positively charged in terms of zeta potential with values ranging between 30-40 mV (Figure 4.16) and lipid recovery after dialysis was around 80% indicating no notable liposome loss (Table 4.5).

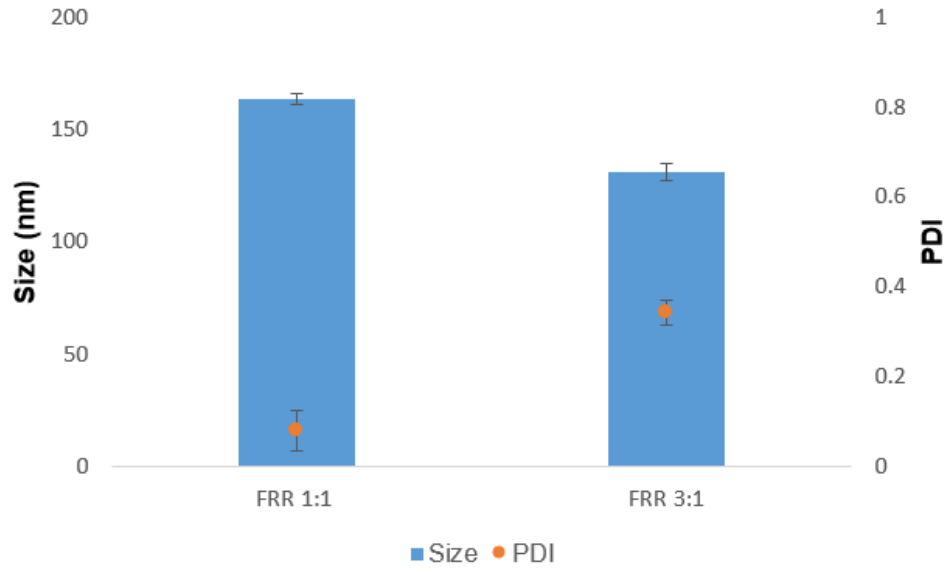

Figure 4.14 *The effect of FRR on size and PDI of liposomes produced by microfluidics. DSPC:Cholesterol:DDA (10:40:50% molar ratio) liposome were manufactured using microfluidics at 1:1 or 3:1 FRR, 12 mL/min TFR and purified using dialysis with a final lipid concentration 10 mg/mL. Purified liposomes were characterised in terms of size and PDI by DLS. Results represent mean ± SD, n = 3 independent batches.*

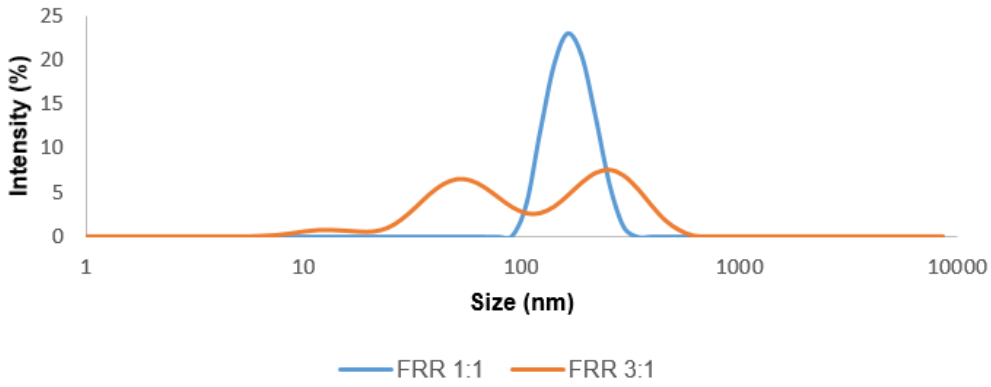

Figure 4.15 *The effect of FRR on size distribution of liposomes produced by microfluidics. DSPC:Cholesterol:DDA (10:40:50% molar ratio) liposome were manufactured using microfluidics at 1:1 or 3:1 FRR, 12 mL/min TFR and purified using dialysis with a final lipid concentration 10 mg/mL. Size distribution plots were obtained by DLS. Results represent mean ± SD, n = 3 independent batches.*

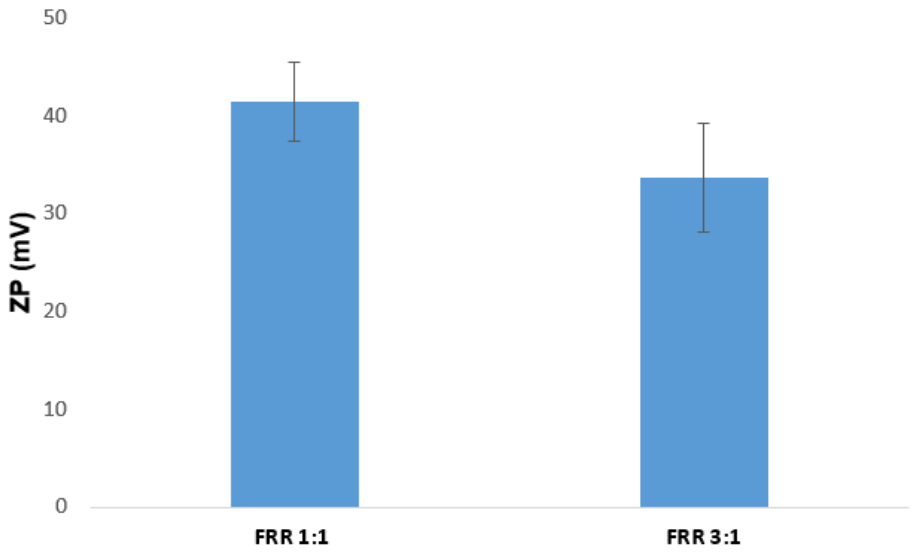

Figure 4.16 *The effect of FRR on zeta potential of liposomes produced by microfluidics. DSPC:Cholesterol:DDA (10:40:50% molar ratio) liposome were manufactured using microfluidics at 1:1 or 3:1 FRR, 12 mL/min TFR and purified using dialysis with a final lipid concentration 10 mg/mL. Purified liposomes were characterised in terms of zeta potential by DLS. Results represent mean ± SD, n = 3 independent batches.*

Table 4.5 *Lipid recovery in liposomes produced by microfluidics. DSPC:Cholesterol:DDA (10:40:50% molar ratio) liposome formulations were manufactured using microfluidics at 1:1 or 3:1 FRR, 12 mL/min TFR and purified using dialysis with a final lipid concentration 10 mg/mL. Lipid recovery was calculated by fluorescense. Results represent mean ± SD, n = 3 independent batches.*

FRR		Recovery (%)
1:1	Dialysis	78 ± 5
3:1	Dialysis	80 ± 7

4.5.4 Short-term stability of liposomes

The physical appearance of DSPC: Cholesterol: DDA liposomal formulations stored at 4 °C for 1 week was evaluated to evaluate their short-term stability. The results in Figure 4.17 demonstrate that after 7 days, all liposome formulations were stable. No visual changes in the colour and viscosity of the liposomal suspension was observed. In addition, test of liposomes characteristics by DLS demonstrated that size, zeta potential and also size distribution of formulations remained the same in all the sample concentrations tested (Figure 4.17-Figure 4.19).

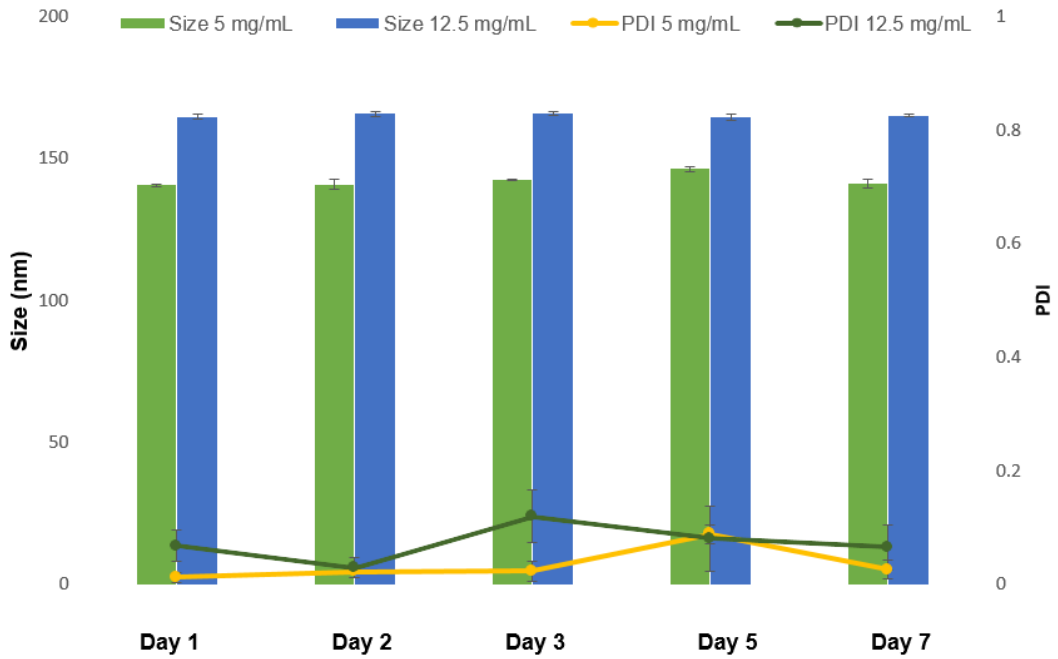

Figure 4.17 *Short-term stability of liposomes. DSPC:Cholesterol:DDA (10:40:50% molar ratio) liposome were manufactured using microfluidics at a 1:1 FRR, 12 mL/min TFR and purified using dialysis with a final lipid concentration of 5 and 12.5 mg/mL. Purified liposomes were characterised in terms of size and PDI by DLS. Results represent mean ± SD, n = 3 independent batches.*

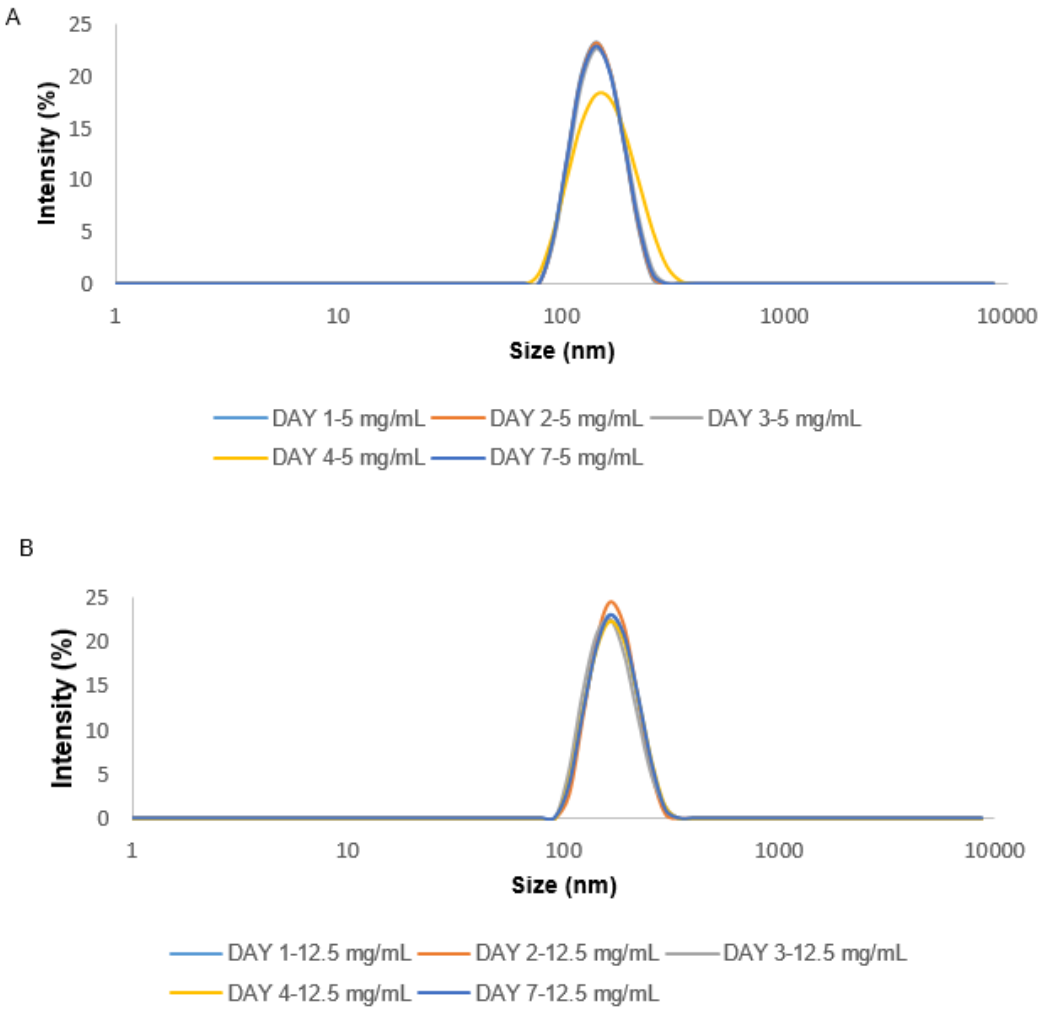

Figure 4.18 *Short-term stability of liposomes. DSPC:Cholesterol:DDA (10:40:50% molar ratio) liposome were manufactured using microfluidics at a 1:1 FRR, 12 mL/min TFR and purified using dialysis with a final lipid concentration of (A) 5 and (B) 12.5 mg/mL. Size distribution plots were obtained by DLS. Results represent mean ± SD, n = 3 independent batches.*

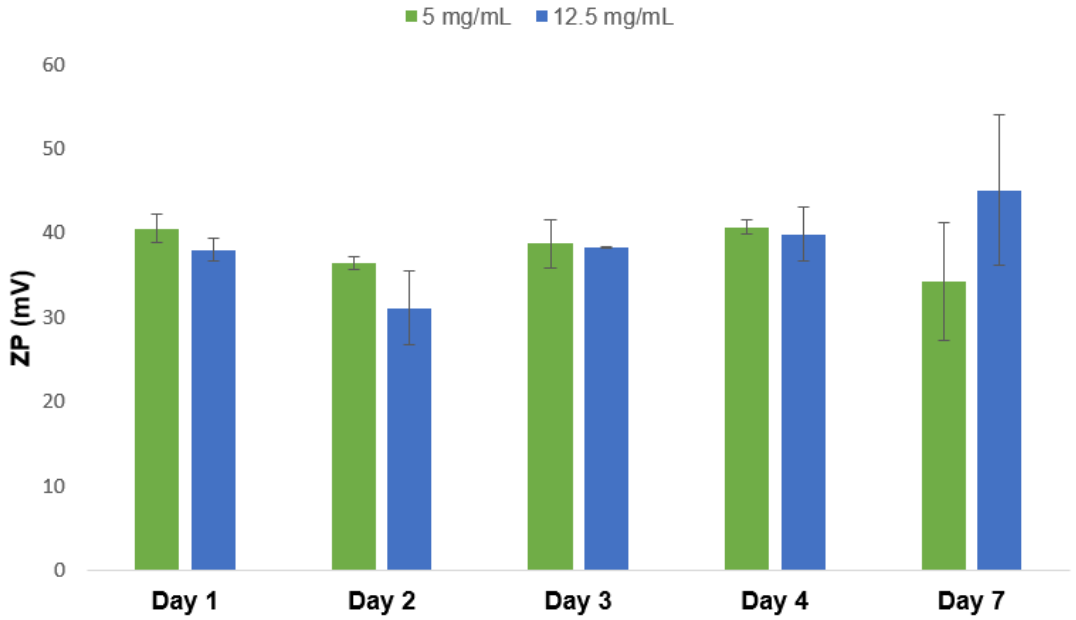

Figure 4.19 *Short-term stability of liposomes. DSPC:Cholesterol:DDA (10:40:50% molar ratio) liposome were manufactured using microfluidics at a 1:1 FRR, 12 mL/min TFR and purified using dialysis with a final lipid concentration of 5 and 12.5 mg/mL. Purified liposomes were characterised in terms of zeta potential by DLS. Results represent mean ± SD, n = 3 independent batches.*

4.5.5 The impact of protein-liposome ratio on liposomes characteristics

Given that the manufacture, purification and short-term stability of the liposome formulations had been confirmed, the next step was to investigate their ability to electrostatically absorb protein antigens. Cationic liposomes have been previously reported to be able to adsorb and deliver electrostatically adsorbed antigen, however the amount of protein loaded has been shown to impact on the particle size (Hamborg *et al.*, 2014). Therefore within these studies, three proteins were studied: OVA (MW 45 kDa, pI=4.5), GBS67 (MW 98 kDa, pI=6.46) and CRM197 (58 kDa, pI=5.85) and a fix final liposome concentration of 0.25 mg/mL was used (equivalent to 315 µg of cationic lipid).

Surface association studies demonstrated that the size of particles increased with increased amounts of protein used for all the proteins tested (Figure 4.20). In the case of OVA, liposomes started aggregating for amount of protein higher than 10 µg indicating saturation for liposomes: OVA weight/weight ratio lower than 1:5 (w/w). This increase in size corresponded with an increase in PDI values where values around 0.6 obtained (Figure 4.21) and size distribution (Figure 4.22). Similar results obtained

with CRM197 protein where PDI values and size distribution indicated different size populations in the solution and thus non-uniform particle formation. Interestingly, GBS67-liposomes particles demonstrated uniformity across the range of protein amount tested with particles having a size between the range 145-170 nm (Figure 4.20) and PDI values of 0.02-0.09 (Figure 4.21) with no change in size distribution noted over the concentration range tested (Figure 4.22).

With an increase in ratio of anionic protein to cationic liposomes, the zeta potential decreased from 40 mV to 10 mV for OVA and GBS67, where the lowest zeta potential value for CRM197 obtained was 31 mV at 20 µg (Figure 4.23). Interestingly whilst GBS67 showed the least impact on overall particle size of the liposome-protein complexes, it did results in the greatest reduction in zeta potential compared to OVA and CRM197 (Figure 4.23).

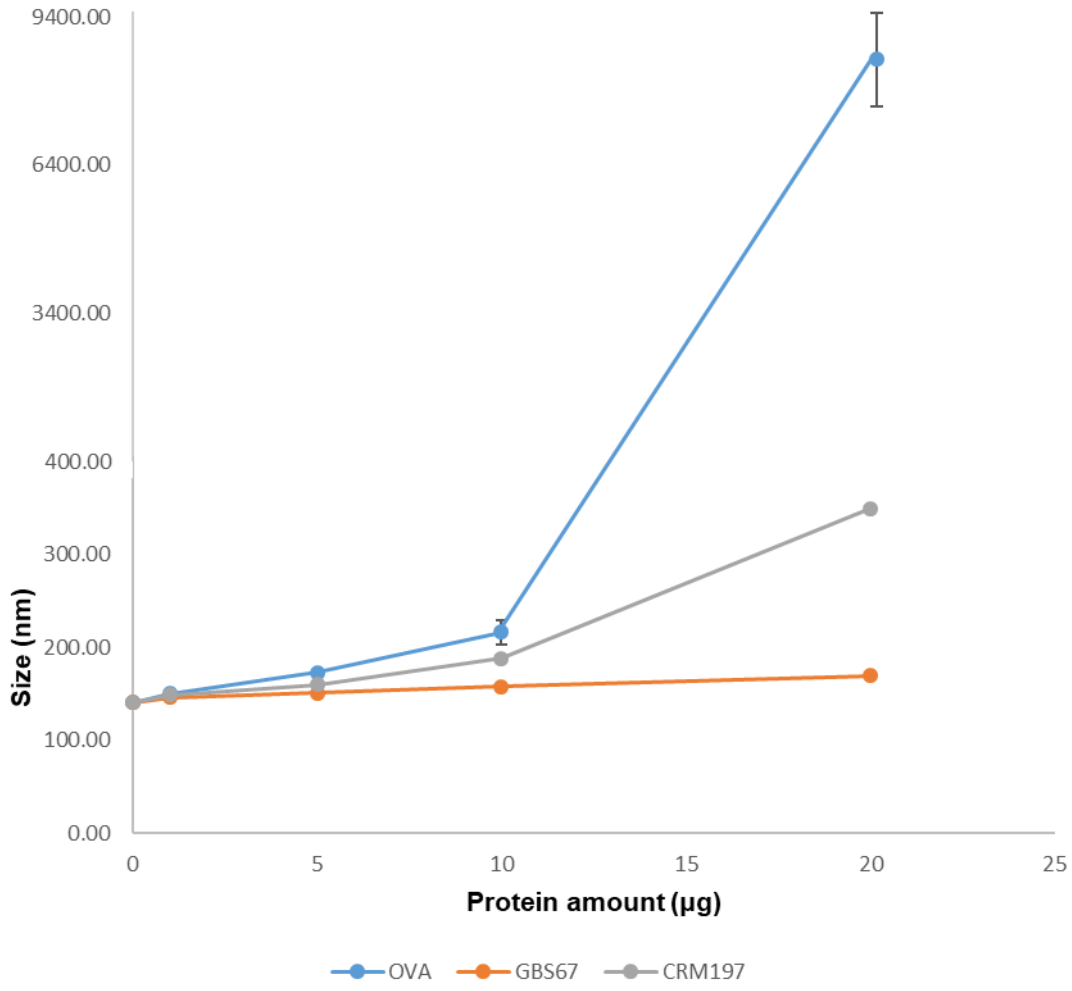

Figure 4.20 *The effect of protein loading on liposomes size. DSPC:Cholesterol:DDA (10:40:50% molar ratio) liposome were manufactured using microfluidics at 1:1 FRR, 12 mL/min TFR and purified using dialysis. Liposomes were mixed with different amounts of protein and purified by dialysis. The final liposome concentration in all the samples was constant (0.25 mg/mL). Liposomes adsorbed protein were characterised in terms of size and PDI by DLS. Results represent mean ± SD, n = 3 independent batches.*

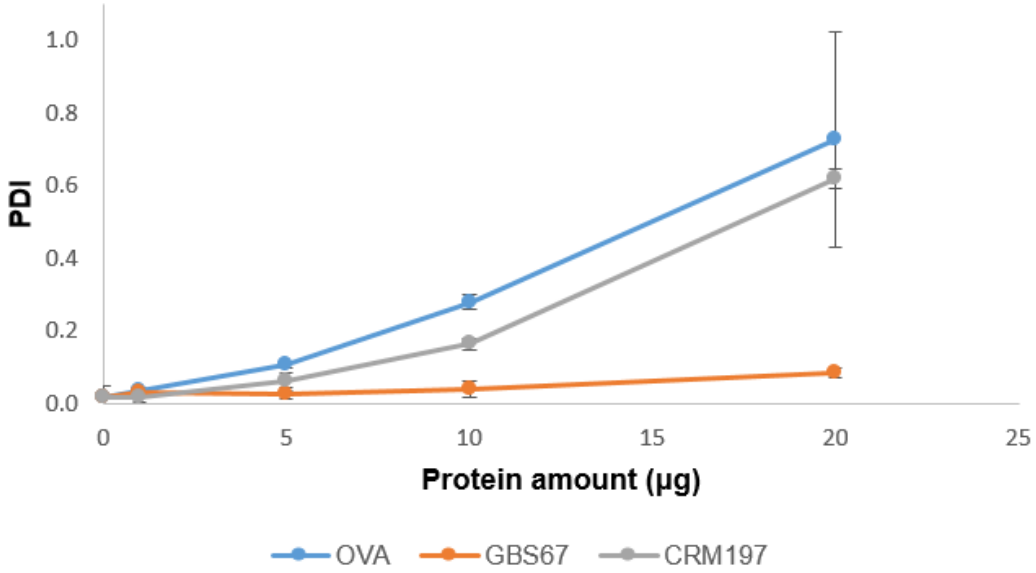

Figure 4.21 *The effect of protein loading on liposomes PDI. DSPC:Cholesterol:DDA (10:40:50% molar ratio) liposome were manufactured using microfluidics at 1:1 FRR, 12 mL/min TFR and purified using dialysis. Liposomes were mixed with different amounts of protein and purified by dialysis. The final liposome concentration in all the samples was constant (0.25 mg/mL). Liposomes adsorbed protein were characterised in terms of size and PDI by DLS. Results represent mean ± SD, n = 3 independent batches.*

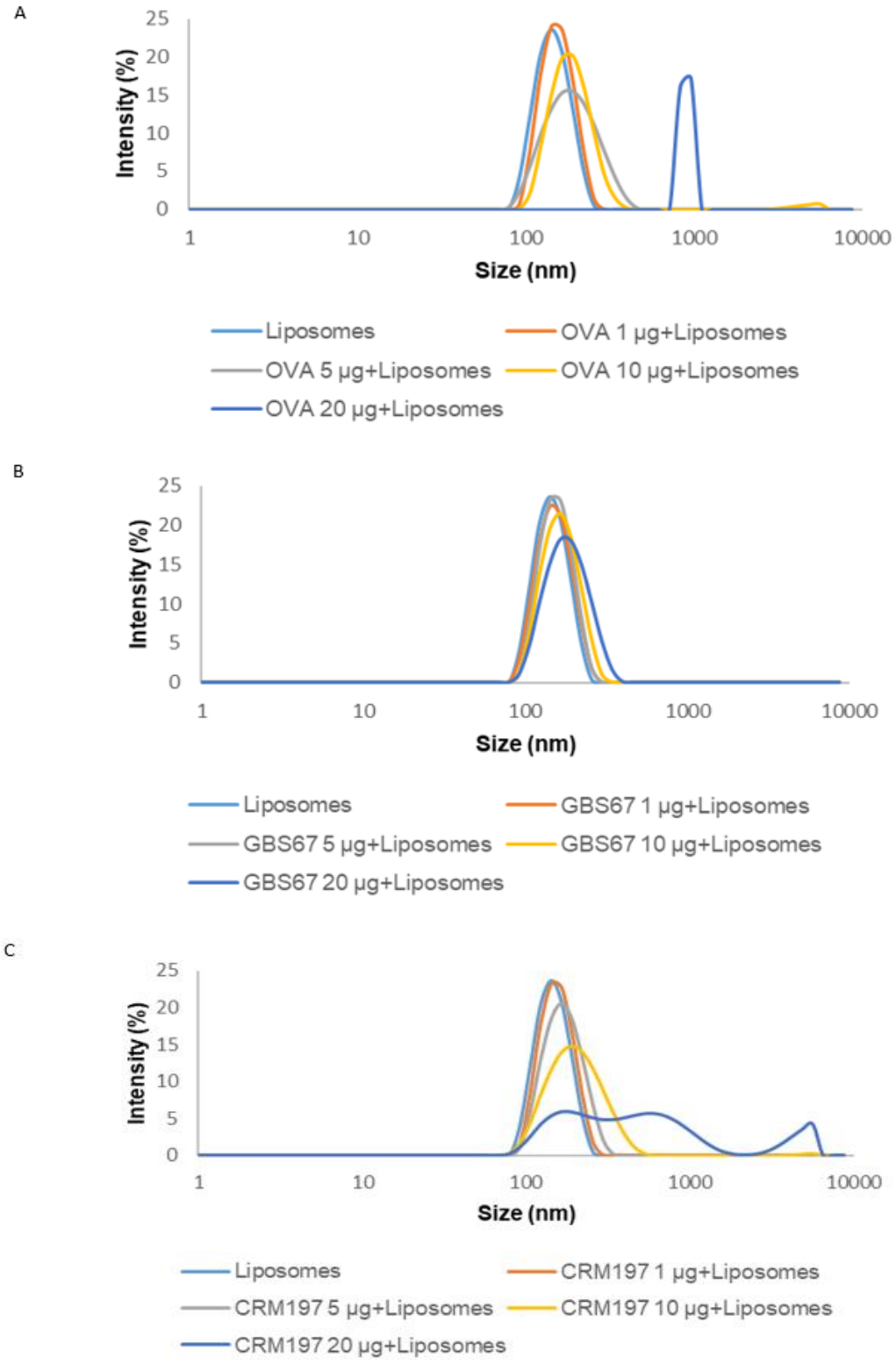

Figure 4.22 *The effect of protein loading on size distribution of liposomes using (A) OVA (B) GBS67 and (C) CRM197 proteins. DSPC:Cholesterol:DDA (10:40:50% molar ratio) liposome were manufactured using microfluidics at 1:1 FRR, 12 mL/min TFR and purified using dialysis. Liposomes were mixed with different amounts of protein and purified by dialysis. The final liposome concentration in all the samples was constant (0.25 mg/mL). Size distribution plots were obtained by DLS. Results represent mean ± SD, n = 3 independent batches.*

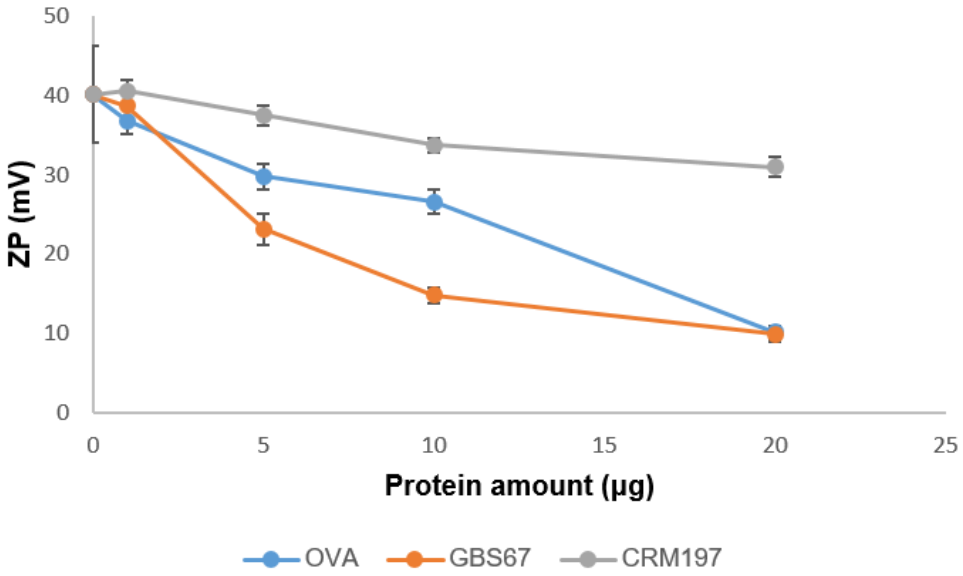

Figure 4.23 *The effect of protein loading on zeta potential of liposomes. DSPC:Cholesterol:DDA (10:40:50% molar ratio) liposome were manufactured using microfluidics at 1:1 FRR, 12 mL/min TFR and purified using dialysis. Liposomes were mixed with different amounts of protein and purified by dialysis. The final liposome concentration in all the samples was constant (0.25 mg/mL). Liposomes were characterised in terms of zeta potential by DLS. Results represent mean ± SD, n = 3 independent batches.*

4.5.6 Association of protein with liposomes

The final stage in building the liposomal adjuvants was to consider the addition of CpGODN. After confirming the adsorption of free protein on liposomes surface, protein-CpGODN conjugate adsorption was attempted and the characteristics and behaviour of liposomes were investigated (represented by yellow bars; Figure 4.24-Figure 4.27). A physical mixture of CpGODN with protein was also added in one of liposome formulations as control (represented by grey bars). The mixture of CpGODN, protein and liposomes has been previously tested with success (Kovacs-Nolan *et al.*, 2009; de Titta *et al.*, 2013; Zhao *et al.*, 2014). In all the samples tested, the final concentrations of liposomes (5 mg/mL), protein (0.25 mg/mL) and CpGODN (0.038 mg/mL) were equal.

Adsorption of the negatively charged protein and CpGODN onto the cationic liposomes surface resulted in the increase of liposomes size and reduction of their surface charge as expected (Figure 4.24). The highest increase in size was observed for the protein+liposomes+CpGODN for all the protein tested. Interestingly, almost no size increase was obtained when protein conjugate was mixed with DSPC:

Cholesterol: DDA liposomes with the size remaining at 136 nm (Figure 4.24). PDI values were lower than 0.3 across the formulation range tested which in conjunction with size distribution indicate uniform particles (Figure 4.25-Figure 4.26). The lowest zeta potential measurements were observed when liposomes were mixed with protein alone for all the proteins (Figure 4.27). On the other hand, when liposomes mixed with protein conjugates a 10 mV reduction was noticed from 41 mV to 31 mV for free liposomes and protein conjugates, respectively. Regarding the protein and CpGODN loading on proteins, more than 90% protein and CpGODN loading was achieved for all the formulations tested (Table 4.6).

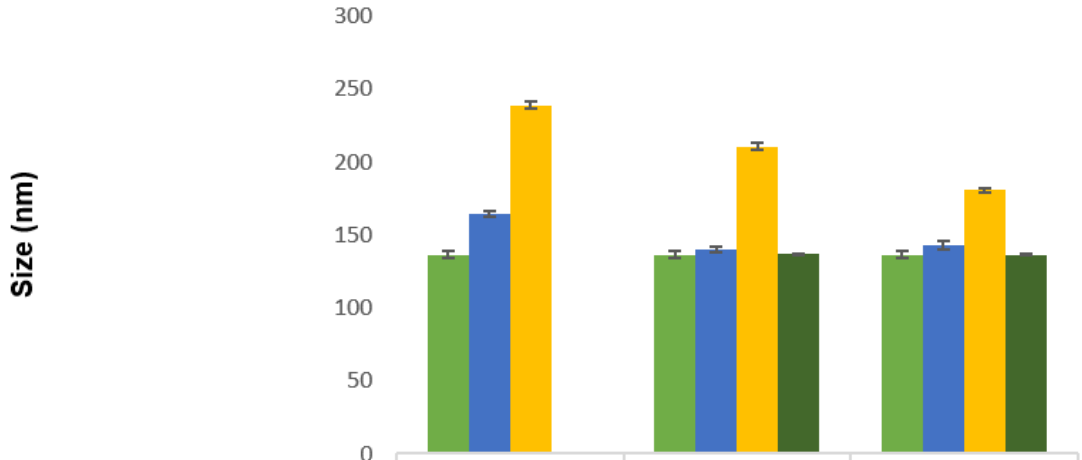

	OVA	GBS67	CRM197
Liposomes	136.33	136.33	136.33
Protein+Liposomes	164.43	139.90	142.80
Protein+Liposomes+CpGODN	238.73	210.40	180.57
Protein-CpGODN+Liposomes	0	136.73	136.43

Figure 4.24 *The effect of CpGODN loading on size of liposomes. DSPC:Cholesterol:DDA (10:40:50% molar ratio) liposome were manufactured using microfluidics at 1:1 FRR, 12 mL/min TFR and purified using dialysis. Liposomes were mixed with free protein, protein+CpGODN mixture or protein-CpGODN conjugate and purified by dialysis. The final liposome (5 mg/mL), protein (0.25 mg/mL) and CpGODN (0.038 mg/mL) concentrations in all the samples were the same. Liposomes were characterised in terms of size and PDI by DLS. Results represent mean ± SD, n = 3 independent batches.*

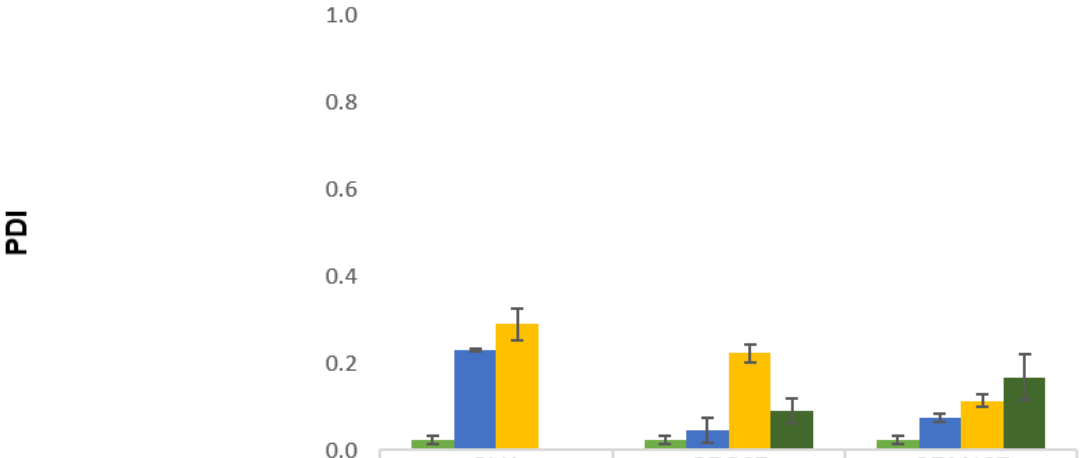

	OVA	GBS67	CRM197
Liposomes	0.02	0.02	0.02
Protein+Liposomes	0.23	0.05	0.07
Protein+Liposomes+CpGODN	0.29	0.22	0.11
Protein-CpGODN+Liposomes	0	0.09	0.17

Figure 4.25 *The effect of CpGODN loading on PDI of liposomes. DSPC:Cholesterol:DDA (10:40:50% molar ratio) liposome were manufactured using microfluidics at 1:1 FRR, 12 mL/min TFR and purified using dialysis. Liposomes were mixed with free protein, protein+CpGODN mixture or protein-CpGODN conjugate and purified by dialysis. The final liposome (5 mg/mL), protein (0.25 mg/mL) and CpGODN (0.038 mg/mL) concentrations in all the samples were the same. Liposomes were characterised in terms of size and PDI by DLS. Results represent mean ± SD, n = 3 independent batches.*

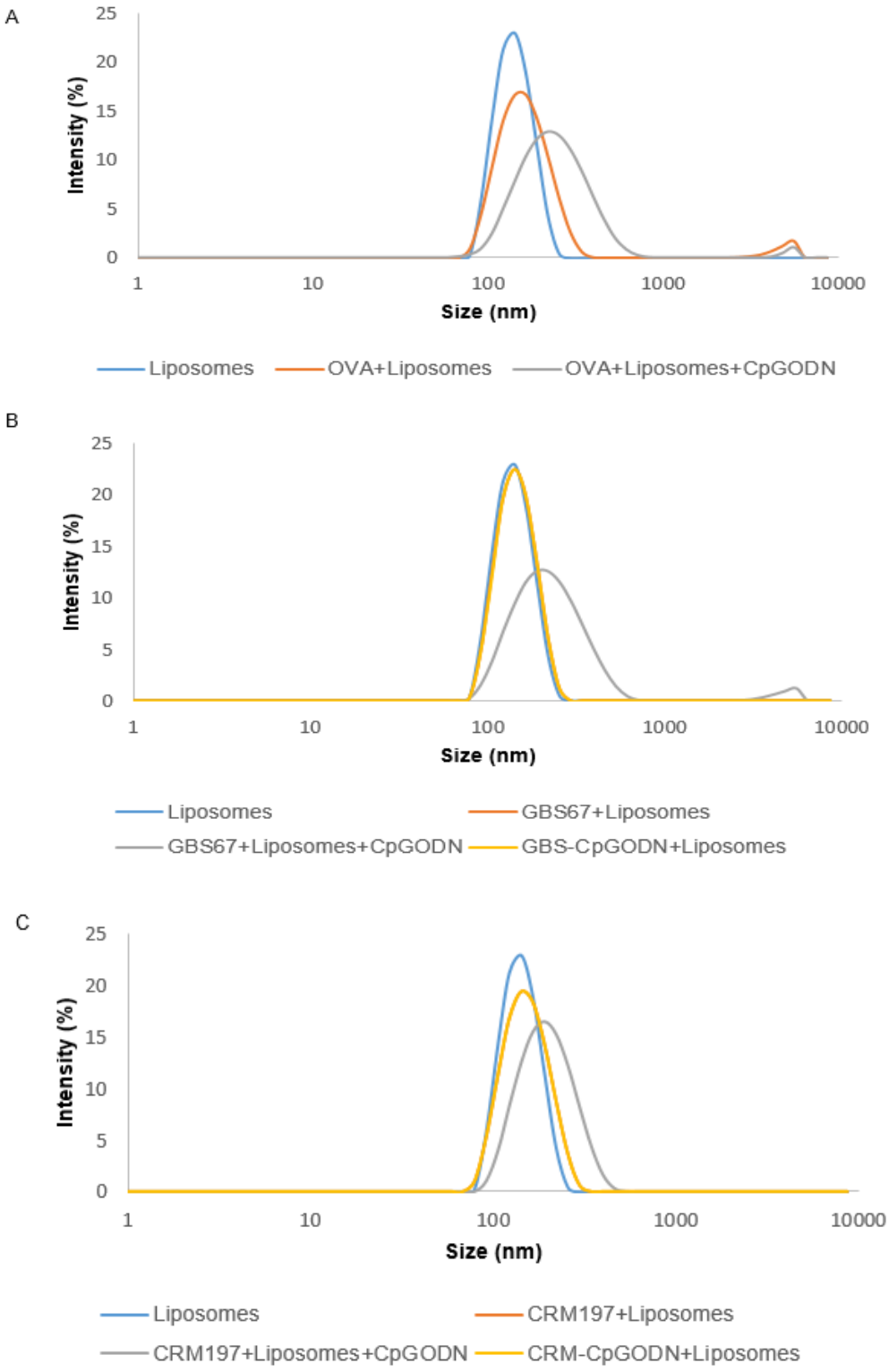

Figure 4.26 *The effect of CpGODN loading on size distribution of liposomes using (A) OVA (B) GBS67 and (C) CRM197 proteins. DSPC:Cholesterol:DDA (10:40:50% molar ratio) liposome were manufactured using microfluidics at 1:1 FRR, 12 mL/min TFR and purified using dialysis. Liposomes were mixed with free protein, protein+CpGODN mixture or protein-CpGODN conjugate and purified by dialysis. The final liposome (5 mg/mL), protein (0.25 mg/mL) and CpGODN (0.038 mg/mL) concentrations in all the samples were the same. Size distribution plots were obtained by DLS. Results represent mean ± SD, n = 3 independent batches.*

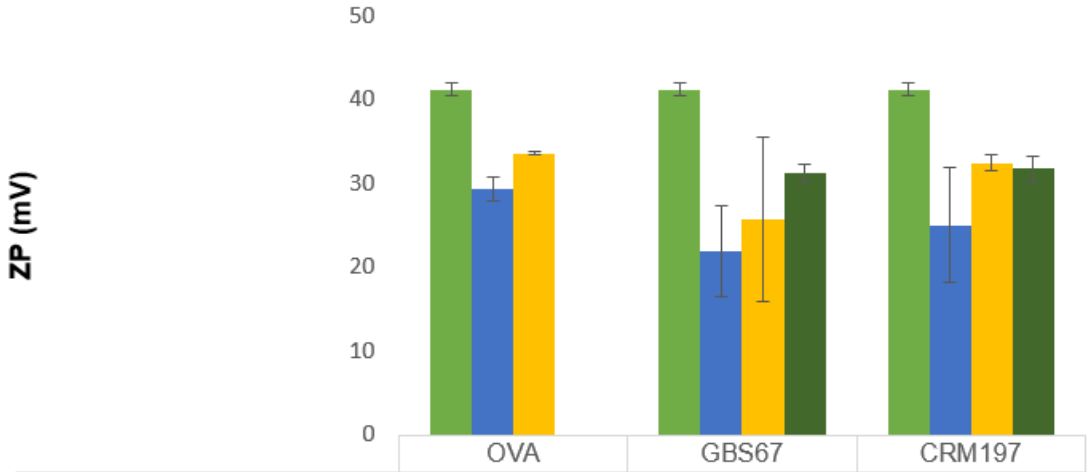

	OVA	GBS67	CRM197
Liposomes	41.3	41.3	41.3
Protein+Liposomes	29.4	22.0	25.0
Protein+Liposomes+CpGODN	33.6	25.8	32.5
Protein-CpGODN+Liposomes	0.0	31.4	31.8

Figure 4.27 *The effect of CpGODN loading on zeta potential of liposomes. DSPC:Cholesterol:DDA (10:40:50% molar ratio) liposome were manufactured using microfluidics at 1:1 FRR, 12 mL/min TFR and purified using dialysis. Liposomes were mixed with free protein, protein+CpGODN mixture or protein-CpGODN conjugate and purified by dialysis. The final liposome (5 mg/mL), protein (0.25 mg/mL) and CpGODN (0.038 mg/mL) concentrations in all the samples were the same. Liposomes were characterised in terms of zeta potential by DLS. Results represent mean ± SD, n = 3 independent batches.*

Table 4.6 *Protein and CpGODN loading on liposomes. DSPC:Cholesterol:DDA (10:40:50% molar ratio) liposome were manufactured using microfluidics at 1:1 FRR, 12 mL/min TFR and purified using dialysis. Liposomes were mixed free with protein, protein+CpGODN mixture or protein-CpGODN conjugate and purified by dialysis. The final (5 mg/mL), protein (0.25 mg/mL) and CpGODN (0.038 mg/mL) concentrations in all the samples were the same. Protein and CpGODN quantification was carried out by BCA and UV, respectively. Results represent mean ± SD, n = 3 independent batches.*

Protein	Formulation	Protein loading (%)	CpGODN loading (%)
OVA	Protein+Liposomes	91 ± 3	-
	Protein+Liposomes+CpGODN	93 ± 8	93 ± 9
	Protein-CpGODN+Liposomes	-	-
GBS67	Protein+Liposomes	96 ± 3	-
	Protein+Liposomes+CpGODN	95 ± 1	96 ± 5
	Protein-CpGODN+Liposomes	95 ± 3	96 ± 1
CRM197	Protein+Liposomes	90 ± 3	-
	Protein+Liposomes+CpGODN	92 ± 4	93 ± 4
	Protein-CpGODN+Liposomes	96 ± 1	98 ± 1

4.5.7 Liposome morphology

The structure and morphology of the liposomes and GBS67-CpGODN+liposomes complexes have been evaluated by using transmission electron microscopy techniques. For that purpose, cryo-TEM experiments were run for samples of DSPC: Cholesterol: DDA liposomes and DSPC: Cholesterol: DDA protein conjugate complex at protein ratio 1:50 w/w. Cryo-TEM characterisation of free liposomes (Figure 4.28A) reveal the presence of a homogeneous population of unilamellar spherical liposomes, characterised by an average diameter of around 100 nm and size distribution that matched with DLS measurements. The formation of protein conjugate-liposome complexes induces a clear change in liposome morphology (Figure 4.28B). Analysis revealed a rich distribution of complex morphologies, from unilamellar conjugate coated liposomes to multilamellar lipoplexes. The formation of cluster-like structures coexisting with more elongated lipid structures including several intermediate morphologies was also observed. In all of the cases, the protein conjugate-coated liposomes show diameters of around 100-120 nm indicating that the addition of GBS67-CpGODN mainly affects the structure and morphology of the liposome but not its size. Finally, the presence of protein conjugate on liposomes surface caused increase of the thickness bilayer of the vehicles compared to the normal bilayer thickness observed (Figure 4.28A).

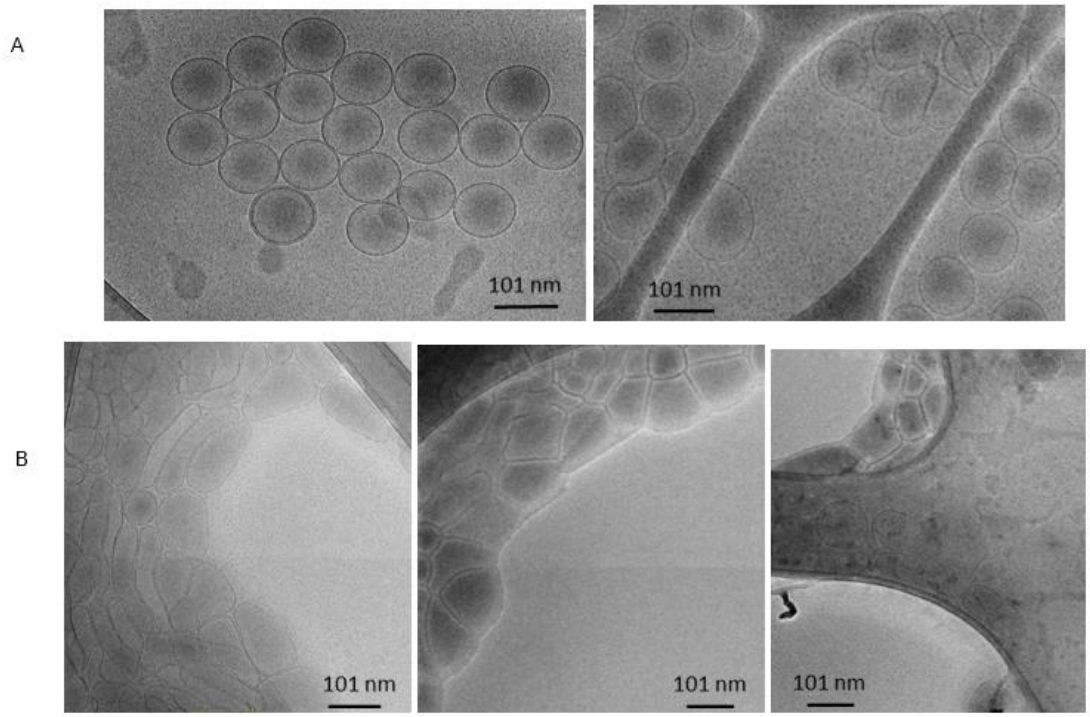

Figure 4.28 *The effect of GBS67-CpGODN adsorption on liposomes morphology. Cryo-EM images of liposomes (A) before and (B) after protein-conjugate adsorption. DSPC:Cholesterol:DDA (10:40:50% molar ratio) liposome were manufactured using microfluidics at 1:1 FRR, 12 mL/min TFR and purified using dialysis. GBS67-CpGODN was mixed with liposomes at 1:50 w/w. The final liposome and GBS67-CpGODN conjugate concentrations in the sample were 5 mg/mL and 0.1 mg/mL , respectively. Scale bars, 101 nm.*

4.6 Discussion

In the present chapter, DSPC: Cholesterol: DDA cationic liposomal formulations were prepared using microfluidics. Overall, microfluidics offers a rapid, reproducible and scalable manufacturing process for nanoparticles including liposomes (Belliveau *et al.*, 2012; Zhigaltsev *et al.*, 2012). Initially, the impact of cationic composition and purification method was tested in order to decide the cationic lipid ratio as also the preferable purification method will be used for the upcoming studies. It was demonstrated that the cationic lipid ratio has a significant impact only on the zeta potential and not on the size and size distribution of particles. Interestingly, a small increase in size observed from low molar ratio of DDA cationic lipid which was then stabilised at higher DDA molar ratios possibly due to electrostatic interactions occur among lipid head groups which are increasing by increased charge (Lombardo *et al.*, 2016). Results were as expected as cationic charge increases by increasing cationic lipid concentration as has been reported previously (Bose *et al.*, 2015; Lou *et al.*, 2019). Studies contacted by Lou *et al*. evidenced that the increase of cationic content

on liposomes in low ionic strength aqueous phases did not cause major changes in particle size (Lou *et al.*, 2019).

To purify the liposomes, two methods were tested, TFF and dialysis, and results demonstrated purification using TFF is not suitable for purification of cationic liposomes. It is assumed that cationic liposomes interact with the TFF column, which is composed of Polyethersulfone (PES) which is anionic in nature and may results in electrostatic interaction/fouling of the membrane and hence low recovery. Such electrostatic interactions do not occur with dialysis membranes, which are composed of cellulose acetate. Indeed, previous studies using this cross-flow TFF system have only been used successfully for purification of neutral and anionic particles and cationic formulations were not considered (Forbes *et al.*, 2019). Furthermore, a prototype method compatible with cationic liposomes has been reported in the literature where microfluidics werecoupled with TFF for a continuous manufacture and purification of liposomes using exchangeable cellulose membranes (van Reis and Zydney, 2007; Dimov *et al.*, 2017). The membrane used in this set-up is similar to the dialysis membrane used within the studies in this chapter and suggests it may be applicable for the DSPC: Cholesterol: DDA formulations being developed. However, although this prototype TFF method allowed high particle recovery, the PDI values obtained were higher than the ones can be achieved using dialysis as has been demonstrated by others (Kastner *et al.*, 2014; Joshi *et al.*, 2016; Lou *et al.*, 2019). In contrast with TFF, dialysis had no impact on liposome characteristics and 100% particles recovery was achieved after purification. Thus, further refinements of a TFF process is required prior to it being applicable to cationic liposomes.

Both vesicle size and charge have been considered as factors controlling trafficking, processing, and presentation of antigens in lipid vesicles (Brewer *et al.*, 1998; Khadke *et al.*, 2019). Thus, size controlling is of major importance when it comes to modulation of immunological properties of nanocarriers-antigen complexes. Manufacturing conditions are high importance when controlling the liposome size in a microfluidics method (Kastner *et al.*, 2014) and the impact of manufacturing parameters on the product critical attributes mustbe understood in the development of a manufacturing process. There is a broad range of applications that microfluidics can be applied to, thus a setup time is required in order to determine the optimal parameters based on the purpose of the study. Parameters such as the lipid selection, initial lipid concentration, FRR, TFR, manufacturing temperature as also the buffer

ionic strength can affect liposome properties (Kastner *et al.*, 2014; Joshi *et al.*, 2016; Forbes *et al.*, 2019; Lou *et al.*, 2019). In order to test any potential impact of manufacturing conditions on liposomes characteristics, formulations with the same composition were reproduced using a different FRR. Results demonstrated that FRR has an essential role in particle size controlling as increase of FRR at constant TFR led to reduction of particle size. These results are in agreement with previous work showing that the increase in FRR reduces the resulting size of the liposomes (Jahn *et al.*, 2010; Kastner *et al.*, 2015; Joshi *et al.*, 2016; Forbes *et al.*, 2019). It is reported that the overall lower amount of solvent present at higher FRR employed decreases of the particle fusion (Ostwald ripening), which leads to the formation of smaller particles (Zhigaltsev *et al.*, 2012). On the contrary, an increase in the PDI values was noted which is in line with previous work reported by Kastner *et al.* where again it was shown that the FRR has impact on PDI. It is supported that, this increase may be a result of increased dilution at higher FRR reducing the rate of diffusional mixing within the micromixer (Kastner *et al.*, 2014). Reduction in the rate of diffusion eventually results in partly incomplete nucleation and a lower rate of liposome formation inside the micromixer (Kastner *et al.*, 2014; Balbino *et al.*, 2015). On the other hand, the zeta potential of the liposomes was maintained despite alternations in FRR.

Interesting also were the findings of Lou *et al.* who demonstrated that the concentration of aqueous phase is a crucial point on controlling liposomes properties. Their experiments revealed that the hydrodynamic diameter of cationic liposomes DOPE: DOTAP and DOPE: DDA was increased from 40 up to >500 nm by increasing the concentration of the aqueous phase (TRIS pH 7.4) in the range of 10-1000 mM. Further experiments using DSPC: Cholesterol: DOTAP liposomes (0, 5, 13 and 23% DOTAP) showed that liposome size was also influenced by the cationic lipid within the formulation. Interestingly, no change on liposome size observed in the range of 10 to 1000 mM TRIS, with DSPC: Cholesterol: DDA (13 and 23% DDA). Thus, different buffer-dependent liposome sizes are expected for specific combinations of cationic and structural lipids due to their mean packing parameter into the formulations which can inhibit the effect of buffer ionic strength (Lou *et al.*, 2019).

As with any conventional pharmaceutical product which is designated for parenteral administration, sterilisation is required to ensure the absence of any bacterial into the product. Filtration is recommended for the preparation of sterilised liposomes products. This sterilisation technique is suitable for thermolabile products, which

include liposomes, since it does not involve any form of heating nor conditions that can result in the formation of degradation products or leakage of liposomal contents (Toh and Chiu, 2013). This method can be applied as sterilisation technique on liposomes particles with a diameter less than 200 nm and is very convenient as is fast and simple as method. Herein, it was demonstrated that filtration is not a suitable technique for sterilisation of cationic liposomes. The passage of cationic particles through 0.22 μm filter composes by a hydrophilic polyethersulfone (PES) membrane resulted in liposome loss with liposome loss increases by increased cationic lipid concentration regardless their small size (<200 nm). It is speculated that liposomes were interacting with the filter membrane and stacked on the membrane filter. Interestingly, these results are in agreement with what was observed with TFF where a polyethersulfone (mPES) column was used indicating the incompatibility of this material for cationic liposomes. Nevertheless, filtration have limitations as the size restrictions which limits its applicability as also its high cost. Most importantly, there are concerns regarding the filtration efficiency on formulations such as some adjuvanted vaccines, liposome-based drug delivery solutions, and similar surfactant or emulsion-based product fluids. Not all the filters are suitable for all the formulations, thus matching of the solution with the appropriate sterilising-grade filter and process conditions should be considered. The limitations of this technique have prompted research of the other sterilisation techniques. An alternative to filtration is γ-irradiation. It is supported that this technique cannot be used in liposome sterilisation as can cause lipids peroxidation, thus liposome degradation after radiation exposure (Toh and Chiu, 2013; Turker *et al.*, 2013). However, protection of liposomal lipids against irradiation damage in some degree can be achieved by the use of nitroxides or by freezing (Samuni *et al.*, 1997). Also, γ-irradiation of liposomes in dry state has been proven beneficial for preventing alternation of physicochemical properties of liposomes attributes post γ-irradiation (Mohammed *et al.*, 2006).

Another important aspect on particle preparation is their shelf-life. Whilst the use of liposomes as carriers for drug and vaccine delivery is well-documented, their potential application as therapeutic agents is still challenged by their inherent physical and chemical instabilities in aqueous dispersions. A crucial factor influencing liposome stability is their lipid composition and their between interactions and forces. These forces and interactions will produce an overall effect that is strong enough to hold different molecular subunits together as well as ensure their stability in solution. Moreover, the weakness of the involved interactions makes the structure more

flexible, thereby enabling the system to withstand minor perturbation while preserving the reversibility of the self-assembled structure (Lombardo *et al.*, 2016). It is referred that dispersions of DDA liposomes are physically unstable and prolonged storage at 4°C is not possible without formation of aggregates and precipitation. This instability cause change in the liposomes parameters. However, incorporation of the glycolipid TDB in to DDA formulations, help the stability of formulations and prolonged their shelf-life (Davidsen *et al.*, 2005). The particle size, size distribution, change in mean particle size with time, and physical appearance of the liposomal suspension are sensible indicators of the kinetic stability of liposomal suspensions. Stability studies proved that DSPC: Cholesterol: DDA liposomes were stable for 1 week. Results are in line with the literature where it is referred that the high stability of charged liposomes relies on the presence of surface charge induces electrostatic repulsion which prevents their aggregation and flocculation (Lombardo *et al.*, 2016).

Electrostatic interactions between cationic liposomes and negatively charged proteins favour adsorption of proteins on liposome surface. Liposome: protein ratio used for adsorption has an essential role in the protein loading as also on particles characteristics as affects the colloidal and protein stability. It is important to achieve the optimal balance between liposomes and protein in order to have enough excess of liposomes present in solution for protein binding but not high enough causing aggregation of the protein. From the adsorption studies, it was proven that more uniform particles were produced with increasing liposomes: protein ratio with protein saturation occurring at a certain protein: liposomes ratio. These findings are in accordance with Hamborg *et al*. who proved that the adsorption process for OVA (pI=4.5) reached saturation above approximately 0.7 mg/mL in the presence of DDA/TDB liposomes at a lipid concentration of 1.5 mg/mL (Liposomes: protein 2.14:1) (Hamborg *et al.*, 2013).

Incorporation of protein and CpGODN in unconjugated form, resulted in a size increase due to aggregation of vesicles promoted by antigen interactions and a drop in zeta potential as expected. Results are in line with what has been reported previously by others (Shargh *et al.*, 2012; Mansourian *et al.*, 2014; Nikoofal-Sahlabadi *et al.*, 2018). Interestingly, addition of CpGODN did not affect protein loading on particles as previously observed by Milicic *et al.* who proved that combination of CpGODN and OVA on DDA: TDB liposomes cause protein loading reduction (Milicic *et al.*, 2012). This is probably due to the very low amount of CpGODN incorporated

into the formulations, which was not high enough to affect protein loading. On the other hand, addition of protein conjugate on liposomes did not alter their size but decreased their zeta potential indicating that material was electrostatically adsorbed to the surface of the particles, thereby masking part of the cationic nature of the liposome surface. Cryo-TEM experiments confirmed also the above observations. The presence of the GBS67-CpGODN protein conjugate induces liposome aggregation to form cluster-like structures, where the liposomes are deformed at the surface of contact with adjacent liposomes, without rupture. Rodriguez-Pulido *et al.* reported that when a complex is formed, positive charges are partially compensated on only one side of the bilayer because negatively charged molecules is adsorbed and compacted only at the outer positive-charged surface of the liposome, reducing the effective head group of the cationic lipids and provoking a clear asymmetry in packing pressure. This stresses and destabilises the membrane, thus promoting liposomes fusion and/or aggregation (Rodríguez-Pulido *et al.*, 2008; Kuvichkin *et al.*, 2009). The wall of liposome attributes adsorbed protein conjugate was clearly thicker than that observed for the lipid bilayer of the liposomes. This increase was attributed to the presence on protein-CpGODN on the membrane surface. Similar conclusions were reached also by Hamborg *et al*. and Sangra *et al*. after protein adsorption on the surface of cationic liposomes (Hamborg *et al.*, 2014; Sangra *et al.*, 2017). It is worth pointing out that the presence of CpGODN chains on liposomes surface is also responsible for the change in morphological properties of liposomes. It has been evidenced that lipoplexes of DNA or oligonucleotides and cationic liposomes demonstrate similar behaviour to that observed herein (Almgren *et al.*, 2000; Meidan *et al.*, 2000; Weisman *et al.*, 2004; Kuntsche *et al.*, 2011; Balbino *et al.*, 2015). It is supported that the formation of aggregated and/or multilamellar structures is a result of insufficient oligonucleotide to interact with all the cationic lipid. The lateral phase separation leads to membrane defects at the upper part of the bilayer acyl chains which permit water penetration through the membrane into this region of the lipid bilayer. In order to overcome these defects, thermodynamic factors cause aggregation and probably fusion of the lipoplexes to form larger particles (Meidan *et al.*, 2000).

4.7 Conclusion

In summary, the preparation of DSPC: Cholesterol: DDA liposomes using an on-chip method was demonstrated. These liposomes are well defined, and produced by a scalable, process-controlled method and are capable to adsorbed negatively charged proteins and adjuvants as CpGODN TLR9 with high efficiency. The immunological properties of the double adjuvanted designed system composed by antigenic protein-CpGODN conjugate adsorbed on cationic liposomes surface will be investigated *in vivo*.

Chapter 5 Immunisation studies

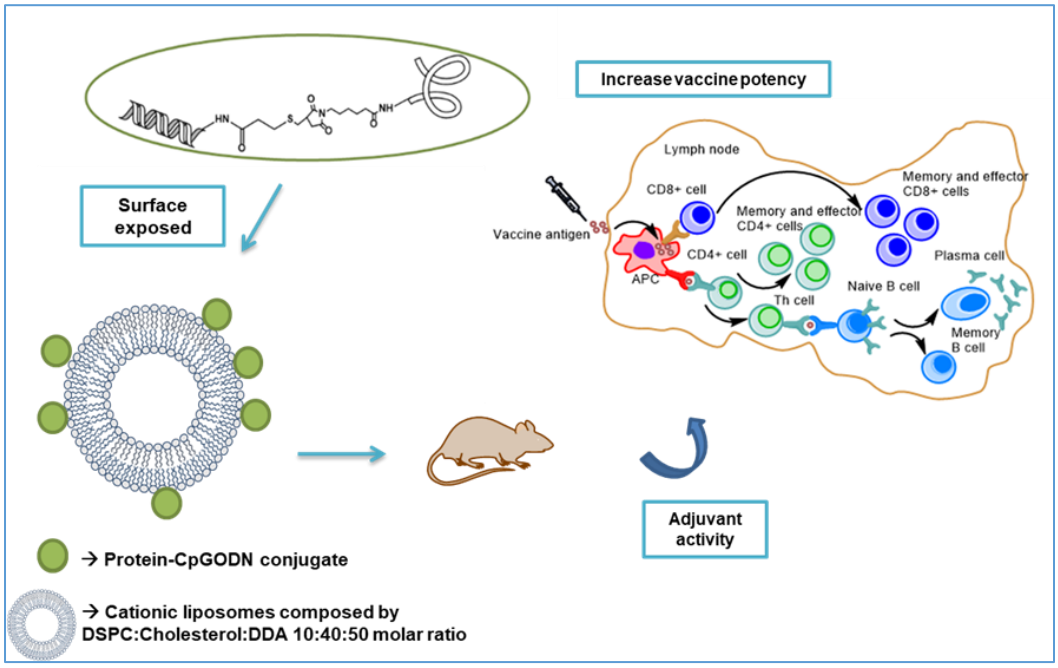

5.1 Introduction

A protective immune response to infectious pathogens relies on activation of innate and adaptive immunity. Innate immunity relies on pathogen-associated molecular patterns, which are recognised by pathogen recognition receptors localised in APCs. After antigen processing and presentation, CD4+ T cell polarisation occurs, further leading to B cell and CD8+ activation and humoral and cell-mediated adaptive immune responses (De Serrano and Burkhart, 2017).

Synthetic subunit vaccines that can elicit strong antibody-mediated and CD4+ T cell immunity are highly desirable for prophylactic vaccination against infectious diseases (Ignacio *et al.*, 2018; Clauson *et al.*, 2019). IgG is the major class of the five classes of immunoglobulins in human beings, IgM, IgD, IgG, IgA, and IgE. IgG can be further divided in four subclasses, named, in order of decreasing abundance IgG1, IgG2, IgG3, and IgG4. Although they are more than 90% identical on the amino acid level, each subclass has a unique profile with respect to antigen binding, immune complex formation, complement activation, triggering of effector cells, half-life, and placental transport (Dekkers *et al.*, 2017). Antibody responses to soluble protein antigens and membrane proteins primarily induce IgG1, but are accompanied with lower levels of the other subclasses. IgG2 has an essential role in the defence against pathogens, as an increased susceptibility to certain bacterial infections is associated with IgG2 deficiency (Vidarsson *et al.*, 2014). Translation of these antibody subclasses from human to mice for preclinical studies purpose, gives the IgG1 and IgG2a subclasses, with IgG2c being the equivalent of IgG2a in some mouse strains such as C47Bl/6 mice (Nimmerjahn *et al.*, 2005; Zhang *et al.*, 2012; Dekkers *et al.*, 2017). CD4+ T cells play critical roles in mediating adaptive immunity to a variety of pathogens. They help B cells make antibody, enhance and maintain responses of CD8+ T cells, regulate macrophage function, orchestrate immune responses against a wide variety of pathogenic microorganisms, and regulate/suppress immune responses both to control autoimmunity and to adjust the magnitude and persistence of responses. CD4+ T cells are important mediators of immunologic memory, and when their numbers are diminished or their functions are impaired, the individual becomes susceptible to a wide range of infectious disorders (Zhu *et al.*, 2010).

T-helper cells can be further divided into subpopulations distinguished from each other by the type of cytokines produced and particular transcription factors. The two main subpopulations associated with infection are Th1 and Th2. Their main function

is to stimulate proliferation of all T-cell populations (both CD4+ and CD8+ T cells) via IL-2, as well as to activate tissue macrophages via IFNγ. In contrast, Th2 cells produce IL-4, IL-5 and IL-10. Th2 cells influence B-cell activation, proliferation and immunoglobulin production. IL-4 stimulates B-cell growth and heavy chain switch from IgM to IgG, IgE and IgA and stimulates high affinity antibody synthesis. These T-cell subpopulations can inhibit as well as stimulate. Th1-produced IFNγ can act to suppress Th2 cells and Th2-produced IL-4 can inhibit some Th1 responses (Glimcher and Murphy, 2000; Nash *et al.*, 2015; Walker and McKenzie, 2017). T helper 17 (Th17) cells belong to a recently identified T helper subset, in addition to the traditional Th1 and Th2 subsets. These cells are characterised as preferential producers of IL-17A, IL-17F, IL-21, and IL-22 and their signalling is critical especially for extracellular pathogens (Yao *et al.*, 1995; Dumoutier *et al.*, 2000; Ouyang *et al.*, 2008). However, their biological function is not completely clear yet. Treg cells is a class of cells, which their function is based on a number of suppressive, tolerance and regulatory mechanisms. Their activity is triggered in an antigen-specific fashion (Corthay, 2009). Th9 has an essential role in allergic and autoimmune diseases; however, the functional properties of this Th cell subset are not fully cleared yet (Schmitt *et al.*, 2014).

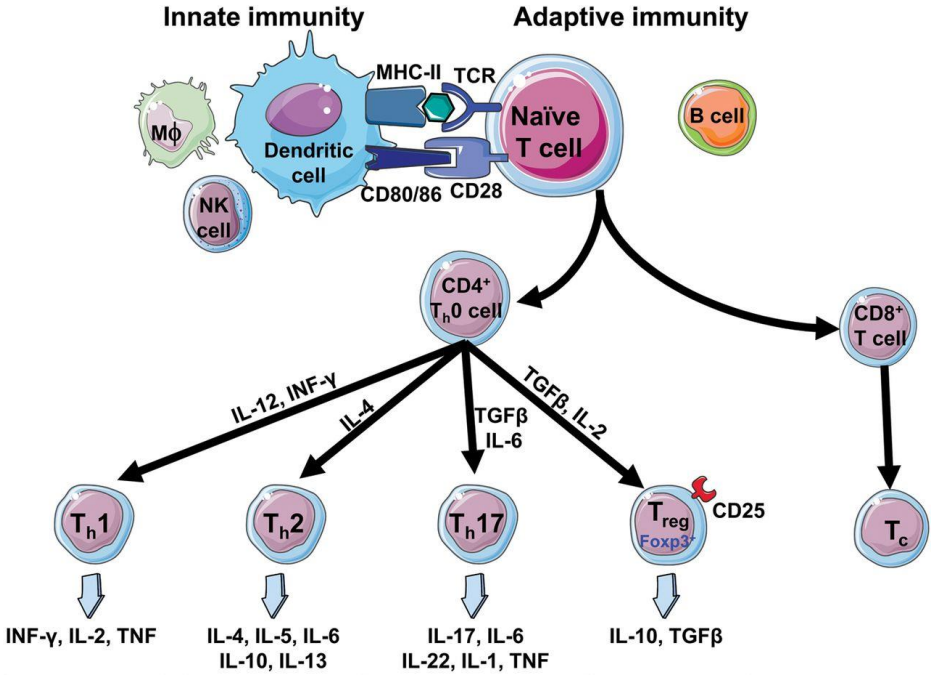

Figure 5.1 *Differentiation of naïve T lymphocytes into various subsets. APC (dendritic cells and monocyte/macrophages) present antigens on MHC-II to naïve T cells (Th0) in secondary lymphoid tissues, leading to T-cell clonal expansion and differentiation into effector T cells, such as T helper (Th)1, Th2, and Th17 or T regulatory (Treg) cells according to combined stimulation by different cytokines (Idris-Khodja et al., 2014).*

CpG ODN adjuvant action relies on the activation of B-cell differentiation into plasma cells, resulting in enhancement of antibody production. Generally, naïve B cells never express TLR9, so they do not respond to CpGODN. Accordingly, it is essential to stimulate naïve B cells in advance with antigens, to ensure that the cells differentiate into plasma cells following CpG ODN activation. These antigen-stimulated naïve B cells mature into antigen-specific B cells, which express TLR9. When antigen-specific B cells are stimulated by CpGODN, the expression of costimulatory molecules such as MHC-II, CD40, CD80, and CD86, as well as Fc receptors is increased, and the B cells differentiate into antigen secreting plasma cells (Hanagata, 2017).

Progress in research demonstrated that covalent attachment of CpGODN to antigens can improve antigen uptake, antigen presentation and cross-priming of cytotoxic T-lymphocytes (Tighe *et al.*, 2000; Khan *et al.*, 2007). However, preclinical studies revealed that CpGODN is susceptible to digestion by endonucleases. In addition, CpGODN demonstrates unfavourable pharmacokinetic and biodistribution profiles (Tam, 2006). Thus, focus has been given on enhancing lymph node targeting through nanoparticulate materials. Techniques such as surface engineering of CpGODN and incorporation into or onto particles have been extensively tested aiming to improve pharmacokinetics, and pharmacodynamics (Liu and Irvine, 2015; Yu *et al.*, 2017). Vaccine formulations comprising engineered materials that control antigen and adjuvant biodistribution, regulate uptake of vaccine by APC, optimise triggering of antigen-specific B cells, and influence vaccine kinetics have a role to play in the design of future vaccines.

5.2 Aim and objectives

The aim of the work described in this chapter is the immunological evaluation of the double adjuvanted vaccine formulations prepared. Immunisation studies had been focused on GBS67 antigen and corresponding conjugate/formulations. Maleimide-thiol conjugates are prone to hydrolysis, thus stability evaluation of conjugates was necessary prior to immunisations. Stability tests showed that GBS67-CpGODN was proven more stable than NadA-CpGODN conjugate, so GBS67-CpGODN was used for all the upcoming immunisation studies. The objectives of the work presented in this chapter were:

1. The investigation of the impact of chemical conjugation between CpGODN TLR9 agonist and protein compared to the physical mixture

2. The evaluation of impact of cationic liposome formulations on the kinetic, quality and magnitude of immune responses
3. Investigate any potential synergistic effect between liposomes and CpGODN

5.3 Materials

Table 5.1 lists the materials used for within the work reported in this chapter.

Table 5.1 *List of materials.*

Material	**Supplier**
Alexa Fluor 790 protein labelling kit	ThermoFisher Scientific, UK
Cholesterol	Sigma Aldrich, UK
CpGODN 1826 (5'-[AmC6]TCCATGACGTTCCTGACGTT)	Sigma Aldrich, Italy
DSPC	Avanti lipids, USA
DDA	Avanti lipids, USA
DiD	ThermoFisher Scientific, UK
GBS67	GSK, Siena, Italy

5.4 Methods

5.4.1 Preparation and characterisation of liposome formulations for *in vivo*

Liposomes were prepared by microfluidics (with and without DiD lipophilic dye tracker) with the liposomes adsorbing protein-CpGODN conjugate (Group 5) or protein and CpGODN on their surface (Group 6), as has been previously described in Chapter 4 of this study. Antigen dose selection was based on previous *in vivo* studies performed with GBS67 (Nilo *et al.*, 2015). The final antigen, CpGODN and liposomes concentrations in formulations, are presented in the Table 5.2. For the biodistribution study, DiD lipophilic dye was added in lipid stock solution in a ratio of 1:100 w/v DiD: Total lipid and liposomes were prepared in the same manner as before.

Table 5.2 *Vaccines composition for all the immunisation groups. Mixture and conjugate are represented by (+) and (-), respectively. Liposome formulation are composed by DSPC: Cholesterol: DDA (10: 40: 50 molar ratio).*

Group	Immunisation group	Antigen amount (µg/dose)	CpGODN amount (µg/dose)	Liposomes amount (µg/dose)
1	GBS67	1	-	-
2	GBS67-CpGODN	1	0.15	-
3	GBS67+CpGODN	1	0.15	-
4	GBS67+Liposomes	1	-	50
5	GBS67-CpGODN+Liposomes	1	0.15	50
6	GBS67+CpGODN+Liposomes	1	0.15	50

5.4.2 Fluorolabelling of GBS67 protein and GBS67-CpGODN protein conjugate

GBS67 protein and GBS67-CpGODN protein conjugate were labelled using Alexa Fluor 790 protein labelling kit (Molecular probes) according to the manufacturer's instructions.

5.4.3 Biodistribution study

All experiments were undertaken in accordance with the regulations of the Directive 2010/63/EU. Female BALB/c mice, 7–12 weeks old were split into 3 groups of 3 mice. All mice were immunised intramuscularly into the right thigh (50 µL/dose) at day 0 with fluorolabeled antigens and liposomes. Anesthetised mice were placed into the IVIS chamber, and images were captured using the IVIS spectrum camera (Perkin Elmer) at day 0-4 and then every 2 days until day 11. A non-immunised mouse was used as negative control and for quantifying the background level. Mice were terminated at day 14 and organs (spleen, kidneys, liver, and intestines) were isolated for *ex vivo* imaging. The final antigen, CpGODN and liposomes concentrations in formulations are presented in the Table 5.3.

Table 5.3 *Vaccines composition for all the groups used for the biodistribution study. Mixture and conjugate are represented by (+) and (-), respectively. Liposome formulation are composed by DSPC: Cholesterol: DDA (10: 40: 50 molar ratio) and have a final concentration of 4 mg/mL lipid and 0.04 mg/mL DiD.*

Group	Immunisation group	Antigen amount (µg/dose)	CpGODN amount (µg/dose)	Liposomes amount (µg/dose)
1	GBS67	10	-	-
2	GBS67-CpGODN	10	1.5	-
3	GBS67-CpGODN+Liposomes	10	1.5	200

5.4.4 Immunisations

All experiments were undertaken in accordance with the regulations of the Directive 2010/63/EU. Female BALB/c mice, 6–8 weeks old were split into 6 groups of 5 mice. All mice were immunised intramuscularly (50 µL/dose) two times (days 0 and 21) and at scheduled time points, blood samples were taken from the tail (day 0, 21) and stored at −20°C for future analysis of antibodies. Mice were terminated at day 42 and further processed for isolation of splenocytes.

5.4.5 Antibody responses analysis

Enzyme-linked immunosorbent assay titres of protein antibodies were determined using the coating reagent GBS67. Microtiter plates (Nunc Maxisorp) were coated by adding 100 µL per well of coating reagent (2 µg/mL) in PBS pH 7.4. The plates were incubated overnight at 4 °C and were washed with PBS containing 0.05% v/v TWEEN20 and then blocked with 2% w/v BSA in PBS for 1 hour at 37 °C. The wells were then filled with 100 µL of serum serially diluted in PBS and incubated at 37 °C for 2 hours. After 3 washes, 100 µL per well of peroxidase-labelled goat anti-mouse (IgG 1:1000, IgG1 1:20,000, IgG2a 1:1000) was added (Sigma-Aldrich) and plates incubated for 1 hour at 37 °C. The plates were again washed 3 times with PBS containing 0.05% v/v TWEEN20, and finally 100 µL of peroxidase substrate solution (Sigma-Aldrich) was added to each well, following incubation of the plates for 30 minutes at RT. The reaction was stopped by the addition of 100 µL of a solution of H_2SO_4 0.2M and the plates were read immediately at 450 nm.

5.4.6 Isolation and stimulation of splenocytes

Mice spleens were removed aseptically and placed into universals containing 5 mL of complete media (RPMI 1640 containing 10% v/v FCS, 1% v/v Penicillin-Streptomycin and 1% v/v L-glutamine) and kept ice-cold until ready to proceed. Cell suspensions were prepared by breaking about the spleens with the plunger of a 2 mL syringe using cell strainers. Cells were transferred to a 50 mL centrifuge tubes and cell strainers were washed with another 5 mL of media, respectively. After centrifugion (1200 rpm, 4 °C) for 5 minutes, cell pellets resuspended in 3 mL Boyle's solution (1:9 v/v 0.17 M Tris: 0.16 M ammonium chloride) and centrifuged at 1200 rpm for 5 minutes for erythrocytes removal. Pellets are then washed twice in 5 mL complete medium and centrifuged at 1200 rpm for 5 minutes. After final wash, pellets were resuspended in 5 mL complete media. Viable cell numbers were estimated by trypan blue exclusion. Briefly, cells were dyed with trypan blue in a 1:10 v/v ratio (10 µL cells: 90 µL trypan blue). Subsequently, 100 µL were placed on a haemocytometer and cells were counted (Figure 5.2). Trypan blue allows to check the viability of the cells, since cells take up trypan blue, they are considered non-viable. The number of cells was estimated based on the following calculation:

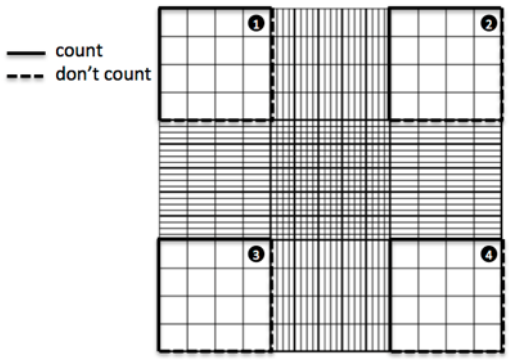

$$Number\ of\ \frac{cells}{mL} = number\ of\ \frac{cells}{square}\ x\ DF\ x\ 10{,}00$$

where

DF=Dilution factor

Number of cells/square=average cells from 4 indicated squares

Figure 5.2 *Schematic representation of the haemocytometer grid for the cell count and equation followed for calculation of the viable cells.*

After counting, cells were diluted in complete RPMI so that there were $5x10^6$ cells/mL. A volume of 100 µL of cells were added to the appropriate wells of Nunclon 96-well round bottom plate (Figure 5.3). The same procedure was followed for splenocytes coming from the rest of immunisation groups. Cells were stimulated with either RPMI media as a negative control or GBS67 antigen (4 µg/mL) as the investigated antigen.

Splenocytes were incubated at 37 °C, 5% CO_2 for 72 hours. After 3 days, plates were stored at -20 °C for cytokine analysis at a later date.

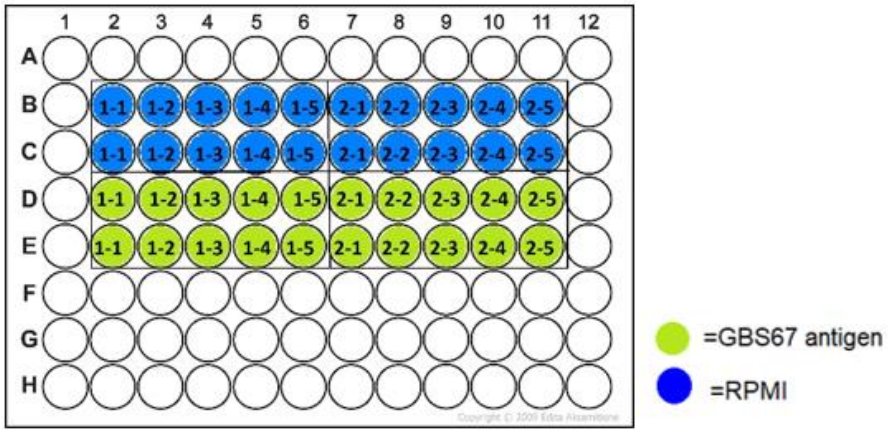

Figure 5.3 *Outline of the ELISA plate set-up used for splenocytes stimulation. Samples were plated in duplicate. RPMI media was used as a negative control and GBS67 antigen for the quantification of antigen-specific responses.*

5.4.7 Cytokine analysis of stimulated splenocytes

Cytokine profiles of supernatants from restimulated splenocytes were analysed using LEGENDplex mouse Th cytokine (13-plex) multi-analyte flow assay kit (Biolegend) according to the manufacturer's instructions.

5.4.8 Opsonophagocytosis Killing Assay (OPKA)

The functional activity of the sera was determined by OPKA as previously described by Nilo *et al.* (Nilo *et al.*, 2015). HL60 cells were grown in RPMI 1640 with 10%FCS, incubated at 37 °C, 5% CO_2. HL-60 cells were differentiated to neutrophils with 0.78% dimethylformamide (DMF) and after 4−5 days were used as source of phagocytes. Serum antibodies serially diluted in HBSS red were mixed with $6x10^4$ CFU per well of GBS type V CJB111. HL-60 cells ($2x10^6$ cell/well) and rabbit complement (diluted at 10% in water) were added and incubated at 37 °C for 1 hour under shaking. Before (T_0) and after (T_{60}) incubation, the mixtures were diluted and plated in blood agar plates. (Nunc Polysorp; Nalge Nunc International Corp., Rochester, NY). Each plate was then incubated overnight at 37 °C with 5% of CO_2 counting CFUs the next day. OPA titre was expressed as the reciprocal serum dilution leading to 50% killing of bacteria and the % of killing was estimated based on the following calculation:

$$\%killing = \frac{T_{0-}T_{60}}{T_0}$$

where T_0 is the mean of the CFU counted at T_0 and T_{60} is the average of the CFU counted at T_{60} for the two replicates of each serum dilution.

5.4.9 Statistical analysis

Statistical significance was determined by ANOVA followed by Tukey's (HSD) test. Significance was acknowledged for p values less than 0.05. All calculations were made in Minitab 18.

5.5 Results

5.5.1 Characterisation of liposome-based formulations for *in vivo* immunisation studies

As shown in Table 5.4, the addition of CpGODN (0.15 μg) and GBS67 (1 μg) results in an increase on particle size of the liposomal formulations without loss of the particle uniformity (PDI between 0.02-0.05). The highest increase in size (183 nm) was observed when GBS67+CpGODN mixture was added on liposomes. Interestingly, addition of free GBS67 protein or GBS67-CpGODN conjugate on liposomes did not cause a significant change in liposomes size. At the same time, a reduction in zeta potential was noted in all the formulations, due the electrostatic interaction of the negatively charged CpGODN and GBS67 with the cationic liposomes, with liposomes having a net surface charge of between +34-39 mV (Table 5.4). The GBS67 antigen and the GBS67-CpGODN conjugate have pI values of 6.46 and 6.15 respectively, and therefore confer a net anionic charge, favours the adsorption to cationic liposomes, as has been confirmed and discussed in Chapter 4 (Sections 4.5.5-4.5.7). Loading of protein and CpGODN was assumed 100% based on previous experiments performed.

Table 5.4 *Physicochemical characteristics of liposomal formulations with or without GBS67 and/or CpGODN. Liposomes were mixed with free protein, protein+CpGODN mixture or protein-CpGODN conjugate. The final liposome (1 mg/mL), protein (0.02 mg/mL) and CpGODN (0.003 mg/mL) concentrations in all the samples were the equal. Liposomes were characterised in terms of size and PDI by DLS. Results represent the mean ± SD of two immunisations.*

	Size (nm)	PDI	ZP (mV)
Liposomes	164 ± 26	0.02 ± 0.01	45 ± 5
GBS67+Liposomes	166 ± 26	0.03 ± 0.02	35 ± 2
GBS67-CpGODN+Liposomes	169 ± 24	0.05 ± 0.02	39 ± 3
GBS67+CpGODN+Liposomes	183 ± 9	0.03 ± 0.02	34 ± 1

5.5.2 Antibody responses analysis

The effect of conjugation of TLR9 to GBS67 as well as the effect of liposome inclusion, was evaluated by i.m. immunisation of groups of 5 BALB/c mice with two 1 µg protein-based doses of vaccine, 3 weeks apart, corresponding to the administration of 0.15 µg of TLR9. Ser from pre-immunised mice was used as negative control.

The anti GBS67 IgG titres after the first dose and boost dose were measured (Figure 5.4A and B). Mice immunised with GBS67-CpGODN conjugate showed significantly ($p<0.001$) higher anti-GBS67 IgG titres (2-fold) compared to physical mixture of GBS67 and CpGODN even after the primary dose. The combination of DSPC: Cholesterol: DDA cationic liposomes with either conjugate or physical mixture, further increased the immune responses, with the combination of conjugate and liposomes vaccine giving the highest titre observed after the first injection (Figure 5.4A). Immunisation of the mice with a second dose significantly ($p<0.05$) boosted the anti-GBS67 IgG total titres further. Again, a similar trend was followed with the GBS67-CpGODN conjugate elicited IgG titres significantly ($p<0.001$) higher (2-fold) than the physical unconjugated mixture. When cationic liposomes were combined with the conjugate, a 2-fold increase of anti-GBS67 IgG titres was observed, with the total IgG response being significantly ($p<0.001$) higher compared to those achieved after vaccination with physical mixture+liposomes. Interestingly, incorporation of liposomes with GBS67 in absence of CpGODN, induced a 4-fold increase of anti-GBS67 titres compared to GBS67 alone. Despite the adjuvant effect of free liposomes on GBS67, the mixture of liposomes with free CpGODN and GBS67 or GBS67-CpGODN conjugate induced significantly ($p<0.001$) higher immune responses (Figure 5.4B).

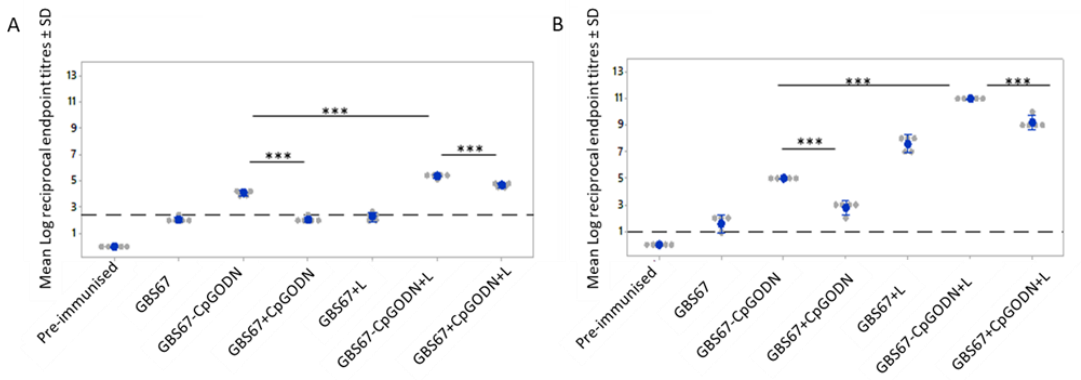

Figure 5.4 *Total IgG responses after primary dose (A) Day 21 and boost dose (B) Day 42. Six groups of mice were injected twice intramuscularly with the corresponding formulations. The study was split over two experiments with 2 mice from each group in study 1 and 3 mice in study 2. The results are then combined to give an n = 5. Results are plotted for individual mice (◦) and also an average (•), to show variability across the studies and mice. Blood samples were taken from the tail at day 21. Mice were terminated at day 42 and ELISA was performed for determination of total GBS67-specific antibody titre levels. Mixture and conjugate are represented by (+) and (-), respectively. Results are the average of two independent experiments (mean±SD). ***p<0.001. Dash line represents the limit of detection.*

To determine the impact of the conjugated CpGODN TLR9 ligand and cationic liposomes on Th1 and Th2 antibody-mediated responses, the levels of antibody subclasses were analysed by ELISA (Figure 5.5). After the first dose, increased levels of IgG1 were observed for GBS67-CpGODN conjugate group which were significantly ($p<0.01$) higher (2-fold) than free GBS67 and CpGODN physical mixture (Figure 5.5A). The same trend was observed when conjugate and physical mixture of GBS67, CpGODN were combined with liposomes, with GBS67-CpGODN+liposomes giving the higher IgG1 response. Interestingly, no significant differences obtained between GBS67 and GBS67+CpGODN, as also GBS67+liposomes and GBS67+CpGODN+liposomes, after primary dose. Regarding IgG2a, no significant differences were observed between the groups after vaccination with the first dose (Figure 5.5C).

The second dose further boosted the production of IgG1 and IgG2a antibodies (Figure 5.5B and D respectively) with a stronger effect on the IgG1 isotype. In particular, the conjugation of TLR9 ligand resulted in an enhanced level of both IgG1 and IgG2a compared to GBS67 alone and GBS67+CpGODN mixture. Interestingly, no IgG2a titres observed after boost vaccination with GBS67+CpGODN mixture with the titres being lower than the limit of detection of the assay. The highest level of IgG isotypes was measured for the group immunised with GBS67-CpGODN conjugate in combination with liposomes. IgG2a were significantly higher than the ones obtained with GBS67+liposomes ($p<0.001$) and GBS67+CpGODN+liposomes mixture

(p<0.01). Noteworthy is the fact that, no significant differences observed between GBS67+liposomes and GBS67+CpGODN+liposomes groups for both, IgG1 and IgG2a titres (Figure 5.5B and D).

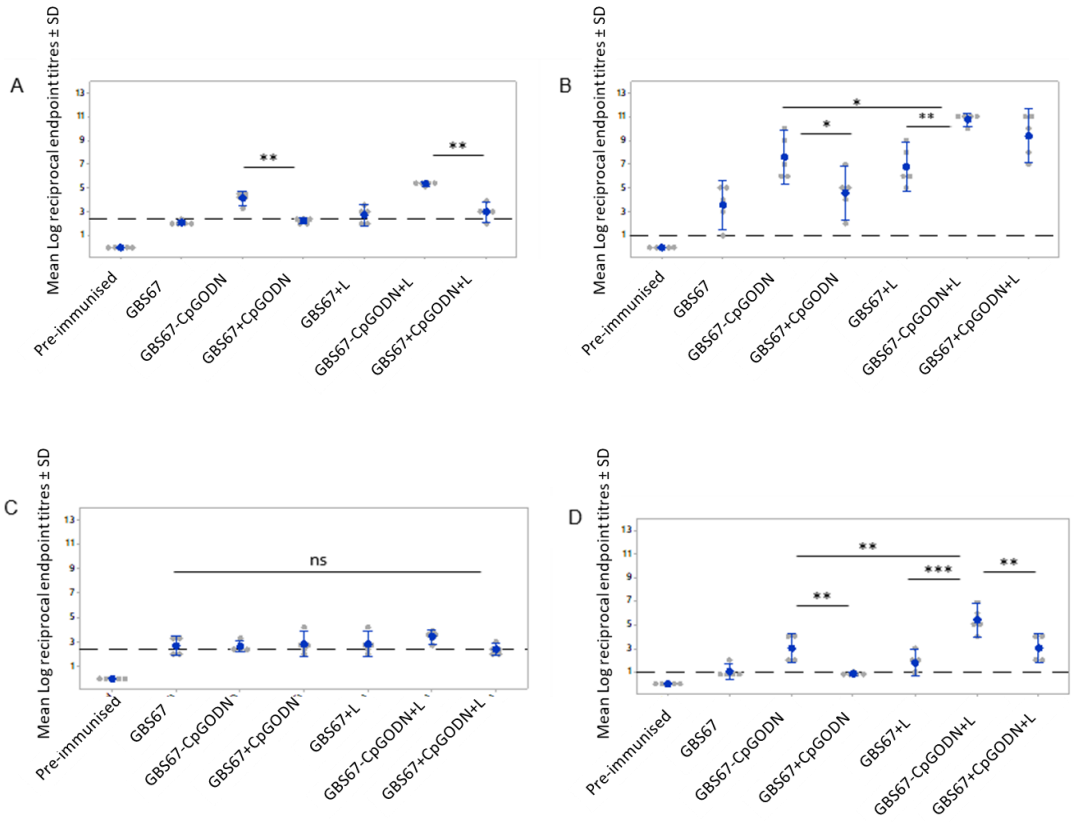

Figure 5.5 *IgG1 and IgG2a subclasses after primary dose (Day 21, Figure A for IgG1 and C for IgG2a) and boost dose (Day 42, Figure B for IgG1 and D for IgG2a). Six groups of mice (n=2 for 1st study 1 and n=3 for 2nd study) were injected twice intramuscularly with the corresponding formulations. Blood samples were taken from the tail at day 21. Mice were terminated at day 42 and ELISA was performed for determination of Th1 and Th2 antibody-mediated responses. Mixture and conjugate are represented by (+) and (-), respectively. Results are plotted for individual mice (◦) and also an average (•), to show variability across the studies and mice. Results are the average of two independent experiments (mean±SD). *p<0.05; **p<0.01;***p<0.001; ns: non-significant. Dash line represents the limit of detection.*

5.5.3 Opsonophagocytosis Killing Assay (OPKA)

To assess the antibody functionality, the pooled sera from vaccinated mice were tested by *in vitro* killing-based opsonophagocytosis assay (OPKA). This is a well-established assay that mimics *in vivo* bacterial killing by host effector cells, following opsonisation by specific antibodies and therefore considered a robust surrogate of the protection induced by GBS vaccines (Brigtsen *et al.*, 2002; Guttormsen *et al.*, 2008; Nilo *et al.*, 2015). A serotype V CJB1111 strain was used to determine effects of the antibodies against GBS67 protein.

As shown in Table 5.5, protein conjugate and protein conjugate+liposomes elicited anti-GBS67 antibody levels, which mediated opsonophagocytic killing of type V GBS. The OPKA titres measured against strain CJB1111 showed that the serum from GBS67-CpGODN conjugate was able to induce 3-fold higher opsonophagocytic killing of the tested strain compared to serum coming from GBS67 and physical mixture of GBS67 and CpGODN. Adsorption of protein conjugate on the surface of cationic liposomes resulted in a 2-fold and 6-fold increase of functional activity in comparison to GBS67-CpGODN and GBS67, respectively. In contrary, inclusion of liposomes into GBS67, CpGODN mixture did not offer any further benefit, as the obtained functional activity titre was at the same levels with free GBS67 control. Interestingly, the combination of GBS67 and liposomes was similar to GBS67, GBS67+CpGODN and GBS67+CpGODN+liposomes.

Table 5.5 *Functional activity of vaccine and correspoding controls. Serum antibodies serially diluted, were mixed with GBS type V CJB111. HL-60 cells and rabbit complement were added (T_0) and incubated at 37 °C for 1 hour under shaking (T_{60}). Before (T_0) and after (T_{60}) incubation, the mixtures were diluted and plated in blood agar plates. Each plate was then incubated overnight at 37 °C with 5% of CO_2 counting CFUs the next day. OPKA titre was expressed as the reciprocal serum dilution leading to 50% killing of bacteria. Mixture and conjugate are represented by (+) and (-), respectively. Values represent the mean ± SD of three different experiments using pooled sera from each single group (5 single mice serum/ group). ***p<0.001.*

Immunisation group	**OPKA titre**
GBS67	131 ± 42
GBS67-CpGODN	388 ± 224
GBS67+CpGODN	150 ± 20
GBS67+Liposomes	134 ± 55
GBS67-CpGODN+Liposomes	823 ± 78 ***
GBS67+CpGODN+Liposomes	134 ± 88

5.5.4 Cytokine analysis of stimulated splenocytes

After the last immunisation, splenocytes were isolated from all the mice and stimulated with GBS67 antigen (4 μg/mL) and RPMI, which represents the negative control. Cytokine profiles for 13 different cytokines were obtained by flow cytometry using mouse Th cytokine panel kit.

Overall, no significant differences were observed between the different groups tested, with the exception of group 5 (GSB67-CpGODN protein conjugate with DSPC: Cholesterol: DDA cationic liposomes). Interestingly, no significant differences were noted between the GBS67-CpGODN conjugate and GBS67, CpGODN mixture. Inclusion of liposomes in protein conjugate led to the highest cytokine levels obtained

which were significantly higher than the ones obtained when liposomes were combined with protein+CpGODN mixture (Figure 5.6-Figure 5.10).

In general, cytokine responses obtained did not polarise immune response (Th1 or Th2). Notably, a combination of Th1, Th2, Th17 and Th9 responses was observed. Regarding Th1, IFNγ and IL-2 cytokine levels were analysed. IFNγ levels obtained after vaccination with GBS67-CpGODN+liposomes were significantly ($p<0.05$) higher than the ones obtained with GBS67-CpGODN conjugate (Figure 5.6A). The combination of conjugate and liposomes induced a 10-fold higher production of IFNγ compared to GBS67+CpGODN+liposomes, even though differences were not significant ($p=0.07$). Noteworthy is the fact that, no significance differences obtained between groups 2 and 3, which refer to protein conjugate and protein+CpGODN physical mixture, respectively. Similarly, no significant differences were noted between the groups regarding IL-2 cytokine, with RPMI giving higher values that expected (Figure 5.6B).

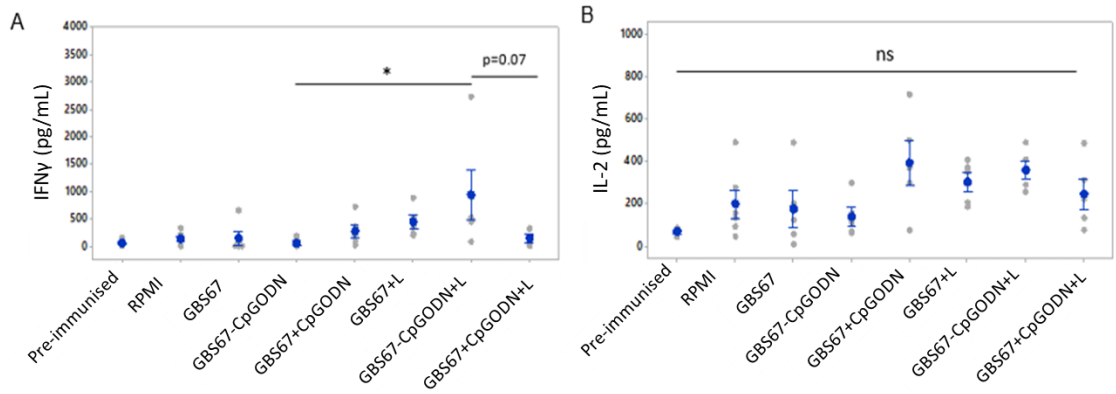

Figure 5.6 *Th1 Cytokine panel (A) IFNγ (B) IL-2 for cell-mediated responses. Mice were immunised with two injections spaced at 3-week intervals with the different formulations, as described in Section. 5.4.2. At day 42, spleen cells were prepared and restimulated in vitro with 4 μg/mL GBS67 and were incubated at 37 °C, 5% CO_2 for 72 hours. RPMI media was used as negative control. Culture supernatants were harvested after 72 hours and tested for cytokine levels by LEGENDplex mouse Th cytokine (13-plex) multi-analyte flow assay kit. Mixture and conjugate are represented by (+) and (-), respectively. Results are plotted for individual mice (◦) and also an average (•), to show variability across the mice. Values represent the mean ± SE from cells of five mice. *p<0.05; ns: non-significant.*

Signature cytokines of Th2 cells are the IL-4, IL-5 and IL-13. Analysis of IL-4 and IL-5 cytokines (Figure 5.7A and B) did not reveal any significant difference between all the groups tested. Although no statistical significance was observed, GBS67+CpGODN mixture showed higher cytokine levels than protein conjugate. Similarly, the combination of liposomes with GBS67-CpGODN conjugate shows the highest cytokine values for both IL-4 and IL5. In contrast, IL-13 cytokine levels

obtained, with GBS67-CpGODN+liposomes were significantly higher ($p<0.01$) than the ones obtained after immunisation with GBS67+CpGODN. The combination of protein conjugate and liposomes elicited the highest production of IL-13, which were 3-fold higher than those elicited by liposomes were physically mixed with GBS67, CpGODN ($p=0.06$). Interestingly, no significance differences were noted between GBS67+liposomes and GBS67-CpGODN+liposomes (Figure 5.7C).

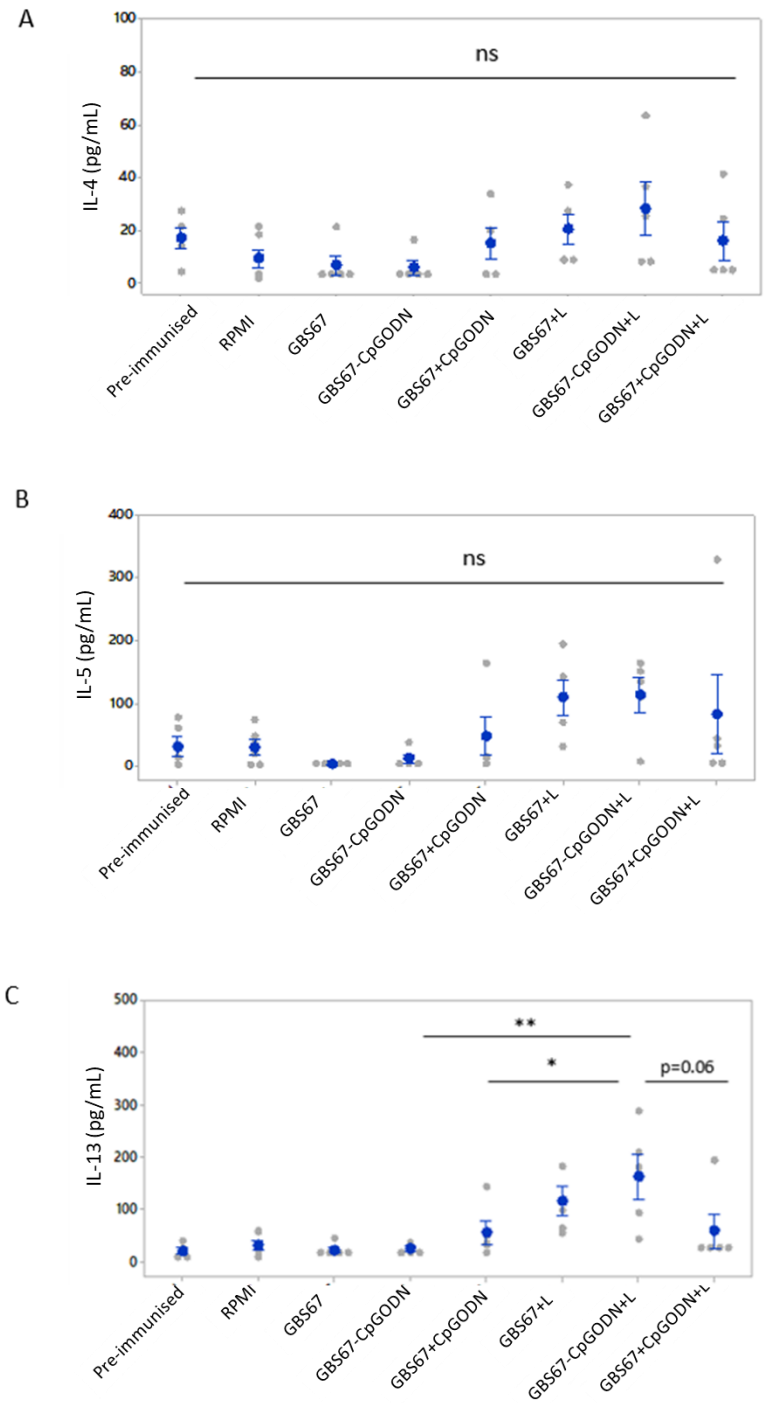

Figure 5.7 *Th2 Cytokine panel (A) IL-4 (B) IL-5 (C) IL-13 for cell-mediated responses. Mice were immunised with two injections spaced at 3-week intervals with the different formulations, as described in Section. 5.4.2. At day 42, spleen cells were prepared and restimulated in vitro with 4 µg/mL GBS67 and were incubated at 37 °C, 5% CO_2 for 72 hours. RPMI media was used as negative control. Culture supernatants were harvested after 72 hours and tested for cytokine levels by LEGENDplex mouse Th cytokine (13-plex) multi-analyte flow assay kit. Mixture and conjugate are represented by (+) and (-), respectively. Results are plotted for individual mice (◦) and also an average (•), to show variability across the mice. Values represent the mean ± SE from cells of five mice. *p<0.05; **p<0.01; ns: non-significant.*

Th17 cells are characterised by the production of IL-17A, IL-17F, and IL-22 as signature cytokines, and they are also good producers of IL-21. For all the cytokines tested, vaccination with GBS67-CpGODN+liposomes resulted in the highest cytokine levels obtained (Figure 5.8). Interestingly, no significant increase in cytokine production was observed after addition of CpGODN, regardless if is in a conjugate or physical mixture form. Similar results were obtained when GBS67 antigen was combined with cationic liposomes, with cytokine levels not being significantly different than the ones obtained with free GBS67 or combinations of GBS67 with CpGODN. However, when the protein conjugate was adsorbed on liposomes, a 4-fold increase in IL-17A levels was noted, which was significantly different than GBS67-CpGODN ($p<0.01$) and GBS67+liposomes ($p<0.5$). In contrast, combination of liposomes with GBS67 and CpGODN in the physical mixture form was not able to give any cytokine responses (Figure 5.8A). Similar results were obtained after analysis of IL-17F, with the combination of GBS67-CpGODN and liposomes inducing significantly highest cytokine levels obtained (Figure 5.8B). Regarding IL-21, no significantly difference was obtained between free GBS67, GBS67-CpGODN and GBS67+CpGODN (Figure 5.8C and D). Adsorption of protein conjugate onto cationic liposomes significantly augmented cytokine levels (2-fold) compared to GBS67-CpGODN alone ($p<0.001$). IL-21 levels obtained with combination of liposomes and protein conjugate were significantly higher ($p<0.001$) than that obtained with GBS67+liposomes and GBS67+CpGODN+liposomes (Figure 5.8C). In contrast, no differences were obtained between GBS67+liposomes and GBS67+CpGODN+liposomes groups. Finally, IL-22 cytokine levels obtained were in line with previous results obtained, demonstrating that combination of protein conjugate with liposomes induced a 4-fold and 5-fold increase on IL-22 cytokine levels compared to GBS67-CpGODN and GBS67+CpGODN+liposomes group, respectively ($p<0.01$) (Figure 5.8D).

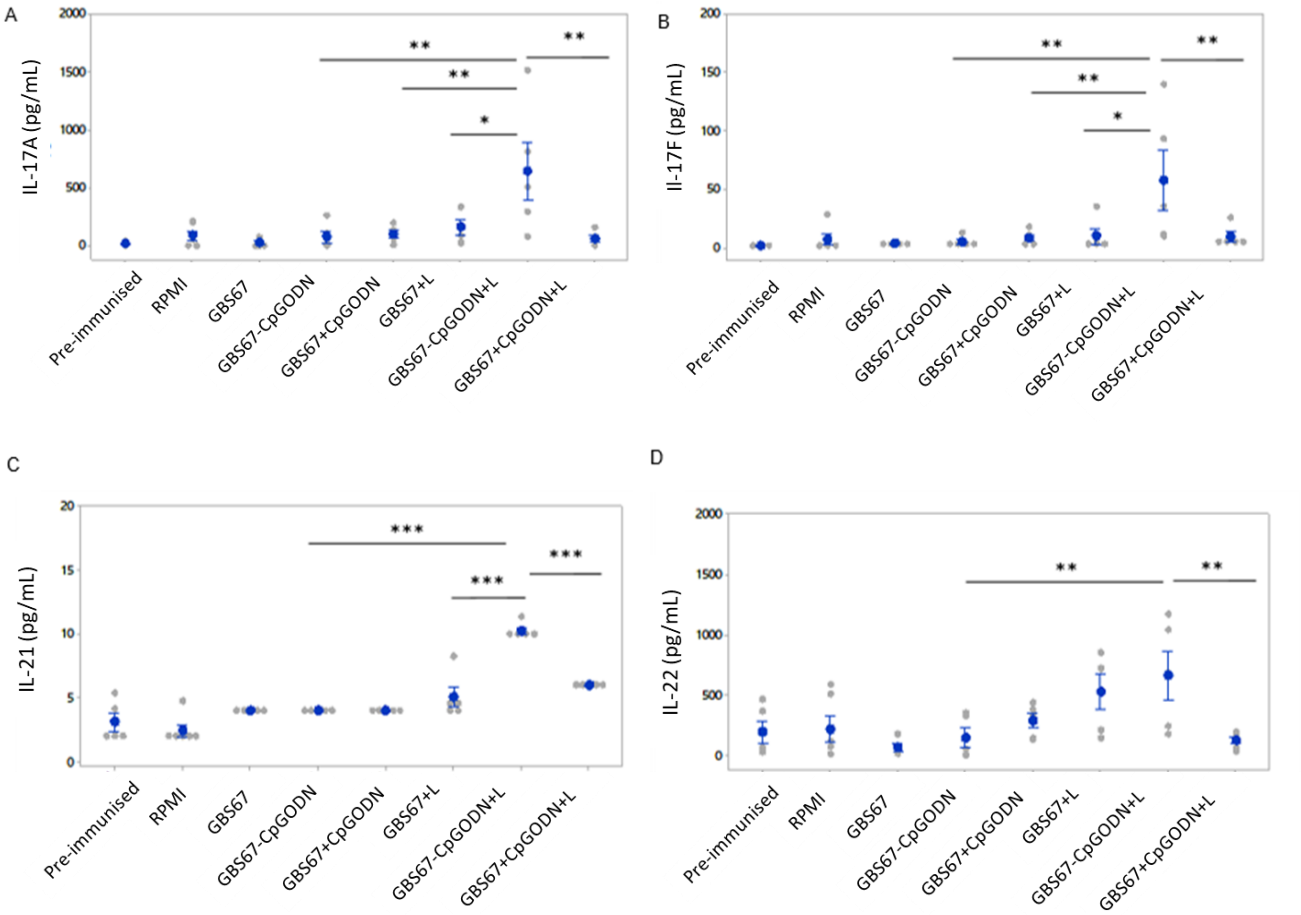

Figure 5.8 *Th17 Cytokine panel (A) IL-17A (B) IL-17F (C) IL-21 (D) IL-22 for cell-mediated responses. Mice were immunised with two injections spaced at 3-week intervals with the different formulations, as described in Section. 5.4.2. At day 42, spleen cells were prepared and restimulated in vitro with 4 µg/mL GBS67 and were incubated at 37 °C, 5% CO_2 for 72 hours. RPMI media was used as negative control. Culture supernatants were harvested after 72 hours and tested for cytokine levels by LEGENDplex mouse Th cytokine (13-plex) multi-analyte flow assay kit. Results are plotted for individual mice (◦) and also an average (•), to show variability across the mice. Values represent the mean ± SE from cells of five mice. *p<0.05; **p<0.01;***p<0.001.*

A different category of Th cells is T9. T9 cells are identified by the potent production of IL-9. Following on from the previous results, no significant differences were observed between all the groups tested with exception the difference between free GBS67 and GBS67-CpGODN+liposomes and GBS67-CpGODN with GBS67-CpGODN+liposomes (Figure 5.9). GBS67-CpGODN+liposomes IL-9 levels were 14-fold higher than the ones obtained with free GBS67 and GBS67-CpGODN ($p<0.05$). Interestingly, no significant differences were reached between GBS67-CpGODN+liposomes and GBS67+CpGODN+liposomes groups, despite the boosted IL-9 levels (2-fold) obtained with protein conjugate+liposomes (Figure 5.9).

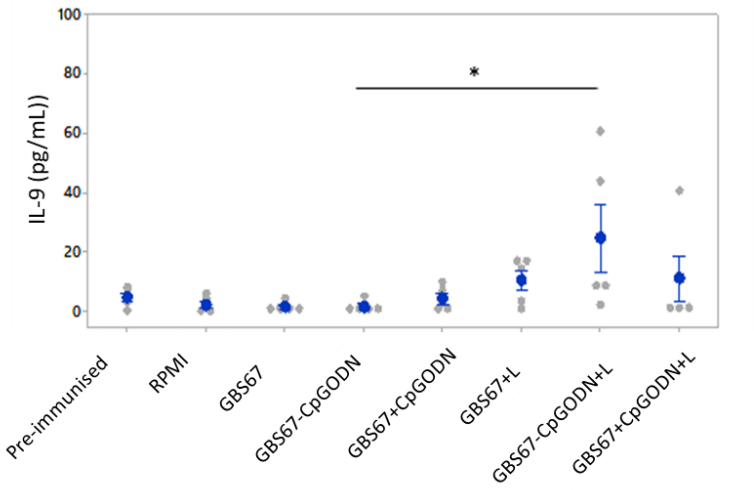

Figure 5.9 *Th9 Cytokine panel for cell-mediated responses. Figure presents the IL-9 cytokine levels obtained. Mice were immunised with two injections spaced at 3-week intervals with the different formulations, as described in Section. 5.4.2. At day 42, spleen cells were prepared and restimulated in vitro with 4 µg/mL GBS67 and were incubated at 37 °C, 5% CO_2 for 72 hours. RPMI media was used as negative control. Culture supernatants were harvested after 72 hours and tested for cytokine levels by LEGENDplex mouse Th cytokine (13-plex) multi-analyte flow assay kit. Mixture and conjugate are represented by (+) and (-), respectively. Results are plotted for individual mice (◦) and also an average (•), to show variability across the mice. Values represent the mean ± SE from cells of five mice. *p<0.05.*

A group of cytokines, which can be produced by different Th cells, is presented in Figure 5.10. Although no significant differences were reached between the groups tested regarding TNF-α, combination of GBS67-CpGODN+liposomes gave the highest TNF-α mean value obtained (Figure 5.10A). Interestingly, the combination of GBS67 and liposomes appeared to be the most potent group giving the highest IL-6 cytokine obtained (not significant) (Figure 5.10B). Regarding IL-10, results followed the same trends observed for other cytokines. Group 5 (GBS67-CpGODN+liposomes) induced 10-fold higher IL-10 cytokine responses compared to free GBS67 ($p<0.05$) as presented in Figure 5.10C. Similarly, IL-10 levels induced by combination of protein conjugate and liposomes were 6-fold boosted compared to

GBS67-CpGODN alone, even though differences did not reach significance (p=0.08). On the other hand, mixture of GBS67, CpGODN and liposomes did not augment further IL-10 levels compared to free GBS67 and GBS67+CpGODN, with the IL-10 cytokine levels being 5-fold lower than the ones obtained by combination of GBS67-CpGODN conjugate with liposomes (Figure 5.10).

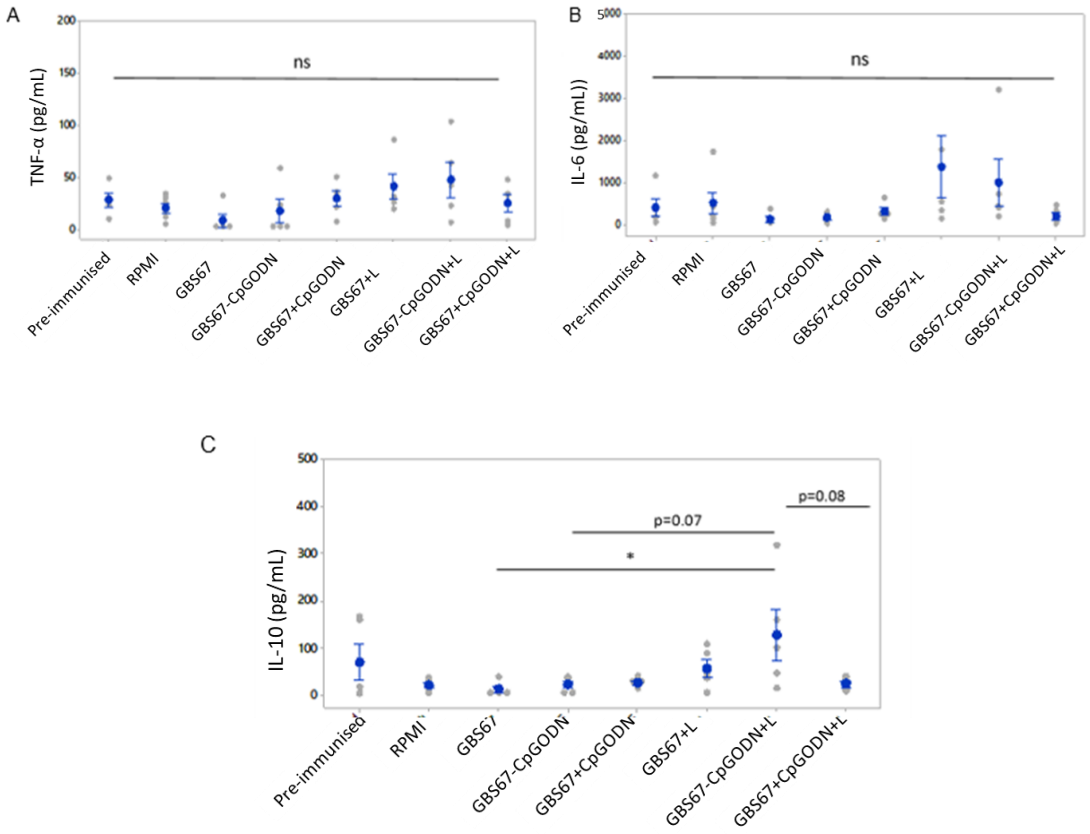

Figure 5.10 *Cytokine panel (A) TNF-α (B) IL-6 (C) IL-10 from cytokines which can be produced by several Th cell types. Mice were immunised with two injections spaced at 3-week intervals with the different formulations, as described in Section. 5.4.2. At day 42, spleen cells were prepared and restimulated in vitro with 4 µg/mL GBS67 and were incubated at 37 °C, 5% CO_2 for 72 hours. RPMI media was used as negative control. Culture supernatants were harvested after 72 hours and tested for cytokine levels by LEGENDplex mouse Th cytokine (13-plex) multi-analyte flow assay kit. Mixture and conjugate are represented by (+) and (-), respectively. Results are plotted for individual mice (◦) and also an average (•), to show variability across the mice. Values represent the mean ± SE from cells of five mice. *p<0.05; ns: non-significant.*

5.5.5 Biodistribution study

The biodistribution profiles of free GBS67, GBS67-CpGODN and GBS67-CpGODN+liposomes were compared in order to evaluate the ability of DSPC: Cholesterol: DDA cationic liposome formulation to retain the GBS67 protein within the body. Groups of 3 female mice BALB/c mice were immunised intramusculary with one 10 µg protein-based dose of vaccine, corresponding to the administration of 1.5

μg of TLR9. A 200 μg dose of cationic liposomes was used in one of the groups. Non-immunised mice was used as negative control.

Images were analysed and the total amount of radiated energy (total flux) was calculated for all the days. Overall, full mice body images showed that signal is concentrated at the site of injection for all the groups tested. After intramuscular injection of GBS67 either alone or conjugated with CpGODN, rapid reduction of protein signal was noted over a period of 11 days (Figure 5.11-Figure 5.12A). Interestingly, part of the free protein and GBS67-conjugate dose was accumulated at the site of injection for 11 days (14% and 21% remaining at day 11 post injection for GBS67 and GBS67-CpGODN, respectively; Figure 5.12A). Regarding GBS67-CpGODN, incorporation of CpGODN TLR9 agonist in conjugated form, had no significant effect on protein retention at the injection site, at all-time points measured (Figure 5.11-Figure 5.12A). Comparable levels of GBS67 remained at the injection site (75% remaining at day 1, 44% after 4 days, and 21% of the dose remaining at day 11 post injection) when TLR9 agonist CpGODN was conjugated to GBS67 protein, although a slower signal reduction was noted during the first 4 days of the study (Figure 5.12A). When considering GBS67-CpGODN+liposomes retention at the site of injection, high levels of GBS67-CpGODN (114%, 128% and 116% of the initial signal at days 1, 7 and 11 post injection, respectively; Figure 5.11-Figure 5.12A) were retained at the injection site, which they were 8-fold and 5-fold significantly higher than those obtained with free GBS67 and GBS67-CpGODN protein conjugate at day 11 ($p<0.001$). Interestingly, no DiD fluorescence signal was detected immediately after injection. However, liposomes signal was increasing as the study was progressing with the final value at day 11 being 2-fold higher than that obtained at day 1 (Figure 5.12B).

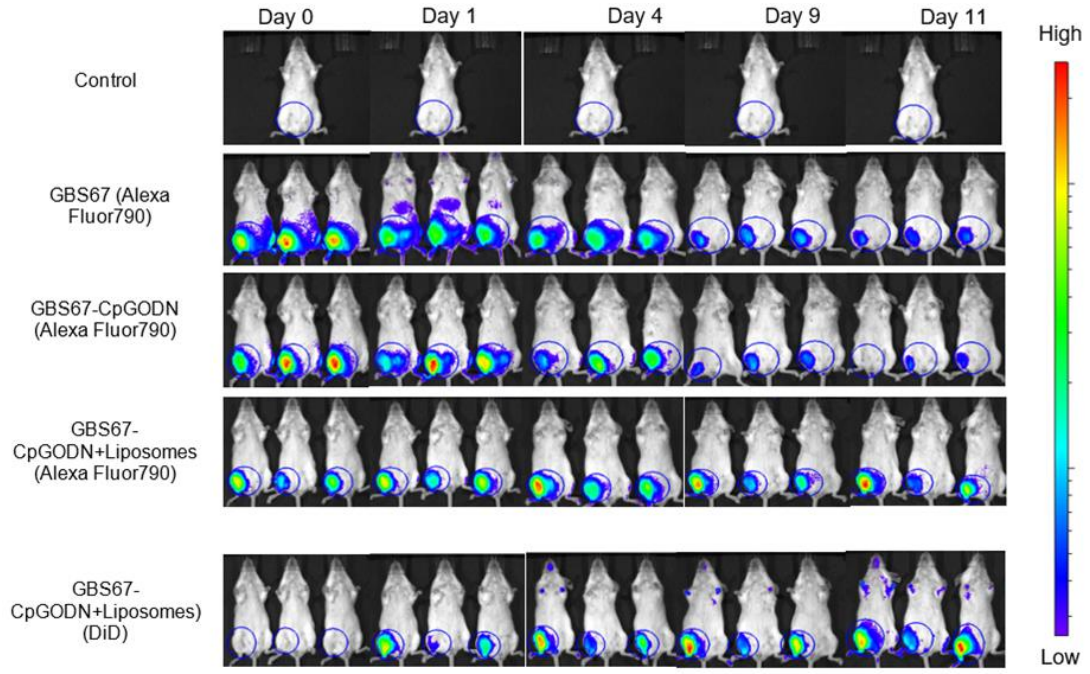

Figure 5.11 *Biodistribution profile of protein and liposomes. Whole-body fluorescence intensity images for selective days, following i.m. injection of either free GBS67, GBS67 conjugated to CpGODN (GBS67-CpGODN) or GBS67-CpGODN adsorbed on the surface of DSPC: Cholesterol: DDA cationic liposomes (GBS67-CpGODN+Liposomes). Mice received 10 µg protein-based dose of vaccine, corresponding to the administration of 1.5 µg of TLR9. A 200 µg dose of cationic liposomes was used in one of the groups. Non-immunised mouse was used as negative control. Scale bar refers to the fluorescence intensity.*

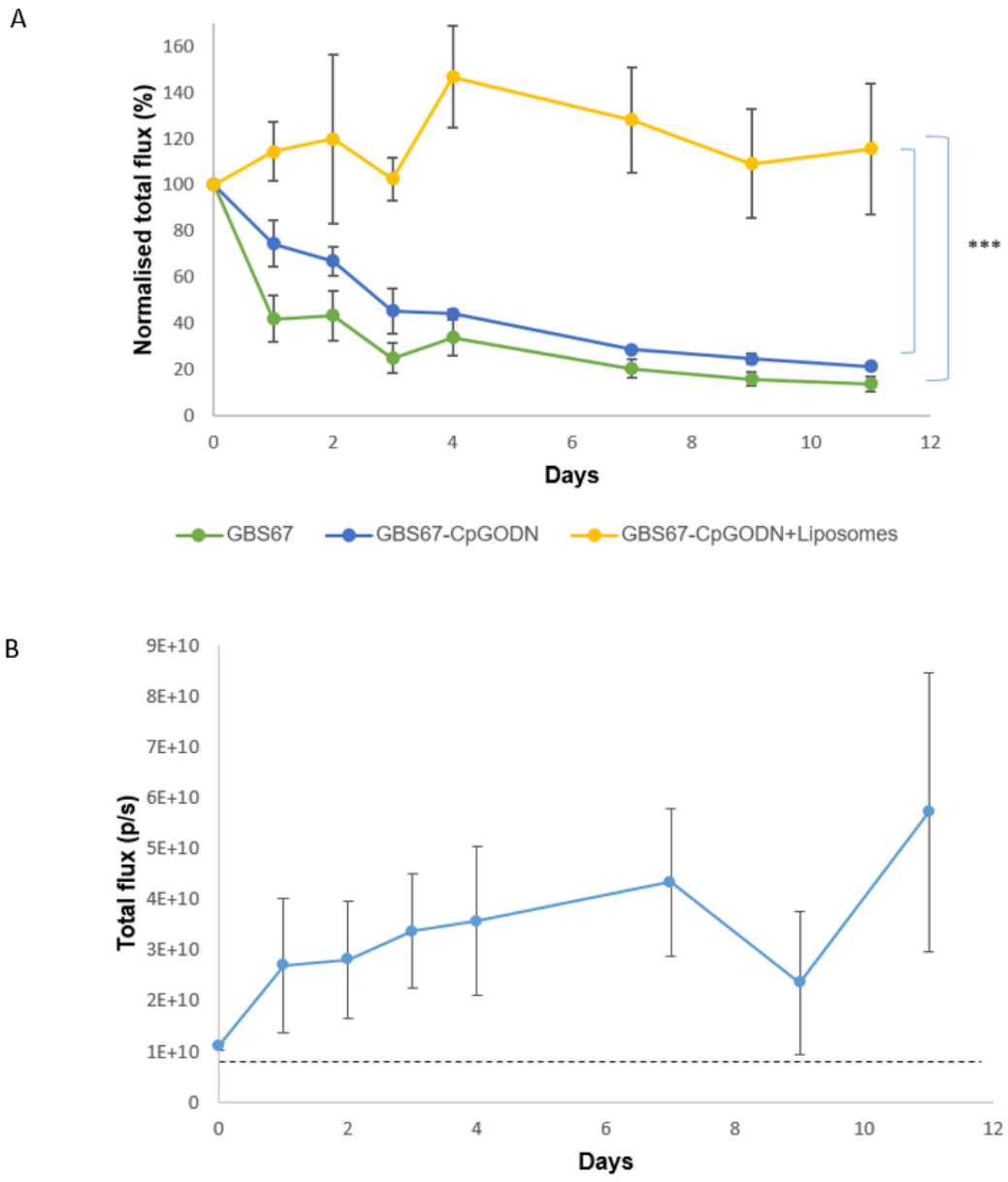

Figure 5.12 *Biodistribution profile of protein and liposomes. (A) Protein and (B) liposomes dose retention at the site of injection following i.m. injection of either free GBS67, GBS67 conjugated to CpGODN (GBS67-CpGODN) or GBS67-CpGODN adsorbed on the surface of DSPC: Cholesterol: DDA cationic liposomes (GBS67-CpGODN+Liposomes). Mice received 10 µg protein-based dose of vaccine, corresponding to the administration of 1.5 µg of TLR9. A 200 µg dose of cationic liposomes was used in one of the groups. Non-immunised mouse was used as negative control. The proportion of Alexa Fluor 790 tracking dye at the injection site as a percentage of the initial dose was calculated. Mixture and conjugation are represented by (+) and (-), respectively. Dash line on Figure (C) represents the background level. Results represent the mean ± SD of three mice per group. ***p<0.001.*

On day 14 spleens, kidneys, livers and intestines were isolated and total flux was determined. When considering the movement of antigen to the organs, antigen demonstrated to be predominantly localised in the kidneys, which eventually plays a dominant role in the clearance and eventual elimination of protein (Figure 5.13). Interestingly, antigen conjugate adsorbed on liposomes showed the highest intensity in the kidneys compared to free protein and protein conjugate administrated in the absence of liposomes. When tracking the presence of liposomes, no predominant signal was observed in any of organs tested (Figure 5.13).

Figure 5.13B and C show the total flux intensity for all the organs and groups. When considering the movement of antigen and liposomes to the organs, intestines showed the strongest signal obtained for all the groups, which contrasts with Figure 5.13A. Interestingly, high total flux value was also obtained for the non-immunised mouse.

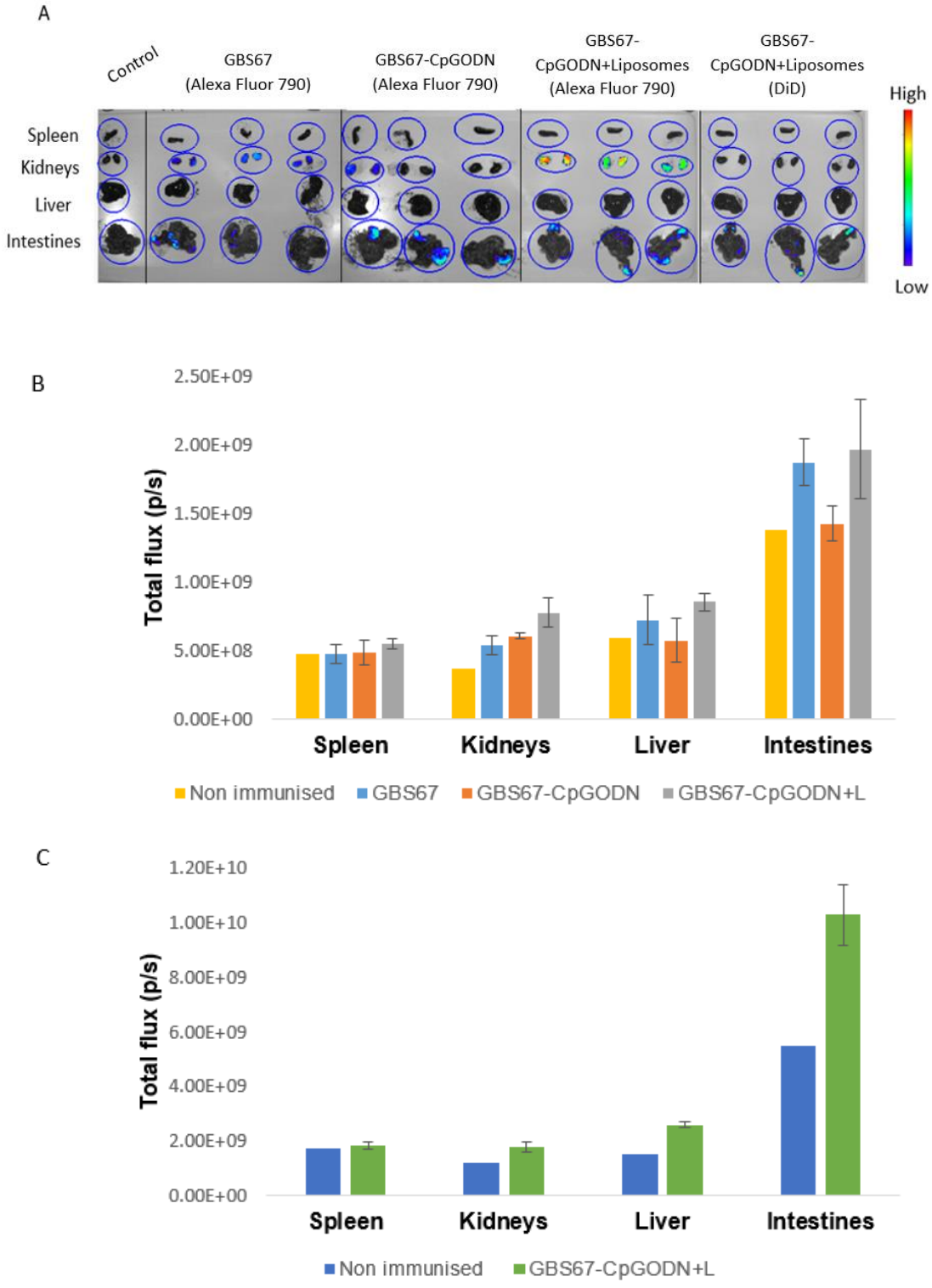

Figure 5.13 *(A) Organs ex-vivo imaging for all groups at Day 14. Fluorescence intensity of (B) protein and (C) liposomes for different organs. Group of 3 female mice was immunised with free GBS67 or GBS67 conjugated to CpGODN (GBS67-CpGODN) or GBS67-CpGODN adsorbed on the surface of DSPC: Cholesterol: DDA cationic liposomes (GBS67-CpGODN+Liposomes) at day 0. Mice received 10 µg protein-based dose of vaccine, corresponding to the administration of 1.5 µg of TLR9. A 200 µg dose of cationic liposomes was used in one of the groups. Mice were terminated at day 14 and spleen, kidneys, liver and intestines were isolated for ex-vivo imaging. Mixture and conjugation are represented by (+) and (-), respectively. A non-immunised mousewas used as negative control. Results represent the mean ± SD of three mice per group. Scale bar refers to the fluorescence intensity.*

5.6 Discussion

This chapter refers to the immunological evaluation of the designed system composed by the GBS67-CpGODN conjugate adsorbed on the surface of DSPC: Cholesterol: DDA cationic liposomes. Overall, the designed formulation was tested *in vivo* demonstrating high antibody and cell-mediated responses in mice.

Vaccines mainly induce humoral immunity to prevent infection. Therefore, vaccines induce the production of antibodies, and the pathogens are prevented from infecting the host cells through the action of antibody neutralisation or opsonisation (Moyer *et al.*, 2016). Thus, strategies to promote the humoral response are of key importance in vaccine development. The ability of the designed protein conjugate GSB67-CpGODN to induce B-cell responses, was evaluated. Total antigen specific-antibody responses proved that the chemical linkage of TLR9 agonist CpGODN with antigenic protein confers a strong adjuvant effect towards protein antigen, in comparison with the simple coadministration of the antigen with CpGODN. In agreement with the total IgG titres, the estimation of IgG subclasses, IgG1 and IgG2a, proves that the GBS67-CpGODN elicited the highest IgG1 and IgG2a titres compared to physical mixture and free protein, with IgG2a titres being negligible in response to protein and protein/CpGODN mixture after the 2nd dose. These findings are in agreement with the literature where it has been previously demonstrated that the chemical conjugation of CpGODN to the antigen induces earlier kinetics and greater magnitude of immune responses (Tighe *et al.*, 2000; Shirota *et al.*, 2001; Maurer *et al.*, 2002; Heit *et al.*, 2003; Heit *et al.*, 2005; Kramer *et al.*, 2017). It is supported that, when CpGODN and the protein antigen are conjugated, the colocalization of antigen and adjuvant into the same cells is favoured. In contrary, when antigen and adjuvant are physically mixed, efficient codelivery cannot be ensured. Recent research has reported that self-assembled CpGODN, protein/peptide-CpGODN conjugates, and nanomaterial-CpG ODN complexes demonstrate higher adjuvant effects than free CpGODN, owing to their improved uptake efficiency into cells expressing TLR9. Therefore, the close proximity of the protein antigen and CpG oligonucleotides adjuvant, especially, direct linkage of CpGODN to an antigen, ensuring that antigens and CpG ODN can codeliver to the same APCs, which directs the response towards the antigen, thereby lowering the required dose for an effective immune response (Tao *et al.*, 2014; Hanagata, 2017; Ignacio *et al.*, 2018).

It is supported that particle formation improves vaccine potency through improved antigen stability, repetitive antigen display (providing optimal B cell stimulation), and

improved antigen uptake (Moyer *et al.*, 2016). The adjuvant and the immunostimulatory properties of liposomes are very well known. Special focus has been given on cationic liposomes, as it has been demonstrated that the immunogenicity of cationic liposomes is stronger than that of neutral and anionic liposomes (Davidsen *et al.*, 2005; Vangala *et al.*, 2006; Yan *et al.*, 2007). This superiority of cationic liposomal formulations has been related to the association between negatively charged antigen and the liposomes, which increases the antigen presentation to APCs by forming antigen depot effect at the site of injection (Henriksen-Lacey *et al.*, 2010b).

In this study, different particulate vaccines in the 160-180 nm size range and high positive charge were developed composed by GBS67 antigen, CpGODN adjuvant and DSPC: Cholesterol: DDA cationic liposomes. Liposome size and charge are of major importance for optimal vaccine potency, as they influence their biodistribution, thus affecting the induced immune responses, although other factors such as the administration route and the lipid composition can also affect those (Tandrup Schmidt *et al.*, 2016). Despite, positive charge being the predominant factor for cationic particles, it was observed previously that a smaller particle size (200-500 nm) favors the lymphatic uptake (Henriksen-Lacey *et al.*, 2011b; Perrie *et al.*, 2016) as also the uptake by APCs demonstrating enhanced immunogenicity (Carstens *et al.*, 2011). Immunological studies demonstrated that combination of liposomes with CpGODN either in conjugation or mixture form, further boosted immunity revealing a synergistic effect between the two adjuvants. These findings are in accordance with what has been reported before by other studies where CpGODN and antigen were mixed (Gursel *et al.*, 2001; Mansourian *et al.*, 2014) or encapsulated (Jaafari *et al.*, 2007; Bal *et al.*, 2011; Bayyurt *et al.*, 2017) with or into liposomes. The immune-enhancing effect is maximised when TLR agonist and antigen are coassociated in the same particle, such that TLR and antigen are colocalised to the same endosome/phagosome within APCs (Moyer *et al.*, 2016).

Herein, it was demonstrated for the first time that the adsorption of protein conjugate GBS67-CpGODN on DSPC: Cholesterol: DDA cationic liposomes resulted in significant enhancement of immune responses. Notable is the fact that this response is unequivocally higher than the individual adjuvant effects of CpGODN and liposomes, as also the mixture of all the components together. Although total IgG levels induced by protein conjugate-liposomes and the physical mixture of CpGODN, GBS67 and liposomes are comparable, IgG subclasses analysis revealed major differences between the two formulations. While inducing an immune response

phenotypically similar, protein conjugate-liposomes vaccine was clearly superior in magnitude showing that conjugation between protein and CpGODN was necessary for eliciting high IgG2a titres. It is assumed that the superiority of liposomes-conjugate combination relies on the fact that conjugation ensures the colocalisation of CpGODN and antigen, as conjugation secures coadsorption of CpGODN and antigen on liposomes surface. In contrast, adsorption of free CpGODN and free antigen on liposomes cannot ensure that both will be adsorbed on the same liposome. Some liposomes could potentially adsorb protein, whereas some others many only display CpGODN and finally some particles could adsorb both CpGODN and antigen.

In agreement with the elicited anti-GBS67 IgG levels, the OPKA titres obtained against serotype V CJB1111 strain demonstrated that when TLR9 agonist CpGODN is included in vaccine in conjugated form, combined or not with cationic liposomes, a significant enhancement in functional activity of serum is noted. This result highlights once again the importance of conjugation for the immunological behaviour of the designed system and confirms that conjugation of CpGODN on GBS67 protein through thiol-maleimide addition resulted in the highest anti-protein antibody levels in the set, which were sufficient to induce efficacious bacterial killing. In agreement with previous investigations on other conjugates, protein-CpGODN conjugate vaccine elicited higher-tittered antibodies of greater functional activity than those elicited by the protein alone, perhaps due to stabilisation and/or multivalency of immunogenic epitopes on the protein following conjugation and adsorption on liposomes, antigen presentation, or a depot effect resulting from the increased mass of the conjugate and the presence of cationic liposomes (Yang *et al.*, 2007).

Naïve CD4+ T (Th0) cells that recognise the antigen on MHC-II proliferate and differentiate into a variety of effector CD4+ T cells, including antigen-specific helper 1 T (Th1) cells or antigen-specific helper 2 T (Th2) cells. These effector CD4+ T secrete a range of cytokines cells and are responsible of activating the differentiation of B cells into plasma cells, resulting in the induction of antigen-specific antibodies. The predominance of Th1 and Th2 T helper cell subsets is known to result in distinct patterns of cytokine secretion. TLR ligands as also cationic liposomes can shift this balance to higher Th1-biased CD4+ T-cell responses (Donadei *et al.*, 2016; Perrie *et al.*, 2016). An increase in this isotype levels with Th1-biased response has been associated with the protection conferred by different vaccines (Zhu *et al.*, 2010).

Cytokine responses analysis revealed overall no significant differences between cytokines levels elicited by GBS67-CpGODN conjugate and GBS67, CpGODN

mixture. Many factors could potentially be responsible for this effect. First, the low antigen and CpGODN doses used for the immunisation might not be sufficient for detectable T-cell proliferation induction. As it is supported by the literature, CpG-B ODNs are recognised by endosomal TLR9 of B cells, pDCs, mDCs, and macrophages, inducing inflammatory cytokines. However, B class CpGODN is known for its lack of T-cell activity (Hartmann and Krieg, 2000; Krug *et al.*, 2001; Hanagata, 2017). Thus, the type of immunological activity of CpGODN in combination with the very low immunisation dose could be responsible for its T-cell behaviour *in vivo*. On the other hand, the conjugation strategy used can have further impact on the agonist activity. The absence of a linker spacer between antigen and CpGODN might cause alteration of intracellular signalling resulting in suppression of T-cell-stimulatory cytokines production from APCs (Liu and Irvine, 2015).

Stronger B cell responses is a characteristic of B-class CpGODN which was chosen for this study. Honda *et al.* refers that B-class CpGODN are strong stimulators of B cell responses with moderate effect on IFN (Honda *et al.*, 2005). However, by forming complexes between CpG-B-ODN and a cationic nanomaterial using electrostatic interactions, the production of cytokines can be modulated (Chinnathambi *et al.*, 2012; Hanagata, 2017). In the current study, DDA cationic lipid was chosen for the formation of liposomes. DDA has a dual role in the designed system. First, DDA confers a positive net charge favouring the adsorption of negative molecules on liposomes surface but the same time provides significant immunostimulatory and adjuvanting properties (Davidsen *et al.*, 2005; Henriksen-Lacey *et al.*, 2010a; Schwendener, 2014; De Serrano and Burkhart, 2017). Indeed, adsorption of antigen-CpGODN complex on DDA-based cationic liposomes significantly shifted immunity. Combination of cationic liposomes with protein conjugate demonstrated the highest cytokine responses observed. Obtained responses were not characterised by a specific T cell-driven response. Interestingly, a combination of cytokines released by Th1, Th2, Th17 and Th9 cells were noted, demonstrating the multifunctional activity of the protein conjugate-liposomes system. Generally, mixture of liposomes with CpGODN and GBS67 was not able to induce T cell responses. These results demonstrate that in order to achieve cell-mediated responses in such a low antigen and CpGODN dose, the covalent linkage of the CpGODN immunopotentiator to the protein prior to adsorption on particles surface, was needed.

Pharmacokinetic, biodistribution, and metabolic clearance characteristics are important properties that can influence the overall efficacy of novel therapeutics (Vasquez *et al.*, 2011). It has been previously demonstrated by others that cationic

liposomes form a depot effect at the site of injection whereby liposomes and consequently antigen are retained in the tissue for an extended period of time (Henriksen-Lacey *et al.*, 2010a; Henriksen-Lacey *et al.*, 2011a; Wilkinson *et al.*, 2018; Roces *et al.*, 2019). Formation of a depot effect results in attraction of APCs that engulf antigen and become activated (Perrie *et al.*, 2016). Based on that, it was speculated that the obtained immunological activity of the GBS67-CpGODN+liposomes system is also related with the deposition of liposomes at the site of injection in conjunction with the CpGODN targeting ligand. Indeed, biodistribution studies revealed that liposomes promoted high accumulation of GBS67-CpGODN protein conjugate within the body of the mice, which lasts up to 11 days.

Ex-vivo organs imaging showed predominant accumulation of antigen in the kidneys highlighting that at day 14 protein is already got into the clearance process from the body through urine. The high accumulation of antigen and liposomes observed in the intestines was comparable to background levels, which indicates that intestines signal is presumably not related to antigen and liposomes signals, but to interfering signal coming from mouse food. It has been previously demonstrated that the diet fed to an animal prior to imaging can have dramatic effects on image quality and clarity, due largely to the chlorophyll component of many plant-based ingredients used in regular mouse chows (Nooshabadi *et al.*, 2016). Inoue *et al.* refers that intestinal autofluorescence may mask the signal from fluorescent probes localised in or near the abdomen and may also mimic the excretion and/or accumulation of probes in the intestine (Inoue *et al.*, 2008). Thus, tissue biodistribution should be repeated with termination of mice in an earlier time point, in order to track the antigen and liposomes in the different tissue and following low-fluorescence diet requirements in order to avoid food interference with the results. Finally, the use of larger number of mice is recommended for determination of background levels (controls) and for statistics purpose.

Whilst the full mechanism of immunostimulatory action of cationic liposomes is not yet fully understood, it can safely be assumed that the obtained B and T cell responses are a result of the liposomes and thus protein conjugate retention at the site of injection (Christensen *et al.*, 2011). High accumulation of the formulation at the injection induced recruitment of immune cells. As a result, antigen is taken up by the cells and digested meanwhile CpGODN can bind to TLR9 in the endosome of the cells, activate them leading to strong B and T cell responses. In line with observations from this study, work from others proved that injection of cationic liposomes and

antigen significantly increased the attraction of immune cells at the site of injection, increased trafficking of liposomes to the draining lymph nodes and thus the immune responses (Korsholm *et al.*, 2010; Henriksen-Lacey *et al.*, 2011a; Awate *et al.*, 2013).

5.7 Conclusion

Conjugation of CpGODN to protein confer on a protein vaccine the ability to induce a more potent immune response, compared to CpGODN/protein mixture vaccination. Building on the principle that multivalency can increase the immunogenicity of subunit antigens, it was also shown that presentation of protein conjugate on the surface of cationic nanoparticles elicited enhanced humoral and cell-mediated immune responses. Overall, the multifaceted immune response elicited with CpGODN and liposomes-based immunisation highlights the potential for harnessing the immunostimulatory properties of different adjuvants to develop more effective nanostructure-based vaccine platforms.

Chapter 6 Concluding remarks and future perspectives

During the past decades, intensive research has been conducted to develop vaccines able to prevent and treat all the kinds of infections. Live attenuated vaccines are currently the most efficient vaccines being used for the elimination of many diseases (Moyle, 2017). Despite their high efficacy, the use of conventional vaccines is restricted by their low safety profile. Protein and peptide-based vaccines have attracted interest as safer alternative compared to traditional vaccines. Nevertheless, the immune responses induced by subunit vaccines are still weaker compared to live-attenuated vaccines. Current research is focused on improving the efficiency of subunit vaccines, which are believed to be the most promising of the vaccines (Rappuoli *et al.*, 2011).

Nanotechnology offers several solutions for enhanced vaccine formulations (Peek *et al.*, 2008). Recently, adjuvants have received more attention for their ability to increase the efficacy of vaccines and drug formulations. Liposomes (Perrie *et al.*, 2016), polymeric nanoparticles and emulsions are some of the most used adjuvants in vaccine development (Mohan *et al.*, 2013). Nanoparticles have the advantage of the small size which gives them longer circulation time in bloodstream, allowing them to reach the target cells (Solaro *et al.*, 2010). In addition, studies demonstrated that the efficiency of a nanotechnology-based system can be improved when nanoparticle is conjugated with a specific ligand which can bind specific receptors on the cell surface, such as TLRs (Ghosh and Heston, 2004; Peer *et al.*, 2007).

The strong self adjuvanting activity of TLR2 agonist, Pam_3Cys has been established along the years. The lipid moiety presented on these lipopeptides is the reason behind their adjuvant properties. Research has been focused on the use of acyl moieties for lipopeptide vaccine development with Pam_3Cys being one of the most studied examples (Bueno *et al.*, 2004; Moyle *et al.*, 2006). In an effort to utilise the adjuvant properties of Pam_3Cys, its chemical conjugation with protein was attempted at the beginning of this study. However, it has been concluded that incorporation of Pam_3Cys into protein is not straight forward. The solubility issues due to the lipid nature of Pam_3Cys made its addition on protein and peptide antigens challenging. Due to the challenges described in this Chapter 2 of this study, the replacement of a Pam_3Cys TLR2 agonist with the hydrophilic TLR9 agonist CpGODN was decided.

The potency of CpGODN TLR9 agonist has been demonstrated by many researchers with some of its formulations being tested in clinical trials. CpGODN has been used for stimulation of immune responses physically mixed with antigens and other adjuvants or encapsulated into nanoparticles for delivery to lymph nodes in an effort

to protect it from degradation. Despite the research has been done so far, no research has been focused on the use of protein conjugates in conjunction with liposomes attributes. Conjugation efficiency has been proven extensively, especially when it is compared with simple coadministration of antigens and adjuvants (Heit *et al.*, 2005). It is supported that conjugation can ensure codelivery of protein and adjuvant to the same cell (Vollmer and Krieg, 2009). Similarly, cationic liposomes use as adjuvants/delivery systems have attracted interest the last years due to their high potential and efficiency (Christensen *et al.*, 2011; Perrie *et al.*, 2016). Special focus has been given on the use of cationic liposomes as their positive nature favors formation of the depot effect at the injection site. Building on the previous work in the field, this project aimed to study the liposomal delivery of CpGODN conjugated on antigenic proteins in an effort to maximise the vaccination potency.

In the Chapter 3 of this study it has been described the conjugation strategy followed for the conjugation of CpGODN on proteins. Three different model proteins NadA, CRM197 and GBS67, have been successfully conjugated on CpGODN motifs using maleimide-thiol chemistry as has been previously used for the preparation of other protein-CpGODN conjugates (Maurer *et al.*, 2002; Clauson *et al.*, 2019). Based on the isoelectric point of the conjugates and their negative charge, cationic liposomes were selected for their delivery ensuring the adsorption of protein conjugates on their surface due to electrostatic interactions. Cationic liposomes composed of DSPC: Cholesterol: DDA (10:40:50 molar ratio) were manufactured by microfluidics and fully characterised by DLS demonstrating an average size of 180-190 nm. These formulations had the capability to efficiently adsorb negatively charged molecules as antigens and adjuvants on their surface. After intramuscular administration, liposomes absorbing protein conjugate resulted in a 1.2-fold and 2-fold increase in antibody-mediated responses compared to those observed with unconjugated form/liposomes mixture and protein conjugate alone, respectively. DSPC: Cholesterol: DDA liposomes-bearing protein-CpGODN induced significantly higher production of cytokines compared to protein/CpGODN/liposomes physical mixture. Finally, biodistribution study revealed high accumulation of protein conjugate+liposomes complex on the site of injection compared to the protein conjugate alone, highlighting the benefit of liposomes incorporation for a depot effect. Deposition of the vaccine formulation at the site of injection has been proven to be important factor for immunostimulatory action of vaccine as increases antigen exposure time within the body (Christensen *et al.*, 2011).

Overall, a double adjuvanted system composed by CpGODN, antigen and cationic liposomes was designed. It has been evidenced that coadministration of CpGODN and liposomes with antigen is not efficient enough for the occurrence of synergy between the adjuvants and thus induction of strong B and T cell responses. In contrary, it has been highlighted that chemical ligation of CpGODN with antigen was essential for achieving strong immunopotency, strongly emphasising the believe that conjugation facilitates the codelivery and couptake of antigen and adjuvant into the same cell.

The multifaceted immune response elicited with CpGODN and liposomes-based immunisation highlights the potential for harnessing the mechanisms of actions of different adjuvants to develop more effective nanostructure-based vaccines. Despite the wide use of vaccine adjuvants in billions of doses of human and animal vaccines, the mechanisms of action by which they potentiate immune responses are not fully characterised. Adjuvants may act by a combination of various mechanisms including formation of depot, induction of cytokines and chemokines, recruitment of immune cells, enhancement of antigen uptake and presentation, and promoting antigen transport to draining lymph nodes.

The ultimate goal of vaccination is to generate protection against disease causing pathogens. Protective immunity against different pathogens requires different immune responses that can be generated by using appropriate vaccine adjuvants. The activation of immunity via various mechanisms is favoured by combination of adjuvants, which results in more potent formulation that can enhance the quality and quantity of immune response against vaccine antigens. The future of vaccine adjuvant research is heading toward developing novel combination adjuvants that consist primarily of Pattern recognition receptors (PRRs) agonists and particulate adjuvants (Awate *et al.*, 2013; Ulmer, 2013). Herein, an APC targeting ligand as is TLR9 agonist has been combined with liposome particles. The use of cationic liposomes created the deposition of immunogen-CpGODN conjugate at the site of injection and the recruitment of APCs. Thus, CpGODN binds to the receptor of APCs, activates them meanwhile antigen is digested and processed leading to the induction of high antibody and cell-mediated responses.

The conjugation approach as also the nanoparticle contribution described in this study, can be particularly helpful for enhancement of immunity using low doses of antigen and increasing the speed and reducing the number of immunisations required to achieve effectiveness. The work described within this study gives initial evidencefor

the immunopotency of the designed system using a combination of delivery systems and immunopotentiators technology approaches.

Future studies could potentially investigate in depth the mechanism of action of the design system (e.g. antigen uptake and presentation by different cell populations). In addition, cytotoxicity studies are needed for reactogennicity test of the formulation taking into consideration the safety concerns regarding the use of CpGODN and cationic liposomes, as they can be toxic. Nevertheless, no side effects were observed during the immunisation studies, maybe further optimisation of the system is required for achieving the correct balance between potency and safety.

More in depth investigation of the pharmacokinetic profile of the prepared conjugate-formulation complex is required for tissue trafficking. An earlier termination time point is required for isolation and *ex-vivo* organs imaging, following by specific dietary requirements for avoiding fluorescent contribution to the fluorescent animal signalling. Special focus has to be given on the selection of fluorescent probes for liposomes and antigen tracking as they may be FRET pairs (Bajar *et al.*, 2016). In addition, studies should be conducted in order to investigate further the identity of fluorescence signals observed as the lipophilic nature of DiD could potentially cause interactions with the lipophilic components of the body compromising the results.

Finally, the same approach could potentially be applied using different antigens and targeting different diseases. The work described in this thesis gives a first indication about the utilisation of antigen-TLR conjugation and formulation combination for the design of more potent vaccines. It may worth to investigate the application of the approached proposed during this study using different TLR agonist for evaluate the impact on the immune obtained immune responses.

References

Al-Dosari, M.S., and Gao, X. (2009). Nonviral gene delivery: principle, limitations, and recent progress. AAPS J *11*, 671-681.

Almgren, M., Edwards, K., and Karlsson, G. (2000). Cryo transmission electron microscopy of liposomes and related structures. Colloids and Surfaces A: Physicochemical and Engineering Aspects *174*, 3-21.

Awate, S., Babiuk, L.A., and Mutwiri, G. (2013). Mechanisms of action of adjuvants. Frontiers in immunology *4*, 114-114.

Badescu, G., Bryant, P., Swierkosz, J., Khayrzad, F., Pawlisz, E., Farys, M., Cong, Y., Muroni, M., Rumpf, N., Brocchini, S., and Godwin, A. (2014). A New Reagent for Stable Thiol-Specific Conjugation. Bioconjugate Chemistry *25*, 460-469.

Bajar, B.T., Wang, E.S., Zhang, S., Lin, M.Z., and Chu, J. (2016). A Guide to Fluorescent Protein FRET Pairs. Sensors (Basel) *16*, 1488.

Baker, C.J., Carey, V.J., Rench, M.A., Edwards, M.S., Hillier, S.L., Kasper, D.L., and Platt, R. (2014). Maternal antibody at delivery protects neonates from early onset group B streptococcal disease. J Infect Dis *209*, 781-788.

Bal, S.M., Hortensius, S., Ding, Z., Jiskoot, W., and Bouwstra, J.A. (2011). Co-encapsulation of antigen and Toll-like receptor ligand in cationic liposomes affects the quality of the immune response in mice after intradermal vaccination. Vaccine *29*, 1045-1052.

Balbino, T.A., Correa, G.S.C., Favaro, M.T.P., Toledo, M.A.S., Azzoni, A.R., and de la Torre, L.G. (2015). Physicochemical and in vitro evaluation of cationic liposome, hyaluronic acid and plasmid DNA as pseudo-ternary complexes for gene delivery. Colloids and Surfaces A: Physicochemical and Engineering Aspects *484*, 262-270.

Bambini, S., De Chiara, M., Muzzi, A., Mora, M., Lucidarme, J., Brehony, C., Borrow, R., Masignani, V., Comanducci, M., Maiden, M.C.J*., et al.* (2014). Neisseria adhesin A variation and revised nomenclature scheme. Clin Vaccine Immunol *21*, 966-971.

Bangham, A.D., and Horne, R.W. (1964). Negative staining of phospholipids and their structural modification by surface-active agents as observed in the electron microscope. Journal of Molecular Biology *8*, 660-IN610.

Bayyurt, B., Tincer, G., Almacioglu, K., Alpdundar, E., Gursel, M., and Gursel, I. (2017). Encapsulation of two different TLR ligands into liposomes confer protective immunity and prevent tumor development. J Control Release *247*, 134-144.

Belliveau, N.M., Huft, J., Lin, P.J., Chen, S., Leung, A.K., Leaver, T.J., Wild, A.W., Lee, J.B., Taylor, R.J., Tam, Y.K*., et al.* (2012). Microfluidic Synthesis of Highly Potent Limit-size Lipid Nanoparticles for In Vivo Delivery of siRNA. Mol Ther Nucleic Acids *1*, e37-e37.

Blokesch, M., and Schoolnik, G.K. (2008). The extracellular nuclease Dns and its role in natural transformation of Vibrio cholerae. Journal of bacteriology *190*, 7232-7240.

Bose, R.J.C., Arai, Y., Ahn, J.C., Park, H., and Lee, S.-H. (2015). Influence of cationic lipid concentration on properties of lipid-polymer hybrid nanospheres for gene delivery. Int J Nanomedicine *10*, 5367-5382.

Boylan, N.J., Zhou, W., Proos, R.J., Tolbert, T.J., Wolfe, J.L., and Laurence, J.S. (2013). Conjugation site heterogeneity causes variable electrostatic properties in Fc conjugates. Bioconjug Chem *24*, 1008-1016.

Brewer, J.M., Tetley, L., Richmond, J., Liew, F.Y., and Alexander, J. (1998). Lipid Vesicle Size Determines the Th1 or Th2 Response to Entrapped Antigen. The Journal of Immunology *161*, 4000.

Brigtsen, A.K., Kasper, D.L., Baker, C.J., Jennings, H.J., and Guttormsen, H.-K. (2002). Induction of Cross-Reactive Antibodies by Immunization of Healthy Adults with Types Ia and Ib Group B Streptococcal Polysaccharide-Tetanus Toxoid Conjugate Vaccines. The Journal of Infectious Diseases *185*, 1277-1284.

Bueno, C., Lee, K.K., Chau, L.A., Lee-Chan, E., Singh, B., Strejan, G.H., and Madrenas, J. (2004). Mechanism of modulation of T cell responses by N-palmitoylated peptides. European journal of immunology *34*, 3497-3507.
Bulbake, U., Doppalapudi, S., Kommineni, N., and Khan, W. (2017). Liposomal Formulations in Clinical Use: An Updated Review. Pharmaceutics *9*, 12.
Capecchi, B., Adu-Bobie, J., Di Marcello, F., Ciucchi, L., Masignani, V., Taddei, A., Rappuoli, R., Pizza, M., and Aricò, B. (2005). Neisseria meningitidis NadA is a new invasin which promotes bacterial adhesion to and penetration into human epithelial cells. Molecular Microbiology *55*, 687-698.
Carstens, M.G., Camps, M.G.M., Henriksen-Lacey, M., Franken, K., Ottenhoff, T.H.M., Perrie, Y., Bouwstra, J.A., Ossendorp, F., and Jiskoot, W. (2011). Effect of vesicle size on tissue localization and immunogenicity of liposomal DNA vaccines. Vaccine *29*, 4761-4770.
Castor, M.L., Whitney, C.G., Como-Sabetti, K., Facklam, R.R., Ferrieri, P., Bartkus, J.M., Juni, B.A., Cieslak, P.R., Farley, M.M., Dumas, N.B.*, et al.* (2008). Antibiotic resistance patterns in invasive group B streptococcal isolates. Infectious diseases in obstetrics and gynecology *2008*, 727505.
Chen, V.L., Avci, F.Y., and Kasper, D.L. (2013). A maternal vaccine against group B Streptococcus: past, present, and future. Vaccine *31 Suppl 4*, D13-D19.
Chinnathambi, S., Chen, S., Ganesan, S., and Hanagata, N. (2012). Binding Mode of CpG Oligodeoxynucleotides to Nanoparticles Regulates Bifurcated Cytokine induction via Toll-like Receptor 9. Scientific Reports *2*, 534.
Christensen, D., Korsholm, K.S., Andersen, P., and Agger, E.M. (2011). Cationic liposomes as vaccine adjuvants. Expert Rev Vaccines *10*, 513-521.
Chua, B.Y., Eriksson, E.M., Brown, L.E., Zeng, W., Gowans, E.J., Torresi, J., and Jackson, D.C. (2008). A self-adjuvanting lipopeptide-based vaccine candidate for the treatment of hepatitis C virus infection. Vaccine *26*, 4866-4875.
Clauson, R.M., Berg, B., and Chertok, B. (2019). The Content of CpG-DNA in Antigen-CpG Conjugate Vaccines Determines Their Cross-Presentation Activity. Bioconjug Chem *30*, 561-567.
Cluff, C.W., Baldridge, J.R., Stöver, A.G., Evans, J.T., Johnson, D.A., Lacy, M.J., Clawson, V.G., Yorgensen, V.M., Johnson, C.L., Livesay, M.T.*, et al.* (2005). Synthetic Toll-Like Receptor 4 Agonists Stimulate Innate Resistance to Infectious Challenge. Infect Immun *73*, 3044.
Comanducci, M., Bambini, S., Brunelli, B., Adu-Bobie, J., Aricò, B., Capecchi, B., Giuliani, M.M., Masignani, V., Santini, L., Savino, S.*, et al.* (2002). NadA, a novel vaccine candidate of Neisseria meningitidis. J Exp Med *195*, 1445-1454.
Comberlato, A., Paloja, K., and Bastings, M.M.C. (2019). Nucleic acids presenting polymer nanomaterials as vaccine adjuvants. Journal of Materials Chemistry B.
Corthay, A. (2009). How do regulatory T cells work? Scand J Immunol *70*, 326-336.
Courant, T., Bayon, E., Reynaud-Dougier, H.L., Villiers, C., Menneteau, M., Marche, P.N., and Navarro, F.P. (2017). Tailoring nanostructured lipid carriers for the delivery of protein antigens: Physicochemical properties versus immunogenicity studies. Biomaterials *136*, 29-42.
Datta, S.K., Cho, H.J., Takabayashi, K., Horner, A.A., and Raz, E. (2004). Antigen–immunostimulatory oligonucleotide conjugates: mechanisms and applications. Immunological Reviews *199*, 217-226.
Davidsen, J., Rosenkrands, I., Christensen, D., Vangala, A., Kirby, D., Perrie, Y., Agger, E.M., and Andersen, P. (2005). Characterization of cationic liposomes based on dimethyldioctadecylammonium and synthetic cord factor from M. tuberculosis (trehalose 6,6'-dibehenate)—A novel adjuvant inducing both strong CMI and antibody responses. Biochimica et Biophysica Acta (BBA) - Biomembranes *1718*, 22-31.

De Serrano, L.O., and Burkhart, D.J. (2017). Liposomal vaccine formulations as prophylactic agents: design considerations for modern vaccines. J Nanobiotechnology *15*, 83.
de Titta, A., Ballester, M., Julier, Z., Nembrini, C., Jeanbart, L., van der Vlies, A.J., Swartz, M.A., and Hubbell, J.A. (2013). Nanoparticle conjugation of CpG enhances adjuvancy for cellular immunity and memory recall at low dose. Proc Natl Acad Sci U S A *110*, 19902-19907.
Dekkers, G., Bentlage, A.E.H., Stegmann, T.C., Howie, H.L., Lissenberg-Thunnissen, S., Zimring, J., Rispens, T., and Vidarsson, G. (2017). Affinity of human IgG subclasses to mouse Fc gamma receptors. MAbs *9*, 767-773.
Dermer, P., Lee, C., Eggert, J., and Few, B. (2004). A history of neonatal group B streptococcus with its related morbidity and mortality rates in the United States. Journal of pediatric nursing *19*, 357-363.
Dimov, N., Kastner, E., Hussain, M., Perrie, Y., and Szita, N. (2017). Formation and purification of tailored liposomes for drug delivery using a module-based micro continuous-flow system. Scientific reports *7*, 12045-12045.
Donadei, A., Balocchi, C., Mancini, F., Proietti, D., Gallorini, S., O'Hagan, D.T., D'Oro, U., Berti, F., Baudner, B.C., and Adamo, R. (2016). The adjuvant effect of TLR7 agonist conjugated to a meningococcal serogroup C glycoconjugate vaccine. Eur J Pharm Biopharm *107*, 110-119.
Dumoutier, L., Louahed, J., and Renauld, J.-C. (2000). Cloning and Characterization of IL-10-Related T Cell-Derived Inducible Factor (IL-TIF), a Novel Cytokine Structurally Related to IL-10 and Inducible by IL-9. The Journal of Immunology *164*, 1814.
Erikci, E., Gursel, M., and Gursel, I. (2011). Differential immune activation following encapsulation of immunostimulatory CpG oligodeoxynucleotide in nanoliposomes. Biomaterials *32*, 1715-1723.
Esposito, V., Musi, V., de Chiara, C., Veggi, D., Serruto, D., Scarselli, M., Kelly, G., Pizza, M., and Pastore, A. (2011). Structure of the C-terminal domain of Neisseria heparin binding antigen (NHBA), one of the main antigens of a novel vaccine against Neisseria meningitidis. J Biol Chem *286*, 41767-41775.
Fabbrini, M., Rigat, F., Rinaudo, C.D., Passalaqua, I., Khacheh, S., Creti, R., Baldassarri, L., Carboni, F., Anderloni, G., Rosini, R*., et al.* (2016). The Protective Value of Maternal Group B Streptococcus Antibodies: Quantitative and Functional Analysis of Naturally Acquired Responses to Capsular Polysaccharides and Pilus Proteins in European Maternal Sera. Clinical infectious diseases : an official publication of the Infectious Diseases Society of America *63*, 746-753.
Falloon, J., Talbot, H.K., Curtis, C., Ervin, J., Krieger, D., Dubovsky, F., Takas, T., Yu, J., Yu, L., Lambert, S.L*., et al.* (2017). Dose Selection for an Adjuvanted Respiratory Syncytial Virus F Protein Vaccine for Older Adults Based on Humoral and Cellular Immune Responses. Clin Vaccine Immunol *24*, e00157-00117.
Fernando, O., Tagalakis, A.D., Awwad, S., Brocchini, S., Khaw, P.T., Hart, S.L., and Yu-Wai-Man, C. (2018). Development of Targeted siRNA Nanocomplexes to Prevent Fibrosis in Experimental Glaucoma Filtration Surgery. Molecular Therapy *26*, 2812-2822.
Fletcher, L.D., Bernfield, L., Barniak, V., Farley, J.E., Howell, A., Knauf, M., Ooi, P., Smith, R.P., Weise, P., Wetherell, M*., et al.* (2004). Vaccine potential of the Neisseria meningitidis 2086 lipoprotein. Infect Immun *72*, 2088-2100.
Flexner, S. (1913). THE RESULTS OF THE SERUM TREATMENT IN THIRTEEN HUNDRED CASES OF EPIDEMIC MENINGITIS. J Exp Med *17*, 553-576.
Forbes, N., Hussain, M.T., Briuglia, M.L., Edwards, D.P., Horst, J.H.t., Szita, N., and Perrie, Y. (2019). Rapid and scale-independent microfluidic manufacture of liposomes entrapping protein incorporating in-line purification and at-line size monitoring. International Journal of Pharmaceutics *556*, 68-81.

Gdowski, A., Johnson, K., Shah, S., Gryczynski, I., Vishwanatha, J., and Ranjan, A. (2018). Optimization and scale up of microfluidic nanolipomer production method for preclinical and potential clinical trials. Journal of Nanobiotechnology *16*, 12.
Ghosh, A., and Heston, W.D. (2004). Tumor target prostate specific membrane antigen (PSMA) and its regulation in prostate cancer. Journal of cellular biochemistry *91*, 528-539.
Giannini, G., Rappuoli, R., and Ratti, G. (1984). The amino-acid sequence of two non-toxic mutants of diphtheria toxin: CRM45 and CRM197. Nucleic Acids Res *12*, 4063-4069.
Glimcher, L.H., and Murphy, K.M. (2000). Lineage commitment in the immune system: the T helper lymphocyte grows up. Genes & Development *14*, 1693-1711.
Guan, H.H., Budzynski, W., Koganty, R.R., Krantz, M.J., Reddish, M.A., Rogers, J.A., Longenecker, B.M., and Samuel, J. (1998). Liposomal formulations of synthetic MUC1 peptides: effects of encapsulation versus surface display of peptides on immune responses. Bioconjug Chem *9*, 451-458.
Guimarães Sá Correia, M., Briuglia, M.L., Niosi, F., and Lamprou, D.A. (2017). Microfluidic manufacturing of phospholipid nanoparticles: Stability, encapsulation efficacy, and drug release. International Journal of Pharmaceutics *516*, 91-99.
Gullotti, E., and Yeo, Y. (2009). Extracellularly activated nanocarriers: a new paradigm of tumor targeted drug delivery. Mol Pharm *6*, 1041-1051.
Gursel, I., Gursel, M., Ishii, K.J., and Klinman, D.M. (2001). Sterically stabilized cationic liposomes improve the uptake and immunostimulatory activity of CpG oligonucleotides. J Immunol *167*, 3324-3328.
Guttormsen, H.-K., Liu, Y., and Paoletti, L.C. (2008). Functional activity of antisera to group B streptococcal conjugate vaccines measured with an opsonophagocytosis assay and HL-60 effector cells. Hum Vaccin *4*, 370-374.
Hamborg, M., Jorgensen, L., Bojsen, A.R., Christensen, D., and Foged, C. (2013). Protein antigen adsorption to the DDA/TDB liposomal adjuvant: effect on protein structure, stability, and liposome physicochemical characteristics. Pharm Res *30*, 140-155.
Hamborg, M., Rose, F., Jorgensen, L., Bjorklund, K., Pedersen, H.B., Christensen, D., and Foged, C. (2014). Elucidating the mechanisms of protein antigen adsorption to the CAF/NAF liposomal vaccine adjuvant systems: Effect of charge, fluidity and antigen-to-lipid ratio. Biochimica et Biophysica Acta (BBA) - Biomembranes *1838*, 2001-2010.
Hanagata, N. (2017). CpG oligodeoxynucleotide nanomedicines for the prophylaxis or treatment of cancers, infectious diseases, and allergies. Int J Nanomedicine *Volume 12*, 515-531.
Hartmann, G., and Krieg, A.M. (2000). Mechanism and Function of a Newly Identified CpG DNA Motif in Human Primary B Cells. The Journal of Immunology *164*, 944.
Heit, A., Maurer, T., Hochrein, H., Bauer, S., Huster, K.M., Busch, D.H., and Wagner, H. (2003). Cutting edge: Toll-like receptor 9 expression is not required for CpG DNA-aided cross-presentation of DNA-conjugated antigens but essential for cross-priming of CD8 T cells. J Immunol *170*, 2802-2805.
Heit, A., Schmitz, F., O'Keeffe, M., Staib, C., Busch, D.H., Wagner, H., and Huster, K.M. (2005). Protective CD8 T cell immunity triggered by CpG-protein conjugates competes with the efficacy of live vaccines. J Immunol *174*, 4373-4380.
Henriksen-Lacey, M., Bramwell, V.W., Christensen, D., Agger, E.M., Andersen, P., and Perrie, Y. (2010a). Liposomes based on dimethyldioctadecylammonium promote a depot effect and enhance immunogenicity of soluble antigen. J Control Release *142*, 180-186.
Henriksen-Lacey, M., Christensen, D., Bramwell, V.W., Lindenstrom, T., Agger, E.M., Andersen, P., and Perrie, Y. (2010b). Liposomal cationic charge and antigen adsorption are important properties for the efficient deposition of antigen at the injection site and ability of the vaccine to induce a CMI response. J Control Release *145*, 102-108.

Henriksen-Lacey, M., Christensen, D., Bramwell, V.W., Lindenstrøm, T., Agger, E.M., Andersen, P., and Perrie, Y. (2011a). Comparison of the Depot Effect and Immunogenicity of Liposomes Based on Dimethyldioctadecylammonium (DDA), 3β-[N-(N',N'-Dimethylaminoethane)carbomyl] Cholesterol (DC-Chol), and 1,2-Dioleoyl-3-trimethylammonium Propane (DOTAP): Prolonged Liposome Retention Mediates Stronger Th1 Responses. Molecular Pharmaceutics *8*, 153-161.
Henriksen-Lacey, M., Devitt, A., and Perrie, Y. (2011b). The vesicle size of DDA:TDB liposomal adjuvants plays a role in the cell-mediated immune response but has no significant effect on antibody production. Journal of Controlled Release *154*, 131-137.
Hermanson, G.T. (2013). Chapter 3 - The Reactions of Bioconjugation. In Bioconjugate Techniques (Third Edition), G.T. Hermanson, ed. (Boston: Academic Press), pp. 229-258.
Hoffman, O., and Weber, R.J. (2009). Pathophysiology and treatment of bacterial meningitis. Ther Adv Neurol Disord *2*, 1-7.
Holland, C., Numata, K., Rnjak-Kovacina, J., and Seib, F.P. (2019). The Biomedical Use of Silk: Past, Present, Future. Advanced Healthcare Materials *8*, 1800465.
Honda, K., Yanai, H., Negishi, H., Asagiri, M., Sato, M., Mizutani, T., Shimada, N., Ohba, Y., Takaoka, A., Yoshida, N., and Taniguchi, T. (2005). IRF-7 is the master regulator of type-I interferon-dependent immune responses. Nature *434*, 772-777.
Idris-Khodja, N., Mian, M.O.R., Paradis, P., and Schiffrin, E.L. (2014). Dual opposing roles of adaptive immunity in hypertension†. European Heart Journal *35*, 1238-1244.
Ignacio, B.J., Albin, T.J., Esser-Kahn, A.P., and Verdoes, M. (2018). Toll-like Receptor Agonist Conjugation: A Chemical Perspective. Bioconjug Chem *29*, 587-603.
Inoue, Y., Izawa, K., Kiryu, S., Tojo, A., and Ohtomo, K. (2008). Diet and Abdominal Autofluorescence Detected by in Vivo Fluorescence Imaging of Living Mice. Molecular Imaging *7*, 7290.2008.0003.
Ippolito, D.L., James, W.A., Tinnemore, D., Huang, R.R., Dehart, M.J., Williams, J., Wingerd, M.A., and Demons, S.T. (2010). Group B streptococcus serotype prevalence in reproductive-age women at a tertiary care military medical center relative to global serotype distribution. BMC Infect Dis *10*, 336-336.
Jaafari, M.R., Badiee, A., Khamesipour, A., Samiei, A., Soroush, D., Kheiri, M.T., Barkhordari, F., McMaster, W.R., and Mahboudi, F. (2007). The role of CpG ODN in enhancement of immune response and protection in BALB/c mice immunized with recombinant major surface glycoprotein of Leishmania (rgp63) encapsulated in cationic liposome. Vaccine *25*, 6107-6117.
Jahn, A., Stavis, S.M., Hong, J.S., Vreeland, W.N., DeVoe, D.L., and Gaitan, M. (2010). Microfluidic Mixing and the Formation of Nanoscale Lipid Vesicles. ACS Nano *4*, 2077-2087.
Janssen, R.S., Mangoo-Karim, R., Pergola, P.E., Girndt, M., Namini, H., Rahman, S., Bennett, S.R., Heyward, W.L., and Martin, J.T. (2013). Immunogenicity and safety of an investigational hepatitis B vaccine with a toll-like receptor 9 agonist adjuvant (HBsAg-1018) compared with a licensed hepatitis B vaccine in patients with chronic kidney disease. Vaccine *31*, 5306-5313.
Johri, A.K., Paoletti, L.C., Glaser, P., Dua, M., Sharma, P.K., Grandi, G., and Rappuoli, R. (2006). Group B Streptococcus: global incidence and vaccine development. Nature reviews. Microbiology *4*, 932-942.
Jones, D.S., Rowe, C.G., Chen, B., Reiter, K., Rausch, K.M., Narum, D.L., Wu, Y., and Duffy, P.E. (2016). A Method for Producing Protein Nanoparticles with Applications in Vaccines. PloS one *11*, e0138761-e0138761.
Joshi, S., Hussain, M.T., Roces, C.B., Anderluzzi, G., Kastner, E., Salmaso, S., Kirby, D.J., and Perrie, Y. (2016). Microfluidics based manufacture of liposomes simultaneously entrapping hydrophilic and lipophilic drugs. International Journal of Pharmaceutics *514*, 160-168.

Kabanova, A., and Rappuoli, R. (2011). CHAPTER 34 - Diphtheria. In Tropical Infectious Diseases: Principles, Pathogens and Practice (Third Edition), R.L. Guerrant, D.H. Walker, and P.F. Weller, eds. (Edinburgh: W.B. Saunders), pp. 223-227.
Kastner, E., Kaur, R., Lowry, D., Moghaddam, B., Wilkinson, A., and Perrie, Y. (2014). High-throughput manufacturing of size-tuned liposomes by a new microfluidics method using enhanced statistical tools for characterization. International Journal of Pharmaceutics *477*, 361-368.
Kastner, E., Verma, V., Lowry, D., and Perrie, Y. (2015). Microfluidic-controlled manufacture of liposomes for the solubilisation of a poorly water soluble drug. International Journal of Pharmaceutics *485*, 122-130.
Kaur, R., Bramwell, V.W., Kirby, D.J., and Perrie, Y. (2012). Pegylation of DDA:TDB liposomal adjuvants reduces the vaccine depot effect and alters the Th1/Th2 immune responses. J Control Release *158*, 72-77.
Kaur, R., Henriksen-Lacey, M., Wilkhu, J., Devitt, A., Christensen, D., and Perrie, Y. (2014). Effect of Incorporating Cholesterol into DDA:TDB Liposomal Adjuvants on Bilayer Properties, Biodistribution, and Immune Responses. Molecular Pharmaceutics *11*, 197-207.
Khadke, S., Roces, C.B., Cameron, A., Devitt, A., and Perrie, Y. (2019). Formulation and manufacturing of lymphatic targeting liposomes using microfluidics. Journal of Controlled Release *307*, 211-220.
Khan, S., Bijker, M.S., Weterings, J.J., Tanke, H.J., Adema, G.J., van Hall, T., Drijfhout, J.W., Melief, C.J., Overkleeft, H.S., van der Marel, G.A*., et al.* (2007). Distinct uptake mechanisms but similar intracellular processing of two different toll-like receptor ligand-peptide conjugates in dendritic cells. J Biol Chem *282*, 21145-21159.
Khan, S., Weterings, J.J., Britten, C.M., de Jong, A.R., Graafland, D., Melief, C.J.M., van der Burg, S.H., van der Marel, G., Overkleeft, H.S., Filippov, D.V., and Ossendorp, F. (2009). Chirality of TLR-2 ligand Pam3CysSK4 in fully synthetic peptide conjugates critically influences the induction of specific CD8+ T-cells. Molecular Immunology *46*, 1084-1091.
Kim, M.-G., Park, J.Y., Shon, Y., Kim, G., Shim, G., and Oh, Y.-K. (2014). Nanotechnology and vaccine development. Asian Journal of Pharmaceutical Sciences *9*, 227-235.
Kobayashi, M., Vekemans, J., Baker, C.J., Ratner, A.J., Le Doare, K., and Schrag, S.J. (2016). Group B Streptococcus vaccine development: present status and future considerations, with emphasis on perspectives for low and middle income countries. F1000Research *5*, 2355.
Kolb, H.C., Finn, M.G., and Sharpless, K.B. (2001). Click Chemistry: Diverse Chemical Function from a Few Good Reactions. Angewandte Chemie (International ed. in English) *40*, 2004-2021.
Kolb, H.C., and Sharpless, K.B. (2003). The growing impact of click chemistry on drug discovery. Drug Discov Today *8*, 1128-1137.
Korsholm, K.S., Petersen, R.V., Agger, E.M., and Andersen, P. (2010). T-helper 1 and T-helper 2 adjuvants induce distinct differences in the magnitude, quality and kinetics of the early inflammatory response at the site of injection. Immunology *129*, 75-86.
Kovacs-Nolan, J., Latimer, L., Landi, A., Jenssen, H., Hancock, R.E., Babiuk, L.A., and van Drunen Littel-van den Hurk, S. (2009). The novel adjuvant combination of CpG ODN, indolicidin and polyphosphazene induces potent antibody- and cell-mediated immune responses in mice. Vaccine *27*, 2055-2064.
Kovacs-Simon, A., Titball, R.W., and Michell, S.L. (2011). Lipoproteins of Bacterial Pathogens. Infect Immun *79*, 548.
Kramer, K., Shields, N.J., Poppe, V., Young, S.L., and Walker, G.F. (2017). Intracellular Cleavable CpG Oligodeoxynucleotide-Antigen Conjugate Enhances Anti-tumor Immunity. Mol Ther *25*, 62-70.

Krug, A., Towarowski, A., Britsch, S., Rothenfusser, S., Hornung, V., Bals, R., Giese, T., Engelmann, H., Endres, S., Krieg, A.M., and Hartmann, G. (2001). Toll-like receptor expression reveals CpG DNA as a unique microbial stimulus for plasmacytoid dendritic cells which synergizes with CD40 ligand to induce high amounts of IL-12. European journal of immunology *31*, 3026-3037.
Kumar, S., Chaturvedi, V.K., Kumar, B., Kumar, P., Somarajan, S.R., Mishra, A.K., and Sharma, B. (2015). Effect of alum co-adjuvantation of oil adjuvant vaccine on emulsion stability and immune responses against haemorhagic septicaemia in mice. Iran J Microbiol *7*, 79-87.
Kuntsche, J., Horst, J.C., and Bunjes, H. (2011). Cryogenic transmission electron microscopy (cryo-TEM) for studying the morphology of colloidal drug delivery systems. International Journal of Pharmaceutics *417*, 120-137.
Kuramoto, Y., Kawakami, S., Zhou, S., Fukuda, K., Yamashita, F., and Hashida, M. (2008). Efficient peritoneal dissemination treatment obtained by an immunostimulatory phosphorothioate-type CpG DNA/cationic liposome complex in mice. J Control Release *126*, 274-280.
Kuvichkin, V.V., Danev, R.S., Shigematsu, H., and Nagayama, K. (2009). DNA-Induced Aggregation and Fusion of Phosphatidylcholine Liposomes in the Presence of Multivalent Cations Observed by the Cryo-TEM Technique. Journal of Membrane Biology *227*, 95.
Lachenauer, C.S., Kasper, D.L., Shimada, J., Ichiman, Y., Ohtsuka, H., Kaku, M., Paoletti, L.C., Ferrieri, P., and Madoff, L.C. (1999). Serotypes VI and VIII Predominate among Group B Streptococci Isolated from Pregnant Japanese Women. The Journal of Infectious Diseases *179*, 1030-1033.
Lamagni, T.L., Keshishian, C., Efstratiou, A., Guy, R., Henderson, K.L., Broughton, K., and Sheridan, E. (2013). Emerging trends in the epidemiology of invasive group B streptococcal disease in England and Wales, 1991-2010. Clinical infectious diseases : an official publication of the Infectious Diseases Society of America *57*, 682-688.
Lancefield, R.C. (1938). TWO SEROLOGICAL TYPES OF GROUP B HEMOLYTIC STREPTOCOCCI WITH RELATED, BUT NOT IDENTICAL, TYPE-SPECIFIC SUBSTANCES. J Exp Med *67*, 25.
Landwehr-Kenzel, S., and Henneke, P. (2014). Interaction of Streptococcus agalactiae and Cellular Innate Immunity in Colonization and Disease. Front Immunol *5*, 519.
Lay, M., Callejo, B., Chang, S., Hong, D.K., Lewis, D.B., Carroll, T.D., Matzinger, S., Fritts, L., Miller, C.J., Warner, J.F*., et al.* (2009). Cationic lipid/DNA complexes (JVRS-100) combined with influenza vaccine (Fluzone) increases antibody response, cellular immunity, and antigenically drifted protection. Vaccine *27*, 3811-3820.
Lemaitre, B., Nicolas, E., Michaut, L., Reichhart, J.-M., and Hoffmann, J.A. (1996). The Dorsoventral Regulatory Gene Cassette spätzle/Toll/cactus Controls the Potent Antifungal Response in Drosophila Adults. Cell *86*, 973-983.
Li, M., Du, C., Guo, N., Teng, Y., Meng, X., Sun, H., Li, S., Yu, P., and Galons, H. (2019). Composition design and medical application of liposomes. European Journal of Medicinal Chemistry *164*, 640-653.
Lin, F.-Y.C., Weisman, L.E., Azimi, P.H., Philips, J.B., III, Clark, P., Regan, J., Rhoads, G.G., Frasch, C.E., Gray, B.M., Troendle, J*., et al.* (2004). Level of Maternal IgG Anti-Group B Streptococcus Type III Antibody Correlated with Protection of Neonates against Early-Onset Disease Caused by This Pathogen. The Journal of Infectious Diseases *190*, 928-934.
Lin, F.Y., Philips, J.B., 3rd, Azimi, P.H., Weisman, L.E., Clark, P., Rhoads, G.G., Regan, J., Concepcion, N.F., Frasch, C.E., Troendle, J*., et al.* (2001). Level of maternal antibody required to protect neonates against early-onset disease caused by group B Streptococcus type Ia: a multicenter, seroepidemiology study. J Infect Dis *184*, 1022-1028.
Lin, S.M., Zhi, Y., Ahn, K.B., Lim, S., and Seo, H.S. (2018). Status of group B streptococcal vaccine development. Clin Exp Vaccine Res *7*, 76-81.

Liu, H., and Irvine, D.J. (2015). Guiding principles in the design of molecular bioconjugates for vaccine applications. Bioconjug Chem *26*, 791-801.
Lombardo, D., Calandra, P., Barreca, D., Magazù, S., and Kiselev, M.A. (2016). Soft Interaction in Liposome Nanocarriers for Therapeutic Drug Delivery. Nanomaterials (Basel) *6*, 125.
Lou, G., Anderluzzi, G., Woods, S., Roberts, C.W., and Perrie, Y. (2019). A novel microfluidic-based approach to formulate size-tuneable large unilamellar cationic liposomes: Formulation, cellular uptake and biodistribution investigations. European Journal of Pharmaceutics and Biopharmaceutics *143*, 51-60.
Ludewig, B., Barchiesi, F., Pericin, M., Zinkernagel, R.M., Hengartner, H., and Schwendener, R.A. (2000). In vivo antigen loading and activation of dendritic cells via a liposomal peptide vaccine mediates protective antiviral and anti-tumour immunity. Vaccine *19*, 23-32.
Luo, Y., Friese, O.V., Runnels, H.A., Khandke, L., Zlotnick, G., Aulabaugh, A., Gore, T., Vidunas, E., Raso, S.W., Novikova, E*., et al.* (2016). The Dual Role of Lipids of the Lipoproteins in Trumenba, a Self-Adjuvanting Vaccine Against Meningococcal Meningitis B Disease. AAPS J *18*, 1562-1575.
Madhi, S.A., Cutland, C.L., Jose, L., Koen, A., Govender, N., Wittke, F., Olugbosi, M., Meulen, A.S., Baker, S., Dull, P.M*., et al.* (2016). Safety and immunogenicity of an investigational maternal trivalent group B streptococcus vaccine in healthy women and their infants: a randomised phase 1b/2 trial. The Lancet. Infectious diseases *16*, 923-934.
Madhi, S.A., Dangor, Z., Heath, P.T., Schrag, S., Izu, A., Sobanjo-Ter Meulen, A., and Dull, P.M. (2013). Considerations for a phase-III trial to evaluate a group B Streptococcus polysaccharide-protein conjugate vaccine in pregnant women for the prevention of early- and late-onset invasive disease in young-infants. Vaccine *31 Suppl 4*, D52-57.
Maji, M., Mazumder, S., Bhattacharya, S., Choudhury, S.T., Sabur, A., Shadab, M., Bhattacharya, P., and Ali, N. (2016). A Lipid Based Antigen Delivery System Efficiently Facilitates MHC Class-I Antigen Presentation in Dendritic Cells to Stimulate CD8(+) T Cells. Sci Rep *6*, 27206.
Malito, E., Biancucci, M., Faleri, A., Ferlenghi, I., Scarselli, M., Maruggi, G., Lo Surdo, P., Veggi, D., Liguori, A., Santini, L*., et al.* (2014). Structure of the meningococcal vaccine antigen NadA and epitope mapping of a bactericidal antibody. Proceedings of the National Academy of Sciences *111*, 17128-17133.
Malito, E., Bursulaya, B., Chen, C., Lo Surdo, P., Picchianti, M., Balducci, E., Biancucci, M., Brock, A., Berti, F., Bottomley, M.J*., et al.* (2012). Structural basis for lack of toxicity of the diphtheria toxin mutant CRM197. Proceedings of the National Academy of Sciences of the United States of America *109*, 5229-5234.
Malito, E., Faleri, A., Lo Surdo, P., Veggi, D., Maruggi, G., Grassi, E., Cartocci, E., Bertoldi, I., Genovese, A., Santini, L*., et al.* (2013). Defining a protective epitope on factor H binding protein, a key meningococcal virulence factor and vaccine antigen. Proceedings of the National Academy of Sciences *110*, 3304.
Manetsch, R., Krasiński, A., Radić, Z., Raushel, J., Taylor, P., Sharpless, K.B., and Kolb, H.C. (2004). In Situ Click Chemistry: Enzyme Inhibitors Made to Their Own Specifications. Journal of the American Chemical Society *126*, 12809-12818.
Mansourian, M., Badiee, A., Jalali, S.A., Shariat, S., Yazdani, M., Amin, M., and Jaafari, M.R. (2014). Effective induction of anti-tumor immunity using p5 HER-2/neu derived peptide encapsulated in fusogenic DOTAP cationic liposomes co-administrated with CpG-ODN. Immunol Lett *162*, 87-93.
Marasini, N., Ghaffar, K.A., Skwarczynski, M., and Toth, I. (2017). Chapter Twelve - Liposomes as a Vaccine Delivery System. In Micro and Nanotechnology in Vaccine Development, M. Skwarczynski, and I. Toth, eds. (William Andrew Publishing), pp. 221-239.

Margarit, I., Rinaudo, C.D., Galeotti, C.L., Maione, D., Ghezzo, C., Buttazzoni, E., Rosini, R., Runci, Y., Mora, M., Buccato, S.*, et al.* (2009). Preventing Bacterial Infections with Pilus-Based Vaccines: the Group B Streptococcus Paradigm. The Journal of Infectious Diseases *199*, 108-115.
Marshall, H.S., Richmond, P.C., Nissen, M.D., Wouters, A., Baber, J., Jiang, Q., Anderson, A.S., Jones, T.R., Harris, S.L., Jansen, K.U., and Perez, J.L. (2013). A phase 2 open-label safety and immunogenicity study of a meningococcal B bivalent rLP2086 vaccine in healthy adults. Vaccine *31*, 1569-1575.
Martinez-Jothar, L., Doulkeridou, S., Schiffelers, R.M., Sastre Torano, J., Oliveira, S., van Nostrum, C.F., and Hennink, W.E. (2018). Insights into maleimide-thiol conjugation chemistry: Conditions for efficient surface functionalization of nanoparticles for receptor targeting. J Control Release *282*, 101-109.
Mascioni, A., Bentley, B.E., Camarda, R., Dilts, D.A., Fink, P., Gusarova, V., Hoiseth, S.K., Jacob, J., Lin, S.L., Malakian, K.*, et al.* (2009). Structural Basis for the Immunogenic Properties of the Meningococcal Vaccine Candidate LP2086. J Biol Chem *284*, 8738-8746.
Masignani, V., Comanducci, M., Giuliani, M.M., Bambini, S., Adu-Bobie, J., Arico, B., Brunelli, B., Pieri, A., Santini, L., Savino, S.*, et al.* (2003). Vaccination against Neisseria meningitidis using three variants of the lipoprotein GNA1870. J Exp Med *197*, 789-799.
Matsubara, K., Katayama, K., Baba, K., Nigami, H., Harigaya, H., and Sugiyama, M. (2002). Seroepidemiologic Studies of Serotype VIII Group B Streptococcus in Japan. The Journal of Infectious Diseases *186*, 855-858.
Maurer, N., Wong, K.F., Stark, H., Louie, L., McIntosh, D., Wong, T., Scherrer, P., Semple, S.C., and Cullis, P.R. (2001). Spontaneous Entrapment of Polynucleotides upon Electrostatic Interaction with Ethanol-Destabilized Cationic Liposomes. Biophysical Journal *80*, 2310-2326.
Maurer, T., Heit, A., Hochrein, H., Ampenberger, F., O'Keeffe, M., Bauer, S., Lipford, G.B., Vabulas, R.M., and Wagner, H. (2002). CpG-DNA aided cross-presentation of soluble antigens by dendritic cells. European journal of immunology *32*, 2356-2364.
Mbua, N.E., Guo, J., Wolfert, M.A., Steet, R., and Boons, G.-J. (2011). Strain-promoted alkyne-azide cycloadditions (SPAAC) reveal new features of glycoconjugate biosynthesis. Chembiochem *12*, 1912-1921.
McNeil, L.K., Zagursky, R.J., Lin, S.L., Murphy, E., Zlotnick, G.W., Hoiseth, S.K., Jansen, K.U., and Anderson, A.S. (2013). Role of factor H binding protein in Neisseria meningitidis virulence and its potential as a vaccine candidate to broadly protect against meningococcal disease. Microbiology and molecular biology reviews : MMBR *77*, 234-252.
Medini, D., Stella, M., and Wassil, J. (2015). MATS: Global coverage estimates for 4CMenB, a novel multicomponent meningococcal B vaccine. Vaccine *33*, 2629-2636.
Meidan, V.M., Cohen, J.S., Amariglio, N., Hirsch-Lerner, D., and Barenholz, Y. (2000). Interaction of oligonucleotides with cationic lipids: the relationship between electrostatics, hydration and state of aggregation1A preliminary report of this study was presented by V.M. Meidan et al. at the Monte Verita Workshop on Gene and Oligonucleotide Delivery of Therapeutics and Vaccines, organized by the Department of Pharmacy, ETH Zurich, Ascona, Switzerland, April 23–24, 1999.1. Biochimica et Biophysica Acta (BBA) - Biomembranes *1464*, 251-261.
Melin, P., and Efstratiou, A. (2013). Group B streptococcal epidemiology and vaccine needs in developed countries. Vaccine *31 Suppl 4*, D31-42.
Milicic, A., Kaur, R., Reyes-Sandoval, A., Tang, C.-K., Honeycutt, J., Perrie, Y., and Hill, A.V.S. (2012). Small cationic DDA:TDB liposomes as protein vaccine adjuvants obviate the need for TLR agonists in inducing cellular and humoral responses. PloS one *7*, e34255-e34255.

Mohammed, A.R., Bramwell, V.W., Coombes, A.G.A., and Perrie, Y. (2006). Lyophilisation and sterilisation of liposomal vaccines to produce stable and sterile products. Methods *40*, 30-38.
Mohan, T., Verma, P., and Rao, D.N. (2013). Novel adjuvants & delivery vehicles for vaccines development: a road ahead. Indian J Med Res *138*, 779-795.
Moyer, T.J., Zmolek, A.C., and Irvine, D.J. (2016). Beyond antigens and adjuvants: formulating future vaccines. J Clin Invest *126*, 799-808.
Moyle, P.M. (2017). Biotechnology approaches to produce potent, self-adjuvanting antigen-adjuvant fusion protein subunit vaccines. Biotechnology Advances *35*, 375-389.
Moyle, P.M., Dai, W., Zhang, Y., Batzloff, M.R., Good, M.F., and Toth, I. (2014). Site-specific incorporation of three toll-like receptor 2 targeting adjuvants into semisynthetic, molecularly defined nanoparticles: application to group a streptococcal vaccines. Bioconjug Chem *25*, 965-978.
Moyle, P.M., Hartas, J., Henningham, A., Batzloff, M.R., Good, M.F., and Toth, I. (2013). An efficient, chemically-defined semisynthetic lipid-adjuvanted nanoparticulate vaccine development system. Nanomedicine: Nanotechnology, Biology and Medicine *9*, 935-944.
Moyle, P.M., Olive, C., Ho, M.F., Burgess, M., Karpati, L., Good, M.F., and Toth, I. (2006). Method for the synthesis of multi-epitopic Streptococcus pyogenes lipopeptide vaccines using native chemical ligation. J Org Chem *71*, 6846-6850.
Nash, A.A., Dalziel, R.G., and Fitzgerald, J.R. (2015). Chapter 6 - The Immune Response to Infection. In Mims' Pathogenesis of Infectious Disease (Sixth Edition), A.A. Nash, R.G. Dalziel, and J.R. Fitzgerald, eds. (Boston: Academic Press), pp. 119-144.
Nikoofal-Sahlabadi, S., Matbou Riahi, M., Sadri, K., Badiee, A., Nikpoor, A.R., and Jaafari, M.R. (2018). Liposomal CpG-ODN: An in vitro and in vivo study on macrophage subtypes responses, biodistribution and subsequent therapeutic efficacy in mice models of cancers. Eur J Pharm Sci *119*, 159-170.
Nilo, A., Passalacqua, I., Fabbrini, M., Allan, M., Usera, A., Carboni, F., Brogioni, B., Pezzicoli, A., Cobb, J., Romano, M.R.*, et al.* (2015). Exploring the Effect of Conjugation Site and Chemistry on the Immunogenicity of an anti-Group B Streptococcus Glycoconjugate Vaccine Based on GBS67 Pilus Protein and Type V Polysaccharide. Bioconjugate Chemistry *26*, 1839-1849.
Nimmerjahn, F., Bruhns, P., Horiuchi, K., and Ravetch, J.V. (2005). FcγRIV: A Novel FcR with Distinct IgG Subclass Specificity. Immunity *23*, 41-51.
Nisini, R., Poerio, N., Mariotti, S., De Santis, F., and Fraziano, M. (2018). The Multirole of Liposomes in Therapy and Prevention of Infectious Diseases. Front Immunol *9*, 155.
Nobbs, A.H., Rosini, R., Rinaudo, C.D., Maione, D., Grandi, G., and Telford, J.L. (2008). Sortase A utilizes an ancillary protein anchor for efficient cell wall anchoring of pili in Streptococcus agalactiae. Infect Immun *76*, 3550-3560.
Nolan, T., O'Ryan, M., Wassil, J., Abitbol, V., and Dull, P. (2015). Vaccination with a multicomponent meningococcal B vaccine in prevention of disease in adolescents and young adults. Vaccine *33*, 4437-4445.
Nooshabadi, F., Yang, H.-J., Bixler, J.N., Kong, Y., Cirillo, J.D., and Maitland, K.C. (2016). Intravital Fluorescence Excitation in Whole-Animal Optical Imaging. PloS one *11*, e0149932-e0149932.
Nuccitelli, A., Rinaudo, C.D., and Maione, D. (2015). Group B Streptococcus vaccine: state of the art. Ther Adv Vaccines *3*, 76-90.
Nudelman, Y., and Tunkel, A.R. (2009). Bacterial meningitis: epidemiology, pathogenesis and management update. Drugs *69*, 2577-2596.
Ouyang, W., Kolls, J.K., and Zheng, Y. (2008). The biological functions of T helper 17 cell effector cytokines in inflammation. Immunity *28*, 454-467.

Oyewumi, M.O., Kumar, A., and Cui, Z. (2010). Nano-microparticles as immune adjuvants: correlating particle sizes and the resultant immune responses. Expert Rev Vaccines *9*, 1095-1107.
Patil, S.D., Rhodes, D.G., and Burgess, D.J. (2005). DNA-based therapeutics and DNA delivery systems: a comprehensive review. AAPS J *7*, E61-E77.
Peek, L.J., Middaugh, C.R., and Berkland, C. (2008). Nanotechnology in vaccine delivery. Adv Drug Deliv Rev *60*, 915-928.
Peer, D., Karp, J.M., Hong, S., Farokhzad, O.C., Margalit, R., and Langer, R. (2007). Nanocarriers as an emerging platform for cancer therapy. Nature Nanotechnology *2*, 751-760.
Perez, H.L., Cardarelli, P.M., Deshpande, S., Gangwar, S., Schroeder, G.M., Vite, G.D., and Borzilleri, R.M. (2014). Antibody-drug conjugates: current status and future directions. Drug Discov Today *19*, 869-881.
Perrie, Y., Crofts, F., Devitt, A., Griffiths, H.R., Kastner, E., and Nadella, V. (2016). Designing liposomal adjuvants for the next generation of vaccines. Adv Drug Deliv Rev *99*, 85-96.
Pfister, H.W., Koedel, U., Haberl, R.L., Dirnagl, U., Feiden, W., Ruckdeschel, G., and Einhäupl, K.M. (1990). Microvascular Changes during the Early Phase of Experimental Bacterial Meningitis. Journal of Cerebral Blood Flow & Metabolism *10*, 914-922.
Presolski, S.I., Hong, V.P., and Finn, M.G. (2011). Copper-Catalyzed Azide-Alkyne Click Chemistry for Bioconjugation. Curr Protoc Chem Biol *3*, 153-162.
Qiao, C., Liu, J., Yang, J., Li, Y., Weng, J., Shao, Y., and Zhang, X. (2016). Enhanced non-inflammasome mediated immune responses by mannosylated zwitterionic-based cationic liposomes for HIV DNA vaccines. Biomaterials *85*, 1-17.
Quagliarello, V., and Scheld, W.M. (1992). Bacterial meningitis: pathogenesis, pathophysiology, and progress. The New England journal of medicine *327*, 864-872.
Quagliarello, V.J., Wispelwey, B., Long, W.J., Jr., and Scheld, W.M. (1991). Recombinant human interleukin-1 induces meningitis and blood-brain barrier injury in the rat. Characterization and comparison with tumor necrosis factor. The Journal of Clinical Investigation *87*, 1360-1366.
Raabe, V.N., and Shane, A.L. (2019). Group B Streptococcus (Streptococcus agalactiae). Microbiol Spectr *7*, 10.1128/microbiolspec.GPP1123-0007-2018.
Rajagopal, L. (2009). Understanding the regulation of Group B Streptococcal virulence factors. Future microbiology *4*, 201-221.
Ramilo, O., Sáez-Llorens, X., Mertsola, J., Jafari, H., Olsen, K.D., Hansen, E.J., Yoshinaga, M., Ohkawara, S., Nariuchi, H., and McCracken, G.H. (1990). Tumor necrosis factor alpha/cachectin and interleukin 1 beta initiate meningeal inflammation. J Exp Med *172*, 497.
Rappuoli, R. (2000). Reverse vaccinology. Current opinion in microbiology *3*, 445-450.
Rappuoli, R., Mandl, C.W., Black, S., and De Gregorio, E. (2011). Vaccines for the twenty-first century society. Nature reviews. Immunology *11*, 865-872.
Ricard, J.D., Wolff, M., Lacherade, J.C., Mourvillier, B., Hidri, N., Barnaud, G., Chevrel, G., Bouadma, L., and Dreyfuss, D. (2007). Levels of vancomycin in cerebrospinal fluid of adult patients receiving adjunctive corticosteroids to treat pneumococcal meningitis: a prospective multicenter observational study. Clinical infectious diseases : an official publication of the Infectious Diseases Society of America *44*, 250-255.
Richmond, P.C., Nissen, M.D., Marshall, H.S., Lambert, S.B., Roberton, D., Gruber, W.C., Jones, T.R., and Arora, A. (2012). A bivalent Neisseria meningitidis recombinant lipidated factor H binding protein vaccine in young adults: results of a randomised, controlled, dose-escalation phase 1 trial. Vaccine *30*, 6163-6174.

Roces, C.B., Khadke, S., Christensen, D., and Perrie, Y. (2019). Scale-Independent Microfluidic Production of Cationic Liposomal Adjuvants and Development of Enhanced Lymphatic Targeting Strategies. Molecular Pharmaceutics *16*, 4372-4386.
Rodríguez-Pulido, A., Ortega, F., Llorca, O., Aicart, E., and Junquera, E. (2008). A Physicochemical Characterization of the Interaction between DC-Chol/DOPE Cationic Liposomes and DNA. The Journal of Physical Chemistry B *112*, 12555-12565.
Rosenstein, N.E., and the Active Bacterial Core Surveillance, T., Perkins, B.A., and the Active Bacterial Core Surveillance, T., Stephens, D.S., and the Active Bacterial Core Surveillance, T., Lefkowitz, L., and the Active Bacterial Core Surveillance, T., Cartter, M.L., and the Active Bacterial Core Surveillance, T*., et al.* (1999). The Changing Epidemiology of Meningococcal Disease in the United States, 1992–1996. The Journal of Infectious Diseases *180*, 1894-1901.
Rosini, R., Rinaudo, C.D., Soriani, M., Lauer, P., Mora, M., Maione, D., Taddei, A., Santi, I., Ghezzo, C., Brettoni, C*., et al.* (2006). Identification of novel genomic islands coding for antigenic pilus-like structures in Streptococcus agalactiae. Molecular Microbiology *61*, 126-141.
Sablan, B.P., Kim, D.J., Barzaga, N.G., Chow, W.C., Cho, M., Ahn, S.H., Hwang, S.G., Lee, J.H., Namini, H., and Heyward, W.L. (2012). Demonstration of safety and enhanced seroprotection against hepatitis B with investigational HBsAg-1018 ISS vaccine compared to a licensed hepatitis B vaccine. Vaccine *30*, 2689-2696.
Saez-Llorens, X., and McCracken, G.H., Jr. (2003). Bacterial meningitis in children. Lancet (London, England) *361*, 2139-2148.
Samuni, A.M., Barenholz, Y., Crommelin, D.J.A., and Zuidam, N.J. (1997). γ-Irradiation Damage to Liposomes Differing in Composition and Their Protection by Nitroxides. Free Radical Biology and Medicine *23*, 972-979.
Sangra, M., Estelrich, J., Sabate, R., Espargaro, A., and Busquets, M.A. (2017). Evidence of Protein Adsorption in Pegylated Liposomes: Influence of Liposomal Decoration. Nanomaterials (Basel) *7*.
Scheiermann, J., and Klinman, D.M. (2014). Clinical evaluation of CpG oligonucleotides as adjuvants for vaccines targeting infectious diseases and cancer. Vaccine *32*, 6377-6389.
Schmitt, E., Klein, M., and Bopp, T. (2014). Th9 cells, new players in adaptive immunity. Trends in Immunology *35*, 61-68.
Schrag, S.J., and Verani, J.R. (2013). Intrapartum antibiotic prophylaxis for the prevention of perinatal group B streptococcal disease: experience in the United States and implications for a potential group B streptococcal vaccine. Vaccine *31 Suppl 4*, D20-26.
Schuchat, A. (1999). Group B streptococcus. Lancet (London, England) *353*, 51-56.
Schuchat, A., Robinson, K., Wenger, J.D., Harrison, L.H., Farley, M., Reingold, A.L., Lefkowitz, L., and Perkins, B.A. (1997). Bacterial meningitis in the United States in 1995. Active Surveillance Team. The New England journal of medicine *337*, 970-976.
Schwendener, R.A. (2014). Liposomes as vaccine delivery systems: a review of the recent advances. Ther Adv Vaccines *2*, 159-182.
Seib, F.P. (2017). Silk nanoparticles-an emerging anticancer nanomedicine. AIMS Bioeng. *4*, 239-258.
Sekiya, T., Yamagishi, J., Gray, J.H.V., Whitney, P.G., Martinelli, A., Zeng, W., Wong, C.Y., Sugimoto, C., Jackson, D.C., and Chua, B.Y. (2017). PEGylation of a TLR2-agonist-based vaccine delivery system improves antigen trafficking and the magnitude of ensuing antibody and CD8(+) T cell responses. Biomaterials *137*, 61-72.
Shabayek, S., and Spellerberg, B. (2018). Group B Streptococcal Colonization, Molecular Characteristics, and Epidemiology. Frontiers in Microbiology *9*.

Shargh, V.H., Jaafari, M.R., Khamesipour, A., Jaafari, I., Jalali, S.A., Abbasi, A., and Badiee, A. (2012). Liposomal SLA co-incorporated with PO CpG ODNs or PS CpG ODNs induce the same protection against the murine model of leishmaniasis. Vaccine *30*, 3957-3964.
Sharma, P., Lata, H., Arya, D.K., Kashyap, A.K., Kumar, H., Dua, M., Ali, A., and Johri, A.K. (2013). Role of pilus proteins in adherence and invasion of Streptococcus agalactiae to the lung and cervical epithelial cells. J Biol Chem *288*, 4023-4034.
Shi, S., Zhu, H., Xia, X., Liang, Z., Ma, X., and Sun, B. (2019). Vaccine adjuvants: Understanding the structure and mechanism of adjuvanticity. Vaccine *37*, 3167-3178.
Shirota, H., Sano, K., Hirasawa, N., Terui, T., Ohuchi, K., Hattori, T., Shirato, K., and Tamura, G. (2001). Novel roles of CpG oligodeoxynucleotides as a leader for the sampling and presentation of CpG-tagged antigen by dendritic cells. J Immunol *167*, 66-74.
Shirota, H., Sano, K., Kikuchi, T., Tamura, G., and Shirato, K. (2000). Regulation of murine airway eosinophilia and Th2 cells by antigen-conjugated CpG oligodeoxynucleotides as a novel antigen-specific immunomodulator. J Immunol *164*, 5575-5582.
Silva, A., Mount, A., Krstevska, K., Pejoski, D., Hardy, M.P., Owczarek, C., Scotney, P., Maraskovsky, E., and Baz Morelli, A. (2015). The combination of ISCOMATRIX adjuvant and TLR agonists induces regression of established solid tumors in vivo. J Immunol *194*, 2199-2207.
Slotved, H.C., Kong, F., Lambertsen, L., Sauer, S., and Gilbert, G.L. (2007). Serotype IX, a Proposed New Streptococcus agalactiae Serotype. Journal of clinical microbiology *45*, 2929-2936.
Slutter, B., Soema, P.C., Ding, Z., Verheul, R., Hennink, W., and Jiskoot, W. (2010). Conjugation of ovalbumin to trimethyl chitosan improves immunogenicity of the antigen. J Control Release *143*, 207-214.
Smith, A.J., Li, Y., Bazin, H.G., St-Jean, J.R., Larocque, D., Evans, J.T., and Baldridge, J.R. (2016). Evaluation of novel synthetic TLR7/8 agonists as vaccine adjuvants. Vaccine *34*, 4304-4312.
Solaro, R., Chiellini, F., and Battisti, A. (2010). Targeted Delivery of Protein Drugs by Nanocarriers. Materials (Basel) *3*, 1928-1980.
Stephens, D.S., Greenwood, B., and Brandtzaeg, P. (2007). Epidemic meningitis, meningococcaemia, and Neisseria meningitidis. Lancet (London, England) *369*, 2196-2210.
Taha, M.K., Hawkins, J.C., Liberator, P., Deghmane, A.E., Andrew, L., Hao, L., Jones, T.R., McNeil, L.K., O'Neill, R.E., Perez, J.L.*, et al.* (2017). Bactericidal activity of sera from adolescents vaccinated with bivalent rLP2086 against meningococcal serogroup B outbreak strains from France. Vaccine *35*, 1530-1537.
Tam, Y.K. (2006). Liposomal encapsulation enhances the activity of immunostimulatory oligonucleotides. Future Lipidology *1*, 35-46.
Tandrup Schmidt, S., Foged, C., Korsholm, K.S., Rades, T., and Christensen, D. (2016). Liposome-Based Adjuvants for Subunit Vaccines: Formulation Strategies for Subunit Antigens and Immunostimulators. Pharmaceutics *8*.
Tao, Y., Ju, E., Li, Z., Ren, J., and Qu, X. (2014). Engineered CpG-Antigen Conjugates Protected Gold Nanoclusters as Smart Self-Vaccines for Enhanced Immune Response and Cell Imaging. Advanced Functional Materials *24*, 1004-1010.
Thakur, K.K., Saini, J., Mahajan, K., Singh, D., Jayswal, D.P., Mishra, S., Bishayee, A., Sethi, G., and Kunnumakkara, A.B. (2017). Therapeutic implications of toll-like receptors in peripheral neuropathic pain. Pharmacological Research *115*, 224-232.
Thoryk, E.A., Swaminathan, G., Meschino, S., Cox, K.S., Gindy, M., Casimiro, D.R., and Bett, A.J. (2016). Co-Administration of Lipid Nanoparticles and Sub-Unit Vaccine Antigens Is Required for Increase in Antigen-Specific Immune Responses in Mice. Vaccines (Basel) *4*, 47.

Tighe, H., Takabayashi, K., Schwartz, D., Van Nest, G., Tuck, S., Eiden, J.J., Kagey-Sobotka, A., Creticos, P.S., Lichtenstein, L.M., Spiegelberg, H.L., and Raz, E. (2000). Conjugation of immunostimulatory DNA to the short ragweed allergen amb a 1 enhances its immunogenicity and reduces its allergenicity. J Allergy Clin Immunol *106*, 124-134.
Toh, M.-R., and Chiu, G.N.C. (2013). Liposomes as sterile preparations and limitations of sterilisation techniques in liposomal manufacturing. Asian Journal of Pharmaceutical Sciences *8*, 88-95.
Tornøe, C.W., Christensen, C., and Meldal, M. (2002). Peptidotriazoles on Solid Phase: [1,2,3]-Triazoles by Regiospecific Copper(I)-Catalyzed 1,3-Dipolar Cycloadditions of Terminal Alkynes to Azides. The Journal of Organic Chemistry *67*, 3057-3064.
Tunkel, A.R., Hartman, B.J., Kaplan, S.L., Kaufman, B.A., Roos, K.L., Scheld, W.M., and Whitley, R.J. (2004). Practice guidelines for the management of bacterial meningitis. Clinical infectious diseases : an official publication of the Infectious Diseases Society of America *39*, 1267-1284.
Tunkel, A.R., and Scheld, W.M. (1993). Pathogenesis and pathophysiology of bacterial meningitis. Clinical microbiology reviews *6*, 118-136.
Tureen, J.H., Dworkin, R.J., Kennedy, S.L., Sachdeva, M., and Sande, M.A. (1990). Loss of cerebrovascular autoregulation in experimental meningitis in rabbits. J Clin Invest *85*, 577-581.
Turker, S., Ozer, A.Y., Kilic, E., Ozalp, M., Colak, S., and Korkmaz, M. (2013). Gamma-irradiated liposome/noisome and lipogelosome/niogelosome formulations for the treatment of rheumatoid arthritis. Interv Med Appl Sci *5*, 60-69.
Ulmer, J. (2013). Vaccine Adjuvants: Mode of Action. Frontiers in Immunology *4*.
Vacca, I., Del Tordello, E., Gasperini, G., Pezzicoli, A., Di Fede, M., Rossi Paccani, S., Marchi, S., Mubaiwa, T.D., Hartley-Tassell, L.E., Jennings, M.P*., et al.* (2016). Neisserial Heparin Binding Antigen (NHBA) Contributes to the Adhesion of Neisseria meningitidis to Human Epithelial Cells. PLOS ONE *11*, e0162878.
van de Beek, D., Brouwer, M.C., Thwaites, G.E., and Tunkel, A.R. (2012). Advances in treatment of bacterial meningitis. The Lancet *380*, 1693-1702.
van der Vlies, A.J., O'Neil, C.P., Hasegawa, U., Hammond, N., and Hubbell, J.A. (2010). Synthesis of Pyridyl Disulfide-Functionalized Nanoparticles for Conjugating Thiol-Containing Small Molecules, Peptides, and Proteins. Bioconjugate Chemistry *21*, 653-662.
van Dissel, J.T., Joosten, S.A., Hoff, S.T., Soonawala, D., Prins, C., Hokey, D.A., O'Dee, D.M., Graves, A., Thierry-Carstensen, B., Andreasen, L.V*., et al.* (2014). A novel liposomal adjuvant system, CAF01, promotes long-lived Mycobacterium tuberculosis-specific T-cell responses in human. Vaccine *32*, 7098-7107.
van Reis, R., and Zydney, A. (2007). Bioprocess membrane technology. Journal of Membrane Science *297*, 16-50.
Vangala, A., Kirby, D., Rosenkrands, I., Agger, E.M., Andersen, P., and Perrie, Y. (2006). A comparative study of cationic liposome and niosome-based adjuvant systems for protein subunit vaccines: characterisation, environmental scanning electron microscopy and immunisation studies in mice. Journal of Pharmacy and Pharmacology *58*, 787-799.
Vasquez, K.O., Casavant, C., and Peterson, J.D. (2011). Quantitative whole body biodistribution of fluorescent-labeled agents by non-invasive tomographic imaging. PLoS One *6*, e20594.
Vidarsson, G., Dekkers, G., and Rispens, T. (2014). IgG subclasses and allotypes: from structure to effector functions. Frontiers in immunology *5*, 520-520.
Vollmer, J., and Krieg, A.M. (2009). Immunotherapeutic applications of CpG oligodeoxynucleotide TLR9 agonists. Adv Drug Deliv Rev *61*, 195-204.
Wagner, H. (2009). The immunogenicity of CpG-antigen conjugates. Adv Drug Deliv Rev *61*, 243-247.

Walker, J.A., and McKenzie, A.N.J. (2017). TH2 cell development and function. Nature Reviews Immunology *18*, 121.
Wang, J.Q., Jeelall, Y.S., Ferguson, L.L., and Horikawa, K. (2014). Toll-Like Receptors and Cancer: MYD88 Mutation and Inflammation. Front Immunol *5*, 367.
Watson, D.S., Endsley, A.N., and Huang, L. (2012). Design considerations for liposomal vaccines: influence of formulation parameters on antibody and cell-mediated immune responses to liposome associated antigens. Vaccine *30*, 2256-2272.
Weisman, S., Hirsch-Lerner, D., Barenholz, Y., and Talmon, Y. (2004). Nanostructure of Cationic Lipid-Oligonucleotide Complexes. Biophysical Journal *87*, 609-614.
Wilkinson, A., Lattmann, E., Roces, C.B., Pedersen, G.K., Christensen, D., and Perrie, Y. (2018). Lipid conjugation of TLR7 agonist Resiquimod ensures co-delivery with the liposomal Cationic Adjuvant Formulation 01 (CAF01) but does not enhance immunopotentiation compared to non-conjugated Resiquimod+CAF01. J Control Release *291*, 1-10.
Wilson, K.D., de Jong, S.D., and Tam, Y.K. (2009). Lipid-based delivery of CpG oligonucleotides enhances immunotherapeutic efficacy. Adv Drug Deliv Rev *61*, 233-242.
Wongpinyochit, T., Totten, J.D., Johnston, B.F., and Seib, F.P. (2019). Microfluidic-assisted silk nanoparticle tuning. Nanoscale Advances *1*, 873-883.
Yan, W., Chen, W., and Huang, L. (2007). Mechanism of adjuvant activity of cationic liposome: Phosphorylation of a MAP kinase, ERK and induction of chemokines. Molecular Immunology *44*, 3672-3681.
Yang, H.-H., Madoff, L.C., Guttormsen, H.-K., Liu, Y.-D., and Paoletti, L.C. (2007). Recombinant group B streptococcus Beta C protein and a variant with the deletion of its immunoglobulin A-binding site are protective mouse maternal vaccines and effective carriers in conjugate vaccines. Infect Immun *75*, 3455-3461.
Yao, Z., Fanslow, W.C., Seldin, M.F., Rousseau, A.M., Painter, S.L., Comeau, M.R., Cohen, J.I., and Spriggs, M.K. (1995). Herpesvirus Saimiri encodes a new cytokine, IL-17, which binds to a novel cytokine receptor. Immunity *3*, 811-821.
Yu, C., An, M., Li, M., and Liu, H. (2017). Immunostimulatory Properties of Lipid Modified CpG Oligonucleotides. Mol Pharm *14*, 2815-2823.
Zaman, M., and Toth, I. (2013). Immunostimulation by synthetic lipopeptide-based vaccine candidates: structure-activity relationships. Front Immunol *4*, 318.
Zeng, W., Ghosh, S., Lau, Y.F., Brown, L.E., and Jackson, D.C. (2002). Highly immunogenic and totally synthetic lipopeptides as self-adjuvanting immunocontraceptive vaccines. J Immunol *169*, 4905-4912.
Zeng, W., Horrocks, K.J., Robevska, G., Wong, C.Y., Azzopardi, K., Tauschek, M., Robins-Browne, R.M., and Jackson, D.C. (2011). A modular approach to assembly of totally synthetic self-adjuvanting lipopeptide-based vaccines allows conformational epitope building. The Journal of biological chemistry *286*, 12944-12951.
Zhang, L., Chen, X., Xue, P., Sun, H.H.Y., Williams, I.D., Sharpless, K.B., Fokin, V.V., and Jia, G. (2005). Ruthenium-Catalyzed Cycloaddition of Alkynes and Organic Azides. Journal of the American Chemical Society *127*, 15998-15999.
Zhang, R., Qin, X., Kong, F., Chen, P., and Pan, G. (2019). Improving cellular uptake of therapeutic entities through interaction with components of cell membrane. Drug Deliv *26*, 328-342.
Zhang, Z., Goldschmidt, T., and Salter, H. (2012). Possible allelic structure of IgG2a and IgG2c in mice. Molecular Immunology *50*, 169-171.
Zhao, B.G., Vasilakos, J.P., Tross, D., Smirnov, D., and Klinman, D.M. (2014). Combination therapy targeting toll like receptors 7, 8 and 9 eliminates large established tumors. Journal for ImmunoTherapy of Cancer *2*, 12.

Zhigaltsev, I.V., Belliveau, N., Hafez, I., Leung, A.K.K., Huft, J., Hansen, C., and Cullis, P.R. (2012). Bottom-Up Design and Synthesis of Limit Size Lipid Nanoparticle Systems with Aqueous and Triglyceride Cores Using Millisecond Microfluidic Mixing. Langmuir *28*, 3633-3640.
Zhu, J., Yamane, H., and Paul, W.E. (2010). Differentiation of effector CD4 T cell populations (*). Annu Rev Immunol *28*, 445-489.
Zimmermann, P., Gwee, A., and Curtis, N. (2017). The controversial role of breast milk in GBS late-onset disease. The Journal of infection *74 Suppl 1*, S34-s40.
Zwijnenburg, P.J.G., van der Poll, T., Roord, J.J., and van Furth, A.M. (2006). Chemotactic factors in cerebrospinal fluid during bacterial meningitis. Infect Immun *74*, 1445-1451.

Appendix I

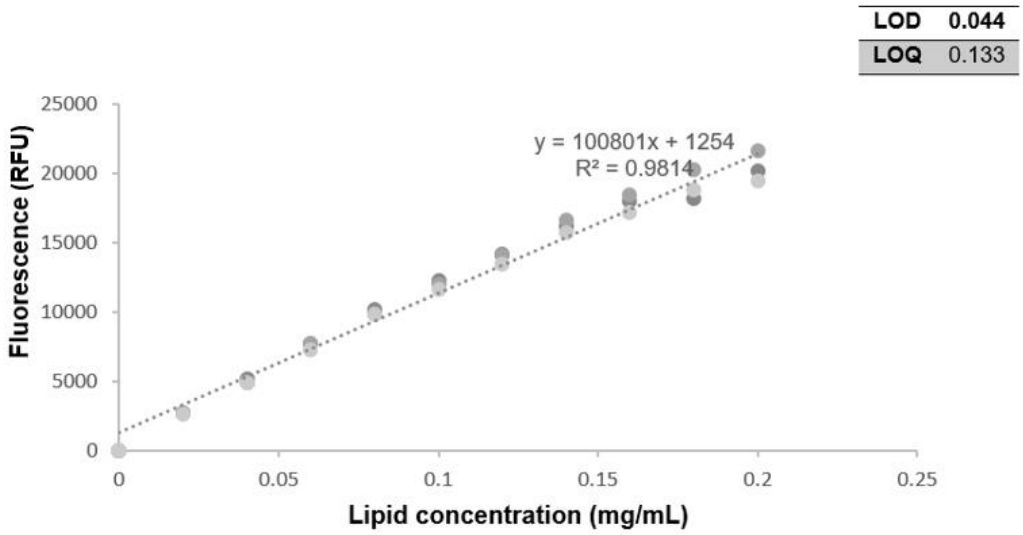

Figure A.1 *Calibration curve for the calculation of lipid recovery after dialysis, TFF, filtration for DSPC: Cholesterol: DDA liposomes. DSPC: Cholesterol: DDA liposomes were prepared by microfluidics. DiI fluorescent dye was included in lipid stocks at 0.2 mol% before microfluidic production of the liposomes. The lipid recovery after purification and sterilisation was determined from a calibration standard curve as a direct function of the measured absorbance. A POLARstar Omega plate reader spectrophotometer was used for the measurement of the fluorescence using an excitation wavelength of 482 nm and emission wavelength of 520 nm. Equation represents the average of a triplicate. LOD and LOQ represent the limit of detection and limit of quantification respectively.*

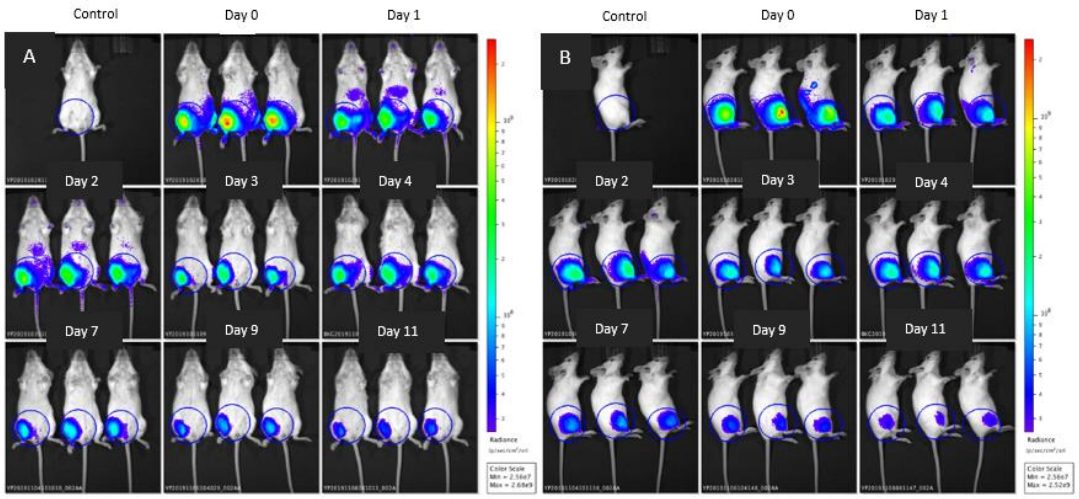

Figure A.2 *Fluorescense intensity images taken from (A) back and (B) side for GBS67 for all the days of the study. GBS67 protein and GBS67-CpGODN protein conjugate were labelled using Alexa Fluor 790 protein labelling kit (Molecular probes) according to the manufacturer's instructions. DiD lipophilic tracking dye was included in liposomes formulation for tracking. Female BALB/c mice, 7–12 weeks old were split into 3 groups of 3 mice. All mice were immunised intramuscularly (50 µL/dose) at day 0 with fluorolabeled antigens and liposomes. Anesthetised mice were placed into the IVIS chamber, and images were captured using the IVIS spectrum camera (Perkin Elmer) at day 0-4 and then every 2 days until day 11. A non-immunised mouse was used as negative control and for quantifying the background level.*

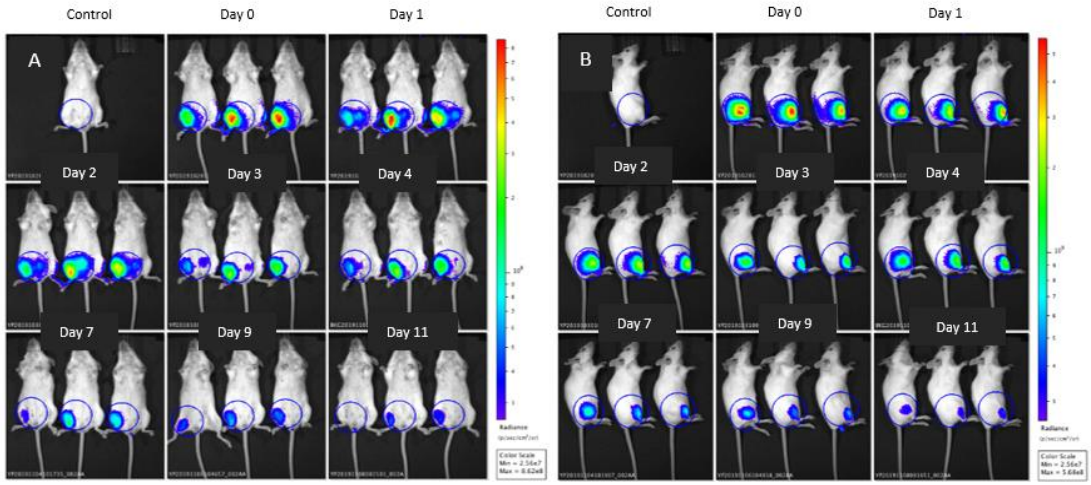

Figure A.3 *Fluorescense intensity images for GBS67-CpGODN taken from (A) back and (B) side for all the days of the study. GBS67 protein and GBS67-CpGODN protein conjugate were labelled using Alexa Fluor 790 protein labelling kit (Molecular probes) according to the manufacturer's instructions. DiD lipophilic tracking dye was included in liposomes formulation for tracking. Female BALB/c mice, 7–12 weeks old were split into 3 groups of 3 mice. All mice were immunised intramuscularly (50 µL/dose) at day 0 with fluorolabeled antigens and liposomes. Anesthetised mice were placed into the IVIS chamber, and images were captured using the IVIS spectrum camera (Perkin Elmer) at day 0-4 and then every 2 days until day 11. A non-immunised mouse was used as negative control and for quantifying the background level.*

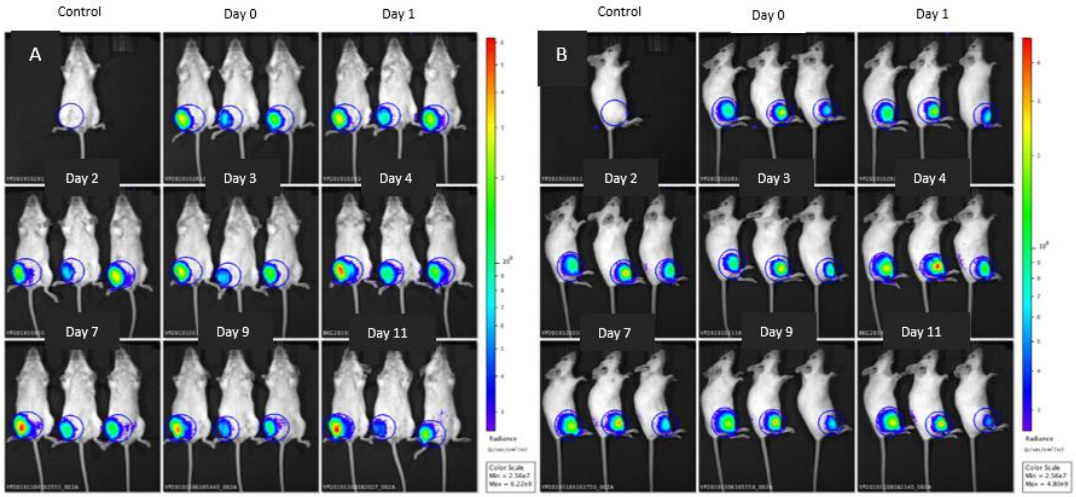

Figure A.4 *Fluorescense intensity images for GBS67-CpGODN+liposomes group (AlexaFluor 790) taken from (A) back and (B) side for all the days of the study. GBS67 protein and GBS67-CpGODN protein conjugate were labelled using Alexa Fluor 790 protein labelling kit (Molecular probes) according to the manufacturer's instructions. DiD lipophilic tracking dye was included in liposomes formulation for tracking. Female BALB/c mice, 7–12 weeks old were split into 3 groups of 3 mice. All mice were immunised intramuscularly (50 µL/dose) at day 0 with fluorolabeled antigens and liposomes. Anesthetised mice were placed into the IVIS chamber, and images were captured using the IVIS spectrum camera (Perkin Elmer) at day 0-4 and then every 2 days until day 11. A non-immunised mouse was used as negative control and for quantifying the background level.*

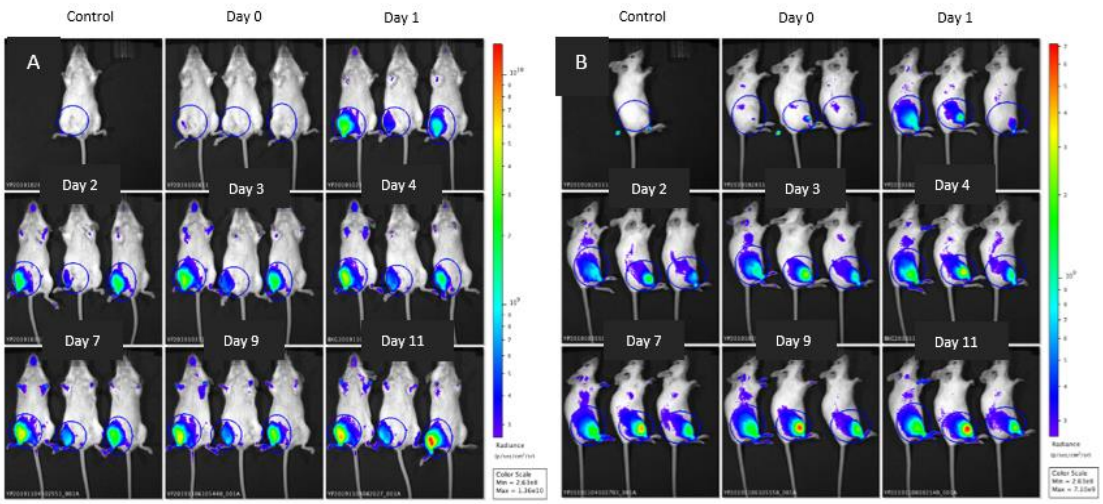

Figure A.5 *Fluorescense intensity images for GBS67-CpGODN+liposomes group (DiD) taken from (A) back and (B) side for all the days of the study. GBS67 protein and GBS67-CpGODN protein conjugate were labelled using Alexa Fluor 790 protein labelling kit (Molecular probes) according to the manufacturer's instructions. DiD lipophilic tracking dye was included in liposomes formulation for tracking. Female BALB/c mice, 7–12 weeks old were split into 3 groups of 3 mice. All mice were immunised intramuscularly (50 µL/dose) at day 0 with fluorolabeled antigens and liposomes. Anesthetised mice were placed into the IVIS chamber, and images were captured using the IVIS spectrum camera (Perkin Elmer) at day 0-4 and then every 2 days until day 11. A non-immunised mouse was used as negative control and for quantifying the background level.*

Appendix II

Conference attendance

Chatzikleanthous D, Paciello I, Carboni F, D'Oro U, Romano M.R, Roberts C.W, Perrie Y, Adamo R (2019). Design of vaccine delivery systems: The conjugation of CpG-ODN TLR9 agonist to protein antigens anchored to liposomes. Bioinspired nanomaterials meeting 2019. 18th-19th March 2019, Glasgow, UK.

Chatzikleanthous D, Paciello I, Carboni F, D'Oro U, Romano M.R, Roberts C.W, Perrie Y, Adamo R (2019). Design of vaccine nanotechnology-based delivery systems: The effect of CpG-ODN-protein conjugate anchored to liposomes. UK Ireland Controlled Release Society annual meeting (UKICRS). 3th-4th June, Liverpool, UK.

Chatzikleanthous D, Paciello I, Carboni F, D'Oro U, Romano M.R, Roberts C.W, Perrie Y, Adamo R (2019). Design of vaccine nanotechnology-based delivery systems: The effect of CpG-ODN-protein conjugate anchored to liposomes. Controlled Release Society annual meeting (CRS). 20th-23rd July, Valencia, Spain.

Chatzikleanthous D, Paciello I, Carboni F, D'Oro U, Romano M.R, Roberts C.W, Perrie Y, Adamo R (2019). The effect of CpG-ODN-protein conjugates anchored to liposomes. British Society of Nanomedicine: Early career researchers meeting 2019. 25th-26th July 2019, Glasgow, UK.

Chatzikleanthous D, Paciello I, Carboni F, D'Oro U, Romano M.R, Roberts C.W, Perrie Y, Adamo R (2019). Synthesis and immunological properties of protein conjugate adsorbed on cationic liposomes surface. Liposome Research Days (LRD). 15th-18th September 2019, Sapporo, Japan.

Publications

Chatzikleanthous *et al*. – submitted, under revision